WEAK LYAPUNOV FUNCTIONS FOR HYBRID DYNAMICAL SYSTEMS: APPLICATIONS TO ELECTRICAL AND MECHANICAL SYSTEMS

ANDREA BISOFFI

May 15, 2017

WEAK LYAPUNOV FUNCTIONS FOR HYBRID DYNAMICAL SYSTEMS: APPLICATIONS TO ELECTRICAL AND MECHANICAL SYSTEMS

ANDREA BISOFFI

University of Trento
Department of Industrial Engineering
May 15, 2017

APPROVED BY

Luca Zaccarian, Supervisor
Department of Industrial Engineering & Laboratoire d'analyse et d'architecture des systèmes
University of Trento, Italy & Centre National de la Recherche Scientifique, France

Mauro Da Lio, Co-supervisor
Department of Industrial Engineering
University of Trento

REFEREES

Sophie Tarbouriech
Laboratoire d'analyse et d'architecture des systèmes
Centre National de la Recherche Scientifique, France

Pietro Tesi
Faculty of Science and Engineering
University of Groningen

PH. D. COMMISSION

Marco Fontana
Department of Industrial Engineering
University of Trento

Sophie Tarbouriech
Laboratoire d'analyse et d'architecture des systèmes
Centre National de la Recherche Scientifique, France

Isabelle Queinnec
Laboratoire d'analyse et d'architecture des systèmes
Centre National de la Recherche Scientifique, France

Giulio Panzani
Dipartimento di Elettronica, Informazione e Bioingegneria
Politecnico di Milano

Daniele Fontanelli
Department of Industrial Engineering
University of Trento

ABSTRACT

In this work we propose a number of relevant engineering applications that exhibit both a continuous and a discrete evolution, and are therefore suitably described by a recent formalism for hybrid dynamical systems. More specifically, *(i)* we design observer schemes for a nonsmooth disturbance arising in AC/DC conversion, which we then cancel from a desirable signal; *(ii)* we show how reset actuation applied to nonlinear mechanical systems can at the same time sustain or damp oscillations; *(iii)* we study the feedback interconnection of a classical proportional-integral-derivative controller with a sliding mass under Coulomb friction through differential inclusions. In the context of dynamical systems, we analyze the properties of these applications in terms of asymptotic stability through Lyapunov functions tailored for hybrid systems. Instead of the standard Lyapunov conditions, we prove asymptotic stability through weaker, or relaxed, conditions that are compensated by additional (structural) properties that may be easier to verify.

SOMMARIO

In questo lavoro è proposta una serie di rilevanti applicazioni ingegneristiche che mostrano un'evoluzione sia continua sia discreta, e perciò si prestano ad essere descritte da un recente formalismo per sistemi dinamici ibridi. Nello specifico, *(i)* si progettano degli osservatori per un disturbo non differenziabile rinvenibile nella conversione da corrente alternata a corrente continua che viene quindi opportunamente cancellato dal segnale desiderato; *(ii)* si mostra come un'attuazione a reset applicata a sistemi meccanici non lineari possa allo stesso tempo sostenere o attenuare le oscillazioni; *(iii)* si studia tramite un'inclusione differenziale l'interconnessione in anello chiuso di un classico controllore proporzionale-integrale-derivativo con una massa che si muove sotto l'azione dell'attrito di Coulomb. Nel contesto dei sistemi dinamici, si analizzano le proprietà di queste applicazioni in termini di stabilità asintotica tramite funzioni di Lyapunov adattate per sistemi ibridi. Invece delle condizioni Lyapunov standard, si prova la stabilità asintotica attraverso condizioni più deboli, o rilassate, che sono compensate da ulteriori proprietà (strutturali) più facilmente verificabili.

CONTENTS

LIST OF TABLES

INTRODUCTION

In control theory, the broad term of hybrid systems refers to all those systems that present a continuous-time dynamics, typically described by differential equations, and a discrete-time dynamics, typically described by difference equations: these two dynamics are intertwined and both necessary for describing the evolution of those systems. The interest in hybrid dynamical systems, which has a strong motivation in the pervasive presence of digital control for continuous-time plants, is witnessed by several special issues in the main control journals [2, 3, 35, 87].

Whereas the continuous-time dynamics is typically embedded "as it is" in hybrid dynamical systems, different approaches are proposed to deal with the discrete-time dynamics. One widespread approach is to consider an event-driven discrete-time dynamics: events can be determined by a switching signal [72], or by an automaton [76]. The approach taken here embeds also the discrete-time dynamics "as it is", and follows [47, 48]. (This last approach can include the ones before, as detailed in [47, §1.4.4] and [47, §1.4.2], respectively.) In this sense, the approach in [47, 48] builds on classical notions and tools for nonlinear systems described either by differential or difference equations (and inclusions).

We discuss briefly the modeling power of this *hybrid* systems formalism on the basis of the problems addressed in the next chapters. The ripple disturbances in Chapter 3 are nonsmooth (that is, not continuously differentiable) continuous-time signals. This feature partly makes them "defective" signals from a continuous-time perspective. On the other hand, they are totally legitimate hybrid signals if we interpret this nonsmoothness as a result of a jump in their derivative, which allows to build suitable observers for the estimation of these ripple disturbances. Regarding Chapters 4-5, a very common modus operandi of the control engineer (for instance when designing linear controllers on linearized plants) is to ascertain which dynamics are the fastest and which the slowest, and then concentrate on the slowest for the design, as a first approximation. The models of Chapters 4-5 rest upon the approximation that the actuator dynamics is typically fast as compared to the natural mechanical dynamics, and can then be associated to an instantaneous dynamics (that is, a jump), for which we design a reset control (a jump map) and a reset surface (a jump set) in order to sustain or damp oscillations. In Chapter 6 we use another potential strength of the hybrid systems formalism in [47], specifically the fact that it allows for differential inclusions instead of differential equations for describing continuous-time dynamics. This more general description of friction enables us to establish stability properties of the feedback interconnection of a proportional-integral-derivative controller with Coulomb friction. Finally, a relevant modeling feature of the formalism in [47] is allowing for the study of stability properties of *sets*, instead of mere equilibrium points.

Besides hybrid dynamical systems, the second key ingredient of this work are Lyapunov functions. Starting from his seminal work [75], Lyapunov functions have been constantly used in control to prove asymptotic stability properties. Their main advantage is that they enable us to prove asymptotic stability without resorting to solutions, which are in general hard to compute. Although converse theorems (see [59, §4.7] and Section 2.5.2) guarantee that a Lyapunov function exists if an attractor enjoys asymptotic stability, they do not provide a constructive way to build a Lyapunov function. A main disadvantage of Lyapunov functions is then the fact that obtaining them often relies on (energy) intuition (see the Lyapunov function in Chapter 4), and preliminary trial and error.

This is even more true for hybrid dynamical systems, where a (strict) Lyapunov function has to satisfy a decrease condition along the flow and also across the jumps.

One way to partially simplify the daunting quest of a Lyapunov function is to obtain one that satisfies this decrease condition in a weak, or relaxed, sense. This is the spirit with which we approach the search of a Lyapunov function that can guarantee asymptotic stability for the problems of Chapters 3-6. More specifically, we deal with Lyapunov functions such that: *(i)* nonnegative decrease along flow and across jumps is balanced by observability and average dwell time (see Section 2.5.3 and its use in Chapter 3), *(ii)* nonnegative decrease along flow is balanced by some persistent jumping (see Section 2.5.4 and its use in Chapters 3 and 4), *(iii)* differentiability of the Lyapunov function is given up for establishing stability (see Section 2.5.5 and its use in Chapter 6), *(iv)* mild integrability conditions determine a superset of the ω-limit set of a hybrid solution in the context of invariance principles (see Section 2.5.6 and its use in Chapter 6).

Each chapter is strongly rooted in a specific engineering application. Chapter 3 deals with a typical disturbance arising in AC/DC conversion, the so-called ripple, and applies the presented observer schemes to cancel the ripple from experimental signals coming from the Joint European Torus. The framework of Chapters 4 and 5 is applied to a one-legged robotic hopper (for sustaining oscillations) or to an automotive suspension (for damping oscillations). Chapter 6 addresses the asymptotic stability properties of the feedback interconnection of a proportional-integral-derivative controller with a sliding point mass under the action of Coulomb friction.

From the point of view of the structure of this work, Chapter 2 collects the fundamentals of the hybrid system formalism in [47] that are used in the subsequent chapters: we have chosen to illustrate these notions and results by using only examples and applications that are extracted from the subsequent chapters themselves. Chapters 3-6 present the problems that we address with the hybrid system formalism and at which we have already hinted above: each chapter is preceded by an abstract summarizing the content, and in each following introduction the state of the art for the specific problem is also discussed in detail. Finally, Chapter 7 presents conclusions and future perspectives.

1.2   SCIENTIFIC PRODUCTION

The research activity as a Ph.D. candidate has led to the following publications, on some of which this thesis is built.

IN PREPARATION OR UNDER REVIEW

[17] A. Bisoffi, F. Forni, M. Da Lio, and L. Zaccarian. "Reset control of minimal-order mechanical systems with applications." In preparation.

[16] A. Bisoffi, M. Da Lio, A. R. Teel, and L. Zaccarian. "Global asymptotic stability of a PID control system with Coulomb friction." In: *arXiv* (2016). Available at `https://arxiv.org/abs/1609.09103`. Under review in the IEEE Transactions on Automatic Control.

[13] A. Bisoffi, F. Biral, M. Da Lio, and L. Zaccarian. "Longitudinal jerk estimation of driving intentions for intelligent vehicle applications." Under review in the IEEE/ASME Transactions on Mechatronics.

JOURNAL

[20] A. Bisoffi, L. Zaccarian, M. Da Lio, and D. Carnevale. "Hybrid cancellation of ripple disturbances arising in AC/DC converters." In: *Automatica* 77 (2017), pp. 344–352

PEER-REVIEWED CONFERENCE

[18] A. Bisoffi, F. Forni, M. Da Lio, and L. Zaccarian. "Global results on reset-induced periodic trajectories of planar systems." In: *European Control Conference*. 2016, pp. 2644–2649

[14] A. Bisoffi, F. Biral, M. Da Lio, and L. Zaccarian. "Longitudinal Jerk Estimation for Identification of Driver Intention." In: *IEEE 18th International Conference on Intelligent Transportation Systems*. 2015, pp. 1855–1861

[38] S. Formentin, A. Bisoffi, and T. Oomen. "Asymptotically exact direct data-driven multivariable controller tuning." In: *IFAC-PapersOnLine* 48.28 (2015), pp. 1349–1354

[29] M. Corno, A. Bisoffi, C. Ongini, and S. M. Savaresi. "An energy-driven road-to-driver assistance system for intersections." In: *European Control Conference*. 2015, pp. 3035–3040

[19] A. Bisoffi, M. Da Lio, and L. Zaccarian. "A hybrid ripple model and two hybrid observers for its estimation." In: *IEEE 53rd Conference on Decision and Control*. Los Angeles (CA), USA, 2014

PATENT

[15] A. Bisoffi, M. Corno, C. Ongini, and S. M. Savaresi. "Sistema di segnalazione per ottimizzare i consumi di un veicolo nella percorrenza di strade semaforizzate." Italian Patent MI 2014A001024. Applicant: Politecnico di Milano. 2014

The next chapters correspond to the previous publications as follows:

<div align="center">

Chapter 3:   [19], [20];

Chapter 4:   [18];

Chapter 5:   [17];

Chapter 6:   [16].

</div>

The publications [15] and [29] are a continuation of the author's M. Sc. thesis, and are therefore not included in this work. The publication [38] arose from the attendance of a Ph. D. course on "Advanced data-driven methods for modeling and control", and is then out of the scope of this work. The publications [13, 14] are related to an automotive application of an enhanced Kalman filter.

This chapter introduces the reader to the formalism of hybrid dynamical systems, and the use of Lyapunov methods to certify stability and attractivity. The chapter is entirely based on [47, 48], and aims at providing the reader with the minimal set of definitions and results that are needed in the problems that are addressed in the next Chapters.

We do not provide here a comparison of this formalism with other hybrid dynamical system formalisms because the reader can already find a thorough comparison in [47, §1.4-1.5] and [48, pp. 40-41]. (An additional and up-to-date resource could be [73].)

The reader should note that in the parts of this chapter denoted as Examples and Applications, we make use of variables that are *local* to the specific example or application, are defined within it and are *not* used in the rest of the chapter.

Notation: $\mathbb{R}_{\geqslant 0}$ denotes the nonnegative real numbers. $\mathbb{Z}_{\geqslant 0}$ denotes the nonnegative integers. For a set $\mathcal{S}$, its closure is denoted by $\overline{\mathcal{S}}$. $\mathrm{co}\mathcal{S}$ is the convex hull of the set $\mathcal{S}$, so that $\overline{\mathrm{co}}\mathcal{S}$ denotes the closure of the convex hull of the set $\mathcal{S}$. $\mathbb{B}$ is the closed unit ball and $\mathbb{B}^{\circ}$ is the open unit ball.

2.1 HYBRID SYSTEMS FORMALISM

In this section we introduce the specific formalism of hybrid dynamical systems together with its concept of solution.

The following definition of a set-valued mapping is instrumental for considering differential inclusions in our hybrid dynamical system model, which we present in (2.1).

DEFINITION 2.1 (Set-valued mapping and domain [47, Def. 2.1]) *A set-valued mapping* F *from* $\mathbb{R}^{n}$ *(resp., from* $S \subset \mathbb{R}^{n}$*) to* $\mathbb{R}^{n}$ *associates every point* $x \in \mathbb{R}^{n}$ *(resp.,* $x \in S$*) with a subset of* $\mathbb{R}^{n}$ *and is denoted by* $F : \mathbb{R}^{n} \rightrightarrows \mathbb{R}^{n}$ *(resp.,* $F : S \rightrightarrows \mathbb{R}^{n}$*). The domain of* F *is the set* $\mathrm{dom}F := \{x \in \mathbb{R}^{n} : F(x) \neq \emptyset\}$ *(resp.,* $\mathrm{dom}F := \{x \in S : F(x) \neq \emptyset\}$ *because one trivially sets* $F(x) = \emptyset$ *for all* $x \notin S$*).*
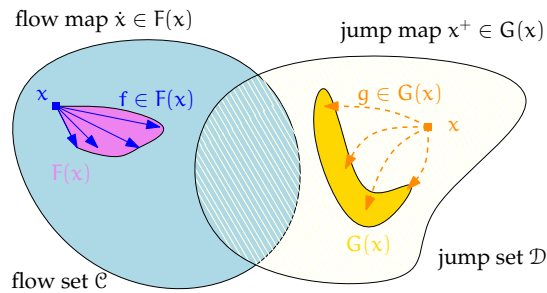
Figure 2.1: Quantities appearing in the hybrid system of Equation (2.1): the *flow set* is $\mathcal{C}$ (light blue set), the *jump set* is $\mathcal{D}$ (light yellow set), the *flow map* at a point $x \in \mathcal{C}$ is given by a the set $F(x)$ (violet) within which the velocity vector $f \in F(x)$ can be chosen (some examples are the blue arrows), the *jump map* at a point $x \in \mathcal{D}$ is given by a set $G(x)$ (gold) within which the next-value vector $g \in G(x)$ can be chosen (some examples are the orange dashed arrows).

With Definition 2.1, we can state the type of hybrid dynamical systems we consider in this work:

$$\mathcal{H}: \begin{cases} \dot{x} \in F(x), & x \in \mathcal{C} \\ x^+ \in G(x), & x \in D \end{cases} \qquad \begin{matrix} (2.1a) \\ (2.1b) \end{matrix}$$

where we denote:

- as *flow set* the set $\mathcal{C} \subset \mathbb{R}^n$,

- as *flow map* the set-valued mapping $F : \mathbb{R}^n \rightrightarrows \mathbb{R}^n$ with $\mathrm{dom} F \supset \mathcal{C}$,

- as *jump set* the set $\mathcal{D} \subset \mathbb{R}^n$,

- as *jump map* the set-valued mapping $G : \mathbb{R}^n \rightrightarrows \mathbb{R}^n$ with $\mathrm{dom} G \supset \mathcal{D}$.

In the following we refer coincisely to these data of the hybrid system $\mathcal{H}$ as $\mathcal{H} = (\mathcal{C}, F, \mathcal{D}, G)$. x is the *state* of the hybrid system and its functional dependence from the two notions of time will be addressed when talking about solutions to (2.1). At an intuitive level, we may think of Equations 2.1 in the following way.

- Equation (2.1b): whenever the state belongs to $\mathcal{D}$, the state *can* evolve discrete-wise, that is, with a jump. The set $G(x)$ gives the collection of values associated to the current state x, which the state can evolve to. The next value for the state is denoted by x^+.

- Equation (2.1a), in a parallel way: whenever the state belongs to $\mathcal{C}$, the state *can* evolve continuous-wise, that is, with a flow. The set $F(x)$ gives the collection of values associated to the current state x for its velocity. The velocity is the time derivative $\dot{x}$ of the state.

This description is complemented by the pictorial illustration in Figure 2.1.

The intuitive explanation of (2.1) already anticipates that many possible evolutions are allowed in (2.1). A first source for multiple evolutions is the presence of the differential and difference inclusions, as explained in the points above. A second source for multiple evolutions is that when the state belongs to $\mathcal{C} \cap \mathcal{D}$, there is no prescription whether the state should flow or jump, so that both evolutions are possible. We come back to this consideration more rigorously after introducing the concept of solution.
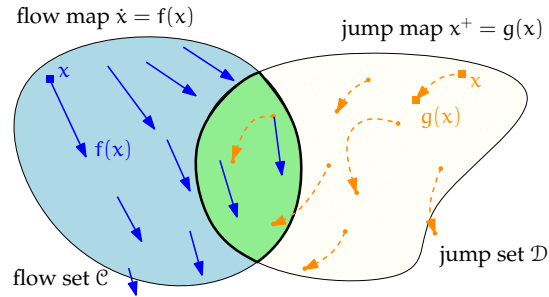
Figure 2.2: Quantities appearing in the hybrid system of Equations (2.2): the flow set $\mathcal{C}$ (light blue set), the jump set $\mathcal{D}$ (light yellow set) and their intersection $\mathcal{C} \cap \mathcal{D}$ (green set). The evolution is governed by the differential equation (for some x's, the corresponding $f(x)$ is given by the blue arrow) and by the difference equation (for some x's, the corresponding $g(x)$ is given by the dashed orange arrow). Note the f can point outside $\mathcal{C}$ and g can induce jumps out of $\mathcal{C} \cup \mathcal{D}$.

A simpler version of (2.1) is obtained by replacing the differential (resp., difference) inclusion with a differential (resp., difference) equation in the following manner

$$\dot{x} = f(x), \quad x \in \mathcal{C} \qquad (2.2a)$$
$$x^+ = g(x), \quad x \in D, \qquad (2.2b)$$

where the flow map is then the function (or single-valued mapping) $f\colon \mathbb{R}^n \to \mathbb{R}^n$, and the jump map is the function (or single-valued mapping) $g\colon \mathbb{R}^n \to \mathbb{R}^n$. Also in this case multiple evolutions can arise, for example when $\mathcal{C} \cap \mathcal{D} \neq \emptyset$. A pictorial illustration of Equation (2.2) is in Figure 2.2.

Through the next example, whose system is taken from Chapter 4, we further illustrate the concept of hybrid dynamical system in (2.1) used in this work and we hint at at the modeling capabilities of this formalism.

EXAMPLE 2.1 (Exemplification of a hybrid dynamical system) *Consider the following hybrid dynamical system from Chapter 4. Specifically, for the state* $x = [\begin{smallmatrix} x_1 \\ x_2 \end{smallmatrix}] \in \mathbb{R}^2$ *consider*

$$\dot{x} = f(x) := \begin{bmatrix} x_2 \\ -\frac{c}{m}x_2 - \frac{k}{m}x_1 \end{bmatrix}, \; x \in \mathcal{C} \tag{2.3a}$$

$$x^+ \in G(x) := \begin{bmatrix} \hat{\theta}\,\overline{\mathrm{sgn}}(x_2) \\ x_2 \end{bmatrix}, \; x \in \mathcal{D} \tag{2.3b}$$

$$\mathcal{C} := \{x\colon x_1 x_2 \leqslant 0\} \cup \{x\colon |x_1| \geqslant \hat{\theta}, x_1 x_2 \geqslant 0\}. \tag{2.3c}$$

$$\mathcal{D} := \{x\colon x_1 = 0\} \tag{2.3d}$$

with

$$\overline{\mathrm{sgn}}(x_2) = \begin{cases} \mathrm{sign}(x_2) & \text{if } x_2 \neq 0 \\ \{1, -1\} & \text{if } x_2 = 0. \end{cases}$$

m, c, k *are respectively the mass, damping and elastic constants of a planar mechanical oscillator, and* $\hat{\theta} > 0$ *is a parameter related to the preload of the spring, as better clarified below. Figure 2.3 provides a graphical illustration of the flow and jump sets.*
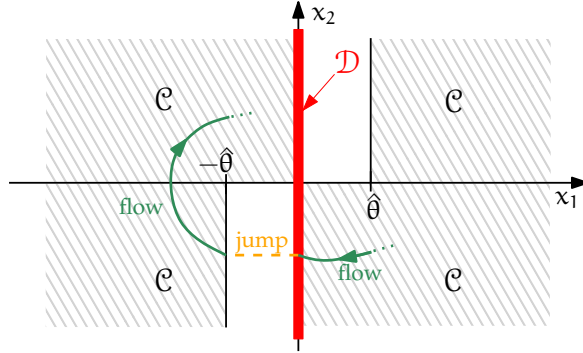
Figure 2.3: Flow set $\mathcal{C}$ and jump set $\mathcal{D}$ on the phase plane for Example 2.1.

Here, $\mathcal{C} \cap \mathcal{D} = \mathcal{D} \supset \{0\}$, *and in particular the solutions from the origin are not unique. Indeed, the solution itself can decide to flow forever in* $\{0\}$ *(since the origin is an equilibrium for (2.3a)), or jump to* $(\hat{\theta}, 0)$ *or* $(-\hat{\theta}, 0)$ *according to the difference inclusion in (2.3b), or flow for some interval staying in* $\{0\}$ *and then jump. The underlying feature of model (2.1) (or (2.2)) is that when in the flow (or jump) set, the solutions are* not *forced to flow (or jump), but they are* allowed *to flow (or jump).*

Finally, we take this example as an opportunity to pinpoint some modeling capabilities of the formalism in (2.1). Consider

$$m\ddot{q} + c\dot{q} + k(q - \theta) = 0, \tag{2.4}$$

with q *being a physical displacement and* θ *a control input that acts as a preload of the spring.* θ *can then enforce a variation in the stored potential energy of the spring. Assume that* θ *is piecewise constant and switches between* $-\hat{\theta}/2$ *and* $\hat{\theta}/2$ *when the solutions to (2.4) pass through the hyperplane defined by* $\{(q, \dot{q}) \in \mathbb{R}^2\colon q - \theta = 0\}$. *With this reset policy for* θ, *(2.4) becomes then (2.3) with the change of coordinates* $x_1 := q - \theta$ *and* $x_2 := \dot{q}$.

In particular, the aforementioned reset policy allows for jumps when $q - \theta =: x_1 = 0$, and $x_2 \neq 0$, toggling θ between $-\hat{\theta}/2$ and $\hat{\theta}/2$, which corresponds to $|q^+ - \theta^+| = |x_1^+| = |q - \theta^+| = \hat{\theta}$. In other words, the jumps of x_1 do not imply that the mass position q changes instantaneously, but are rather related to a very fast actuation *toggling between two values. In this sense, hybrid dynamical systems are a good candidate to address systems with two (or more) timescales (see, for instance, [48, p. 41]). An applicative example of this kind of very fast actuation can be found in [51]: in a hopping robot a spring is preloaded during the flight phase, and the sudden variation of θ can be associated to releasing the spring by a clutch mechanism when touching the ground.*

We have so far illustrated the formulation of a hybrid dynamical system within this work, and illustrated intuitively how the state can evolve according to this formulation. Now we want to be more precise about the evolution of the state, so we introduce the concept of solution. It requires two intermediate steps: the definition of hybrid time domain and hybrid arc.

The concept of hybrid time domain generalizes naturally the concepts of time domain in continuous or discrete time. (Note also that in these two cases, the presence of flow and jump sets generally different from $\mathbb{R}^n$ may induce bounded time domains, and that, even with $\mathcal{C} = \mathbb{R}^n$, finite escape times may be witnessed in the continuous case.) The presence of two distinct time axes is decisive to the current formalism of hybrid dynamical system: t denotes the elapsed continuous time, j denotes the elapsed discrete time, that is, the number of jumps.

DEFINITION 2.2 (Hybrid time domain [47, Def. 2.3] and suprema) *A subset E of $\mathbb{R}_{\geqslant 0} \times \mathbb{Z}_{\geqslant 0}$ is a compact hybrid time domain if for some $J \geqslant 1$,*

$$E = \bigcup_{j=0}^{J-1} [t_j, t_{j+1}] \times \{j\} \tag{2.5}$$

for some finite sequence of times $0 = t_0 \leqslant t_1 \leqslant \cdots \leqslant t_J$. E is a hybrid time domain if for all $(T, J) \in E$, $E \cap ([0, T] \times \{0, 1, \ldots, J\})$ is a compact hybrid time domain. The operations $\sup_t$ and $\sup_j$ on a hybrid time domain E are defined as

$$\sup_t E := \sup\{t \in \mathbb{R}_{\geqslant 0} \colon \exists j \in \mathbb{Z}_{\geqslant 0} \text{ such that } (t, j) \in E\} \tag{2.6a}$$

$$\sup_j E := \sup\{j \in \mathbb{Z}_{\geqslant 0} \colon \exists t \in \mathbb{R}_{\geqslant 0} \text{ such that } (t, j) \in E\}. \tag{2.6b}$$

Some hybrid time domains of Definition 2.2, and their suprema, are illustrated in Figure 2.4.
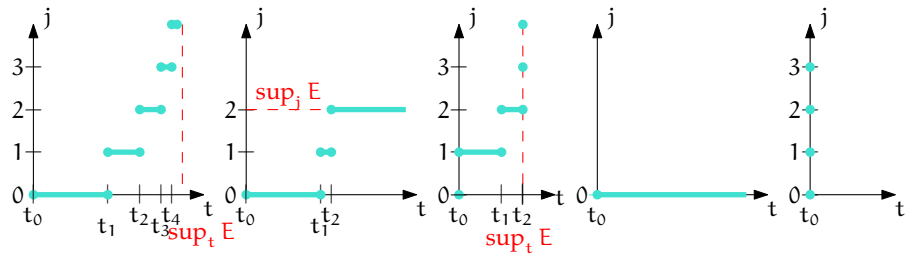
Figure 2.4: Hybrid time domains with suprema indicated. Note that the first (second) one from the right reduces to the time domain of a purely discrete (respectively, continuous) time solution. According to Definition 2.5, the first, third and fifth one from the left correspond to Zeno solutions (the first one is sometimes referred to as genuinely Zeno).

DEFINITION 2.3 (Hybrid arc [47, Def. 2.4] and domain) *A function $\phi : E \to \mathbb{R}^n$ is a hybrid arc if E is a hybrid time domain and if for each $j \in \mathbb{Z}_{\geqslant 0}$, the function $t \mapsto \phi(t, j)$ is*

locally absolutely continuous[1] on the interval $I^j = \{t : (t, j) \in E\}$. *The domain of a hybrid arc is denoted by* $\text{dom}\phi$.

The usefulness of absolute continuity is motivated by the following considerations [9, §0.2]. When considering candidate solutions $\phi(\cdot)$ to an initial value problem $\dot{x} = f(x, t)$ and $x(t_0) = x_0$, one has to consider limits of sequences. To handle the limit, one needs to rewrite the differential equation in integral terms, that is, $x(t) = x_0 + \int_{t_0}^t f(x(s), s)ds$. However, the initial value problem and the integral are equivalent for absolutely continuous functions, but not for continuous functions, because absolutely continuous functions coincide with the integral of their derivative.

A result from real analysis states that an absolutely continuous function has a finite derivative except at most on a set of zero measure, and particularizing this fact for Definition 2.3 yields that on each I^j we can denote $\frac{d}{dt}\phi(t, j)$ by $\dot{\phi}(t, j)$ whenever the time derivative exists.

We are now able to define what we mean by solution to the hybrid dynamical system (2.1) (for a set $\mathcal{S}$, its closure is denoted by $\overline{\mathcal{S}}$).

DEFINITION 2.4 (Solution to a hybrid system [47, Def. 2.6]) *A hybrid arc ϕ is a solution to the hybrid dynamical system* (2.1) *captured by* $(\mathcal{C}, F, \mathcal{D}, G)$ *if*

1. $\phi(0, 0) \in \overline{\mathcal{C}} \cup \mathcal{D}$;

2. *for all $j \in \mathbb{Z}_{\geqslant 0}$ such that $I^j := \{t : (t, j) \in \text{dom}\phi\}$ has a nonempty interior, for all $t \in \text{int }I^j$*

$$\phi(t, j) \in \mathcal{C} \tag{2.7a}$$

and for almost all $t \in I^j$

$$\dot{\phi}(t, j) \in F(\phi(t, j)); \tag{2.7b}$$

3. *for all $(t, j) \in \text{dom}\phi$ such that $(t, j + 1) \in \text{dom}\phi$,*

$$\phi(t, j) \in \mathcal{D} \tag{2.7c}$$
$$\phi(t, j + 1) \in G(\phi(t, j)). \tag{2.7d}$$

It is then clear that when $\phi(t, j) \in \mathcal{C} \cap \mathcal{D}$, this definition does not force $\phi(t, j)$ to flow or jump, but it asks only that if the solution decides to flow, its velocity must (almost always) belong to the flow map as in (2.7b) and that if the solution decides to jump, the next value must belong to jump map as in (2.7d), as we also mentioned in Example 2.1 for the solutions starting from the origin.

Some specific types of solutions are described next.

DEFINITION 2.5 (Types of solutions [47, Def. 2.5, Def. 2.7]) *A solution ϕ to a hybrid system $\mathcal{H} = (\mathcal{C}, F, \mathcal{D}, G)$ is*

- *nontrivial if $\text{dom}\phi$ contains at least two points;*
- *complete if $\text{dom}\phi$ is unbounded, that is, $\sup_t \text{dom}\phi + \sup_j \text{dom}\phi = +\infty$;*
- *Zeno if it is complete and $\sup_t \text{dom}\phi < +\infty$*
- *maximal if there does not exist another solution ψ to $\mathcal{H}$ such that $\text{dom}\phi$ is a proper subset of $\text{dom}\psi$ and $\phi(t, j) = \psi(t, j)$ for all $(t, j) \in \text{dom}\phi$.*

EXAMPLE 2.2 (Hybrid time domain) *Consider again the system of Example 2.1 and a special solution $\phi = (\phi_{x_1}, \phi_{x_2})$ to hybrid system (2.3). We represent its hybrid time domain, and the components ϕ_{x_1} and ϕ_{x_2} as functions of the hybrid time (t, j) in Figure 2.5. We will see in Chapter 4 that the depicted solution is a hybrid periodic solution (see Definition 4.1).*

---

[1] $t \mapsto \phi(t, j)$ is locally absolutely continuous on an interval I^j with nonempty interior if it is absolutely continuous on each compact subinterval of I^j.
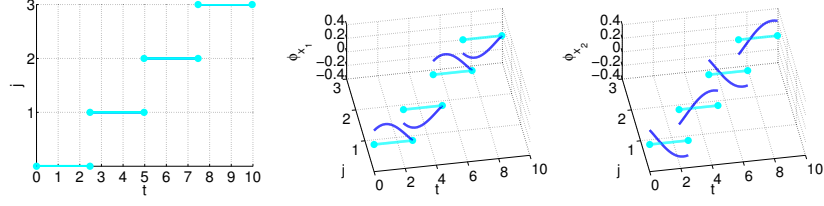
Figure 2.5: A solution ϕ to (2.3) in Examples 2.1 and 2.2: the hybrid time domain of ϕ (left), the graph of the first component ϕ_{x_1} (center) and the graph of the second component ϕ_{x_2} (right) parametrized by the two time directions t and j.

In the following, we use the coincise characterization below.

DEFINITION 2.6 (Set of maximal solutions [47, p. 33]) *Consider a hybrid system* $\mathcal{H} = (\mathcal{C}, F, \mathcal{D}, G)$. $\mathcal{S}_{\mathcal{H}}(S)$ *is the set of all maximal solutions* ϕ *to* $\mathcal{H}$ *with* $\phi(0,0) \in S$. $\mathcal{S}_{\mathcal{H}}$ *is the set of all maximal solutions* ϕ *to* $\mathcal{H}$.

2.2 HYBRID BASIC CONDITIONS

In this section we introduce typical regularity conditions on the data of the hybrid system $\mathcal{H} = (\mathcal{C}, F, \mathcal{D}, G)$, the so-called hybrid basic conditions.

ASSUMPTION 2.1 (Hybrid basic conditions [47, Ass. 6.5]) *We denote by hybrid basic conditions the three following requirements on the data* $(\mathcal{C}, F, \mathcal{D}, G)$ *of* $\mathcal{H}$ *in* (2.1):

1. $\mathcal{C}$ *and* $\mathcal{D}$ *are closed subsets of* $\mathbb{R}^n$;

2. $F \colon \mathbb{R}^n \rightrightarrows \mathbb{R}^n$ *is outer semicontinuous and locally bounded[2] relative to* $\mathcal{C}$, $\mathcal{C} \subset \text{dom} F$, *and* $F(x)$ *is convex[3] for every* $x \in \mathcal{C}$;

3. $G \colon \mathbb{R}^n \rightrightarrows \mathbb{R}^n$ *is outer semicontinuous and locally bounded relative to* $\mathcal{D}$, $\mathcal{D} \subset \text{dom} G$.

To the end of checking the hybrid basic conditions for a given data, note the following equivalence, in light of which we omit here the definition of outer semicontinuity (refer to [47, Def. 5.9]).

FACT 2.1 (Outer semicontinuity and closed graph [47, Lem. 5.10]) *A set-valued mapping* $F \colon \mathbb{R}^n \rightrightarrows \mathbb{R}^n$ *is outer semicontinuous if and only if its graph* $\text{gph} F := \{(x,y) \in \mathbb{R}^n \times \mathbb{R}^n : y \in F(x)\}$ *is closed.*

All the data of the hybrid system models in the next chapters satisfy these hybrid basic conditions. The hybrid basic conditions are not the tightest sufficient conditions that one could ask for a reasonably good behavior of a hybrid dynamical system. Indeed, one could assume only nominal well-posedness and well-posedness of the hybrid system, as it is done for specific results in [47, Chap. 6-7]. In broad terms these two properties ask for a hybrid system that sequences of graphs of solutions, intended as sets, converge to another set that is also the graph of a solution, in the case of no perturbations (nominal well-posedness) and of vanishing perturbations (well-posedness). Proving directly nominal well-posedness (see [47, Def. 6.2]) and well-posedness (see [47, Def. 6.29]) is typically quite involved. On the other hand, the hybrid basic conditions imply nominal well-posedness and well-posedness ([47, Thm. 6.8, Thm. 6.30]), so one renounces some level of generality and prefers to

---

2 Local boundedness of F comprises that the image of any bounded set is itself bounded.

3 We do not need to ask esplicitly that $F(x)$ should be nonempty for every $x \in \mathcal{C}$ because $\text{dom} F := \{x \in \mathbb{R}^n : F(x) \neq \emptyset\}$ from Definition 2.1 and we are already asking $\mathcal{C} \subset \text{dom} F$. Same for the set-valued mapping G.

choose the data of the hybrid system so that the hybrid basic conditions are satisfied. Moreover, the hybrid basic conditions are mild requirements. Indeed, a continuous $f : \mathbb{R}^n \to \mathbb{R}^n$ in (2.2a) (or g in (2.2b)) satisfy Item 2 (or 3, respectively) of the hybrid basic conditions. For continuous time systems, this is less than the Lipschitz continuity that is typically assumed. Therefore, the hybrid basic conditions are usually considered as a good modeling principle with which it is reasonable to comply.

Under the hybrid basic conditions, we can simplify (see [47, p. 124]) partially Definition 2.4 of solution. Item 1 in Definition 2.4 becomes trivially $\phi(0,0) \in \mathcal{C} \cup \mathcal{D}$. Item 2 can be restated as:

For all $j \in \mathbb{Z}_{\geqslant 0}$ such that $I^j := \{t : (t,j) \in \mathrm{dom}\,\phi\}$ has a nonempty interior, for almost all $t \in I^j$

$$\phi(t,j) \in \mathcal{C}, \tag{2.8a}$$
$$\dot{\phi}(t,j) \in F(\phi(t,j)). \tag{2.8b}$$

Indeed, when $\mathcal{C}$ is closed, $\phi(t,j) \in \mathcal{C}$ for all $t \in \mathrm{int}\, I^j$ is equivalent to $\phi(t,j) \in \mathcal{C}$ for all $t \in I^j$, and thanks to the absolute continuity of $t \mapsto \phi(t,j)$ (see Definition 2.3), the latter is equivalent to $\phi(t,j) \in \mathcal{C}$ for almost all $t \in I^j$.

2.3 (UNIFORM) STABILITY AND ATTRACTIVITY

Thanks to Definition 2.4 (or its simplification in (2.8) under the hybrid basic conditions) for the solution concept, we characterize in this section the notions of (Lyapunov) stability and attractivity, in their local and global versions.

Typically, stability and attractivity are studied for equilibrium points, as in [59]. However, there are many cases where it is natural to consider sets instead of points, as motivated in [48, p. 58]. We propose three examples from the next chapters that illustrate the utility of considering sets as attractors.

EXAMPLE 2.3 (Set attractor: timer) *Consider the system*

$$\left.\begin{array}{l} \dot{z} = f(z,\tau) \\ \dot{\tau} = 1 \end{array}\right\} \quad 0 \leqslant \tau \leqslant T_\tau \tag{2.9a}$$

$$\left.\begin{array}{l} z^+ = g(z,\tau) \\ \tau^+ = 0 \end{array}\right\} \quad \tau = T_\tau, \tag{2.9b}$$

which is an abstraction of system (3.18) in Chapter 3. Consider the variable τ that plays the role of a timer: it grows linearly with time during flow, as in (2.9a), up to a fixed threshold T_τ, and is then reset to 0 when this threshold is reached, as in (2.9b). Whichever the compact attractor $\mathcal{A}_z$ for the z component of the state may be, it is unreasonable to ask the timer τ to converge to a point, whereas it is fair to consider as its attractor

$$\mathcal{A}_\tau = [0, T_\tau].$$

The attractor for (2.9) is then $\mathcal{A} = \mathcal{A}_z \times \mathcal{A}_\tau$.

EXAMPLE 2.4 (Set attractor: periodic orbit) *In Chapter 4 we will establish that for the reset planar mass-spring-damper described in Example 2.1 (see also Equations (2.3) and (2.4)) there exist a unique nontrivial hybrid periodic orbit (see Theorem 4.1). The concept of hybrid periodic orbit is the generalization of the concept of periodic orbit (or limit cycle, since we are considering a planar system) for the hybrid setting (see Definition 4.1). The periodic solution whose image is the hybrid periodic orbit is illustrated in Example 2.2. We will be able to characterize this hybrid periodic orbit as the following locus of points in the flow set $\mathcal{C}$:*

$$\mathcal{A} = \{x \in \mathcal{C} : T_b(x) = T_f(x), x \neq 0\}, \tag{2.10}$$

where T_f and T_b are the kinetic energies of the points that are obtained by integrating the flow equation from x forward and backward, respectively, until no flow is possible (namely,

until the jump set is reached for the point yielding $\mathsf{T_f}$ *and until the image of the jump set is reached for the point yielding* $\mathsf{T_b}$*). For more precise definitions, the reader is referred to Equations (4.5) in Section 4.3.*

It is then clear that the hybrid periodic orbit $\mathcal{A}$ *in (2.10) is a set of points, and we will prove the asymptotic stability of this set as a key result in Chapter 4 in Theorem 4.2. The set* $\mathcal{A}$ *and two solutions converging to it are depicted in Figure 2.6.*
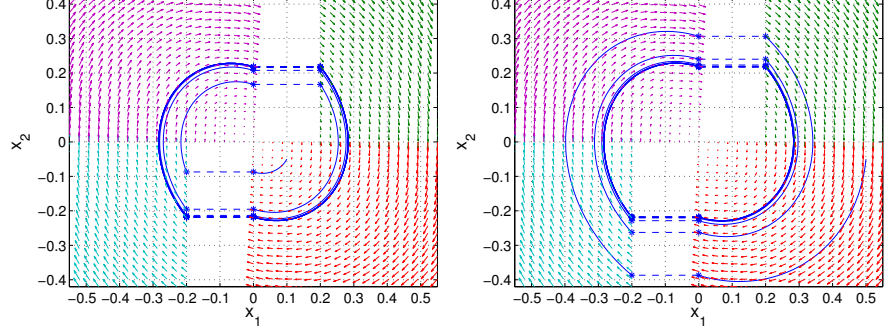
Figure 2.6: Two solutions to system (4.2) in Chapter 4 that converge to the set attractor $\mathcal{A}$ in (2.10).

EXAMPLE 2.5 (Set attractor: friction) *Consider the system in (6.4) that is the subject of Chapter 6 (point mass under Coulomb friction force controlled by a PID feedback) and that we report here for the reader's convenience:*

$$\dot{z} \in \begin{bmatrix} s \\ v \\ -k_i e_i - k_p s - k_v v \end{bmatrix} - f_c \begin{bmatrix} 0 \\ 0 \\ 1 \end{bmatrix} \mathrm{SGN}(v) =: \tilde{F}(z) \tag{2.11a}$$

with SGN *defined by the set-valued mapping*

$$\mathrm{SGN}(v) := \begin{cases} \mathrm{sign}(v) & \text{if } v \neq 0 \\ [-1, 1] & \text{if } v = 0. \end{cases} \tag{2.11b}$$

All possible equilibria of the dynamics in (2.11a) (in this case coinciding with the values $\bar{z}$ *of the right-hand side such that* $0 \in \tilde{F}(\bar{z})$*) are clearly* $\bar{s} = 0$ *and* $\bar{v} = 0$*, but also any value* $\bar{e}_i \in \left[-\frac{f_c}{k_i}, \frac{f_c}{k_i}\right]$*. Indeed, for any such* $\bar{e}_i$ *a value in* $f_c \mathrm{SGN}(0)$ *can be selected that makes* $\dot{v} = 0$*. This leads naturally to considering the set attractor*

$$\mathcal{A} := \left\{ (e_i, s, v) : \ s = 0, \ v = 0, \ e_i \in \left[-\frac{f_c}{k_i}, \frac{f_c}{k_i}\right] \right\}, \tag{2.12}$$

that is depicted in Figure 2.7.

A crucial common feature of all the above attractors is their compactness. Compact (that is, closed and bounded) attractors present additional benefits with respect to closed attractors, and we show partly this claim relative to the conditions to be a Lyapunov function for a closed versus a compact attractor, in Section 2.5. Moreover, all the attractors in the next chapters are compact. For these reasons, the concepts of stability and attractivity in this section are given for compact attractors.

To characterize stability and attractivity, we need first the following notion of distance to a closed set. Note that this notion belongs more generally to metric spaces (see, e.g., [89, Def. 2.2.1]), although we refer here to [47] for uniformity of exposition.

DEFINITION 2.7 (Distance to a closed set [47, Def. 3.5]) *Given a vector* $x \in \mathbb{R}^n$ *and a closed set* $\mathcal{A} \subset \mathbb{R}^n$*, the distance of* x *to* $\mathcal{A}$ *is defined as*

$$|x|_{\mathcal{A}} := \inf_{y \in \mathcal{A}} |x - y|. \tag{2.13}$$
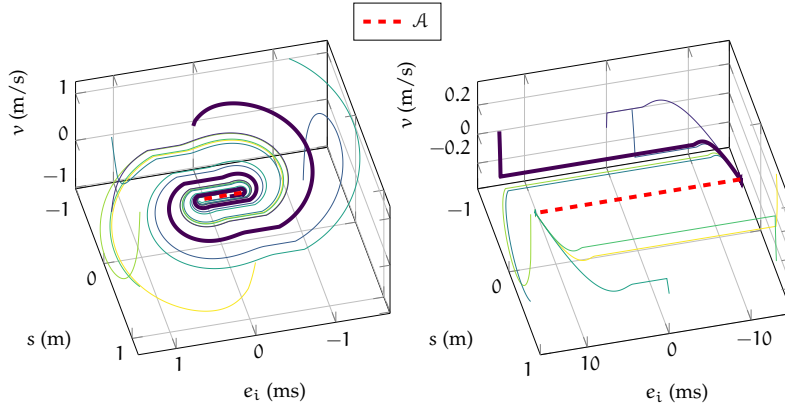
Figure 2.7: Set attractor in (2.12) and some solutions, for the PID parameters $(k_v, k_p, k_i) = (6.4, 3, 4)$ (left) and $(1.5, 0.66, 0.08)$ (right).

EXAMPLE 2.6 (Distance to a set) *Consider the attractor*

$$\mathcal{A} = \{(\sigma, \phi, v) \colon |\phi| \leqslant f_c, \sigma = 0, v = 0\} \tag{2.14}$$

of Chapter 6, which is the same set as (2.12), written in new coordinates. From the definition in (2.13), separate the cases $\phi < -f_c$, $|\phi| \leqslant f_c$, $\phi > f_c$ and obtain

$$|x|_{\mathcal{A}}^2 = \sigma^2 + v^2 + dz_{f_c}(\phi)^2, \tag{2.15}$$

where $dz_{f_c}(\phi) := \phi - \mathrm{sat}_{f_c}(\phi)$ is the symmetric scalar deadzone function returning zero when $\phi \in [-f_c, f_c]$. A level set of $|x|_{\mathcal{A}}^2$ is in Figure 2.8.
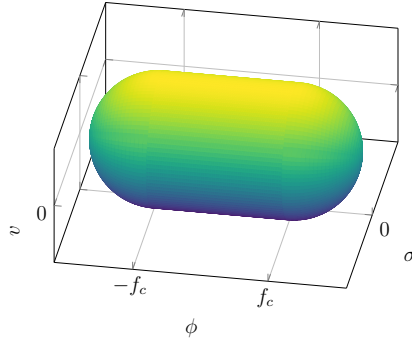
Figure 2.8: Level set of $|x|_{\mathcal{A}}^2$ in (2.15).

We also give the two standard definitions of class-$\mathcal{K}_\infty$ and class-$\mathcal{KL}$ functions. Such comparison functions were introduced in [53] and spread wide within control theory starting from [113] (see [57] for historical details), although we refer here to [47] for uniformity of exposition.

DEFINITION 2.8 (Class-$\mathcal{K}_\infty$ functions [47, Def. 3.4]) *A function $\alpha \colon \mathbb{R}_{\geqslant 0} \to \mathbb{R}_{\geqslant 0}$ is a class $\mathcal{K}_\infty$ function (also written $\alpha \in \mathcal{K}_\infty$) if α is zero at zero, continuous, strictly increasing, and unbounded.*

DEFINITION 2.9 (Class-$\mathcal{KL}$ functions [47, Def. 3.38]) *A function $\beta \colon \mathbb{R}_{\geqslant 0} \times \mathbb{R}_{\geqslant 0} \to \mathbb{R}_{\geqslant 0}$ is a class-$\mathcal{KL}$ function (also written $\beta \in \mathcal{KL}$) if β is continuous, $r \mapsto \beta(r, s)$ is nondecreasing and $\lim_{r \to 0^+} \beta(r, s) = 0$ for each $s \geqslant 0$, $s \mapsto \beta(r, s)$ is nonincreasing and $\lim_{s \to \infty} \beta(r, s) = 0$ for each $r \geqslant 0$.*

We are now in a position to define the notions of (Lyapunov) stability and attractivity that are of interest in this work.

DEFINITION 2.10 ((Lyapunov) stability, local attractivity and asymptotic stability [47, Def. 7.1]) *Let $\mathcal{H} = (\mathcal{C}, F, \mathcal{D}, G)$ be a hybrid system in $\mathbb{R}^n$. A compact set $\mathcal{A} \subset \mathbb{R}^n$ is said to be*

- *(Lyapunov) stable for $\mathcal{H}$ if for every $\epsilon > 0$ there exists $\delta > 0$ such that every solution ϕ to $\mathcal{H}$ with $|\phi(0,0)|_{\mathcal{A}} \leqslant \delta$ satisfies $|\phi(t,j)|_{\mathcal{A}} \leqslant \epsilon$ for all $(t,j) \in \operatorname{dom}\phi$;*
- *locally attractive for $\mathcal{H}$ if there exists $\mu > 0$ such that every solution ϕ to $\mathcal{H}$ with $|\phi(0,0)|_{\mathcal{A}} \leqslant \mu$ is bounded and, if ϕ is complete, $\lim_{t+j\to\infty} |\phi(t,j)|_{\mathcal{A}} = 0$;*
- *locally asymptotically stable for $\mathcal{H}$ if it is both (Lyapunov) stable and locally attractive for $\mathcal{H}$.*

We can then define the basin of attraction of $\mathcal{A}$.

DEFINITION 2.11 (Basin of attraction [47, Def. 7.3]) *Let $\mathcal{H}$ be a hybrid system on $\mathbb{R}^n$ and $\mathcal{A} \subset \mathbb{R}^n$ be locally asymptotically stable for $\mathcal{H}$. The basin of attraction of $\mathcal{A}$ is denoted by $\mathcal{B}_{\mathcal{A}}$ and is the set of points $\xi \in \mathbb{R}^n$ such that every solution ϕ to $\mathcal{H}$ with $\phi(0,0) = \xi$ is bounded and, if it is complete, then $\lim_{t+j\to+\infty} |\phi(t,j)|_{\mathcal{A}} = 0$ with $(t,j) \in \operatorname{dom}\phi$.*

We can deduce from this definition that all $\xi \notin \mathcal{C} \cup \mathcal{D}$ are automatically in the basin of attraction of $\mathcal{A}$ because there are no solutions from outside $\mathcal{C} \cup \mathcal{D}$ (cf. Definition 2.4), so that the for-all statement ("every solution ϕ to $\mathcal{H}$") in the definition above is vacuously satisfied.

We can give the global versions of the Definitions in 2.10. Based on the previous comment, note that asking $\mathcal{B}_{\mathcal{A}}$ to be $\mathbb{R}^n$ amounts to checking if $\mathcal{C} \cup \mathcal{D}$ is in $\mathcal{B}_{\mathcal{A}}$.

DEFINITION 2.12 (Global attractivity, asymptotic stability) *Let $\mathcal{H} = (\mathcal{C}, F, \mathcal{D}, G)$ be a hybrid system in $\mathbb{R}^n$. A compact set $\mathcal{A} \subset \mathbb{R}^n$ is said to be*

- *globally attractive for $\mathcal{H}$ if it is locally attractive for $\mathcal{H}$ with basin of attraction $\mathcal{B}_{\mathcal{A}} = \mathbb{R}^n$.*
- *globally asymptotically stable for $\mathcal{H}$ if it is both stable and globally attractive for $\mathcal{H}$.*

We have the following property for the basin of attraction of a compact attractor of a hybrid system satisfying the hybrid basic conditions. This property is a classical result for equilibrium points of ordinary differential (originally in [61], see also [59, Lem. 8.1]).

FACT 2.2 (Basin of attraction is open [47, Prop. 7.4]) *Let $\mathcal{H}$ satisfy the hybrid basic conditions. If a compact set $\mathcal{A} \subset \mathbb{R}^n$ is locally asymptotically stable for $\mathcal{H}$, then the basin of attraction $\mathcal{B}_{\mathcal{A}}$ of $\mathcal{A}$ is an open set containing $\mathcal{A}$.*

Let us now characterize uniformity of asymptotic stability, and introduce the notion of boundedness of solutions. See Definition 2.6 for the meaning of $\mathcal{S}_{\mathcal{H}}(S)$ for a hybrid system $\mathcal{H}$ and a set S.

DEFINITION 2.13 (Boundedness of solutions [109, Def. 2]) *Let $\mathcal{H} = (\mathcal{C}, F, \mathcal{D}, G)$ be a hybrid system in $\mathbb{R}^n$. The solutions to $\mathcal{H}$ are uniformly bounded from a compact set K if there exists $M > 0$ such that for each $\phi \in \mathcal{S}_{\mathcal{H}}(K)$ and $(t,j) \in \operatorname{dom}\phi$, $|\phi(t,j)| \leqslant M$. The solutions to $\mathcal{H}$ are uniformly bounded from a set $S \subset \mathbb{R}^n$ if they are uniformly bounded from each compact subset of S. The solutions to $\mathcal{H}$ are uniformly globally bounded if they are uniformly bounded from $\mathbb{R}^n$.*

We can now characterize uniformity.

DEFINITION 2.14 (Uniform attractivity and asymptotic stability [47, Def. 6.24]) *Let $\mathcal{H} = (\mathcal{C}, F, \mathcal{D}, G)$ be a hybrid system in $\mathbb{R}^n$. A compact set $\mathcal{A} \subset \mathbb{R}^n$ is said to be:*

- *uniformly attractive from a set* $S \subset \mathbb{R}^n$ *if the solutions to* $\mathcal{H}$ *are uniformly bounded from* S *and for every* $\epsilon > 0$ *there exists* $T > 0$ *such that[4] for every* $\phi \in \mathcal{S}_{\mathcal{H}}(S)$ *and* $(t, j) \in \operatorname{dom}\phi$ *with* $t + j \geqslant T$

$$|\phi(t, j)|_{\mathcal{A}} \leqslant \epsilon;$$

- *uniformly locally asymptotically stable if it is (Lyapunov) stable and uniformly attractive from its basin of attraction* $\mathcal{B}_{\mathcal{A}}$;

- *uniformly globally stable[5] if it is (Lyapunov) stable and solutions are uniformly globally bounded;*

- *uniformly globally attractive[6] if it is uniformly attractive from* $\mathbb{R}^n$;

- *uniformly globally asymptotically stable if it is uniformly globally stable and uniformly globally attractive.*

The definition of uniform local asymptotic stability is stronger, nonetheless it can be proven that asymptotic stability is uniform if the hybrid basic conditions are satisfied and the attractor is compact. In other words, the next result proves the equivalence of asymptotic stability and uniform asymptotic stability for compact attractors and under the hybrid basic conditions.

FACT 2.3 (Uniform AS from AS [47, Lem. 7.8]) *Let* $\mathcal{H}$ *satisfy the hybrid basic conditions and* $\mathcal{A} \subset \mathbb{R}^n$ *be a compact set. If* $\mathcal{A}$ *is locally asymptotically stable, it is also uniformly locally asymptotically stable.*

Analogously, it can be proven that for compact attractors and under the hybrid basic conditions, asymptotic stability implies the (in general) stronger concept of $\mathcal{KL}$ asymptotic stability. To state this result, we define first proper indicators, then we characterize $\mathcal{KL}$ asymptotic stability and finally we report the result linking it with asymptotic stability.

DEFINITION 2.15 (Proper indicator [47, Def. 7.9]) *Let* $\mathcal{U}$ *be an open set. A function* $\omega \colon \mathcal{U} \to \mathbb{R}_{\geqslant 0}$ *is a proper indicator on* $\mathcal{U}$ *if it is continuous and* $\omega(x_i) \to \infty$ *for* $i \to \infty$ *if either* $|x_i| \to \infty$ *or the sequence* $\{x_i\}_{i=1}^{\infty}$ *approaches the boundary of* $\mathcal{U}$. *Let* $\mathcal{A} \subset \mathcal{U}$ *be a compact set. A function* $\omega \colon \mathcal{U} \to \mathbb{R}_{\geqslant 0}$ *is a proper indicator of* $\mathcal{A}$ *on* $\mathcal{U}$ *if it is a proper indicator on* $\mathcal{U}$ *and* $\omega(x) = 0$ *if and only if* $x \in \mathcal{A}$.

Knowing that the basin of attraction $\mathcal{B}_{\mathcal{A}}$ of a compact attractor $\mathcal{A}$ is an open set from Fact 2.2, a proper indicator ω on $\mathcal{B}_{\mathcal{A}}$ is $\omega(x) = 1/|x|_{\mathbb{R}^n \setminus \mathcal{B}_{\mathcal{A}}}$. A proper indicator of a compact attractor $\mathcal{A}$ on $\mathcal{B}_{\mathcal{A}}$ is $\omega(x) = |x|_{\mathcal{A}}/|x|_{\mathbb{R}^n \setminus \mathcal{B}_{\mathcal{A}}}$.

DEFINITION 2.16 ($\mathcal{KL}$ asymptotic stability [47, Def. 7.10]) *Let* $\mathcal{H}$ *be a hybrid system in* $\mathbb{R}^n$, $\mathcal{A} \subset \mathbb{R}^n$ *a compact set, and* $\mathcal{U} \subset \mathbb{R}^n$ *be an open set such that* $\mathcal{A} \subset \mathcal{U}$. *The set* $\mathcal{A}$ *is* $\mathcal{KL}$ *asymptotically stable on* $\mathcal{U}$ *if for every proper indicator* ω *of* $\mathcal{A}$ *on* $\mathcal{U}$ *there exists a function* $\beta \in \mathcal{KL}$ *such that*

$$\omega(\phi(t, j)) \leqslant \beta(\omega(\phi(0, 0)), t + j) \quad \text{for all } (t, j) \in \operatorname{dom}\phi \tag{2.16}$$

for every $\phi \in \mathcal{S}_{\mathcal{H}}(\mathcal{U})$.

FACT 2.4 ($\mathcal{KL}$ AS from AS [47, Thm. 7.12]) *Let* $\mathcal{H}$ *satisfy the hybrid basic conditions. If a compact set* $\mathcal{A} \subset \mathbb{R}^n$ *is locally asymptotically stable, it is also* $\mathcal{KL}$ *asymptotically stable on its basin of attraction* $\mathcal{B}_{\mathcal{A}}$.

---

4 As in Definition 2.10 for local attractivity, this second part of the definition of uniform attractivity imposes an effective requirement only on complete solutions. Indeed, for all *noncomplete* solutions ϕ, pick $T > \sup_t \operatorname{dom}\phi + \sup_j \operatorname{dom}\phi$, so that there are no $(t, j) \in \operatorname{dom}\phi$ such that $t + j \geqslant T$ and what follows is vacuously satisfied.

5 For a compact attractor, the definition in [47, Def. 3.6] coincides with this one.

6 For a compact attractor, the definition in [47, Def. 3.6] coincides with this one.

In addition to the previously stated Facts 2.3 and 2.4, the combination of hybrid basic conditions and compact attractors proves itself useful also for Facts 2.6 and 2.7. Moreover, all these results will enable us in Section 2.5 about Lyapunov functions to provide sufficient conditions simply for asymptotic stability and generalize automatically asymptotic stability to, for example, uniform asymptotic stability or semiglobal practical robust $\mathcal{KL}$ asymptotic stability.

2.4   ROBUST ASYMPTOTIC STABILITY

In this section we introduce the main concepts regarding robust stability. We present the results alongside the points in the next Chapters where they are exploited.

To characterize robust stability, we define first what we mean by a perturbed hybrid system.

DEFINITION 2.17 (ρ-perturbation of $\mathcal{H}$ [47, Def. 6.27]) *Given a hybrid system* $\mathcal{H} = (\mathcal{C}, \mathsf{F}, \mathcal{D}, \mathsf{G})$ *and a function* $\rho\colon \mathbb{R}^n \to \mathbb{R}_{\geqslant 0}$, *the* ρ-*perturbation of* $\mathcal{H}$, *denoted* $\mathcal{H}_\rho$, *is the hybrid system*

$$\dot{x} \in \mathsf{F}_\rho(x), \quad x \in \mathcal{C}_\rho \tag{2.17a}$$

$$x^+ \in \mathsf{G}_\rho(x), \quad x \in \mathcal{D}_\rho \tag{2.17b}$$

where

$$\mathcal{C}_\rho := \{x \in \mathbb{R}^n \colon (x + \rho(x)\mathbb{B}) \cap \mathcal{C} \neq \emptyset\} \tag{2.17c}$$

$$\mathsf{F}_\rho(x) := \overline{\mathrm{co}}\,\mathsf{F}((x + \rho(x)\mathbb{B}) \cap \mathcal{C}) + \rho(x)\mathbb{B} \quad \forall x \in \mathcal{C}_\rho \tag{2.17d}$$

$$\mathcal{D}_\rho := \{x \in \mathbb{R}^n \colon (x + \rho(x)\mathbb{B}) \cap \mathcal{D} \neq \emptyset\} \tag{2.17e}$$

$$\mathsf{G}_\rho(x) := \{v \in \mathbb{R}^n \colon v \in g + \rho(g)\mathbb{B}, g \in \mathsf{G}((x + \rho(x)\mathbb{B}) \cap \mathcal{D})\} \quad \forall x \in \mathcal{D}_\rho, \tag{2.17f}$$

and $\overline{\mathrm{co}}\,S$ *denotes the closure of the convex hull of a set* S.

EXAMPLE 2.7 (Inflation of a set-valued mapping) *As a simple example, consider the inflation of the set-valued mapping* SGN$\colon \mathbb{R} \rightrightarrows \mathbb{R}$ *defined in* (2.11b). *This inflation is used in Chapter 6 where the flow set is* $\mathcal{C} = \mathbb{R}^3$. *For a constant parameter* ρ_v, *define the function* ρ *of Definition 2.17 as* $\rho(x) := |\rho_v|$. *We apply the definition in* (2.17d) *to obtain* $v \rightrightarrows$ SGN$_\rho(v) =:$ SGN$_{\rho_v}(v)$. *For each value of velocity* v_i, SGN$_\rho(v_i)$ *is the* set *sum of the image of the set* $[v_i - |\rho_v|, v_i + |\rho_v|]$ *and the interval* $[-|\rho_v|, |\rho_v|]$: *see Figure 2.9. Applying* $\overline{\mathrm{co}}$ *is superfluous because for each* $v \in \mathbb{R}$, SGN$(v + |\rho_v|\mathbb{B}) + |\rho_v|\mathbb{B}$ *is already a closed and convex set.*
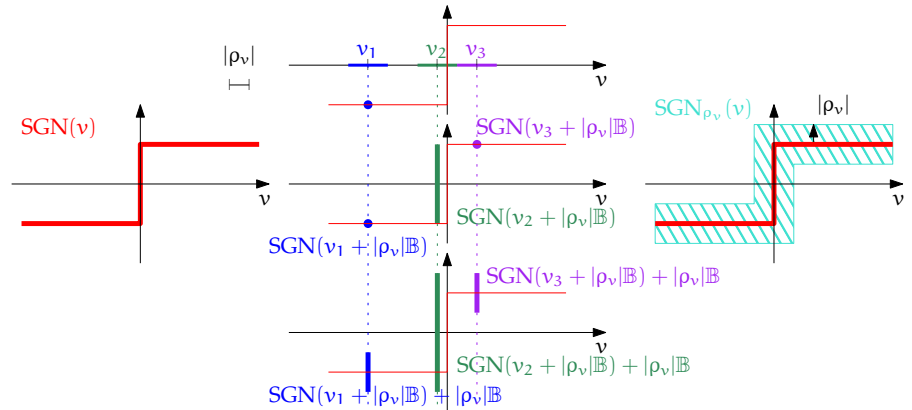
Figure 2.9: From SGN to SGN$_{\rho_v} :=$ SGN$_\rho$ for a given length $|\rho_v|$: SGN$_\rho$ is constructed starting from the points v_i, $i = 1, 2, 3$.

The rationale behind (2.17d), (2.17f) is essentially to inflate the points that one starts from, and to inflate the sets that one arrives at. In particular, the $\overline{\mathrm{co}}$ is needed

in (2.17d) to ensure that the perturbed hybrid system satisfies the hybrid basic conditions, given the importance played by them in the previous sections. The next result can indeed be proven.

FACT 2.5 (Hybrid basic conditions under perturbation [47, Prop. 6.28]) *If $\mathcal{H}$ satisfies the hybrid basic conditions and $\rho\colon \mathbb{R}^n \to \mathbb{R}_{\geqslant 0}$ is continuous, then $\mathcal{H}_\rho$ in (2.17) also satisfies the hybrid basic conditions.*

We report now three possible variants of robust asymptotic stability that call for $\mathcal{H}_\rho$ in (2.17), the ρ-perturbation of $\mathcal{H}$.

DEFINITION 2.18 (Robust asymptotic stability [47, Def. 7.15]) *Let $\mathcal{A} \subset \mathbb{R}^n$ be a compact set that is locally asymptotically stable for $\mathcal{H}$, and let $\mathcal{U} \subset \mathcal{B}_\mathcal{A}$ be an open set such that $\mathcal{A} \subset \mathcal{U}$. The local asymptotic stability of $\mathcal{A}$ is robust on $\mathcal{U}$ if there exists a continuous function $\rho\colon \mathbb{R}^n \to \mathbb{R}_{\geqslant 0}$ that is positive on $\mathcal{U}\backslash\mathcal{A}$ such that $\mathcal{A}$ is locally asymptotically stable for $\mathcal{H}_\rho$ in (2.17) and $\mathcal{U}$ is a subset of the basin of attraction of $\mathcal{A}$ for $\mathcal{H}_\rho$.*

DEFINITION 2.19 (Robust $\mathcal{KL}$ asymptotic stability [47, Def. 7.18]) *Let $\mathcal{A} \subset \mathbb{R}^n$ be a compact set and $\mathcal{U} \subset \mathbb{R}^n$ be an open set such that $\mathcal{A} \subset \mathcal{U}$. The set $\mathcal{A}$ is robustly $\mathcal{KL}$ asymptotically stable on $\mathcal{U}$ for $\mathcal{H}$ if there exists a continuous function $\rho\colon \mathbb{R}^n \to \mathbb{R}_{\geqslant 0}$ that is positive on $\mathcal{U}\backslash\mathcal{A}$ such that $\mathcal{A}$ is $\mathcal{KL}$ asymptotically stable (cf. Def. 2.16) on $\mathcal{U}$ for $\mathcal{H}_\rho$ in (2.17).*

DEFINITION 2.20 (Semiglobal practical robust $\mathcal{KL}$ asymptotic stability [47, Def. 7.18]) *Let $\mathcal{A} \subset \mathbb{R}^n$ be a compact set and $\mathcal{U} \subset \mathbb{R}^n$ be an open set such that $\mathcal{A} \subset \mathcal{U}$. The set $\mathcal{A}$ is semiglobally practically robustly $\mathcal{KL}$ asymptotically stable on $\mathcal{U}$ for $\mathcal{H}$ if for every ω that is a proper indicator of $\mathcal{A}$ on $\mathcal{U}$, every continuous function $\rho\colon \mathbb{R}^n \to \mathbb{R}_{\geqslant 0}$, and every function $\beta \in \mathcal{KL}$ satisfying*

$$\omega(\varphi(t,j)) \leqslant \beta(\omega(\varphi(0,0)), t+j) \quad \forall(t,i) \in \operatorname{dom}\varphi, \forall\varphi \in \mathcal{S}_\mathcal{H}(\mathcal{U}) \tag{2.18}$$

the following holds:
for every compact $K \subset \mathcal{U}$ and every $\epsilon > 0$, there exists $\delta \in (0,1)$ such that every $\varphi \in \mathcal{S}_{\mathcal{H}_{\delta\rho}}(K)$ satisfies

$$\omega(\varphi(t,j)) \leqslant \beta(\omega(\varphi(0,0)), t+j) + \epsilon \quad \forall(t,j) \in \operatorname{dom}\varphi. \tag{2.19}$$

Again, the combination of hybrid basic conditions and compact attractors is powerful because they guarantee that the previous versions of asymptotic stability in Section 2.3 hold in a robust way. We have in particular the following Fact 2.6 and 2.7 for robust $\mathcal{KL}$ asymptotic stability and semiglobal practical robust $\mathcal{KL}$ asymptotic stability, respectively.

FACT 2.6 (Robust $\mathcal{KL}$ AS from LAS [47, Thm. 7.21]) *Let $\mathcal{H}$ satisfy the hybrid basic conditions and $\mathcal{A} \subset \mathbb{R}^n$ be a compact set. If $\mathcal{A}$ is locally asymptotically stable, then it is robustly $\mathcal{KL}$ asymptotically stable on its basin of attraction $\mathcal{B}_\mathcal{A}$.*

EXAMPLE 2.8 (Some cases) *In the next chapters, where the considered systems satisfy the hybrid basic conditions and the attractors are compact, we will use weak Lyapunov functions to certify* simply *(global or local) asymptotic stability: this is done in Theorem 4.2 by Lemma 4.2 within Chapter 4, and in Proposition 6.1 within Chapter 6. This asymptotic stability holds automatically in a robust way (in the sense of the previous Definitions 2.18- 2.20) thanks to Fact 2.6 (and the following Fact 2.7): then, within Chapter 6 we can obtain straightforwardly Theorem 6.1 by applying the previous Fact 2.6.*

FACT 2.7 (Semiglobal practical robust $\mathcal{KL}$ AS from $\mathcal{KL}$ AS [47, Lem. 7.20]) *Let $\mathcal{H}$ satisfy the hybrid basic conditions, $\mathcal{A} \subset \mathbb{R}^n$ be a compact set, and $\mathcal{U} \subset \mathbb{R}^n$ be an open set such that $\mathcal{A} \subset \mathcal{U}$. If $\mathcal{A}$ is $\mathcal{KL}$ asymptotically stable on $\mathcal{U}$ then it is semiglobally practically robustly $\mathcal{KL}$ asymptotically stable on $\mathcal{U}$.*

APPLICATION 2.1 (l-ISS from semiglobal practical robust $\mathcal{KL}$ asymptotic stability)
We present here an application of Facts 2.4 and 2.7 to deduce semiglobal practical robust
$\mathcal{KL}$ *asymptotic stability. Additionally, we further illustrate this last notion by showing that*
it implies local input-to-state stability (l-ISS) with respect to the input $|\rho_\nu|$, *the size of a*
constant perturbation. The motivation for why such an input is of interest is provided in
Chapter 6, page 93.

Proposition 6.1 in Chapter 6 proves that the attractor $\mathcal{A}$ *in (2.12) is globally attractive*
and (Lyapunov) stable for the hybrid system with pure continuous dynamics $\mathcal{H} = (\tilde{F}, \mathcal{C} :=$
$\mathbb{R}^3, \emptyset, \emptyset)$ *and* $\tilde{F}$ *defined in (2.11a).*

Since $\mathcal{H}$ *satisfies the hybrid basic conditions and* $\mathcal{A}$ *is compact,* $\mathcal{A}$ *is also* $\mathcal{KL}$ *asymptoti-*
cally stable on $\mathcal{B}_\mathcal{A} = \mathbb{R}^3$ *by Fact 2.4 and semiglobally practically robustly* $\mathcal{KL}$ *asymptoti-*
cally stable on $\mathcal{B}_\mathcal{A} = \mathbb{R}^3$ *by previous Fact 2.7.*

We show now that semiglobal practical robust $\mathcal{KL}$ *asymptotic stability implies l-ISS with*
respect to the input $|\rho_\nu|$. *Since semiglobal practical robust* $\mathcal{KL}$ *asymptotic stability holds*
globally on $\mathcal{B}_\mathcal{A} = \mathbb{R}^3$, *we can take in Definition 2.20* $\omega(\phi(t,j)) = |\phi(t,j)|_\mathcal{A}$ *(see Defi-*
nition 2.15). Take then a fixed *value* $|\bar{\rho}_\nu| > 0$. *By restating Definition 2.20 in this global*
setting, for every compact K *and every* $\epsilon > 0$, *there exists* $\delta(\epsilon) \in (0,1)$ *such that every*
solution $\phi \in \mathcal{S}_{\mathcal{H}_{\delta(\epsilon)|\bar{\rho}_\nu|}}(K)$ *satisfies*

$$|\phi(t)|_\mathcal{A} \leqslant \beta(|\phi(0,0)|_\mathcal{A}, t) + \epsilon \quad \forall t \in \mathrm{dom}\phi. \tag{2.20}$$

For $|\rho_\nu| \leqslant \delta(\epsilon)|\bar{\rho}_\nu|$, $\mathcal{S}_{\mathcal{H}_{|\rho_\nu|}}(K) \subset \mathcal{S}_{\mathcal{H}_{\delta(\epsilon)|\bar{\rho}_\nu|}}(K)$, *and denote* $\phi_{|\rho_\nu|}$ *any solution* $\phi \in$
$\mathcal{S}_{\mathcal{H}_{|\rho_\nu|}}(K)$. *Then, from (2.20) the following is also true: for every compact* K *and every*
$\epsilon > 0$, *there exists* $\delta(\epsilon) \in (0,1)$ *such that, for* $|\rho_\nu| \leqslant \delta(\epsilon)|\bar{\rho}_\nu|$, *every* $\phi_{|\rho_\nu|}$ *satisfies*

$$|\phi_{|\rho_\nu|}(t)|_\mathcal{A} \leqslant \beta(|\phi_{|\rho_\nu|}(0,0)|_\mathcal{A}, t) + \epsilon \quad \forall t \in \mathrm{dom}\phi_{|\rho_\nu|}. \tag{2.21}$$

By repeating slavishly the steps in [59, Proof of Lemma 4.5, pp. 663-664], for each ϵ *we*
can build $\bar{\delta}(\epsilon)$ *as the supremum of all applicable* δ's *for the given* ϵ. *Although* $\epsilon \mapsto \bar{\delta}(\epsilon)$
is positive, nondecreasing but not necessarily continuous, we can choose $\zeta \in \mathcal{K}$ *(a class-$\mathcal{K}$*
function) such that ζ *bounds from below* $\bar{\delta}$ *for all* ϵ *(that is, there exists* $\kappa \in (0,1)$ *such that*
$\zeta(\epsilon) \leqslant \kappa\bar{\delta}(\epsilon)$ *for all* ϵ). *Define* $c := \lim_{\epsilon \to \infty} \zeta(\epsilon)$ *and* $\alpha := \zeta^{-1} \in \mathcal{K}$. *For all* $|\rho_\nu|$ *such that*
$\frac{|\rho_\nu|}{|\bar{\rho}_\nu|} < c$, *we can then take* ϵ *as* $\epsilon = \alpha\left(\frac{|\rho_\nu|}{|\bar{\rho}_\nu|}\right) = \zeta^{-1}\left(\frac{|\rho_\nu|}{|\bar{\rho}_\nu|}\right)$. *This implies that* $\frac{|\rho_\nu|}{|\bar{\rho}_\nu|} < \bar{\delta}(\epsilon)$
because ζ *bounds from below* $\bar{\delta}$ *and that, from (2.21),*

$$\begin{aligned}|\phi_{|\rho_\nu|}(t)|_\mathcal{A} &\leqslant \beta(|\phi_{|\rho_\nu|}(0,0)|_\mathcal{A}, t) + \alpha\left(\frac{|\rho_\nu|}{|\bar{\rho}_\nu|}\right) \\ &= \beta(|\phi_{|\rho_\nu|}(0,0)|_\mathcal{A}, t) + \gamma_l(|\rho_\nu|), \ \forall t \in \mathrm{dom}\phi_{|\rho_\nu|}\end{aligned} \tag{2.22}$$

with $|\rho_\nu| \mapsto \gamma_l(|\rho_\nu|) := \alpha\left(\frac{|\rho_\nu|}{|\bar{\rho}_\nu|}\right) \in \mathcal{K}$. *Equation (2.22), which is obtained for* $|\rho_\nu| \leqslant c|\bar{\rho}_\nu|$
(hence locally), states precisely a l-ISS notion because, as long as the input $|\rho_\nu|$ *is small, an*
ISS bound can be written for the solution to the system perturbed by $|\rho_\nu|$.

A relevant corollary building on the previous robustness properties claims that
the asymptotic stability of the attractor persists in a semiglobal practical sense in the
presence of mildly changing parameters.

FACT 2.8 (Mildly changing parameters [47, Cor. 7.27]) *Suppose that for* $\mathcal{H} = (\mathcal{C}, F, \mathcal{D}, G)$
having state (x, p), *satisfying the hybrid basic conditions and imposing* $\dot{p} = 0$ *and* $p^+ =$
p, *the compact set* $\mathcal{A}$ *is globally asymptotically stable. Then the hybrid system with data*
$(\mathcal{C}, F_\rho, \mathcal{D}, G_\rho)$ *that imposes* $\dot{p} \in \rho\mathbb{B}$ *and* $p^+ \in p + \rho\mathbb{B}$ *while leaving* $\dot{x}$ *and* x^+ *unchanged*
has the compact set $\mathcal{A}$ *semiglobally practically asymptotically stable in* $\rho > 0$.

Indeed, if $\mathcal{A}$ is globally asymptotically stable for $\mathcal{H}$ on $\mathbb{R}^{n_x + n_p}$, then $\mathcal{A}$ is $\mathcal{KL}$
asymptotically stable on $\mathbb{R}^{n_x + n_p}$ by Fact 2.4, and hence semiglobally practically
robustly $\mathcal{KL}$ asymptotically stable on $\mathbb{R}^{n_x + n_p}$ by Fact 2.7.

The stability and attractivity results in the following chapters will be proven based on Lyapunov methods, so that the current section is a key one in this chapter and in this work.

Loosely speaking, a Lyapunov function for the attractor of a hybrid dynamical system is a function bounded from above and from below by two class-$\mathcal{K}_\infty$ functions of the distance to the attractor, has a negative definite derivative along all the possible evolutions of the differential inclusion (or more, if uniformity is required) and has a negative definite increment across all the possible evolutions of the difference inclusion (or more, if uniformity is required). The advantage of using Lyapunov functions is that the decrease conditions can be checked without explicit knowledge of the solutions to the hybrid dynamical system. The characterization of a strict Lyapunov function is the subject of Section 2.5.1.

Section 2.5.2 introduces briefly converse Lyapunov theorems in order to provide a standard motivation for the search of a Lyapunov function to certify stability and attractivity properties in the case of hybrid dynamical systems.

However, although these converse results imply the existence of a (smooth) strict Lyapunov function in the case of an asymptotically stable attractor, it is oftentimes easier to tailor Lyapunov functions that are nonstrict, which is a well-known fact pointed out, for example, in [77, Preface]. This is indeed what we witness in the problems of the next chapters, where we explicitly construct nonstrict Lyapunov functions, that are generally called weak Lyapunov functions (see, for instance, [58, 82, 83, 115]). With weak Lyapunov functions it is nontrivial to characterize the decay rate of solutions. When one is interested in establishing such a decay rate, resorting to Lyapunov functions tailored for exponential stability might be a better option. However, since the attractors in the next chapters enjoy asymptotic stability and exponential stability does *not* hold for some of them (like in Chapter 6, see page 93), weak Lyapunov functions are sufficient for our scope.

Weakness in Lyapunov functions has then to be balanced by other structural properties, that allow for certifying asymptotic stability nonetheless. Within this typology, the weakness can be balanced by observability and average dwell time as illustrated in Section 2.5.3 (these results will be used in Chapter 3), or by persistent jumping as illustrated in Section 2.5.4 (these results will be used in Chapters 3 and 4). As another source of weakness we consider a not continuously differentiable Lyapunov function for stability in Section 2.5.5, so to explore tools from nonsmooth analysis like the generalized gradient in the sense of Clarke (these results will be used in Chapter 6). Finally, in the context of invariance principles, where Lyapunov functions are used to establish attractivity, we present in Section 2.5.6 a relaxed version of these attractivity Lyapunov functions: the meagre output functions, which are not necessarily continuous (these results will also be used in Chapter 6).

2.5.1 *Strict Lyapunov functions*

In the previous exposition we limited ourselves to the case of hybrid basic conditions and compact attractors, and in the next chapters of this work we operate as well in this setting. However, in this subsection we will first state Lyapunov conditions for the more general case when the attractor may not be compact and the hybrid basic conditions may not hold, so that we can show the simplification brought about in the requirements for a Lyapunov function brought about by compactness and regularity.

Thanks to the following Definition 2.21, we can state the first Lyapunov result in Fact 2.9 for the more general case.

DEFINITION 2.21 (Positive definite function [47, Def. 3.17]) *A function* $\rho\colon \mathbb{R}_{\geqslant 0} \to \mathbb{R}_{\geqslant 0}$ *is positive definite (also written* $\rho \in \mathcal{PD}$*) if* $\rho(s) > 0$ *for all* $s > 0$ *and* $\rho(0) = 0$.

FACT 2.9 (Lyapunov conditions for a closed attractor [47, Thm. 3.18, Def. 3.16]) *Let* $\mathcal{H} = (\mathcal{C}, F, \mathcal{D}, G)$ *be a hybrid system,* $\mathcal{A} \subset \mathbb{R}^n$ *be closed and* V *be a function* $V\colon \mathrm{dom}\, V \to \mathbb{R}$.

If $\overline{\mathcal{C}} \cup \mathcal{D} \cup G(\mathcal{D}) \subset \mathrm{dom}V$ and V is continuously differentiable on an open set containing $\overline{\mathcal{C}}$, and there exists α_1, $\alpha_2 \in \mathcal{K}_\infty$ and a continuous $\rho \in \mathcal{PD}$ such that

$$\alpha_1(|x|_{\mathcal{A}}) \leqslant V(x) \leqslant \alpha_2(|x|_{\mathcal{A}}) \qquad\qquad \forall x \in \mathcal{C} \cup \mathcal{D} \cup G(\mathcal{D}) \qquad (2.23a)$$

$$\langle \nabla V(x), f \rangle \leqslant -\rho(|x|_{\mathcal{A}}) \qquad\qquad \forall x \in \mathcal{C}, \ f \in F(x) \qquad (2.23b)$$

$$V(g) - V(x) \leqslant -\rho(|x|_{\mathcal{A}}) \qquad\qquad \forall x \in \mathcal{D}, \ g \in G(x) \qquad (2.23c)$$

then $\mathcal{A}$ is uniformly globally asymptotically stable for $\mathcal{H}$.

First, when a closed attractor $\mathcal{A}$ is also compact, (2.23a) simplifies as in Lemma 2.1. The proof of this result follows similar steps to the proof of [59, Lem. 4.3], to which this result also boils down when $\mathcal{A} = \{0\}$.

LEMMA 2.1 (Replacement of $\mathcal{K}_\infty$ bounds [59, Lem. 4.3]) *Let $\mathcal{H} = (\mathcal{C}, F, \mathcal{D}, G)$ be a hybrid system, $\mathcal{A} \subset \mathbb{R}^n$ be compact, V be a continuous function $V \colon \mathrm{dom}V \to \mathbb{R}$ such that $\overline{\mathcal{C}} \cup \mathcal{D} \cup G(\mathcal{D}) \subset \mathrm{dom}V$ and $\mathcal{A} \subset \mathrm{dom}V$. If*

$$V(x) = 0 \Leftrightarrow x \in \mathcal{A} \qquad (2.24a)$$

$$V(x) \geqslant 0 \quad \forall x \in \mathcal{C} \cup \mathcal{D} \cup G(\mathcal{D}) \qquad (2.24b)$$

$$\lim_{\substack{|x| \to +\infty \\ x \in \mathcal{C} \cup \mathcal{D} \cup G(\mathcal{D})}} V(x) = +\infty \qquad (2.24c)$$

then there exists α_1, $\alpha_2 \in \mathcal{K}_\infty$ such that (2.23a) holds.

Under the same assumptions, (2.23a) implies trivially (2.24). Therefore, in the case of compact attractors, the use of $\mathcal{K}_\infty$ functions is beneficial to streamlining the proofs, but the previous Lemma provides easier-to-check Lyapunov conditions.

Whenever the attractor is compact and some regularity assumptions are satisfied, the previous Fact 2.9 (and in particular its conditions) can be made easier to check.

FACT 2.10 (Lyapunov conditions for uniform global asymptotic stability [48, Thm. 20]) *Let $\mathcal{H} = (\mathcal{C}, F, \mathcal{D}, G)$ be a hybrid system satisfying the hybrid basic conditions, $\mathcal{A} \subset \mathbb{R}^n$ be compact satisfying*

$$G(\mathcal{A} \cap \mathcal{D}) \subset \mathcal{A}$$

and V be a function $V \colon \mathrm{dom}V \to \mathbb{R}$. If $\mathcal{C} \cup \mathcal{D} \cup G(\mathcal{D}) \subset \mathrm{dom}V$ and V is continuously differentiable on an open set containing $\mathcal{C}$, and there exists α_1, $\alpha_2 \in \mathcal{K}_\infty$

$$\alpha_1(|x|_{\mathcal{A}}) \leqslant V(x) \leqslant \alpha_2(|x|_{\mathcal{A}}) \qquad\qquad \forall x \in \mathcal{C} \cup \mathcal{D} \cup G(\mathcal{D}) \qquad (2.25a)$$

$$\langle \nabla V(x), f \rangle < 0 \qquad\qquad \forall x \in \mathcal{C} \backslash \mathcal{A}, \ f \in F(x) \qquad (2.25b)$$

$$V(g) - V(x) < 0 \qquad\qquad \forall x \in \mathcal{D} \backslash \mathcal{A}, \ g \in G(x) \qquad (2.25c)$$

then $\mathcal{A}$ is uniformly globally asymptotically stable for $\mathcal{H}$.

A local version of the last result can be obtained by invoking the notions of basin of attraction and proper indicator in Definition 2.11 and 2.15, respectively.

FACT 2.11 (Lyapunov conditions for uniform local asymptotic stability) *Let $\mathcal{H} = (\mathcal{C}, F, \mathcal{D}, G)$ be a hybrid system satisfying the hybrid basic conditions, $\mathcal{A} \subset \mathbb{R}^n$ be compact satisfying*

$$G(\mathcal{A} \cap \mathcal{D}) \subset \mathcal{A}$$

and with basin of attraction $\mathcal{B}_{\mathcal{A}}$ and V be a function $V \colon \mathrm{dom}V \to \mathbb{R}$. If $\mathcal{C} \cup \mathcal{D} \cup G(\mathcal{D}) \subset \mathrm{dom}V$ and V is continuously differentiable on an open set containing $\mathcal{C} \cap \mathcal{B}_{\mathcal{A}}$, and for all proper indicators $\omega \colon \mathcal{B}_{\mathcal{A}} \to \mathbb{R}_{\geqslant 0}$ of $\mathcal{A}$ there exists α_1, $\alpha_2 \in \mathcal{K}_\infty$

$$\alpha_1(\omega(|x|_{\mathcal{A}})) \leqslant V(x) \leqslant \alpha_2(\omega(|x|_{\mathcal{A}})) \quad \forall x \in (\mathcal{C} \cup \mathcal{D} \cup G(\mathcal{D})) \cap \mathcal{B}_{\mathcal{A}} \qquad (2.26a)$$

$$\langle \nabla V(x), f \rangle < 0 \quad \forall x \in (\mathcal{C} \backslash \mathcal{A}) \cap \mathcal{B}_{\mathcal{A}}, \ f \in F(x) \qquad (2.26b)$$

$$V(g) - V(x) < 0 \quad \forall x \in (\mathcal{D} \backslash \mathcal{A}) \cap \mathcal{B}_{\mathcal{A}}, \ g \in G(x) \qquad (2.26c)$$

then $\mathcal{A}$ is uniformly locally asymptotically stable for $\mathcal{H}$.

2.5.2 A motivation for Lyapunov functions: converse Lyapunov theorems

The basic idea behind Lyapunov methods is that the existence for an attractor of a suitable Lyapunov function satisfying some decrease conditions implies that the attractor possesses a notion of asymptotic stability: all the current Section 2.5 provides Lyapunov functions with those decrease conditions. Actually, also the converse implication holds. Consider indeed the following result as an exemplification of converse Lyapunov theorems. (Note that the following smooth Lyapunov function[7] V is clearly strict.)

FACT 2.12 (A converse theorem [47, Cor. 7.32, Def. 7.29]) *Let $\mathcal{H}$ be a hybrid system satisfying the hybrid basic conditions and $\mathcal{A} \subset \mathbb{R}^n$ be a compact set that is globally asymptotically stable for $\mathcal{H}$.*
Then, there exists a smooth Lyapunov function V for $\mathcal{A}$, that is,

$V : \mathbb{R}^n \to \mathbb{R}_{\geqslant 0}$ is continuously differentiable and there exists $\alpha_1, \alpha_2 \in \mathcal{K}_\infty$ such that:

$$\alpha_1(|x|_{\mathcal{A}}) \leqslant V(x) \leqslant \alpha_2(|x|_{\mathcal{A}}) \qquad \forall x \in \mathcal{C} \cup \mathcal{D} \cup G(\mathcal{D}) \qquad (2.27a)$$

$$\langle \nabla V(x), f \rangle \leqslant -V(x) \qquad \forall x \in \mathcal{C}, \, f \in F(x) \qquad (2.27b)$$

$$V(g) \leqslant \frac{V(x)}{e} \qquad \forall x \in \mathcal{D}, \, g \in G(x). \qquad (2.27c)$$

This result goes under the name of converse Lyapunov theorem because the fact that an attractor possesses a notion of asymptotic stability implies the existence of a suitable (strict) Lyapunov function satisfying some decrease conditions. Converse Lyapunov theorems are now well-known for continuous-time dynamical systems (see [59, §4.7]): a historical perspective of the succession of results in the continuous-time setting is provided for instance in [48, p. 60-61]. Fact 2.12 (and more general ones as [47, Thm. 7.31] and in [23]) establishes that such converse results also hold for hybrid dynamical systems when the attractor is compact and the hybrid basic conditions hold.

In light of the preceding discussion, the main message of the current section with respect to this work is that, broadly speaking, it is not possible to have asymptotically stable attractors for hybrid systems and not to have a corresponding Lyapunov function certifying that notion of asymptotic stability. Therefore, it is worth searching for a Lyapunov function when the attractor is believed to possess a notion of asymptotic stability. Unfortunately, the Lyapunov functions arising from converse Lyapunov theorems are based on solutions, which are hardly computable, and do not provide a constructive way to build the Lyapunov function.

2.5.3 Weakness is balanced by flow observability and average dwell time

The following result, which will be used in Chapter 3, considers a sufficient exponential stability condition for a hybrid system such that part of its state has a linear flow. The Lyapunov function is weak because the decrease across jump is not strict (compare (2.28b) with (2.25c)), and the function $-y^\top y$ is not *negative* definite in $\mathcal{C}_\mathcal{E} \backslash \{0\}$ (compare (2.28a) with (2.25b)). However, a strict decrease can be recovered by observability and average dwell time. Note that the derivation of this result (see [118, §V.C]) hinges partially on the well known squashing lemma for linear systems (see [86, p. 264] and [91]).

---

7 Since we are speaking of *converse* Lyapunov theorems, one may wonder if (2.27) are actually needed for a compact set $\mathcal{A}$ to be globally asymptotically stable, and why we provided a sufficient condition with the seemingly weaker conditions (2.23). Indeed, it can be proven that given the conditions (2.23) for V, a Lyapunov function $W(x) := \bar{\alpha}(V(x))$ can be obtained through $\bar{\alpha} \in \mathcal{K}_\infty$ such that W verifies (2.27). The details can be found in [57, §2.1 & Lemma 25]. Note however that an exponential decrease in the Lyapunov function is traded off with coarser upper and lower bounds for W.

FACT 2.13 (Sufficient conditions for exponential stability [41, Lem. 1], [118, Thm. 2]) *Consider a hybrid dynamical system $\mathcal{H}$ with partitioned state (x, ξ), with flow and jump sets $\mathcal{C}_\xi$ and $\mathcal{D}_\xi$, and such that all its solutions satisfy an average dwell-time condition (see [47, §2.4]).*

Assume a linear dynamics for the flow restricted to x

$$\dot{x} = Ax, \quad (x, \xi) \in \mathcal{C}_\xi.$$

and the existence of C in

$$y = Cx$$

such that (C, A) is an observable pair.

If there exists $V(x) = x^\top Px$ with P positive definite such that

$$\langle \nabla V(x), Ax \rangle \leqslant -y^\top y \quad \forall (x, \xi) \in \mathcal{C}_\xi \tag{2.28a}$$

$$V(x^+) - V(x) \leqslant 0 \quad \forall (x, \xi) \in \mathcal{D}_\xi, \tag{2.28b}$$

then there exists $\gamma \geqslant 1$ and $\lambda > 0$ such that all solutions to $\mathcal{H}$ satisfy

$$|x(t, j)| \leqslant \gamma e^{-\lambda(t+j)} |x(0, 0)|.$$

APPLICATION 2.2 (Observability and average dwell time) *Consider the hybrid system* (3.3) *and* (3.10) *in Chapter* 3, *which we report here for the reader's convenience.*

$$\left.\begin{aligned} \dot{e} &= A_e e \\ \dot{x}_r &= A_r x_r \\ \dot{\bar{b}} &= 0 \end{aligned}\right\} (e, x_r, \bar{b}) \in \mathcal{C}_{(x_r, \bar{b})}$$

$$\left.\begin{aligned} e^+ &= J_e e \\ x_r^+ &= J_r x_r \\ \bar{b}^+ &= \bar{b} \end{aligned}\right\} (e, x_r, \bar{b}) \in \mathcal{D}_{(x_r, \bar{b})}$$

Partition the state in e and $(x_r, \bar{b})$. Take $P = \begin{bmatrix} 1 & 0 & 0 & 0 \\ 0 & 1 & 0 & 0 \\ 0 & 0 & \omega^3 \ell & 0 \\ 0 & 0 & 0 & \omega \ell \end{bmatrix}$ and $C = [0 \ 0 \ 0 \ 2\omega\sqrt{\ell}]$. These matrices allow to prove (2.28a)-(2.28b) *(*(3.12a)-(3.12b)*, respectively, in Chapter* 3*) relative to e, and conclude that the rate of convergence for the estimation error e is exponential.*

2.5.4 *Weakness is balanced by persistent jumping*

In this section we present two results about Lyapunov functions that are weak because their decrease along flow is not strict (see Equations (2.29b) and (2.42b)). This type of weakness can be balanced out if the decrease across jumps is strict, and some kind of persistent jumping property holds. The first result in Fact 2.14 involves (standard) persistent jumping, and the second one in Fact 2.15 involves semiglobal practical persistent jumping. These two results will be used in Chapter 3 and in Chapter 4, respectively.

The following fact specializes [47, Prop. 3.24] in the case of $\mathcal{A}$ compact and hybrid basic conditions, so that the decrease of V across jumps just needs to be negative definite outside $\mathcal{A}$, in the same way Fact 2.9 could be simplified into Fact 2.10.

FACT 2.14 (Lyapunov conditions with persistent jumping [47, Prop. 3.24]) *Let $\mathcal{H} = (\mathcal{C}, F, \mathcal{D}, G)$ be a hybrid system satisfying the hybrid basic conditions, $\mathcal{A} \subset \mathbb{R}^n$ be compact satisfying*

$$G(\mathcal{A} \cap \mathcal{D}) \subset \mathcal{A}$$

and V *be a function* $V: \operatorname{dom} V \to \mathbb{R}$ *with* $\mathcal{C} \cup \mathcal{D} \cup G(\mathcal{D}) \subset \operatorname{dom} V$ *and continuously differentiable on an open set containing* $\mathcal{C}$. *Suppose that there exists* $\alpha_1, \alpha_2 \in \mathcal{K}_\infty$ *such that*

$$\alpha_1(|x|_{\mathcal{A}}) \leqslant V(x) \leqslant \alpha_2(|x|_{\mathcal{A}}), \quad \forall x \in \mathcal{C} \cup \mathcal{D} \cup G(\mathcal{D}) \tag{2.29a}$$

$$\langle \nabla V(x), f \rangle \leqslant 0, \quad \forall x \in \mathcal{C}, \forall f \in F(x) \tag{2.29b}$$

$$V(g) - V(x) < 0, \quad \forall x \in \mathcal{D} \backslash \mathcal{A}, \forall g \in G(x). \tag{2.29c}$$

Assume also that the following persistent jump property *holds: For each* $r > 0$, *there exist* $\gamma_r \in \mathcal{K}_\infty$, $N_r \geqslant 0$ *such that for every solution* ϕ *to* $\mathcal{H}$

$$\left. \begin{array}{r} |\phi(0,0)|_{\mathcal{A}} \in (0, r] \\ (t, j) \in \operatorname{dom} \phi \\ t + j \geqslant T \end{array} \right\} \Rightarrow j \geqslant \gamma_r(T) - N_r. \tag{2.30}$$

Then $\mathcal{A}$ *is uniformly globally asymptotically stable.*

APPLICATION 2.3 (Periodic jumps) *For the hybrid system in Chapter 3, Section 3.4, we extract here the only relevant dynamics to illustrate how the property of persistent jumping can be exploited. To this end, instead of considering the whole hybrid system of Section 3.4 given by Equations (3.3), (3.15) and (3.18), we restrict the dynamics to the case when* $d = y_r - \bar{y}_r$ *(compare the proof of Theorem 3.2, and the set* $\mathcal{A}_{\bar{y}}$ *within). This allows to reduce the state to* $x = (\theta, \hat{\theta}, \tau)$.

The flow is governed by

$$\begin{bmatrix} \dot{\theta} \\ \dot{\hat{\theta}} \\ \dot{\tau} \end{bmatrix} = \begin{bmatrix} \omega \\ \omega \\ 1 \end{bmatrix} =: f(x), \ x \in \left[-\frac{\pi}{6}, \frac{\pi}{6} \right] \times \left[-\frac{\pi}{3}, \frac{\pi}{6} \right] \times \left[0, \frac{\pi}{3\omega} \right] =: \mathcal{C}, \tag{2.31}$$

where ω *is a fixed parameter representing a frequency.*

On the other hand, we have three possible jump dynamics

$$\begin{bmatrix} \theta^+ \\ \hat{\theta}^+ \\ \tau^+ \end{bmatrix} = \begin{bmatrix} \theta - \frac{\pi}{3} \\ \hat{\theta} \\ \tau \end{bmatrix} =: g_1(x), \ \theta = \frac{\pi}{6} \tag{2.32a}$$

$$\begin{bmatrix} \theta^+ \\ \hat{\theta}^+ \\ \tau^+ \end{bmatrix} = \begin{bmatrix} \theta \\ \hat{\theta} - \frac{\pi}{3} \\ \tau \end{bmatrix} =: g_2(x), \ \hat{\theta} \in \left[\frac{\pi}{6}, \frac{\pi}{3} \right] \tag{2.32b}$$

$$\begin{bmatrix} \theta^+ \\ \hat{\theta}^+ \\ \tau^+ \end{bmatrix} = \begin{bmatrix} \theta \\ \hat{\theta} - \operatorname{sat}_{\frac{\pi}{6}}(-\hat{k}_\theta \rho(\tilde{\theta})) \\ 0 \end{bmatrix} =: g_3(x), \ \tau = \frac{\pi}{3\omega}, \tag{2.32c}$$

where $\operatorname{sat}_{\frac{\pi}{6}}$ *is the symmetric scalar saturation function bounded in* $\left[-\frac{\pi}{6}, \frac{\pi}{6} \right]$, $\hat{k}_\theta$ *is a sufficiently small positive gain,* $\tilde{\theta} \mapsto \rho(\tilde{\theta})\tilde{\theta}$ *is a positive definite function in* $(-\pi/6, \pi/6)$ *(see Lemma 3.3), where*

$$\tilde{\theta} := \theta - \hat{\theta} + i^* \frac{\pi}{3}, \tag{2.33a}$$

$$i^* := \underset{i \in \mathbb{Z}}{\arg\min} \left(\theta - \hat{\theta} + i\frac{\pi}{3} \right)^2. \tag{2.33b}$$

By assembling Equations (2.32) to fit consistently into Equation (2.1b), the jumps are governed by

$$x^+ \in G(x) := \bigcup_{i : \, x \in \mathcal{D}_i} \{g_i(x)\}, \quad x \in \mathcal{D} := \bigcup_{i \in \{1,2,3\}} \mathcal{D}_i. \tag{2.34}$$

For (2.31) and (2.34), we consider the Lyapunov function

$$V_\theta(\theta, \hat{\theta}) = \tilde{\theta}^2 \tag{2.35}$$

with $\tilde{\theta}$ *defined in (2.33a). Due to (2.31),* $\dot{\tilde{\theta}} = \dot{\theta} - \dot{\hat{\theta}} = 0$,

$$\dot{V}_\theta(\theta, \hat{\theta}) = 0 \quad \forall x \in \mathcal{C} \tag{2.36}$$

and, due to the minimizer i^* in (2.33b),

$$V_\theta(\theta^+, \hat\theta^+) - V(\theta, \hat\theta) = 0 \quad \forall x \in \mathcal{D}_1 \cup \mathcal{D}_2. \tag{2.37}$$

On the other hand, it can be proven (see the proof of Theorem 3.2 *and Equation* (3.21)*) that*

$$V_\theta(\theta^+, \hat\theta^+) < V(\theta, \hat\theta) \quad \forall x \in \mathcal{D}_3 \setminus \{x \colon \tilde\theta = 0\}. \tag{2.38}$$

Since the variable τ represents a timer that is periodically reset at $T_\tau := \frac{\pi}{3\omega}$ (see Example 2.3*), each solution ϕ to* (2.31) *and* (2.34) *has a time domain* $\mathrm{dom}\,\phi$ *such that*

$$(t, j) \in \mathrm{dom}\,\phi \Rightarrow \frac{t}{T_\tau} \leqslant j + 1$$

(note that due to the jumps from $\mathcal{D}_1$ and $\mathcal{D}_2$, $\frac{t}{T_\tau} = j + 1$ does not necessarily hold). This structural property induced by the periodic jumps of the timer can be used in (2.30) *to show that*

$$\left.\begin{array}{r}(t, j) \in \mathrm{dom}\,\phi \\ t + j \geqslant T\end{array}\right\} \Rightarrow j \geqslant T - t \geqslant T - (j + 1)T_\tau,$$

that is,

$$j \geqslant \frac{T}{1 + T_\tau} - \frac{T_\tau}{1 + T_\tau} =: \gamma(T) - N,$$

that hold indeed for each size r of the initial condition of the solution ϕ as required by (2.30). *Thanks to Fact* 2.14, *this proves asymptotic stability of the attractor $\tilde\theta = 0$.*

The persistent jumping property required by Fact 2.14 can be further relaxed into semiglobal practical persistent jumping.

FACT 2.15 (Lyapunov conditions with semiglobal practical persistent jumping [97, Thm. 2, Property 1]) *Consider the hybrid system*

$$\dot x \in F(x), \quad x \in \mathcal{C} \tag{2.39a}$$
$$x^+ \in G(x), \quad x \in D \tag{2.39b}$$

satisfying the hybrid basic conditions, and a compact set $\mathcal{A} \subset \mathbb{R}^n$ satisfying

$$G(\mathcal{A} \cap \mathcal{D}) \subset \mathcal{A}.$$

Build for each pair δ, Δ such that $0 < \delta < \Delta$, the set

$$\mathcal{S}_{\delta,\Delta} := (\mathcal{A} + \Delta\mathbb{B}) \setminus (\mathcal{A} + \delta\mathbb{B}^\circ) \tag{2.40}$$

($\mathbb{B}^\circ$ is the open unit ball) and the hybrid system

$$\dot x \in F(x), \quad x \in \mathcal{C} \cap \mathcal{S}_{\delta,\Delta} \tag{2.41a}$$
$$x^+ \in G(x), \quad x \in \mathcal{D} \cap \mathcal{S}_{\delta,\Delta}. \tag{2.41b}$$

Assume that there exists a function V continuously differentiable on a neighborhood of $\mathcal{C}$ and two class $\mathcal{K}_\infty$ functions α_1 and α_2 such that

$$\alpha_1(|x|_{\mathcal{A}}) \leqslant V(x) \leqslant \alpha_2(|x|_{\mathcal{A}}), \quad \forall x \in \mathcal{C} \cup \mathcal{D} \cup G(\mathcal{D}) \tag{2.42a}$$
$$\langle \nabla V(x), f \rangle \leqslant 0, \quad \forall x \in \mathcal{C}, \forall f \in F(x) \tag{2.42b}$$
$$V(g) - V(x) < 0, \quad \forall x \in \mathcal{D} \setminus \mathcal{A}, \forall g \in G(x). \tag{2.42c}$$

Assume also that the following semiglobal practical persistent jump property *holds: For each pair δ, Δ of positive scalars, there exists a class $\mathcal{K}_\infty$ function γ and a scalar $N \geqslant 0$ such that each solution ϕ to* (2.41) *satisfies for all $(t, j) \in \mathrm{dom}\,\phi$*

$$j \geqslant \gamma(t) - N. \tag{2.43}$$

Then the set $\mathcal{A}$ is uniformly globally asymptotically stable for (2.39).

REMARK 2.1 *A semiglobal persistent jumping property holds if δ in Fact 2.15 is taken equal to 0. Semiglobal persistent jumping implies semiglobal practical persistent jumping. Indeed, $\mathcal{S}_{\delta,\Delta} \subset \mathcal{S}_{0,\Delta}$ and then the solutions of the hybrid system with flow and jump sets restricted by $\mathcal{S}_{\delta,\Delta}$ (semiglobal practical) are a subset of the solutions of the hybrid system with flow and jump set restricted by $\mathcal{S}_{0,\Delta}$ (semiglobal). So if the property of semiglobal persistent jumping holds, then the property of semiglobal practical persistent jumping also holds.* ⌟

We apply now Fact 2.15 together with the previous Remark to the system of Chapter 4.

APPLICATION 2.4 (Semiglobal persistent jumping) *Consider the Lyapunov function used in Chapter 4 to prove the asymptotic stability of the periodic orbit $\mathcal{A}$ described in Example 2.4 for the system described in Example 2.1. The attractor $\mathcal{A}$ has basin of attraction $\mathcal{B}_{\mathcal{A}} := \mathbb{R}^2\setminus\{0\}$. Using the forward and backward energies introduced intuitively in Example 2.4 (for details refer to Equations (4.5) in Section 4.3), build the Lyapunov function ($\hat{\theta} > 0$ is the variation of x_1 across jumps)*

$$V(x) = \frac{(U_b(x) + T_b(x) - T_f(x) - \frac{1}{2}k\hat{\theta}^2)^2}{U_b(x)},\qquad(2.44)$$

whose shape and level sets are depicted in Figure 2.10. Under the assumptions of Chapter 4
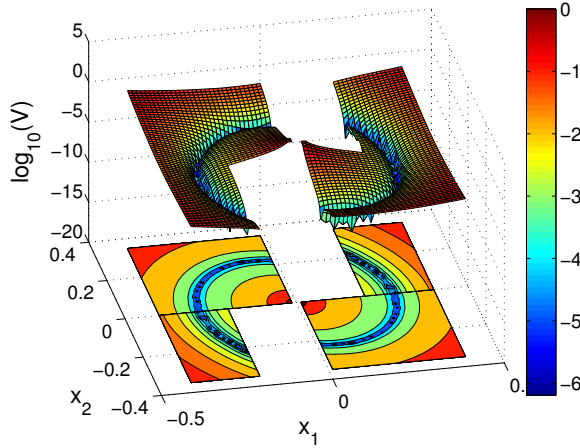
Figure 2.10: The Lyapunov function V of (2.44) in logarithmic scale.

(Assumption 4.1), the Lyapunov function in (2.44) has the following properties.

- *For any indicator function ω of $\mathcal{A}$ on $\mathcal{B}_{\mathcal{A}}$ there exists class $\mathcal{K}_\infty$ functions α_1 and α_2 such that*

$$\alpha_1(\omega(x)) \leqslant V(x) \leqslant \alpha_2(\omega(x)).\qquad(2.45a)$$

- *V is built starting from solutions, and in particular its level sets are the orbits of solutions. Then V remains constant along flow, that is,*

$$\langle \nabla V(x), f(x)\rangle = 0, \forall x \in \mathcal{C}.\qquad(2.45b)$$

- *V is strictly decreasing across jumps in the basin of attraction[8] $\mathcal{B}_{\mathcal{A}}$ and outside the attractor $\mathcal{A}$, that is,*

$$V(G(x)) - V(x) < 0,\ \forall x \in \mathcal{B}_{\mathcal{A}} \cap \mathcal{D}\setminus\mathcal{A}.\qquad(2.45c)$$

---

8 Note that in the basin of attraction $\mathcal{B}_{\mathcal{A}} = \mathbb{R}^2\setminus\{0\}$, the jump map given by (2.3b) becomes single-valued and this allows to write directly (2.45c).

For more details, see Lemma 4.2.

Thanks to Remark 2.1, it is sufficient to show that semiglobal persistent jumping holds to apply Fact 2.15 since Equations (2.45), which are satisfied by V, are just the local version of the conditions in (2.42) and semiglobal persistent jumping holds from Lemma 4.3.

2.5.5 *Nondifferentiable Lyapunov-like functions for stability*

The main result we present in this section in view of Chapter 6 is Fact 2.17. Fact 2.17 holds for a Lyapunov-like function that is not C^1 in order to establish uniform global stability in Definition 2.14, and is a generalization of Fact 2.16 for a C^1 Lyapunov-like function. For this reason, the Lyapunov function required for Fact 2.17 is *weak* with respect to the Lyapunov function required for uniform global stability based on Fact 2.16.

To state these two facts, we introduce first some preliminary concepts, among which the ones of Lyapunov-like functions and bounded growth.

DEFINITION 2.22 (Lyapunov-like function) *Given a hybrid system $\mathcal{H}$ and a function $V : \mathbb{R}^n \to \mathbb{R}$, V is a Lyapunov-like function if for every solution $\phi \in \mathcal{S}_{\mathcal{H}}$ it is nonincreasing along ϕ, that is,*

$$V(\phi(\bar{t}, \bar{j})) \leqslant V(\phi(\underline{t}, \underline{j})) \tag{2.46}$$

for all $(\underline{t}, \underline{j}), (\bar{t}, \bar{j}) \in \operatorname{dom}\phi$ such that[9] $(\underline{t}, \underline{j}) \preceq (\bar{t}, \bar{j})$.

A slightly more general concept is bounding the growth of V along solutions by some functions. This concept is formalized in Definition 2.23, for which we need to define for a hybrid arc ϕ with domain $\operatorname{dom}\phi$ the next two functions (as in [47, p. 170]):

$$t(j) := \min_{(t,j) \in \operatorname{dom}\phi} t \tag{2.47a}$$

$$j(t) := \min_{(t,j) \in \operatorname{dom}\phi} j. \tag{2.47b}$$

DEFINITION 2.23 (Bounded growth of V [47, p. 170]) *Given a hybrid system $\mathcal{H}$ and a function $V : \mathbb{R}^n \to \mathbb{R}$, any functions $u_c, u_d : \mathbb{R}^n \to [-\infty, \infty]$, the growth of V along solutions to $\mathcal{H}$ is bounded by u_c, u_d on $\mathbb{R}^n$ if for any $\phi \in \mathcal{S}_{\mathcal{H}}$*

$$V(\phi(\bar{t}, \bar{j})) - V(\phi(\underline{t}, \underline{j})) \leqslant \int_{\underline{t}}^{\bar{t}} u_c\left(\phi(t, j(t))\right) dt + \sum_{j=\underline{j}+1}^{\bar{j}} u_d\left(\phi(t(j), j-1)\right) \tag{2.48}$$

for all $(\underline{t}, \underline{j}), (\bar{t}, \bar{j}) \in \operatorname{dom}\phi$ such that $(\underline{t}, \underline{j}) \preceq (\bar{t}, \bar{j})$.

The link between bounded growth in Definition 2.23 and Lyapunov-like functions in Definition 2.22 is that if the growth of V is bounded by u_c and u_d on $\mathbb{R}^n$, and u_c and u_d are nonpositive on $\mathbb{R}^n$, then V is a Lyapunov-like function.

For a Lyapunov-like function V, let us introduce two functions u_c and u_d that bound its growth along solutions and are determined *directly* by the data $(F, \mathcal{C}, G, \mathcal{D})$ of the hybrid system (2.1). For a *continuously differentiable* V, define the function $u_{\mathcal{C}} : \mathbb{R}^n \to [-\infty, \infty)$ as

$$u_{\mathcal{C}}(x) = \begin{cases} \max_{f \in F(x)} \langle \nabla V(x), f \rangle & \text{if } x \in \mathcal{C} \\ -\infty & \text{otherwise.} \end{cases} \tag{2.49a}$$

For *any* V, define the function $u_{\mathcal{D}} : \mathbb{R}^n \to [-\infty, \infty)$ as

$$u_{\mathcal{D}}(x) = \begin{cases} \max_{g \in G(x)} \left[V(g) - V(x) \right] & \text{if } x \in \mathcal{D} \\ -\infty & \text{otherwise.} \end{cases} \tag{2.49b}$$

---

9 Points from the same hybrid time domain $\operatorname{dom}\phi$ can be naturally ordered by the order relation $\preceq$, see [47, p. 27].

Indeed, equations (2.49) bound the growth of V along solutions in the sense of Definition 2.23 because:

(i) As for the *flow*, we have that for any continuously differentiable V, any $\phi \in \mathcal{S}_{\mathcal{H}}$, any $j \in \mathbb{Z}_{\geqslant 0}$ such that $I^j := \{t \colon (t,j) \in \operatorname{dom}\phi\}$ has a nonempty interior, almost any $t \in I^j$,

$$\frac{\mathrm{d}}{\mathrm{d}t}V(\phi(t,j)) = \langle \nabla V(\phi(t,j)), \frac{\mathrm{d}}{\mathrm{d}t}\phi(t,j)\rangle \leqslant u_{\mathcal{C}}(\phi(t,j)) \tag{2.50a}$$

since $\frac{\mathrm{d}}{\mathrm{d}t}\phi(t,j) \in F(\phi(t,j))$ for almost all $t \in I^j$ by Definition 2.4 of solution, updated on page 11 under the hybrid basic conditions.

(ii) As for the *jumps*, we have that for any V, any $\phi \in \mathcal{S}_{\mathcal{H}}$ and any (t,j), $(t,j+1)$ both belonging to $\operatorname{dom}\phi$,

$$V(\phi(t,j+1)) - V(\phi(t,j)) \leqslant u_{\mathcal{D}}(\phi(t,j)) \tag{2.50b}$$

since $\phi(t,j+1) \in G(\phi(t,j))$ by Definition 2.4, item 3.

Then, for a V at least continuously differentiable on a neighborhood of $\mathcal{C}$, we can write

$$V(\phi(\bar{t},\bar{j})) - V(\phi(\underline{t},\underline{j}))$$

$$= \int_{\underline{t}}^{\bar{t}} \frac{\mathrm{d}}{\mathrm{d}t}V(\phi(t,j(t)))\,\mathrm{d}t + \sum_{j=\underline{j}+1}^{\bar{j}} V(\phi(t(j),j)) - V(\phi(t(j),j-1))$$

$$\leqslant \int_{\underline{t}}^{\bar{t}} u_{\mathcal{C}}(\phi(t,j(t)))\,\mathrm{d}t + \sum_{j=\underline{j}+1}^{\bar{j}} u_{\mathcal{D}}(\phi(t(j),j-1)) \tag{2.51}$$

bounding each term of the second line by (2.50a)-(2.50b).

Then, a uniform global stability result (see Definition 2.14) follows straightforwardly from the bounded growth in (2.51) when $u_{\mathcal{C}}$ and $u_{\mathcal{D}}$ are nonpositive for all $z \in \mathbb{R}^n$ (which means they are nonpositive in $\mathcal{C}$ or $\mathcal{D}$, respectively because of their definition in (2.49)) and V is bounded from above and below by two class $\mathcal{K}_{\infty}$ functions. For its proof, refer to the end of this section.

FACT 2.16 *Let $\mathcal{H} = (\mathcal{C}, F, \mathcal{D}, G)$ be a hybrid system satisfying the hybrid basic conditions, $\mathcal{A} \subset \mathbb{R}^n$ be compact, α_1 and α_2 be class-$\mathcal{K}_{\infty}$ functions and $V \colon \mathbb{R}^n \to \mathbb{R}$ be continuous on $\mathbb{R}^n$ and continuously differentiable on a neighborhood of $\mathcal{C}$ such that:*

$$\alpha_1(|x|_{\mathcal{A}}) \leqslant V(x) \leqslant \alpha_2(|x|_{\mathcal{A}}) \quad \forall x \in \mathcal{C} \cup \mathcal{D} \cup G(\mathcal{D}) \tag{2.52a}$$

$$u_{\mathcal{C}}(x) \leqslant 0 \quad \forall x \in \mathcal{C} \tag{2.52b}$$

$$u_{\mathcal{D}}(x) \leqslant 0 \quad \forall x \in \mathcal{D}, \tag{2.52c}$$

where $u_{\mathcal{C}}$ and $u_{\mathcal{D}}$ are defined from $\mathcal{H}$ and V as in (2.49). Then $\mathcal{A}$ is uniformly globally stable.

We are able now to present a weaker version of the Lyapunov result in Fact 2.16 that builds on a Lipschitz continuous, but no longer continuously differentiable V.

For a function V Lipschitz continuous at x, we can use the generalized (in the sense of Clarke) gradient $\partial V(x)$ of V at x [28, p. 20, Eq. (22)] given by

$$\partial V(x) := \operatorname{co}\Big\{\lim_{i \to \infty} \nabla V(x_i) \colon x_i \to x, x_i \notin \Xi, \mu(\Xi) = 0\Big\}. \tag{2.53}$$

The meaning of (2.53) is as follows. Take *any* sequence x_i converging to x and avoiding the set Ξ, which is *any* set of (Lebesgue) measure zero, and such that along x_i, $\nabla V(x_i)$ must exist and converge. Taking out a set Ξ of measure zero agrees with Rademacher's Theorem stating that a Lipschitz continuous function on an open set in $\mathbb{R}^n$ is differentiable almost everywhere in the set. Finally, $\operatorname{co}S$ is the convex hull of the set S.

Using the generalized gradient in (2.53), we can introduce the following counterpart of $u_\mathcal{C}$ in (2.49a) as:

$$\hat{u}_\mathcal{C}(x) = \begin{cases} \max_{f \in F(x), v \in \partial V(x)} \langle v, f \rangle & \text{if } x \in \mathcal{C} \\ -\infty & \text{otherwise.} \end{cases} \tag{2.54}$$

FACT 2.17 *Let* $\mathcal{H} = (\mathcal{C}, F, \mathcal{D}, G)$ *be a hybrid system satisfying the hybrid basic conditions,* $\mathcal{A} \subset \mathbb{R}^n$ *be compact,* α_1 *and* α_2 *be class-$\mathcal{K}_\infty$ functions and* $V \colon \mathbb{R}^n \to \mathbb{R}$ *be Lipschitz continuous on* $\mathbb{R}^n$ *such that:*

$$\alpha_1(|x|_\mathcal{A}) \leqslant V(x) \leqslant \alpha_2(|x|_\mathcal{A}) \quad \forall x \in \mathcal{C} \cup \mathcal{D} \cup G(\mathcal{D}) \tag{2.55a}$$

$$\hat{u}_\mathcal{C}(x) \leqslant 0 \quad \forall x \in \mathcal{C} \tag{2.55b}$$

$$u_\mathcal{D}(x) \leqslant 0 \quad \forall x \in \mathcal{D}, \tag{2.55c}$$

where $u_\mathcal{C}$ *and* $u_\mathcal{D}$ *are defined from* $\mathcal{H}$ *and* V *as in* (2.54) *and* (2.49b), *respectively. Then* $\mathcal{A}$ *is uniformly globally stable.*

Also for the proof of the previous fact, refer to the end of this section.

APPLICATION 2.5 (Lipschitz Lyapunov function) *Consider the system of Chapter 6 and already described in Example 2.5 where the flow set was* $\mathbb{R}^3$*. Now for the state* $x = (\sigma, \phi, v)$ *(corresponding to a change of coordinates), consider a restriction of the original system, that is, the hybrid system* $\mathcal{H} = (\mathcal{C}, F, \emptyset, \emptyset)$ *with*

$$F := \begin{bmatrix} -k_i v \\ \sigma - k_p v \\ \phi - k_v v - f_c\,\text{SGN}(v) \end{bmatrix} \tag{2.56}$$

$$\mathcal{C} := \{x \colon (v \geqslant 0, \phi \leqslant f_c) \text{ or } (v \leqslant 0, \phi \geqslant -f_c)\} \cap \{x \colon |\sigma| \leqslant K|v|\},$$

where $K > 0$ *is an arbitrarily large constant.*

The attractor is defined in (2.14) *as* $\mathcal{A} = \{(\sigma, \phi, v) \colon |\phi| \leqslant f_c, \sigma = 0, v = 0\}$*.*

Consider then the Lyapunov-like function

$$\hat{V}(x) := \tfrac{1}{2}k_1\sigma^2 + \tfrac{1}{2}k_2\big(dz_{f_c}(\phi)\big)^2 + k_3|\sigma||v| + \tfrac{1}{2}k_4 v^2$$
$$= \tfrac{1}{2}\begin{bmatrix} |\sigma| \\ |dz_{f_c}(\phi)| \\ |v| \end{bmatrix}^\mathsf{T} \begin{bmatrix} k_1 & 0 & k_3 \\ 0 & k_2 & 0 \\ k_3 & 0 & k_4 \end{bmatrix} \begin{bmatrix} |\sigma| \\ |dz_{f_c}(\phi)| \\ |v| \end{bmatrix}, \tag{2.57}$$

which is Lipschitz continuous on $\mathbb{R}^n$*, but not smooth.*

One can see that

$$\hat{c}_1 |x|_\mathcal{A}^2 \leqslant \hat{V}(x) \leqslant \hat{c}_2 |x|_\mathcal{A}^2 \quad \forall x \in \mathcal{C}, \tag{2.58}$$

as long as *the positive scalars* $k_1, \dots, k_4$ *are chosen so that the inner matrix in* (2.57) *is positive definite (see the proof of Lemma 6.3). Indeed, the squared distance to the attractor* $\mathcal{A}$ *is by* (2.15) $|x|_\mathcal{A}^2 = \sigma^2 + v^2 + dz_{f_c}(\phi)^2$*. Therefore,* (2.58) *verifies easily Condition* (2.55a) *of Fact 2.17.*

We now set out to check condition (2.55b) *of Fact 2.17. The (Clarke) generalized gradient in* (2.53) *is the set*

$$\partial\hat{V}(x) = \bigcup_{\substack{s_\sigma \in \text{SGN}(\sigma), \\ s_v \in \text{SGN}(v)}} (k_1\sigma + k_3|v|s_\sigma, k_2 dz_{f_c}(\phi), k_3|\sigma|s_v + k_4 v). \tag{2.59}$$

Define an element $f \in F(x)$ *as* $f := (-k_i v, \sigma - k_p v, \phi - k_v v - f_c s_v)$ *for some* $s_v \in \text{SGN}(v)$*. Note that for* $x = (\sigma, \phi, v) \in \mathcal{C}$*,* $s_v \in \text{SGN}(v)$ *and* $s_\sigma \in \text{SGN}(\sigma)$*:*

$$-s_v v = -|v|$$
$$|\sigma|s_v(\phi - f_c s_v) \leqslant -|\sigma||dz_{f_c}(\phi)| \tag{2.60}$$
$$v(\phi - f_c s_v) \leqslant -|v||dz_{f_c}(\phi)|.$$

Then, for $x = (\sigma, \phi, \nu) \in \mathcal{C}$

$$\hat{u}_{\mathcal{C}}(x) = \max_{\substack{\nu \in \partial \hat{V}(x) \\ f \in F(x)}} \langle \nu, f \rangle$$

$$= \max_{\substack{s_\nu \in SGN(\nu) \\ s_\sigma \in SGN(\sigma)}} \left\{ \begin{array}{l} [-k_1 k_i \nu \sigma - k_\nu k_3 |\sigma| s_\nu \nu] \\ \quad + [-k_3 k_i \nu |\nu| s_\sigma - k_4 k_\nu \nu^2] \\ \quad\quad + [k_2 dz_{f_c}(\phi)\sigma + k_3 |\sigma| s_\nu(\phi - f_c s_\nu)] \\ \quad\quad\quad + [-k_2 k_p \nu dz_{f_c}(\phi) + k_4 \nu(\phi - f_c s_\nu)] \end{array} \right\}$$

$$\leqslant \max_{\substack{s_\nu \in SGN(\nu) \\ s_\sigma \in SGN(\sigma)}} \left\{ \begin{array}{l} [-k_1 k_i \nu \sigma - k_\nu k_3 |\sigma||\nu|] \\ \quad + [k_3 k_i |\nu|^2 - k_4 k_\nu \nu^2] \\ \quad\quad + [k_2 dz_{f_c}(\phi)\sigma - k_3 |\sigma||dz_{f_c}(\phi)|] \\ \quad\quad\quad + [-k_2 k_p \nu dz_{f_c}(\phi) - k_4 |\nu||dz_{f_c}(\phi)|] \end{array} \right\}$$

$$\leqslant 0$$

where the first inequality holds due to (2.60) *and the second one because for each pair in brackets, the second term is negative semidefinite and the coefficients* $k_1, \ldots, k_4$ *can be chosen such that the second term dominates the first (sign-indefinite or nonnegative) one (for details see the proof of Lemma* 6.3*). Therefore, also condition* (2.55b) *of Fact* 2.17 *is verified.*

A comment on the example is in order. This example, and in particular the choice of $\mathcal{C}$*, stems essentially from the proof of Lemma* 6.3 *and Case* (i) *of the proof of item* 2) *of Proposition* 6.1 *(page* 101*) in Chapter* 6*, but the setting was modified suitably to illustrate Fact* 2.17 *and to have a slightly more involved generalized gradient, which goes well with the purpose of illustrating generalized gradients.*

2.5.5.1 *Proofs of Facts* 2.16 *and* 2.17

Proof of Fact 2.16*.* Note that the continuous differentiability of V is necessary to define the function $u_{\mathcal{C}}$ because of the gradient appearing in (2.49a). For the given V and for each $\phi \in \mathcal{S}_{\mathcal{H}}$, (2.51) holds true. Using there (2.52b) and (2.52c), we obtain $V(\phi(\bar{t}, \bar{j})) \leqslant V(\phi(\underline{t}, \underline{j}))$ for every $(\underline{t}, \underline{j}) \preceq (\bar{t}, \bar{j})$, and in particular

$$V(\phi(t, j)) \leqslant V(\phi(0, 0)) \quad \forall (t, j) \in \text{dom}\phi. \tag{2.61}$$

Using the bounds by the two class $\mathcal{K}_\infty$ functions in (2.52a), we complete (2.61) as

$$\alpha_1(|\phi(t, j)|_{\mathcal{A}}) \leqslant V(\phi(t, j)) \leqslant V(\phi(0, 0)) \leqslant \alpha_2(|\phi(0, 0)|_{\mathcal{A}}) \quad \forall (t, j) \in \text{dom}\phi,$$

and then

$$|\phi(t, j)|_{\mathcal{A}} \leqslant \alpha_1^{-1}\left(\alpha_2(|\phi(0, 0)|_{\mathcal{A}})\right) \quad \forall (t, j) \in \text{dom}\phi, \tag{2.62}$$

where $\alpha_1^{-1} \circ \alpha_2$ is a class-$\mathcal{K}_\infty$ function [59, Lem. 4.2]. (2.62) holds for each $\phi \in \mathcal{S}_{\mathcal{H}}$, and amounts to the property of uniform global stability [47, Def. 3.6]. □

Proof of Fact 2.17*.* To prove this fact, we need to show that also in this weaker setting Equation (2.61) holds, that is,

$$V(\phi(t, j)) \leqslant V(\phi(0, 0)) \quad \forall (t, j) \in \text{dom}\phi. \tag{2.63}$$

If (2.63) holds, then the use of bounds in (2.55a) allows to conclude the uniform global stability of $\mathcal{A}$ with the same reasoning as in Fact 2.16.

1. Consider a generic *jump* for each $\phi \in \mathcal{S}_{\mathcal{H}}$ (that is, both (t, j) and $(t, j + 1)$ belong to $\text{dom}\phi$, $\phi(t, j) \in \mathcal{D}$, $\phi(t, j + 1) \in G(\phi(t, j))$). Then,

$$V(\phi(t, j + 1)) - V(\phi(t, j)) \leqslant \max_{g \in G(\phi(t, j))} [V(g) - V(\phi(t, j))] \leqslant 0 \tag{2.64}$$

   by (2.55c) and (2.49b).

2. Consider for any $\phi \in \mathcal{S}_{\mathcal{H}}$ and any $j \in \mathbb{Z}_{\geqslant 0}$ a single *flow* interval $I^j :=$ $\{t \colon (t, j) \in \mathrm{dom}\,\phi\}$ with nonempty interior, and apply the results in [28, §3.3]. In particular, by [28, Thm. 3.2], we have that for all $t \in I^j$, the function $t \mapsto V(\phi(t, j(t)))$ is decreasing in a nonstrict sense (that is, $t_1 \in I^j$ and $t_2 \in I^j$ and $t_1 < t_2$ imply $V(\phi(t_2, j(t_2))) - V(\phi(t_1, j(t_1))) \leqslant 0$) if and only if for all $x \in \mathcal{C}$ and for all $\nu \in \partial_P V(x)$ it holds

$$\max\{\langle \nu, f \rangle \colon f \in F(x)\} \leqslant 0,$$

where $\partial_P V$ is the proximal subgradient of V (see [28, §3.2]). This implies that: if

$$\max_{\nu \in \partial V(x), f \in F(x)} \langle \nu, f \rangle \leqslant 0$$

(that is, (2.55b) holds), then

$$\max_{\nu \in \partial_P V(x), f \in F(x)} \langle \nu, f \rangle \leqslant 0$$

because, as we shall show next,

$$\max_{\nu \in \partial V(x), f \in F(x)} \langle \nu, f \rangle \geqslant \max_{\nu \in \partial_P V(x), f \in F(x)} \langle \nu, f \rangle. \tag{2.65}$$

But if $\max_{\nu \in \partial_P V(x), f \in F(x)} \langle \nu, f \rangle \leqslant 0$, then for each $t \in I^j$ (such t is greater than or equal to $t(j)$ in (2.47a) by construction)

$$V(\phi(t, j)) - V(\phi(t(j), j)) \leqslant 0. \tag{2.66}$$

Equations (2.64) and (2.66) hold for each solution $\phi \in \mathcal{S}_{\mathcal{H}}$, across each jump and along each flow interval, respectively, so that they prove together the claim (2.63).

To conclude the proof we need then to show that (2.65) is true. This follows from the fact that for a Lipschitz continuous V at x, $\partial_P V(x) \subset \partial V(x)$. Indeed, the generalized notions of gradients ∂V, $\partial_L V$ (the limiting subdifferential) and $\partial_P V$ in [28, §3.1-3.2] all exist for each point x where V is Lipschitz continuous, and we have that

$$\partial_P V(x) \subset \partial_L V(x) \subset \partial V(x) \tag{2.67}$$

for the following reasons.

- Any $\nu \in \partial_P V(x)$ also belongs to $\partial_L V(x)$ because $\partial_L V(x) := \{\lim_{i \to \infty} \nu_i \colon \nu_i \in \partial_P V(x_i), x_i \to x, V(x_i) \to V(x)\}$ [28, p. 21] and the constant sequences $x_i = x$, $\nu_i = \nu \in \partial_P V(x)$ for all $i > 0$ satisfy the properties to be in the set $\partial_L V(x)$. This means then that $\partial_P V(x) \subset \partial_L V(x)$.

- $\partial_L V(x) \subset \partial V(x)$ because $\partial V(x) = \mathrm{co}\{\partial_L V(x)\}$ [28, p. 21].

□

2.5.6   *Meagre output functions and invariance principles*

Invariance principles originating from the well-known LaSalle's invariance principle are by themselves a means to establish attractivity in the presence of weak Lyapunov functions that do not satisfy a strict decrease condition, which they balance with some knowledge of the solutions. A possible route to invariance principles is through the use of weakly meagre output functions. In the context of invariance principles, weakly meagre output functions also constitute a *generalized* version of the Lyapunov functions typically used to prove invariance, as is noted at the end of this Section.

Historically, the name of *output* functions relates to investigating stability properties for the solutions to

$$\dot{x} = f(x)$$
$$y = h(x)$$

in terms of the output function h and the integrability along solutions of $t \mapsto y(t) = h(x(t))$ (see [22]). The use of *meagre* functions in the context of nonlinear dynamical systems probably originated in [33]; the definition of a weakly meagre function follows.

DEFINITION 2.24 (Weakly meagre function [47, p. 178], [74, Def. 4.1]) *A measurable function* $f \colon \mathbb{R}_{\geqslant 0} \to \mathbb{R}$ *is called weakly meagre if*

$$\lim_{n \to \infty} \left(\inf_{t \in I_n} |f(t)| \right) = 0$$

for every family $\{I_n \colon n \in \mathbb{N}\}$ *of nonempty and pairwise disjoint closed intervals* I_n *in* $\mathbb{R}_{\geqslant 0}$ *with length uniformly bounded below by a positive number.*

To simplify the discussion, note that f summable on $\mathbb{R}_{\geqslant 0}$ (that is, f in L^1 on $\mathbb{R}_{\geqslant 0}$) or such that $\lim_{M \to \infty} \int_M^{M+\tau} |f(t)| dt = 0$ for $\tau > 0$ is then weakly meagre.

Before stating Fact 2.19, which is the main result presented in this section, we need to introduce the notions of ω-limit set and invariance. We also provide a standard result about the ω-limit set of a solution.

DEFINITION 2.25 (ω-limit set of a hybrid arc [47, Def. 6.17]) *The ω-limit set of a hybrid arc* $\phi \colon \mathrm{dom}\phi \to \mathbb{R}^n$, *denoted* $\Omega(\phi)$, *is the set of all points* $x \in \mathbb{R}^n$ *for which there exists a sequence* $\{(t,j)_i\}_{i=1}^{\infty}$ *of points* $(t_i, j_i) \in \mathrm{dom}\phi$ *with* $\lim_{i \to \infty} t_i + j_i = \infty$ *and* $\lim_{i \to \infty} \phi(t_i, j_i) = x$. *Every such point is an ω-limit point of* ϕ.

DEFINITION 2.26 (Weak and strong invariance [47, Def. 6.19, Def. 6.25]) *Given a hybrid system* $\mathcal{H}$, *a set* $S \subset \mathbb{R}^n$ *is said to be:*

- *weakly forward invariant if for every* $\xi \in S$ *there exists at least one complete* $\phi \in \mathcal{S}_{\mathcal{H}}(\xi)$ *with*[10] $\mathrm{rge}(\phi) \subset S$;

- *weakly backward invariant if for every* $\xi \in S$, *every* $\tau > 0$, *there exists at least one* $\phi \in \mathcal{S}_{\mathcal{H}}(S)$ *such that for some* $(t^*, j^*) \in \mathrm{dom}\phi$, $t^* + j^* \geqslant \tau$, *it is the case that* $\phi(t^*, j^*) = \xi$ *and* $\phi(t,j) \in S$ *for all* $(t,j) \in \mathrm{dom}\phi$ *with* $t + j \leqslant t^* + j^*$;

- *weakly invariant if it is both weakly forward invariant and weakly backward invariant;*

- *strongly forward invariant if for every* $\phi \in \mathcal{S}_{\mathcal{H}}(S)$, $\mathrm{rge}(\phi) \subset S$.

With Definitions 2.25-2.26, we can have the following result about the ω-limit set of a solution.

FACT 2.18 (Weak invariance of $\Omega(\phi)$ [47, Prop. 6.21]) *If $\mathcal{H}$ satisfies the hybrid basic conditions and* $\phi \in \mathcal{S}_{\mathcal{H}}$ *is complete and bounded, then* $\Omega(\phi)$ *is weakly invariant and* $|\phi(t,j)|_{\Omega(\phi)} \to 0$ *as* $t + j \to \infty$, $(t,j) \in \mathrm{dom}\phi$.

In Chapter 6, only the flow part of (2.1) will be considered, so we provide here an invariance principle limited to the flow that uses weakly meagre functions. The references [105, Lem. 5.1] and [47, Thm. 8.11] provide a full version for hybrid dynamical systems.

FACT 2.19 (Meagre invariance principle [105, Lem. 5.1], [47, Thm. 8.11]) *Let ϕ be a complete solution to*

$$\dot{x} \in F(x), \quad x \in \mathcal{C}$$

with $(F, \mathcal{C})$ *satisfying the hybrid basic conditions in Assumption 2.1.*

---

10 Given a hybrid arc $\phi \colon \mathrm{dom}\phi \to \mathbb{R}^n$, the range of ϕ is the set $\mathrm{rge}(\phi) := \{x \in \mathbb{R}^n : \exists (t,j) \in \mathrm{dom}\phi \text{ such that } x = \phi(t,j)\}$.

1. *If there exists $\ell_c \colon \mathbb{R}^n \to [0, \infty]$ lower semi-continuous[11] such that $t \mapsto \ell_c(\phi(t))$ is weakly meagre, then*

$$\Omega(\phi) \subset \{z \in \overline{\mathrm{rge}\,\phi} \colon \ell_c(z) = 0\}.$$

2. *If there exists $\ell_c \colon \mathbb{R}^n \to [0, \infty]$ such that $t \mapsto \ell_c(\phi(t))$ is weakly meagre, then*

$$\Omega(\phi) \subset \{z \in \overline{\mathrm{rge}\,\phi} \colon \exists z_i \to z, z_i \in \mathrm{rge}\,\phi, \liminf_{i \to \infty} \ell_c(z_i) = 0\}.$$

Proof. In [105, Lem. 5.1], consider a hybrid system that flows only and a global setting (U and O in [105, Lem. 5.1] are taken as $\mathbb{R}^n$). For this case, item 2 rephrases [105, Lem. 5.1], and item 1 is justified in [105, p. 2291]. □

APPLICATION 2.6 (Weakly meagre output function) *The proof of Section 6.4.2 is an application of item 1 of Fact 2.19, with $\ell_c = v^2$. Indeed, all solutions $\phi = (\phi_\sigma, \phi_\phi, \phi_v)$ are complete and bounded, and satisfy*

$$\int_0^{+\infty} \ell_c(\phi)\mathrm{d}t = \int_0^{+\infty} \phi_v(t)^2 \mathrm{d}t < +\infty,$$

that is, $\ell_c \circ \phi$ is summable and consequently weakly meagre (see the discussion after Definition 2.24). By item 1 of Fact 2.19, the ω-limit set $\Omega(\phi)$ is contained in $\{z \in \overline{\mathrm{rge}\,\phi} \colon v = 0\}$.

Finally, we note that Fact 2.19 generalizes [103, Thm. 2.10], which extended the integral-invariance principle in [22] for differential equations to the case of differential inclusions. In particular, item 1 of Fact 2.19 is itself a generalization of [103, Thm. 2.10] since item 1 asks for weakly-meagreness of $\ell_c \circ \phi$, whereas [103, Thm. 2.10] asks for summability of $\ell_c \circ \phi$ (see the discussion after Definition 2.24).

---

11 A function $f \colon \mathbb{R}^n \to \mathbb{R}$ is lower semi-continuous at x_0 if

$$\liminf_{x \to x_0} f(x) \geqslant f(x_0),$$

and is lower semi-continuous if it is lower semi-continuous at every point of its domain.

HYBRID CANCELLATION OF RIPPLE DISTURBANCES
ARISING IN AC/DC CONVERTERS

In AC/DC converters, a peculiar periodic nonsmooth waveform arises, the so-called ripple. In this chapter we propose a novel model that captures this nonsmoothness by means of the hybrid dynamical systems described in Chapter 2, where the state jumps are performed at certain switching instants, and we illustrate its properties with reference to a three phase diode bridge rectifier. As the ripple corrupts an underlying desirable signal, we propound two observer schemes ensuring asymptotic estimation of the ripple, the first with and the second without knowledge of the switching instants. Our theoretical developments are well placed in the context of recent techniques for hybrid regulation and constitute a contribution especially for our second observer, where the switching instants are estimated. Once asymptotic estimation of the ripple is achieved, the ripple can be conveniently canceled from the desirable signal, and thanks to the inherent robustness properties of the proposed hybrid formulation, the two observer schemes require only that the desirable signal is slowly time varying compared to the ripple. Exploiting this fact, we illustrate the effectiveness of our second hybrid observation law on experimental data collected from the Joint European Torus tokamak.

The content of this chapter is entirely based on [19] and [20].

3.1 INTRODUCTION: PROBLEM STATEMENT AND COMPARISON WITH OTHER APPROACHES

Many engineering applications require power electronics in their actuators and often these power electronics are equipped with AC/DC converters whose switching nature produces a peculiar ripple disturbance. A similar disturbance on the torque arises in the presence of split ring commutators on the shaft of DC motors or in brushless DC motor drives [67, 112]. Ripple disturbances may have damaging effects on control design, not only because they affect the actuation signal (like in motors), but also because they often affect the power supply, thus possibly affecting all sensor measurements due to the magnetic coupling. This phenomenon is especially noticed in high-power applications such as tokamaks and plasma control [95]. One of the important features of the ripple is that its frequency is typically a known parameter with little uncertainty, because it is a multiple of the utility frequency in the electrical power grid, which is in turn tuned very finely to the values of either 50 or 60 Hz. Due to this fact, it appears natural to address the problem of ripple estimation and rejection using linear [42] or nonlinear [56, Ch. 8] regulation theory.

However, the peculiar non-smoothness of ripple disturbances makes them less prone to be addressed with classical continuous-time approaches and makes it an interesting problem to be tackled using hybrid regulation theory (see, e.g., the preliminary work in [79] and the more recent results in [25, 26, 30, 80] and references therein). These works, as well as the approach adopted here, are based on the novel framework for the description of nonlinear hybrid dynamical systems described in Chapter 2. In particular, the advantage of adopting that framework will be evident here because it enables us to exploit important robustness properties following from suitable regularity of the dynamics. We make large use of the robustness results outlined in Section 2.4 (and originating from [47, Chap. 7]) to specifically address a "ripple cancellation" problem, wherein the ripple corresponds to a high-frequency perturbation affecting a slowly varying signal within an available measurement. Then the goal of our design is to estimate the ripple component that can be suitably subtracted from the measurement signal. To this end, we consider a general context where an unknown *constant* bias affects the measurement, we take care of this constant bias by incorporating a band-pass filter in our ripple observer, and then rely

on the robustness results from Fact 2.8 [47, Cor. 7.27] to apply the scheme in the presence of slowly varying signals.

Our approach is much inspired by the recent results in [39] and the machinery given in [118, Thm. 2] (also reported in [40, Lemma 1] with a notation that resembles more closely the situation addressed here). We would also like to emphasize that a hybrid approach to tackle this problem does not seem to be the only viable one, because the ripple disturbance is indeed an absolutely continuous function and one may find ways to generate it with a nonsmooth continuous time approach (see, e.g., the results in [78] where a continuous-time exosystem is built that generates the absolute value of a cosine waveform). However, it remains unclear how to do this for the specific waveform characterized in here. Our results are also close in nature to those reported in [30, §4.2], where a hybrid exosystem also generates the absolute value of a cosine waveform. However, as compared to that result, we focus here on ripple signals that perform commutations at phases *different* from $\pm\pi/2$ (see also Remark 3.1). Alternative methods that are relevant in the proposed context pertain to the scientific area of observer design for switched systems, because one may think of the ripple as being generated by a suitable switching system. Then, one may follow the approaches in [93] if the active mode (or, equivalently, the jump times among modes) is known, or rely on the approaches of [12, 92, 94] and references therein, where the active mode is estimated online. In addition to requiring a reformulation of our model as a switched system (which seems to be possible due to the continuity of the ripple output), the problem with applying these switched observation laws is that it is unclear how to take into account the slowly varying signal affecting the output measurement. In our work we incorporate a band-pass filter to remove that component from our ripple observer, and then we use the robustness of our formulation to prove *rigorous* properties of our scheme under a reasonable timescale separation assumption. Conversely, within the active mode detection of the above works, this seems to be a nontrivial goal.

The chapter is organized as follows: in Section 3.2 we introduce the hybrid model for the ripple generation and present the cancellation problem under consideration. In Sections 3.3 and 3.4 we illustrate the two proposed estimation schemes, and state and prove their desirable properties. These properties are illustrated in Section 3.5 in simulations, for ideal nonsmooth signals. Finally, in Section 3.6 we illustrate the effectiveness of the more general scheme on the experimental measurements from the JET tokamak.

3.2   A HYBRID MODEL FOR THE RIPPLE AND PROBLEM STATEMENT

Let us consider a simple physical example where a ripple disturbance arises, that is, the three phase diode bridge rectifier depicted in Figure 3.1, where the valves are ideal diodes. This device converts a three-phase voltage to a mono-phase *almost* direct voltage, which is applied to a load, for example a resistor. The resulting voltage is *almost* direct because, due to the logic of conversion, a non smooth waveform, the ripple, is superposed to the ideal direct voltage.
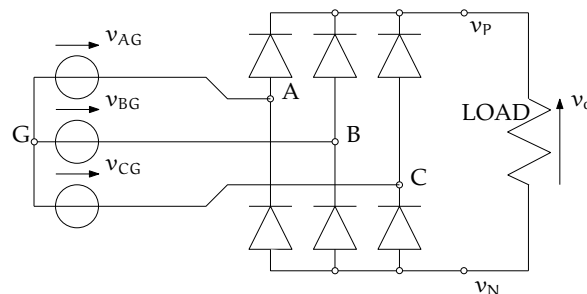
Figure 3.1: A three phase diode bridge rectifier for AC/DC conversion, which results in a waveform affected by a ripple.

Indeed, by denoting ground by G, the three phase voltages have the form:

$$v_{AG} = v_A - v_G = V_f \sin(\omega t + \theta_0)$$
$$v_{BG} = v_B - v_G = V_f \sin\left(\omega t + \theta_0 - \frac{2\pi}{3}\right)$$
$$v_{CG} = v_C - v_G = V_f \sin\left(\omega t + \theta_0 - \frac{4\pi}{3}\right).$$

(3.1)

LEMMA 3.1 *Given the power supply in (3.1), the output voltage v_o of the converter in Figure 3.1 is*

$$v_o = v_P - v_N = \sqrt{3}V_f \max_{i \in \mathbb{Z}} \cos\left(\omega t + \theta_0 - i\frac{\pi}{3}\right).$$

(3.2)

Proof. Without loss of generality, we can set $\theta_0 = 0$ in (3.1). Then, $v_o = v_P - v_N = v_{PG} - v_{NG}$ can be determined using the known rules in electronics that establish which diode is conducting among more than one connected at cathode or anode. We get then from standard results in circuit theory:

$$v_o = v_{PG} - v_{NG} =$$
$$= \max_{i \in \mathbb{Z}} \left\{ V_f \sin\left(\omega t - i\frac{2\pi}{3}\right) \right\} - \min_{j \in \mathbb{Z}} \left\{ V_f \sin\left(\omega t - j\frac{2\pi}{3}\right) \right\}$$
$$= \max_{i,j \in \mathbb{Z}} \left\{ V_f \sin\left(\omega t - i\frac{2\pi}{3}\right) - V_f \sin\left(\omega t - j\frac{2\pi}{3}\right) \right\}$$
$$= V_f \max_{i,j \in \mathbb{Z}} \left\{ 2\cos\left(\omega t - (i+j)\frac{\pi}{3}\right) \sin\left((j-i)\frac{\pi}{3}\right) \right\}$$
$$= \sqrt{3}V_f \max_{i \in \mathbb{Z}} \Big\{ \underbrace{\cos\left(\omega t - (2i+1)\frac{\pi}{3}\right)}_{j-i=1}, \underbrace{\cos\left(\omega t - (2i+2)\frac{\pi}{3}\right)}_{j-i=2},$$
$$\underbrace{-\cos\left(\omega t - (2i-1)\frac{\pi}{3}\right)}_{j-i=-1}, \underbrace{-\cos\left(\omega t - (2i-2)\frac{\pi}{3}\right)}_{j-i=-2} \Big\}$$
$$= \sqrt{3}V_f \max_{i \in \mathbb{Z}} \cos\left(\omega t - i\frac{\pi}{3}\right),$$

where the last step can be carried out via graphical inspection. $\square$

Over an interval $[0, T] = [0, 2\pi/\omega]$, (3.2) can be equivalently obtained by taking at each time the maximum among the three line-to-line voltages and their opposites in sign, as depicted in Figure 3.2.
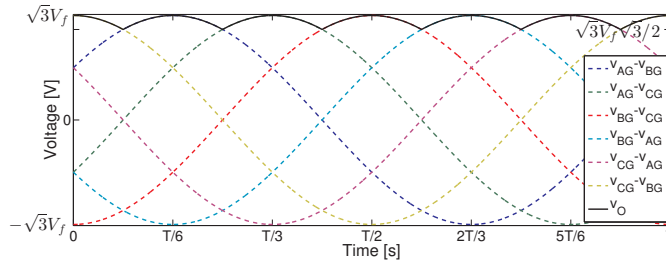
Figure 3.2: Line-to-line voltages in a three-phase diode bridge rectifier.

Based on the hybrid system formalism presented in Section 2.1, we propose a different characterization of the ripple and we show in Proposition 3.1 how it repre-

sents equivalently the physical example we have just introduced. The flow and jump dynamics read

$$
\begin{aligned}
\left.\begin{aligned}
\dot{x}_r &= \begin{bmatrix} 0 & -\omega \\ \omega & 0 \end{bmatrix} \begin{bmatrix} x_{r1} \\ x_{r2} \end{bmatrix} =: A_r x_r \\
\dot{\bar{b}} &= 0
\end{aligned}\right\} \quad (x_r, \bar{b}) \in \mathcal{C}
\end{aligned} \tag{3.3a}
$$

$$
\begin{aligned}
\left.\begin{aligned}
x_r^+ &= \begin{bmatrix} 1 & 0 \\ 0 & -1 \end{bmatrix} \begin{bmatrix} x_{r1} \\ x_{r2} \end{bmatrix} =: J_r x_r \\
\bar{b}^+ &= \bar{b}
\end{aligned}\right\} \quad (x_r, \bar{b}) \in \mathcal{D}.
\end{aligned} \tag{3.3b}
$$

The flow and jump sets $\mathcal{C}$ and $\mathcal{D}$ are specified below. We use the following output equations:

$$
y_r = x_{r1} + \bar{b} = \begin{bmatrix} 1 & 0 \end{bmatrix} x_r + \bar{b} =: C_r x_r + \bar{b} \tag{3.3c}
$$

$$
\theta = \angle(x_r). \tag{3.3d}
$$

Output y_r in (3.3c) is the measured signal comprising a constant bias signal $\bar{b}$, whereas θ is *not* available for measurement (even though we may assume knowledge of its transition times, see Section 3.3). Function $\angle(\cdot)$ returns the phase of the vector at the argument, namely for each $x_r \neq 0$ it is the only angle $\theta \in (-\pi, \pi]$ satisfying $x_r = |x_r| \begin{bmatrix} \cos(\theta) \\ \sin(\theta) \end{bmatrix}$, which is well defined for all x_r satisfying $|x_r| \neq 0$. Note that the function $\angle(\cdot)$ coincides with the well-known function $\text{atan2}(\cdot, \cdot)$ taking values in $(-\pi, \pi]$.

The jump and flow sets in (3.3a)-(3.3b) are defined as

$$
\mathcal{K} := \{(x_r, \bar{b}) : \delta \leqslant |x_r| \leqslant \Delta, |\bar{b}| \leqslant \Delta \text{ with } \Delta \geqslant \delta > 0\} \tag{3.3e}
$$

$$
\mathcal{C} := \{(x_r, \bar{b}) : -\pi/6 \leqslant \theta \leqslant \pi/6\} \cap \mathcal{K} \tag{3.3f}
$$

$$
\mathcal{D} := \{(x_r, \bar{b}) : \theta = \pi/6\} \cap \mathcal{K} \tag{3.3g}
$$

and are depicted in Figure 3.3, where we added a possible solution to (3.3) flowing in $\mathcal{C}$ and jumping when it reaches $\mathcal{D}$. In $\mathcal{C}$ and $\mathcal{D}$, the intersection with the set $\mathcal{K}$ assumes that a nonzero ripple is actually present (strictly positive δ) but is bounded (existence of Δ). Indeed, $\delta \neq 0$ only excludes $|x_r| = 0$, corresponding to no ripple at all, and ensures that $\angle(\cdot)$ in (3.3d) is well defined. However, δ and Δ can be arbitrarily small and large, respectively, and *nowhere* in our design the knowledge of their values is required. Moreover, this choice enables us to deal with compact $\mathcal{C}$ and $\mathcal{D}$, so that (3.3) satisfies the hybrid basic conditions presented in Section 2.2, whose benefits in terms of results were illustrated after Section 2.2 throughout the rest of Chapter 2. In particular, this allows us to derive our main result, Theorem 3.2, for the case of constant $\bar{b}$, but apply the corresponding scheme to the case of a slowly time varying signal $\bar{b}$ based on Fact 2.8.

REMARK 3.1 *If the ripple was not generated by a three-phase system, we would consider a different angle in (3.3f) and (3.3g) instead of $\pi/6$. For example, for a 6-phase or a 12-phase system the angle would be respectively $\pi/12$ or $\pi/24$.* ⌟

The following straightforward Proposition 3.1 motivates the study of ripple disturbances through the hybrid model (3.3). Hybrid time domains in Definition 2.2 allow us to parametrize by the two directions (t, j) the solutions to (3.3) in the sense of Definition 2.4. We constrain θ_0 to be in the set $[-\pi/6, \pi/6]$ because any other value of θ_0 could be shifted to this interval without changing the resulting value of v_o in (3.2). A relevant fact that we also establish below is that all solutions to (3.3) can be continued forward in time and have unbounded domain in the t direction of the hybrid time (t, j) (this implies that all maximal solutions are complete, see Definition 2.5).
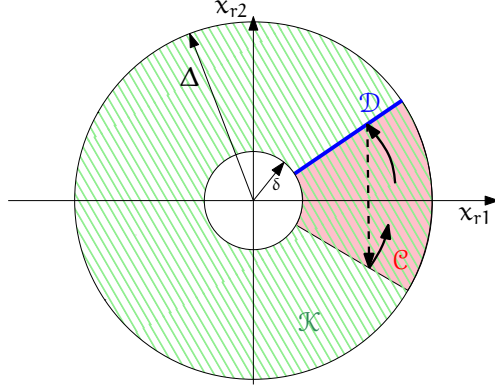
Figure 3.3: Sets $\mathcal{K}$, $\mathcal{C}$, $\mathcal{D}$ (projected on the plane (x_{r1}, x_{r2})) together with a possible trajectory (solid arrow for the flow and dashed arrow for a jump).

PROPOSITION 3.1 *For any value of θ_0 and $V_f > 0$ in (3.2), there exist initial conditions $x_r(0,0) = \sqrt{3}V_f \begin{bmatrix} \cos\theta_0 \\ \sin\theta_0 \end{bmatrix}$ and $\bar{b}(0,0) = 0$ such that the unique solution to (3.3) has unbounded domain in the ordinary time direction and satisfies $y_r(t,j) = v_o(t)$, for all $(t,j) \in \mathrm{dom}(y_r)$.*

Proof. First notice that (3.2) provides the same output for shifts of $\pi/3$ in θ_0 (due to the max). Therefore we consider without loss of generality $\theta_0 \in [-\pi/6, \pi/6]$ and $\bar{\theta}_0 = \theta_0$. We carry out the proof in polar coordinates that are globally defined in $\mathcal{C} \cup \mathcal{D}$. In particular, for a linear oscillator like (3.3a), the coordinate θ in (3.3d) evolves along flows according to $\dot{\theta} = \omega$. Moreover, by the definition of jump set (3.3g), as soon as $\theta = \pi/6$, (3.3b) in polar coordinates reads

$$\left(|x_r| \begin{bmatrix} \cos(\frac{\pi}{6}) \\ \sin(\frac{\pi}{6}) \end{bmatrix} \right)^+ = J_r |x_r| \begin{bmatrix} \cos(\frac{\pi}{6}) \\ \sin(\frac{\pi}{6}) \end{bmatrix} = |x_r| \begin{bmatrix} \cos(-\frac{\pi}{6}) \\ \sin(-\frac{\pi}{6}) \end{bmatrix},$$

showing that $|x_r|$ remains constant and θ changes sign across jumps. Therefore, each pair of consecutive jumps witnesses a dwell time of exactly $\pi/(3\omega)$, which is the time for θ to flow again from $-\pi/6$ to $\pi/6$. This shows dwell time of all solutions and proves that the domain of all solutions is unbounded in the ordinary time direction. Indeed, the flow and jump maps are Lipschitz single-valued functions and no flow is possible from the jump set, because the flow map $\dot{\theta} = \omega$ points out of $\mathcal{C} \cup \mathcal{D}$ (more rigorously, its intersection with the tangent cone to $\mathcal{C} \cup \mathcal{D}$ is empty – see [47, Prop. 6.10]). Therefore, the solution to (3.3) is unique. From (3.3a), $\frac{d}{dt}|x_r| = 0$ along flows and θ keeps revolving in the set $[-\pi/6, \pi/6]$, where $\cos(\theta)$ assumes its maximum. Therefore, all solutions starting from $\bar{b}(0,0) = 0$ satisfy

$$\begin{aligned} y_r(t,j) &= x_{r1}(t,j) = |x_r(t,j)| \cos(\theta(t,j)) \\ &= |x_r(0,0)| \max_{i \in \mathbb{Z}} \cos\left(\theta(0,0) + \omega t - i\frac{\pi}{3} \right), \end{aligned} \tag{3.4}$$

and then for $x_r(0,0) = \sqrt{3}V_f \begin{bmatrix} \cos\theta_0 \\ \sin\theta_0 \end{bmatrix}$ and $\theta(0,0) = \theta_0$ in (3.4), the (unique) solution to (3.3) satisfies the claim. $\qquad\square$

By using Proposition 3.1, it is evident that in our motivating example we would like to track the zero-mean nonsmooth ripple disturbance

$$d(t) := v_o(t) - \frac{\omega}{2\pi} \int_0^{\frac{2\pi}{\omega}} v_o(\tau) d\tau = v_o(t) - \frac{3\sqrt{3}V_f}{\pi}, \tag{3.5a}$$

to get from $y_r(t)$ the direct voltage simply as $y_r(t) - d(t)$. Identity

$$\frac{\omega}{2\pi} \int_0^{\frac{2\pi}{\omega}} v_o(\tau) d\tau = \frac{6\omega}{2\pi} \int_{-\frac{2\pi}{12\omega} - \frac{\theta_0}{\omega}}^{\frac{2\pi}{12\omega} - \frac{\theta_0}{\omega}} \sqrt{3}V_f \cos(\omega\tau + \theta_0) d\tau = \frac{3\sqrt{3}V_f}{\pi} \tag{3.5b}$$

was used in the integral in (3.5a).

More generally, the goal of this chapter can be formulated as follows.

PROBLEM 3.1 *In a measurement y_r, a desirable signal σ is affected by a (nonsmooth, zero-mean) ripple disturbance d, that is,*

$$y_r = \sigma + d. \tag{3.6}$$

Our objective is to estimate asymptotically d only from y_r, so that we recover σ by trivial subtraction. We assume σ slowly varying compared to the timescale of d.

When the hybrid basic conditions are satisfied, Fact 2.8 establishes notably that if stability and convergence of an estimate $\hat{d}$ of d hold for a constant σ, then they are preserved also for a slowly varying σ thanks to inherent robustness properties, therefore in our design we will assume that σ be constant.

We can now specify the quantities of Problem 3.1 with respect to the ripple model in (3.3). The zero-mean ripple disturbance is

$$d(t,j) := y_r(t,j) - \bar{b}(t,j) - \tfrac{3}{\pi}|x_r(t,j)| = x_{r1}(t,j) - \tfrac{3}{\pi}|x_r(t,j)| : \tag{3.7a}$$

$\bar{b}$ and $\tfrac{3}{\pi}|x_r|$ are constant due to (3.3a) and (3.3b), as we noted also within the proof of Proposition 3.1, and $\bar{b} + \tfrac{3}{\pi}|x_r|$ is precisely the mean of the measurement y_r because the mean of the signal $x_{r1}(\cdot, \max_{(\cdot,j)\in \mathrm{dom}\,x_{r1}} j)$ is the constant $\tfrac{3}{\pi}|x_r|$, with analogous steps as in (3.5)[1]. Then, based on (3.6), the desirable signal is

$$\sigma(t,j) := \bar{b}(t,j) + \tfrac{3}{\pi}|x_r(t,j)|, \tag{3.7b}$$

which motivates the introduction of the constant term $\bar{b}$ in order to model an arbitrary constant value for σ. Based on (3.7a), the disturbance estimate is finally

$$\hat{d}(t,j) := \hat{x}_{r1}(t,j) - \tfrac{3}{\pi}|\hat{x}_r(t,j)|. \tag{3.7c}$$

3.3   RIPPLE ESTIMATION WITH KNOWLEDGE OF SWITCHING INSTANTS

If the switching instants of the ripple generator in (3.3) are known, it is possible to design an estimator consisting in a suitable Luenberger observer during flows and performing simultaneous jumps with the ripple generator (namely, the jump and flow sets remain unchanged and do *not* depend on the observer states). This corresponds to a simplified setting for the observer design. The assumption that the switching instants of the hybrid ripple generator are available to the ripple observer may be verified, for example, if the observation algorithm is connected to the circuitry commanding the switches of the rectifier in Figure 3.1, so that the switching times are known. Another case is that of a torque ripple generated by a DC motor where one may assume to measure the shaft angle and then compute the switching times based on the position of the split ring commutator.
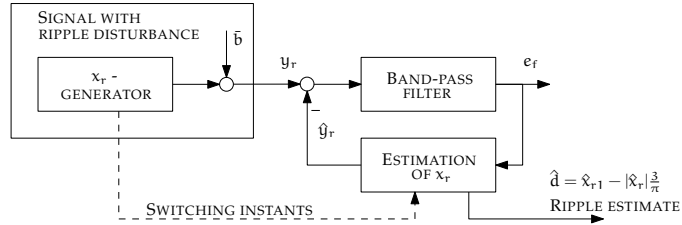
Figure 3.4: Scheme with generator, filter and hybrid observer of x_r when the switching instants are known.

---

1 Or by noting that $x_{r1} = |x_r|\cos\theta$ and computing the mean $\tfrac{6}{\pi}\int_0^{\pi/6}|x_r|\cos\theta\,d\theta$.

The architecture of the proposed solution is sketched in Figure 3.4. The block "SIGNAL WITH RIPPLE DISTURBANCE" corresponds to the hybrid system in (3.3), whereas the block "BAND-PASS FILTER" corresponds to

$$F(s) := \frac{\frac{s}{\omega}}{\left(1 + \frac{s}{\omega}\right)^2},$$ (3.8)

with a double pole at the ripple frequency ω that isolates the dominant mode of the (nonsmooth) signal d from the constant bias and the high-frequency noise. The specific form of $F(s)$ is crucial to obtaining the structure below in (3.10) and the result of Lemma 3.2. The state-space representation of (3.8) is

$$\left[\begin{array}{c|c} A_f & B_f \\ \hline C_f & \end{array}\right] := \left[\begin{array}{cc|c} 0 & 1 & 0 \\ -\omega^2 & -2\omega & 1 \\ \hline 0 & \omega & \end{array}\right].$$ (3.9a)

For the observer (block "ESTIMATION OF x_r") and filter dynamics, we add to (3.3) the following flow and jump equations

$$\left.\begin{array}{l} \dot{x}_f = A_f x_f + B_f(y_r - \hat{y}_r) \\ \dot{\hat{x}}_r = A_r \hat{x}_r + L e_f \end{array}\right\} (x_r, \bar{b}) \in \mathcal{C}$$ (3.9b)

$$\left.\begin{array}{l} x_f^+ = x_f \\ \hat{x}_r^+ = J_r \hat{x}_r \end{array}\right\} (x_r, \bar{b}) \in \mathcal{D},$$ (3.9c)

and the following output equations

$$\begin{array}{l} e_f = C_f x_f \\ \hat{y}_r = C_r \hat{x}_r \end{array}$$ (3.9d)

where $L := \begin{bmatrix} \ell \\ 0 \end{bmatrix}$ is the Luenberger gain and the scalar $\ell > 0$ is a design parameter, whose tuning strategy is commented at the end of this section. The flow and jump sets are the *same* as in (3.3) and depend *only* on output θ in (3.3d). We emphasize that to implement the hybrid observer (3.9) it is *not* necessary to measure θ, but only to know its switching times, that is, the times when the observer state $\hat{x}_r$ should jump.

To suitably analyze the overall system (3.3) and (3.9), let us introduce the error variable

$$e := \begin{bmatrix} \tilde{x}_r \\ \tilde{x}_f \end{bmatrix} := \begin{bmatrix} x_r - \hat{x}_r \\ x_f + A_f^{-1} B_f \bar{b} \end{bmatrix},$$ (3.10a)

where $\tilde{x}_r$ is the error related to the ripple generation and $\tilde{x}_f$ is a coordinate transformation of the filter state variables chosen to satisfy $A_f \tilde{x}_f = A_f x_f + B_f \bar{b}$. Thanks to $\dot{\bar{b}} = 0$ and $C_f A_f^{-1} B_f = 0$, the (hybrid) error dynamics corresponds then to

$$\dot{e} = \begin{bmatrix} A_r & -LC_f \\ B_f C_r & A_f \end{bmatrix} e =: A_e e, \qquad (x_r, \bar{b}) \in \mathcal{C}$$ (3.10b)

$$e^+ = \begin{bmatrix} J_r & 0 \\ 0 & I_2 \end{bmatrix} e =: J_e e, \qquad (x_r, \bar{b}) \in \mathcal{D},$$ (3.10c)

for which Lemma 3.2 holds.

LEMMA 3.2 *Given dynamics (3.3) and (3.9) and the error dynamics (3.10), for every $\ell > 0$, the selection $L := \begin{bmatrix} \ell \\ 0 \end{bmatrix}$ in (3.9b) and (3.10b) ensures the existence of $P = P^\top > 0$ and $H \in \mathbb{R}^{1 \times 4}$ such that (H, A_e) is an observable pair and the function*

$$V(e) := e^\top P e$$ (3.11)

satisfies

$$\langle \nabla V(e), A_e e \rangle = -e^\top H^\top H e, \qquad (x_r, \bar{b}) \in \mathcal{C}$$ (3.12a)

$$V(J_e e) - V(e) = 0, \qquad (x_r, \bar{b}) \in \mathcal{D}.$$ (3.12b)

Proof. Consider the diagonal

$$P := \begin{bmatrix} 1 & 0 & 0 & 0 \\ 0 & 1 & 0 & 0 \\ 0 & 0 & \omega^3\ell & 0 \\ 0 & 0 & 0 & \omega\ell \end{bmatrix}.$$

From $\ell > 0$, it follows $P = P^{\mathsf{T}} > 0$. Moreover, using A_e in (3.10b), one obtains

$$PA_e + A_e^{\mathsf{T}}P = \begin{bmatrix} 0 & 0 & 0 & 0 \\ 0 & 0 & 0 & 0 \\ 0 & 0 & 0 & 0 \\ 0 & 0 & 0 & -4\omega^2\ell \end{bmatrix} = -H^{\mathsf{T}}H,$$

with $H := [0 \ 0 \ 0 \ 2\omega\sqrt{\ell}]$. Then (3.12a) follows. As for H, the observability of the pair (H, A_e) is verified through the observability matrix

$$\begin{bmatrix} H \\ HA_e \\ HA_e^2 \\ HA_e^3 \end{bmatrix},$$

whose determinant is $-16\omega^9\ell^2 \neq 0$. Finally,

$$V(e^+) - V(e) = V(J_e e) - V(e) = e^{\mathsf{T}}(J_e^{\mathsf{T}}PJ_e - P)e$$

$$= e^{\mathsf{T}}\left(\left[\begin{array}{c|c} J_r^{\mathsf{T}}J_r & 0 \\ \hline 0 & \begin{matrix} \omega^3\ell & 0 \\ 0 & \omega\ell \end{matrix} \end{array}\right] - P\right)e = 0$$

proves (3.12b), given that $J_r^{\mathsf{T}}J_r = I_2$.   □

REMARK 3.2 *The proof of Lemma 3.2 applies for any selection of the jump instants. Therefore the scheme in Figure 3.4 is effective at estimating the ripple y_r also when the jump set $\mathcal{D}$ is empty, which boils down to a standard linear disturbance rejection problem with an internal model. Due to this fact, our scheme can be seen as a generalization of the last one, much related to the recent works in [25, 26, 30, 80] and references therein.*   ⌐

Based on the Lyapunov construction of Lemma 3.2 we state next our first main result establishing asymptotic estimation of the ripple signal.

THEOREM 3.1 *For every $\ell > 0$, the selection $L = \begin{bmatrix} \ell \\ 0 \end{bmatrix}$ in (3.9b) and in (3.10b) guarantees that the compact attractor*

$$\mathcal{A} := \{(x_r, \bar{b}, \hat{x}_r, x_f) : \ e = 0 \ \text{and} \ (x_r, \bar{b}) \in \mathcal{K}\}, \tag{3.13}$$

is uniformly globally exponentially stable for the closed-loop dynamics (3.3) and (3.9).

Proof. The proof of this result is illustrated in Application 2.2, and how it is encompassed in the context of weak Lyapunov functions is the subject of Section 2.5.3. As it is explained extensively therein, the result is a direct consequence of [118, Thm. 2] (in [40, Lemma 1] a parallel formulation to the present one is used), given the Lyapunov function (3.11).   □

From (3.7a) and (3.7c) and (3.10a), the disturbance estimation error is

$$d - \hat{d} = \begin{bmatrix} 1 & 0 & 0 & 0 \end{bmatrix}e + \frac{3}{\pi}(|\hat{x}_r| - |x_r|), \tag{3.14}$$

so that Theorem 3.1 implies that for any positive choice of the scalar parameter ℓ, the estimate $\hat{d}$ converges uniformly and exponentially to the ripple disturbance d. Smaller selections of ℓ lead to slower convergence but are less sensitive to noise, whereas larger selections of ℓ lead to faster convergence but larger noise sensitivity should be expected. This is a well-known trade-off when designing linear observers with large gain (see [71, Eq. (3)]) such as (3.10b), and even more for high-gain observers [10]. Possible remedies are taken into consideration in [10, 71] and references therein. We did not consider such remedies in light of the fact that in our final scheme of Section 3.4 we choose a small value of ℓ as specified in Remark 3.5.

3.4 RIPPLE ESTIMATION WITHOUT KNOWLEDGE OF SWITCHING INSTANTS

In most practical cases it is difficult if not impossible to know the switching instants, and the scheme of the previous section cannot be implemented. This calls for the enhanced estimation scheme in Figure 3.5, where we estimate the switching instants by building an estimate $\hat{\theta}$ of the unavailable output θ in (3.3d).
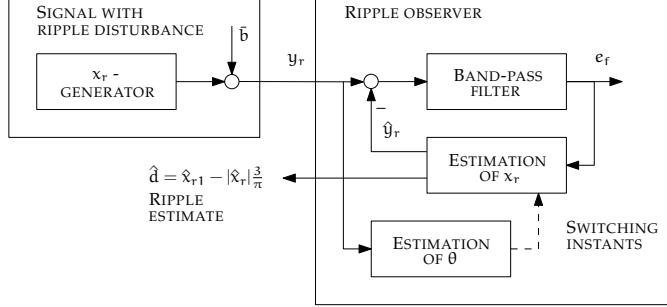
Figure 3.5: Scheme with generator, estimation of the switching instants, filter and hybrid observer of x_r when the switching instants are *not* known.

REMARK 3.3 *In the sequel, to keep the notation simple, we will introduce several coupled dynamical systems representing different components of the scheme in Figure 3.5 and having different jump and flow sets. These jump and flow sets will be specified in terms of only some state variables, implicitly meaning that the other state variables may assume any value within their respective domains. With this simplified notation we refer to the hybrid system constructed having flow set corresponding to the intersection of all the specified flow sets, flow map arising from stacking up all the specified flow equations (no flow equations will be repeated, thus generating no ambiguity), jump set corresponding to the union of all the jump sets, and jump map corresponding to the stack of all the specified jump maps. More concretely, an exemplification of what we mean by this simplified notation, can be found in Application 2.3, where we extracted some of the flow and jump equations of this section and we assembled them consistently with the hybrid system formalism, that is, with a single flow/jump map and set.* ⌟

Using the simplified notation mentioned in Remark 3.3, we preserve the main dynamics in (3.9) using a jump rule now triggered by the new state $\hat{\theta}$

$$
\begin{cases}
\dot{x}_f = A_f x_f + B_f(y_r - \hat{y}_r) \\
\dot{\hat{x}}_r = A_r \hat{x}_r + L e_f \qquad\qquad\qquad \hat{\theta} \in \left[-\dfrac{\pi}{3}, \dfrac{\pi}{6}\right] \\
\dot{\hat{\theta}} = \omega,
\end{cases}
\tag{3.15a}
$$

$$
\begin{cases}
x_f^+ = x_f \\
\hat{x}_r^+ = J_r \hat{x}_r \qquad\qquad\qquad\qquad \hat{\theta} \in \left[\dfrac{\pi}{6}, \dfrac{\pi}{3}\right], \\
\hat{\theta}^+ = \hat{\theta} - \pi/3,
\end{cases}
\tag{3.15b}
$$

with the same output equations (3.9d). Note that the lower bound on $\hat{\theta}$ in (3.15a) and the upper bound in (3.15b) are coarser than those in (3.9b) and (3.9c), because we want to leave some margin for suitable adaptation of $\hat{\theta}$ as in (3.18b).

Clearly, dynamics (3.15) converges to the right estimate when $\hat{\theta} = \theta$. The scheme is then completed by an additional action that updates periodically $\hat{\theta}$ in such a way

that it converges to θ. Such convergence will be established based on the Lyapunov function:

$$V_\theta(\theta, \hat{\theta}) := \min_{i \in \mathbb{Z}} \left(\theta - \hat{\theta} + i\frac{\pi}{3}\right)^2 = \tilde{\theta}^2, \tag{3.16a}$$

$$\tilde{\theta} := \theta - \hat{\theta} + i^*\frac{\pi}{3}, \tag{3.16b}$$

$$i^* := \arg\min_{i \in \mathbb{Z}} \left(\theta - \hat{\theta} + i\frac{\pi}{3}\right)^2. \tag{3.16c}$$

In particular, the following lemma is fundamental to achieve this convergence property.

LEMMA 3.3 *Consider any hybrid solution to solely (3.3) and (3.15). The output $\tilde{\theta}$ defined in (3.16b) and the Lyapunov function V_θ in (3.16a) both remain constant along flows and across jumps. Moreover, defining[2] for each $t \geqslant 0$ the function $j^*(t) := \max_{(t,j) \in \mathrm{dom}\theta} j$, the next identity holds:*

$$\int_t^{t+\frac{\pi}{3\omega}} \hat{\theta}(\tau, j^*(\tau)) d(\tau, j^*(\tau)) d\tau = -|x_r(0,0)|\rho(\tilde{\theta}), \tag{3.17}$$

where ρ is such that $\tilde{\theta} \mapsto \rho(\tilde{\theta})\tilde{\theta}$ is a positive definite function in the interval $\tilde{\theta} \in (-\pi/6, \pi/6)$ and d is in (3.7a), corresponding to $d = |x_r|\cos(\theta) - \frac{3}{\pi}|x_r|$.
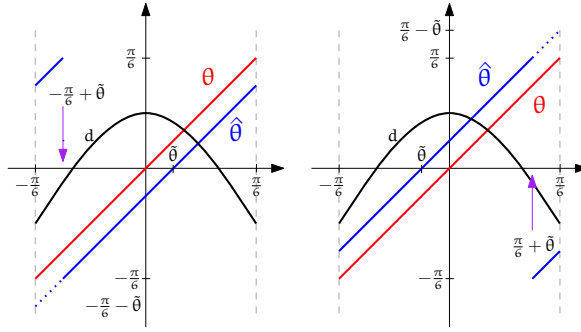
Figure 3.6: Proof for $\tilde{\theta} > 0$ (left) and $\tilde{\theta} < 0$ (right).

Proof. When one considers solely (3.3) and (3.15), $\tilde{\theta}$ and V_θ remain constant along solutions because $\dot{\theta} - \dot{\hat{\theta}} = \omega - \omega = 0$ along flows and $\theta^+ = \theta - \frac{\pi}{3}$ (similarly for $\hat{\theta}^+$) so that across jumps quantity i^* in (3.16c) changes but the minimum in (3.16a) does not.

Regarding integral (3.17), we compute it by dividing the analysis in the two cases shown in Figure 3.6. After some calculations, essentially splitting each integral in two parts, ρ in (3.17) can be found to be

$$\rho(\tilde{\theta}) := \begin{cases} -\frac{1}{6\omega}\left(\pi - 6\tilde{\theta} - 2\pi\sin\left(\frac{\pi}{6} - \tilde{\theta}\right)\right) =: \rho_p(\tilde{\theta}) & \tilde{\theta} \geqslant 0 \\ -\rho_p(-\tilde{\theta}) & \tilde{\theta} < 0 \end{cases}$$

so that $\tilde{\theta} \mapsto \rho(\tilde{\theta})\tilde{\theta}$ is positive definite in $(-\pi/6, \pi/6)$. □

REMARK 3.4 *As graphically illustrated in Figure 3.6, scalar $\tilde{\theta}$ characterized in Lemma 3.3 is the difference between θ and $\hat{\theta}$ modulo $\pi/3$, that is, by $\tilde{\theta}$ one measures their distance in a way that remains constant across jumps.* ⌋

---

2 Note that the definition of $j^*(t)$ is valid for all $t \geqslant 0$ because all solutions have unbounded domain in the ordinary time direction, as established in Proposition 3.1.

Based on the preliminary result of Lemma 3.3, we complete now the hybrid observer (3.15) with an additional dynamics implementing integral (3.17) and imposing a suitable jump rule on $\hat{\theta}$ to ensure its convergence to θ. Consider

$$
\begin{cases}
\dot{\bar{y}}_r = 0 \\
\dot{\bar{y}}_{rI} = y_r - \bar{y}_r \\
\quad \dot{\eta} = \hat{\theta}(y_r - \bar{y}_r) \\
\quad \dot{\tau} = 1,
\end{cases}
\qquad \tau \leqslant \frac{\pi}{3\omega} \qquad (3.18a)
$$

$$
\begin{cases}
\bar{y}_r^+ = \bar{y}_r + k_{av}\dfrac{3\omega}{\pi}\bar{y}_{rI} \\
\bar{y}_{rI}^+ = 0 \\
\eta^+ = 0 \\
\tau^+ = 0 \\
\hat{\theta}^+ = \hat{\theta} - \mathrm{sat}_{\frac{\pi}{6}}(k_\theta \eta),
\end{cases}
\qquad \tau = \frac{\pi}{3\omega}, \qquad (3.18b)
$$

whose quanties are now detailed. τ is a periodic timer ensuring that integral (3.17) is computed periodically; over this period state $\bar{y}_{rI}$ integrates the difference between output y_r and its average value, so that $\bar{y}_r$ can converge to the average value of y_r. η implements the left-hand side of (3.17) by subtracting the (estimated) average value $\bar{y}_r$ from measurement y_r and multiplying it by $\hat{\theta}$. $k_{av} \in (0,1]$ and $k_\theta > 0$ are two positive gains that can be tuned according to the guidelines in Remark 3.5. The function $\mathrm{sat}_{\frac{\pi}{6}}(\cdot)$ is the scalar symmetric saturation function whose output is limited within $[-\pi/6, \pi/6]$: note that this limitation ensures that $\hat{\theta}^+$ always belongs to the union of the flow and jump sets in (3.15), which guarantees existence of solutions (for example, when the timer τ reaches the value $\pi/(3\omega)$, a negative correction term $k_\theta \eta$ could induce $\hat{\theta}^+ > \pi/3$ *without* the saturation, hence bringing the solution outside of $\mathcal{C} \cup \mathcal{D}$).

The overall ripple estimation scheme corresponds to the plant (3.3), the estimator dynamics in (3.15), and the extra flow and jump rules in (3.18), where the role of the different jump and flow sets should be intended as explained in Remark 3.3. The overall state is then given by

$$
\xi := (x_r, \bar{b}, x_f, \hat{x}_r, \theta, \bar{y}_r, \bar{y}_{rI}, \eta, \tau),
$$

where we note that because $(x_r, \bar{b})$ belongs to the compact set $\mathcal{K}$ in (3.3e) and $\tau \in [0, \pi/(3\omega)]$, then there exists a large enough scalar M such that $(\bar{y}_r, \bar{y}_{rI}, \eta, \tau) \in M\mathbb{B}^4$, where $\mathbb{B}^4$ is the four-dimensional closed unit ball. In the next theorem we establish parallel results to those of Theorem 3.1 in terms of stability properties of the compact attractor

$$
\mathcal{A}_e := \mathcal{A} \times [-\pi/3, \pi/3] \times M\mathbb{B}^4, \qquad (3.19)
$$

where $\mathcal{A}$ is defined in (3.13) and corresponds to the set where the estimate $\hat{\theta}$ is correct. Note that Theorem 3.2 only establishes local properties of the scheme although its results could be *strengthened* by relying on a more sophisticated update law for $\hat{\theta}$ (see, e.g., [81] for global asymptotic stabilization of dynamics on bounded manifolds like our angles θ and $\hat{\theta}$) and on global results on cascaded hybrid systems.

THEOREM 3.2 *For every $\ell > 0$, every $k_{av} \in (0,1]$ and a small enough value of $k_\theta > 0$, the selection $L := \begin{bmatrix} \ell \\ 0 \end{bmatrix}$ in (3.15a) guarantees that the compact attractor $\mathcal{A}_e$ is uniformly locally asymptotically stable for the closed-loop dynamics (3.3), (3.15), (3.18).*

Proof. The scheme can be represented as the cascade of three hybrid dynamical systems.

The lowermost system corresponds to the dynamics restricted to the set

$$
\mathcal{A}_\theta := \{\xi : \theta = \hat{\theta}\},
$$

which is clearly forward invariant because the dynamics of $\hat{\theta}$ coincide with that of θ. By using the result of Theorem 3.1 it is readily seen that the dynamics restricted to $\mathcal{A}_\theta$ is UAS (actually UES) to $\mathcal{A}_e$.

The intermediate system corresponds to the dynamics restricted to the set

$$\mathcal{A}_{\bar{y}} := \{\xi : \bar{y}_r = \bar{b}(0,0) + \frac{3}{\pi}|x_r(0,0)|\}, \tag{3.20}$$

which is again forward invariant because, from (3.7a) and (3.3), the scalar $\bar{b}(0,0) + \frac{3}{\pi}|x_r(0,0)|$ is the average value of $y_r(t, j^*(t))$, and $\bar{b}$ and $|x_r|$ remain constant along flows and across jumps. Also, the set $\mathcal{A}_\theta$ is uniformly (locally) asymptotically stable for the dynamics restricted to $\mathcal{A}_{\bar{y}}$. The use of a weak Lyapunov function together with persistent jumping to establish asymptotic stability of $\mathcal{A}_{\bar{y}}$ is also illustrated in Application 2.3 within Section 2.5.4 in a way that hints at the general property. Here, we need to consider a local version of Fact 2.14 but we keep the same Lyapunov function. In particular, to establish uniform local asymptotic stability of $\mathcal{A}_\theta$ for the dynamics restricted to $\mathcal{A}_{\bar{y}}$, we use the Lyapunov function V_θ in (3.16a), which remains constant along flows (as established in Lemma 3.3). To analyze the change of V_θ across jumps, first note that in $\mathcal{A}_{\bar{y}}$ we have that $d = y_r - \bar{y}_r$. Then, due to periodicity of timer τ in (3.18) and due to the results of Lemma 3.3, we have before each jump in (3.18b) that $\eta = -|x_r(0,0)|\rho(\tilde{\theta})$. Therefore, across all such jumps, the quantity in (3.16b) satisfies

$$\begin{aligned}(\tilde{\theta}^+)^2 &= \left(\theta - \hat{\theta}^+ + (i^*)^+ \frac{\pi}{3}\right)^2 \leqslant \left(\theta - \hat{\theta}^+ + i^* \frac{\pi}{3}\right)^2 = \\ &= \left(\tilde{\theta} - \operatorname{sat}_{\frac{\pi}{6}}\left(k_\theta |x_r(0,0)|\rho(\tilde{\theta})\right)\right)^2,\end{aligned} \tag{3.21}$$

where the inequality follows from the fact that i^* in (3.16c) is a minimizer. Then from uniform boundedness of $|x_r(0,0)|$ and positive definiteness of $\tilde{\theta} \mapsto \rho(\tilde{\theta})\tilde{\theta}$ in the set $(-\pi/6, \pi/6)$, it is ensured that the function V_θ is (locally) strictly decreasing as long as $k_\theta > 0$ is sufficiently small. For all other jumps triggered by the jump sets in (3.3b) and (3.15b), function V_θ remains constant as established in Lemma 3.3. Since jumps in (3.18b) are periodic from periodicity of τ, then the asymptotic stability of $\mathcal{A}_\theta$ relative to initial conditions from $\mathcal{A}_{\bar{y}}$ follows from persistent jumping and [47, Prop. 3.24]. We showed in detail in Application 2.3 how the periodic jumps of τ imply the property of persistent jump.

The uppermost system corresponds to the dynamics starting anywhere in the allowable set of initial conditions, which clearly converge to the attractor in (3.20). Indeed, at each jump triggered by (3.18b) it holds that $\frac{3\omega}{\pi}y_{rI}$ is the difference between the average of y_r, $\bar{b}(0,0) + \frac{3}{\pi}|x_r(0,0)|$, and its estimate $\bar{y}_r$, so that the update law in the first equation in (3.18b) leads to uniform convergence to zero of the Lyapunov function $V_y := (\bar{b} + \frac{3}{\pi}|x_r| - \bar{y}_r)^2$ (once again we apply [47, Prop. 3.24] and persistent jumping to establish this fact). Recall that $\bar{b}$ and $|x_r|$ remain constant along solutions, while $\bar{y}_r$ remains constant during flowing, so that V_y remains constant along flows and decreases across jumps thanks to $k_{av} \in (0, 1]$.

Once the three above nested (or cascade-like) results are established, the uniform (local) asymptotic stability of the innermost attractor given by $\mathcal{A}_e$ in (3.19) can be established applying iteratively the reasoning in [48, Corollary 19] by intersecting the flow and jump sets with sufficiently large compact sets. $\qquad\square$

REMARK 3.5 *Small choices of k_{av} may be desired to suitably filter possible noise affecting the measurement. Similarly, k_θ should be selected small in such a way to ensure that Theorem 3.2 applies and that suitable noise rejection is obtained. In general, the tuning of the three parameters k_{av}, k_θ and ℓ should be carried out based on the cascaded structure of the proof. Indeed, to experience a graceful transient performance, it is reasonable to pick the gain k_{av} as the most aggressive one, k_θ in such a way to induce an intermediate speed of convergence, and ℓ as the one that induces the slowest transient. This type of tuning procedure was adopted in Sections 3.5 and 3.6.*

The simulations of this section confirm the effectiveness of the methods presented in Section 3.3 and 3.4 in the case of *ideal nonsmooth* signals. In Section 3.6 we apply then the method of Section 3.4 to experimental signals.

3.5.1   *Estimation with known switching instants*

In this section we will present the simulations related to the results in Section 3.3, for the scheme of Figure 3.4.
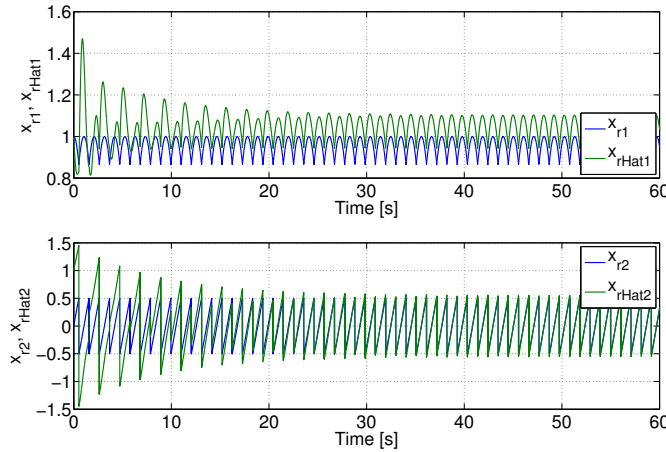
Figure 3.7: Convergence of $\hat{x}_r$ to x_r.

We had to implement slightly inflated versions of $\mathcal{C}$ and $\mathcal{D}$ as compared to (3.3f)-(3.3g) to suitably address numerical issues. In particular, we chose for the simulations

$$\mathcal{C}_s = \{(x_r, \bar{b})\colon -\frac{\pi}{6} - \epsilon \leqslant \theta \leqslant \frac{\pi}{6}\}\cap\mathcal{K} \tag{3.22a}$$

$$\mathcal{D}_s = \{(x_r, \bar{b})\colon \frac{\pi}{6} \leqslant \theta \leqslant \frac{\pi}{6} + \epsilon\}\cap\mathcal{K}, \tag{3.22b}$$

where θ is the output defined in equation (3.3d) and $\epsilon = \frac{\pi}{50}$ is a small angle compared to the ones of the flow set. This modification is important to prevent solutions to exit both flow and jump set due to numerical problems and then stop prematurely. In fact, if we implemented the equality $\theta = \frac{\pi}{6}$ as in (3.3g), it would happen that the numerical errors push any solution θ to slightly overflow from $\frac{\pi}{6}$ before the jump. Then the jump condition is no more satisfied and the solution is terminated. Then, once $\mathcal{D}$ is slightly extended beyond the thin set $\theta = \frac{\pi}{6}$, as in (3.22b), we have to enlarge in a similar way the flow set $\mathcal{C}$ as in (3.22a) at its lower boundary so that after the jump the solution is not terminated because it falls out of the flow set on the opposite side.

For our simulations we choose frequency $\omega = 1$, bias term $\bar{b} = 0.1$, design parameter $\ell = 25$ and initial conditions $x_r(0,0) = \left[\begin{smallmatrix}1\\0\end{smallmatrix}\right]$, $x_f(0,0) = \left[\begin{smallmatrix}0\\0\end{smallmatrix}\right]$, $\hat{x}_r(0,0) = \left[\begin{smallmatrix}1\\1\end{smallmatrix}\right]$.

Figure 3.7 shows the convergence of the error variables defined in (3.10a). We stated in Theorem 3.1 that the compact attractor $\mathcal{A}$ is uniformly globally exponentially stable, and this may seem in contrast with the convergence we are presenting in Figure 3.7, where the magnitude of the state $\hat{x}_r$ does not seem to converge to the one of x_r. What is actually happening is that there is a slow transient where the magnitude error actually goes to zero. This fact is highlighted in Figure 3.8, where we show the convergence of the Lyapunov function used in the proof of Theorem 3.1. By zooming in the final part of the simulation (lower curve of Figure 3.8), we get that the Lyapunov function is still decreasing, though in a very slow fashion, because the difference in magnitude is almost non detectable from the output error.
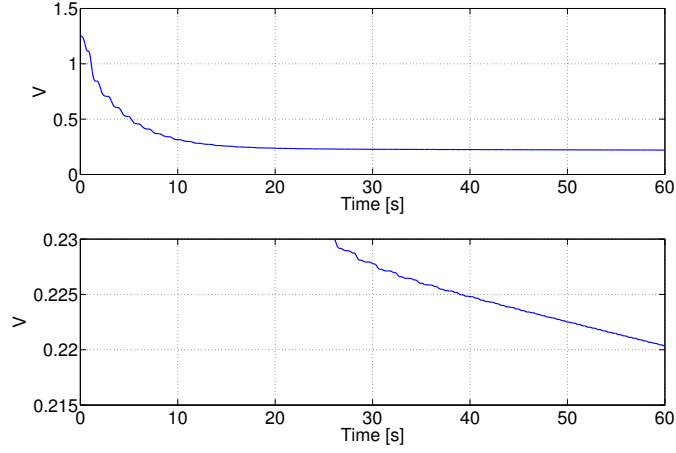
Figure 3.8: Convergence of the Lyapunov function (top) and for the final part of the simulation (bottom).
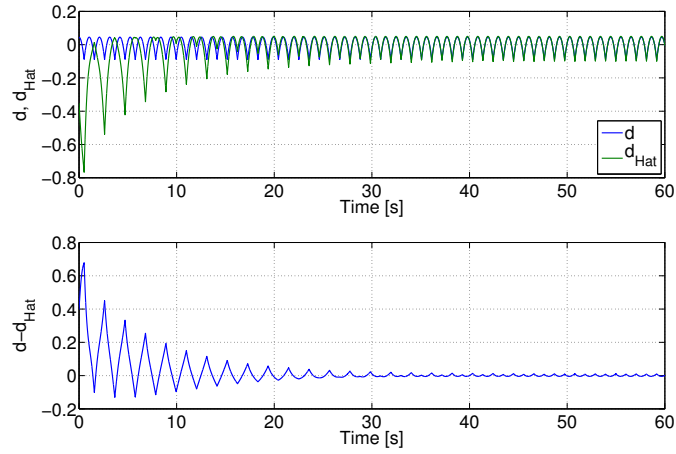
Figure 3.9: Disturbance d and its estimate $\hat{d}$ (top). Convergence to zero of the error $d - \hat{d}$ (bottom).

The fact that the magnitude error is almost non detectable from the output is revealed in the curves of Figure 3.9, corresponding to the disturbance d superimposed to its estimate $\hat{d}$ (upper curve) and the estimation error $d - \hat{d}$ (lower curve). This figure highlights the desirable exponential convergence rate for $d - \hat{d}$ noted after (3.14), despite the fact that the magnitude estimation $|\hat{x}_r|$ is still slowly converging.

3.5.2 *Estimation with unknown switching instants*

In this section we present the simulations related to the scheme proposed in Section 3.4 and represented in Figure 3.5.

For the sake of consistency with the previous Section 3.5.1, we maintained the value $\epsilon = \frac{\pi}{50}$ for the sets (3.22), the frequency $\omega = 1$, the bias term $\bar{b} = 0.1$, the design parameter $\ell = 25$, and the initial conditions $x_r(0,0) = \begin{bmatrix} 1 \\ 0 \end{bmatrix}$, $x_f(0,0) = \begin{bmatrix} 0 \\ 0 \end{bmatrix}$, $\hat{x}_r(0,0) = \begin{bmatrix} 1 \\ 1 \end{bmatrix}$. We have to add two more design parameters, $k_\theta = 10$ and $k_{av} = 0.99$, and the initial states for the other variables $\bar{y}_r(0,0) = \frac{3}{\pi}1.5$, $\tau(0,0) = y_{rI}(0,0) = \eta(0,0) = 0$, $\hat{\theta}(0,0) = \frac{\pi}{10}$.

We show in Figure 3.10 that $\hat{\theta}$ converges asymptotically to θ very fast. In Figure 3.11 we show the convergence of $\hat{x}$ to x: we see a similar tail with slow convergence to zero of the magnitude error, as in Figure 3.7. The convergence of $\hat{d}$ to d is almost identical to the one in Figure 3.9 apart from an initial transient, whose du-
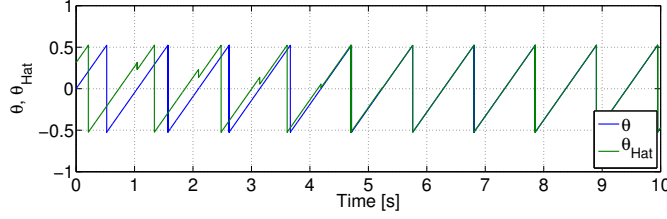
Figure 3.10: Convergence of $\hat{\theta}$ to θ (zoomed time scale).
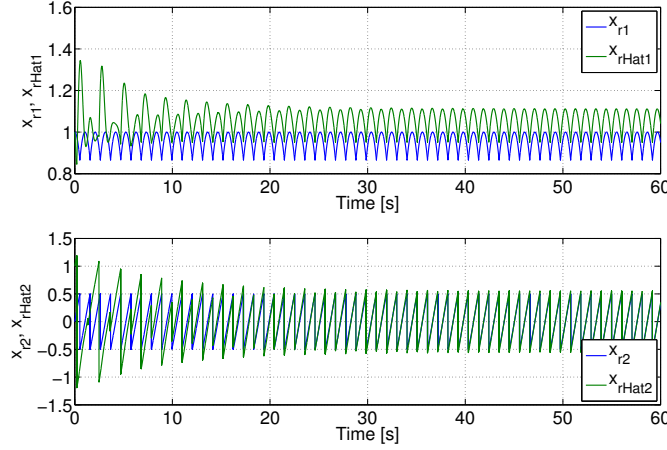
Figure 3.11: Convergence of $\hat{x}_r$ to x_r.

ration is comparable to the one seen for the convergence of $\hat{\theta}$ to θ shown in Figure 3.10.

3.6 JET EXPERIMENTAL MEASUREMENTS

In this Section we apply the scheme in Figure 3.5 from Section 3.4 to experimental data collected from the JET tokamak [88].

The stabilization of the unstable plasma vertical position at JET facilities is achieved by changing the radial magnetic field produced by the current flow on dedicated coils. Such current is regulated by the Vertical Stabilization (VS) system by means of a current amplifier named ERFA. At the time of experiment ♯78000 (used here) a previous amplifier FRFA (Fast Radial Field Amplifier) was in place. The VS system acts on the FRFA requesting a desired current $I_{FRFA,des}$ that is obtained as the sum of two terms: the "fast" velocity loop that reacts promptly to plasma vertical displacements and the "slow" current loop that aims at regulating I_{FRFA} to zero. The ripple generated by the power electronics present in the experiment affects the feedback signal Z_{PD}, which is obtained by combining suitable magnetic measurements (from the Mirnov coils). For the current application we have

$$y_r(t) = \alpha\, I_{FRFA}(t) + Z_{PD}(t) \tag{3.23}$$

where I_{FRFA} is the current flowing within the poloidal coil and the scaling factor $\alpha = 4 \cdot 10^4$ m/s/A. All these quantities are depicted in Figure 3.12, where it is evident that the specific value of α in the linear combination (3.23) is selected to eliminate the current bursts around time 17.72 (to be found whenever a nonzero voltage is applied to the FRFA) and to let the ripple signal emerge in y_r. The resulting signal y_r is of clear graphical significance (the ripple effect was hidden in the oscillations within I_{FRFA} and Z_{PD}) but its experimental meaning goes beyond the goal of this Chapter. The experimental data on which we tested our hybrid observer are the useful 20-second portion of pulse ♯78000.
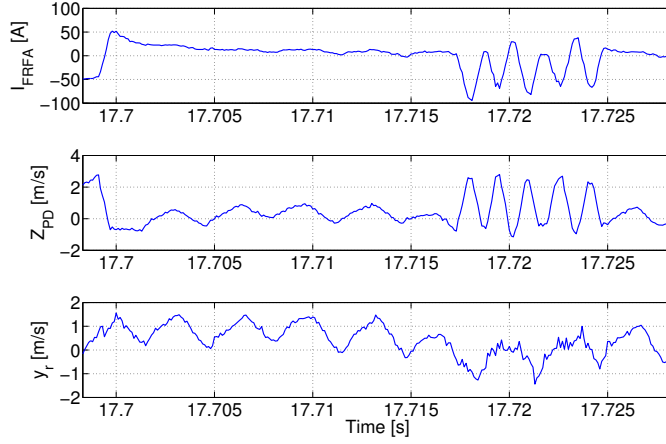
Figure 3.12: Experiment data from the JET tokamak: current I_{FRFA}, measurement Z_{PD} and their combination y_r.

To obtain a ripple-free signal, we apply the scheme in Figure 3.5 where we discard completely the "SIGNAL WITH RIPPLE DISTURBANCE" block and we inject directly into the "RIPPLE OBSERVER" block the signal y_r in (3.23). As a matter of fact, we have no longer a constant signal on which the ripple disturbance is superposed, but a signal that varies slowly with respect to the frequency of the ripple, as one can see from the bottom of Figure 3.12. As clarified after Problem 3.1, our solution also applies to this case, as long as the signal $\bar{b}$ is sufficiently slowly varying. In particular, based on Fact 2.8 we have the following Corollary. Fact 2.8 is itself a consequence of robust asymptotic stability for compact attractors and under the hybrid basic conditions, as illustrated in Section 2.4.

COROLLARY 3.1 *For every $\ell > 0$, every $k_{av} \in (0, 1]$ and a small enough value of $k_\theta > 0$, the selection $L := \begin{bmatrix} \ell \\ 0 \end{bmatrix}$ in (3.15a) guarantees that the compact attractor $\mathcal{A}_e$ in (3.19) is uniformly locally asymptotically stable for the closed-loop dynamics (3.3), (3.15), (3.18), with the second equation in (3.3a) replaced by $\dot{\bar{b}} \in [-\rho_b, \rho_b]$, where ρ_b is a sufficiently small positive constant.*

Note that the modified dynamics for $\bar{b}$ in the above statement enables considering "biases" that are varying at a sufficiently small rate ρ_b. According to the discussion after Problem 3.1 (see Eqs. (3.6) and (3.7c)) the signal resulting from the ripple cancellation filter corresponds to

$$\hat{\sigma} := y_r - \hat{d} = y_r - \left(\hat{x}_{r1} - \tfrac{3}{\pi}|\hat{x}_r|\right). \tag{3.24}$$

Figure 3.13 is obtained for the following parameters and initial values of the hybrid observer in (3.15) and (3.18): $\ell = 7.5$, $k_{av} = 0.9$, $k_\theta = 1$, $\bar{y}_r(0,0) = -0.5 \cdot 10^6$, $\bar{y}_{rI}(0,0) = 0$, $\eta(0,0) = 0$, $\tau(0,0) = 0$, $\hat{\theta}(0,0) = 0$, $x_f(0,0) = \begin{bmatrix} 0 \\ 0 \end{bmatrix}$, $\hat{x}_r(0,0) = \begin{bmatrix} 9.6 \cdot 10^6 \\ 0 \end{bmatrix}$ (leading to a phase shift of roughly $90°$). Following the discussion at the beginning of Section 3.5.1 about implementing slightly inflated versions of flow and jump sets, in the current case of JET measurements we used only $\{\xi: \frac{\pi}{3\omega} \leqslant \tau \leqslant 1.005\frac{\pi}{3\omega}\}$ instead of $\{\xi: \tau = \frac{\pi}{3\omega}\}$ since we have no longer a ripple generator. This forces the maximal hybrid solutions to be also complete (see Definition 2.5) and prevents numerical perturbations from bringing solutions out of $\mathcal{C} \cup \mathcal{D}$, leading to premature termination of complete solutions. At the bottom of Figure 3.13 we have both y_r and $\hat{\sigma}$ on the full timescale. In the upper part, the beginning of the time history is zoomed on the left, and the end on the right (same zoom as in Figure 3.12). The red vertical lines correspond to the instants when the *estimate* $\hat{\theta}$ jumps: at the beginning they are not in phase with the original signal y_r while at the end they are, so that after convergence the hybrid observer effectively removes from y_r the ripple disturbance $\hat{d}$ in the right central part of Figure 3.13.
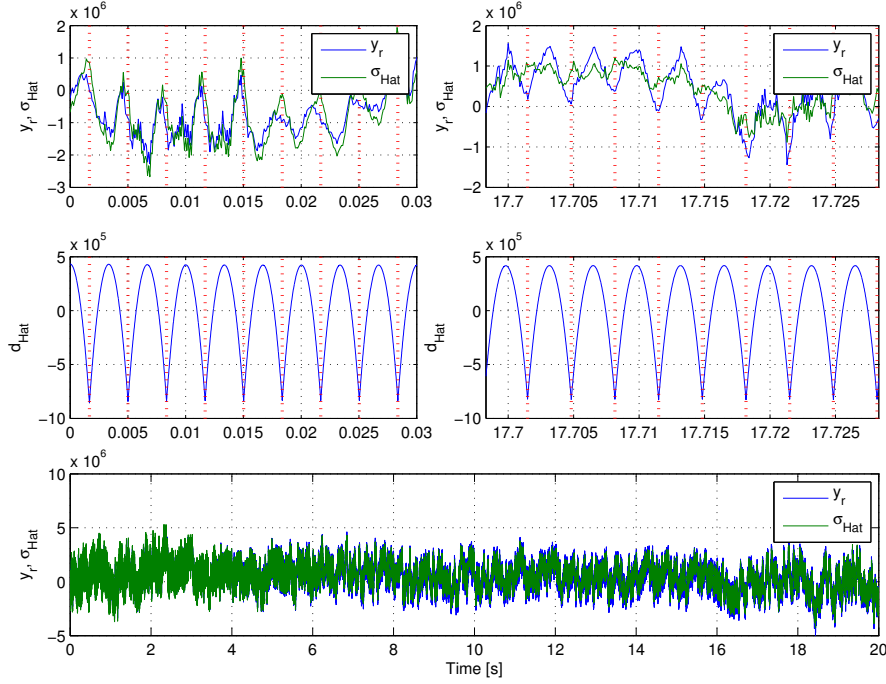
Figure 3.13: Original signal y_r, desirable signal $\hat{\sigma}$ and ripple estimate $\hat{d}$ in different timescales.
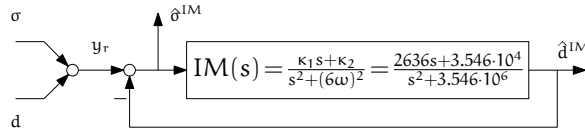
Figure 3.14: Internal model scheme and signals.

We compare our hybrid approach with one based on the internal model (IM) principle for linear systems [42]. According to the internal model principle, we may approximate the ripple disturbance d in y_r by a *pure* sinusoid with frequency 6ω, deliberately neglecting its nonsmoothness and thereby accepting a steady-state residual error. Then a standard unity-feedback system as in Figure 3.14 guarantees that $\hat{d}^{IM}$ approximately manages to converge to the main linear harmonic in d, and by subtracting $\hat{d}^{IM}$ from y_r one gets asymptotically some linear estimate $\hat{\sigma}^{IM}$ of the desirable signal σ. We note that the coefficients κ_1 and κ_2 in $IM(s)$ affect mainly the transient, and are less relevant for the (approximately) asymptotic tracking we want to show in Figure 3.15. The resulting $\hat{\sigma}^{IM}$ from this approach is plotted in Figure 3.15 together with $\hat{\sigma}$ from our hybrid approach, which provides an improved estimation because it is based on a more accurate model of the specific ripple waveform. In particular, note that the linear cancellation scheme exhibits noticeable errors where the ripple waveform is not differentiable.

We also compare our approach with the solution of a (nonlinear) optimization problem exploiting numerical tools. Consider as cost function the squared error between the (sampled) output y_r and the estimated signal $\hat{y}_r$ over a window of N past samples, that is,

$$J_N(k) := \sum_{i=0}^{N-1} \left(y_r(t_{k-i}) - \hat{y}_r(t_{k-i}) \right)^2 \tag{3.25}$$

$$\hat{y}_r(t_j) = \hat{\sigma}_j^J + \sqrt{3}V_f \max_{i \in \mathbb{Z}} \cos\left(\omega t_j + \theta_j - i\frac{\pi}{3} \right) - \frac{3\sqrt{3}}{\pi}V_f,$$

The minimization variables (in $\hat{y}_r$) are θ_k and $\hat{\sigma}_k^J$, and their optimal values are found iterating a numerical gradient descent algorithm on J_N (through `fmincon()` of the optimization toolbox of Matlab®). In our case we have $V_f = 1.8 \cdot 10^6$ and we take $N = 30$ samples, and the result is shown in Figure 3.15. This approach is similar to the one proposed in [85, 108] where Newton and extremum-seeking techniques have been exploited to minimize J_N. With this approach the computational complexity is much higher, the time spent by iterations at each new sample to provide the new value of θ_k and $\hat{\sigma}_k^J$ is not known a priori, and the resulting $\hat{\sigma}_k^J$ can be nonsmooth. Important high frequency information could be canceled out by this approach, whose proof of convergence is in general a difficult problem and has not been addressed for the considered example.
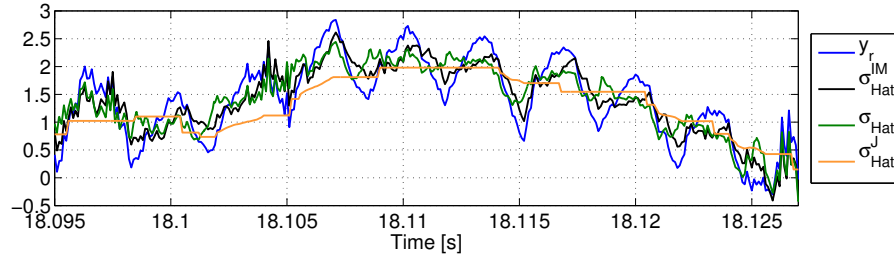
Figure 3.15: Original signal y_r and signals deprived of ripple: $\hat{\sigma}$ with our approach, $\hat{\sigma}^{IM}$ with the internal model scheme, $\hat{\sigma}^J$ by solving an estimation problem.

Although our hybrid observer scheme is presented for offline experimental data, we finally emphasize that it can be used for estimating and removing the ripple *on line*, so that an estimate of the desirable signal $\hat{\sigma}$ in (3.24) is available for feedback purposes.

GLOBAL RESULTS ON RESET-INDUCED PERIODIC SOLUTIONS OF PLANAR SYSTEMS

In this Chapter we study the existence of asymptotically stable periodic solutions induced by reset feedback. The analysis is developed for a planar system. Casting the problem into the setting of hybrid dynamical systems of Chapter 2, we show that a periodic orbit arises from the balance between the energy dissipated during flows and the energy restored by resets, at jumps. The asymptotic stability of the periodic orbit is studied with hybrid Lyapunov tools and the satisfaction of the so-called hybrid basic conditions ensures robustness of asymptotic stability. Extensions of the approach to more general mechanical systems are discussed.

The content of this Chapter is entirely based on [16].

4.1 INTRODUCTION: MOTIVATION AND APPROACH

Starting from the important theorem of Poincaré-Bendixson, many theoretical efforts have been made in the characterization of periodic orbits for planar continuous-time nonlinear systems, motivated by the pervasive presence of oscillators in electronics, mechanics and biology [49, 54]. A recent research direction seeks to extend this effort to the hybrid setting described in Chapter 2 in the sense that for a planar dynamical system, a suitable interplay of continuous flow and discrete jumps of the solutions leads to the existence of attractive periodic hybrid solutions. The relevance of this topic in engineering is readily shown by the studies on bipedal robotic walking, where periodic hybrid solutions arise from the combination of the free motion of the legs (continuous flow) with the impulsive action of the impacts to the ground (discrete jumps) [119, 124].

The paper provides a stability analysis of hybrid periodic solutions for planar mechanical systems based on the hybrid Lyapunov stability tools described in Section 2.5. The main motivation for the paper comes from the literature on variable impedance actuators, typically adopted in robotics. Strongly inspired by biological musculoskeletal systems, these actuators have a tunable stiffness and/or damping, which play a relevant role to improve motion efficiency [51, 63–65]. For multi-body systems with frequency separation between first and subsequent natural modes, [62] and [65] show that periodic oscillations can be obtained by means of simple switching control laws tuned only on the first natural mode. Taking advantage of a number of hybrid tools, we revisit and extend the results in [62]. We model the dynamics in [62] as a hybrid system and we show the existence of a unique (hybrid) periodic orbit corresponding to when the energy dissipated during flow balances the energy restored by the reset control action at a jump. The asymptotic stability of the periodic orbit follows from the decrease along system solutions of a suitable Lyapunov function tailored on the kinetic and potential energies just after and just before a jump.

The most relevant advantage of the approach is the intrinsic (in-the-small) robustness of asymptotic stability (see Section 2.4), which makes possible the use of the reset feedback law in applications. The robustness of the design guarantees that the stability of the attractor persists, and is degraded with continuity, in the presence of small parameter perturbation or when the instantaneous reset law is replaced by a (sufficiently) fast continuous actuation.

The asymptotic stability of the attractor holds for any parameter configuration that allows for a unique periodic orbit. This follows from the fact that the Lyapunov function is based on the mechanical energy just after and just before a jump. Its minimum is represented on the phase space by the set of points such that the dissipated and restored mechanical energy are balanced. Its decay is a natural consequence

of the mechanical features of the system. Indeed, no explicit characterization of the periodic orbit is required.

We anticipate that our Lyapunov-based analysis has similarities with the classical Poincaré analysis of periodic orbits. The level sets of the Lyapunov function are univocally identified by the points of the hyperplane at which resets occur. This hyperplane plays the role of a Poincaré section. Namely, along the portion of solution starting from and returning to this hyperplane, the overall decrease of our Lyapunov function captures the convergence of the return map towards the fixed point. The advantage of a Lyapunov analysis is the characterization of the basin of attraction of the periodic orbit. In this sense, our approach is close in nature to the analysis of the rimless wheel in [104].

The chapter is organized as follows. The hybrid dynamics is discussed in Section 4.2. Sections 4.3 and 4.4 provide conditions for the existence of periodic hybrid solutions and for their stability. The corresponding technical proofs are postponed to Section 4.7. Simulations in Section 4.5 illustrate the convergence towards the unique hybrid periodic orbit of the system. A comparison with the literature and further discussions are reported in Section 4.6.

4.2 DESCRIPTION OF THE SYSTEM

Based on [62], consider the classical mass-spring-damper mechanical system

$$m\ddot{q} + c\dot{q} + k(q - \theta) = 0 \tag{4.1}$$

with mass, damping and elastic constants respectively m, c, k. q is the displacement of the mass and θ is the control input. The elastic force provided by the spring is proportional to the difference $q - \theta$. The role of θ is to enforce a variation in the stored potential energy of the spring. Following [51], θ could represent in a hopping robot the process of preloading the spring during the flight phase; the spring is then released by a clutch mechanism when touching the ground.

In what follows θ is piecewise constant: it toggles between $-\hat{\theta}/2$ and $\hat{\theta}/2$ when the solutions of the system pass through the hyperplane defined by $\{(q, \dot{q}) \in \mathbb{R}^2 \colon q - \theta = 0\}$. $\hat{\theta} > 0$ is a design parameter such that $\frac{1}{2}k\hat{\theta}^2$ is the amount of potential energy loaded in the spring at switches (further comments on its role can be found in Remark 4.2). Switches on θ can be considered as the limit of a very fast continuous action on the spring, a kick of energy, rapidly moving θ from one value to the other in $\{-\hat{\theta}/2, \hat{\theta}/2\}$.

With coordinates $x_1 := q - \theta$ and $x_2 := \dot{q}$, we represent the dynamics of the system according to the formalism of Section 2.1. Since θ is constant, the flow dynamics reads

$$\dot{x} = \begin{bmatrix} \dot{x}_1 \\ \dot{x}_2 \end{bmatrix} = f(x) := \begin{bmatrix} x_2 \\ -\frac{c}{m}x_2 - \frac{k}{m}x_1 \end{bmatrix}, \quad x \in \mathcal{C}. \tag{4.2a}$$

The flow set $\mathcal{C}$ enabling flow dynamics is given by

$$\mathcal{C} := \{x \in \mathbb{R}^2 \colon x_1 x_2 \leqslant 0\} \cup \{x \in \mathbb{R}^2 \colon |x_1| \geqslant \hat{\theta}, x_1 x_2 \geqslant 0\}. \tag{4.2b}$$

The jump dynamics reads

$$x^+ \in G(x) := \begin{bmatrix} \hat{\theta}\,\overline{\mathrm{sgn}}(x_2) \\ x_2 \end{bmatrix}, \quad x \in \mathcal{D} \tag{4.2c}$$

where

$$\overline{\mathrm{sgn}}(x_2) := \begin{cases} \mathrm{sign}(x_2) & \text{if } x_2 \neq 0 \\ \{1, -1\} & \text{if } x_2 = 0. \end{cases}$$

The jump set $\mathcal{D}$ enabling jump dynamics is given by

$$\mathcal{D} := \{x \in \mathbb{R}^2 \colon x_1 = 0\}. \tag{4.2d}$$
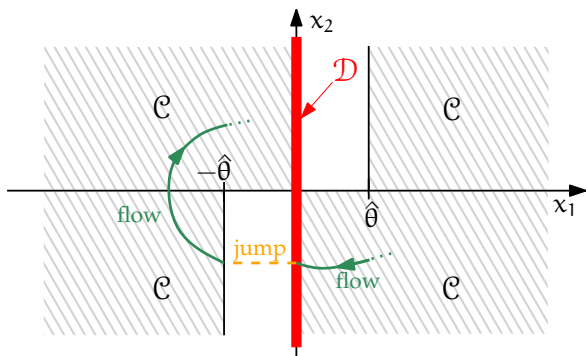
Figure 4.1: Flow set $\mathcal{C}$ and jump set $\mathcal{D}$ on the phase plane.

Figure 4.1 provides a graphical illustration of the flow and jump set on the system phase plane. Equation (4.2d) allows jumps to occur when $q - \theta =: x_1 = 0$. For $x_2 \neq 0$, we have that $|x_1|$ is reset from 0 to $|x_1^+| = \hat{\theta}$, that is, $|q^+ - \theta^+| = |q - \theta^+| = \hat{\theta}$. Indeed, the reset corresponds to a switch in the equilibrium position of the spring, through actuation. We do not reset the mass position q. Because of the described reset policy, it makes sense that when using the coordinates (x_1, x_2) (instead of $(q, \dot{q})$), the set $\mathcal{C} \cup \mathcal{D}$ is not $\mathbb{R}^2$.

The behavior of the solutions is illustrated in Figure 4.2 for a system with parameters $m = 1$ kg, $c = 0.3$ Ns/m, $k = 1$ N/m, $\hat{\theta} = 0.2$ m, for two different initial conditions. The two solutions converge asymptotically to an attractor defined by the image of a hybrid periodic solution, where periodicity must be intended in a hybrid sense as clarified in the next section.
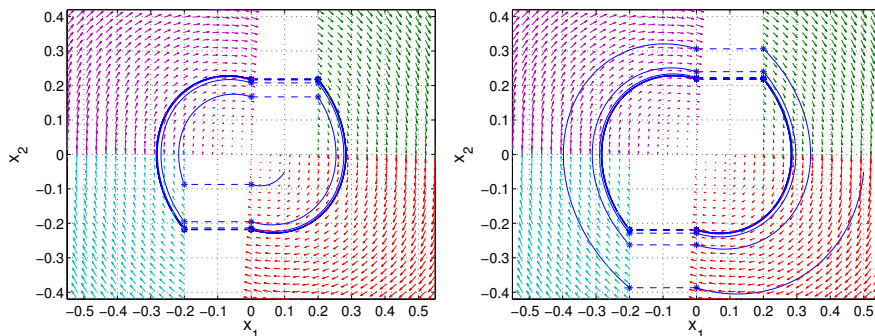
Figure 4.2: Phase plot of hybrid solutions. Left: $(x_{1,0}, x_{2,0}) = (0.1, -0.05)$. Right: $(x_{1,0}, x_{2,0}) = (0.5, -0.05)$.

REMARK 4.1 *In (4.2c) we used the set-valued mapping $\overline{\mathrm{sgn}}$ to guarantee that the graph of the jump map $x \mapsto G(x)$ is a closed set. This feature ensures the outer semicontinuity of G. Outer semicontinuity of G combined with the continuity of f and with the fact that $\mathcal{C}$ and $\mathcal{D}$ are closed sets guarantees that hybrid system (4.2) satisfies the hybrid basic conditions in Section 2.2. In Chapter 2 we noted the manifold benefits induced by these conditions, among which regularity of the solution set and robustness to small perturbations.* ⌙

4.3   UNIQUENESS OF THE HYBRID PERIODIC ORBIT

The notion of periodicity for a hybrid solution in Definition 4.1 is a straightforward extension of the usual notion of periodicity. The notions of solution, complete solution and domain can be found in Definitions 2.4, 2.5 and 2.2, respectively.

DEFINITION 4.1 (Hybrid periodic solution and orbit) *Given any hybrid system* $\mathcal{H} =$ $(\mathcal{C}, f, \mathcal{D}, G)$*, a hybrid periodic solution is a complete solution* x *for which there exists a pair* (T, J) *with either* $T \in \mathbb{R}_{\geqslant 0}$ *and* $J \in \mathbb{Z}_{>0}$ *or* $T \in \mathbb{R}_{>0}$ *and* $J \in \mathbb{Z}_{\geqslant 0}$ *such that* $(t, j) \in \mathrm{dom}(x)$ *implies* $(t + T, j + J) \in \mathrm{dom}(x)$ *and, moreover,*

$$x(t, j) = x(t + T, j + J). \tag{4.3}$$

The image of x *is a hybrid periodic orbit.*

The following standing assumption on the parameters of the hybrid dynamics (4.2) is necessary for the existence of a nontrivial[1] hybrid periodic solution.

ASSUMPTION 4.1 $\hat{\theta}$, m, c *and* k *are strictly positive. The roots of* $ms^2 + cs + k = 0$ *are complex conjugate, that is* $\left(\frac{c}{2m}\right)^2 - \frac{k}{m} < 0$.

Assumption 4.1 guarantees that $m\ddot{x}_1 + c\dot{x}_1 + kx_1 = 0$ is an underdamped mechanical system [84, Chap. 2.2]. When the system is not underdamped, there is no guarantee that a nontrivial hybrid periodic solution exists. With real eigenvalues in the flow map, the solutions of the system may converge to the origin according to the direction of the eigenvector corresponding to the slowest eigenvalue, lying in the second/fourth quadrant for $m, c, k > 0$. In such a case, the solutions to (4.2) exhibit at most one jump and the origin is a globally asymptotically stable equilibrium.

The existence of a nontrivial hybrid periodic orbit follows from energy considerations. Consider the ⌐-shaped curve $\mathcal{C}_0$ represented in Figure 4.3, given by the set

$$\mathcal{C}_0 := \{x \in \mathbb{R}^2 \colon |x_1| = \hat{\theta}, x_1 x_2 \geqslant 0\} \cup \{x \in \mathbb{R}^2 \colon |x_1| \leqslant \hat{\theta}, x_2 = 0\}. \tag{4.4}$$

Under Assumption 4.1, the solutions starting from $\mathcal{C}_0$ necessarily flow until they reach $\mathcal{D}$. More specifically, flowing solutions from any $x \in \mathcal{C}$ in forward (respectively, backward) time reach the set $\mathcal{D}$ (respectively, $\mathcal{C}_0$) in *finite* time because of the revolving nature of the flow solutions. The following quantities are thus well defined.

- *Backward energies.* By denoting by (x_{1b}, x_{2b}) the intersection with $\mathcal{C}_0$ after flowing in backward time from x,

$$T_b(x) := \frac{1}{2}mx_{2b}^2 \qquad U_b(x) := \frac{1}{2}kx_{1b}^2 \tag{4.5a}$$

  are the *backward kinetic* and *backward potential* energies, respectively.

- *Forward energies.* By denoting by (x_{1f}, x_{2f}) the intersection with $\mathcal{D}$ after flowing in forward time from x,

$$T_f(x) := \frac{1}{2}mx_{2f}^2 \tag{4.5b}$$

  is the *forward kinetic* energy.

Figure 4.3 shows the level sets of T_b, U_b and T_f, which coincide indeed to flowing portions of solutions to (4.2), because on such flowing portions T_b, U_b and T_f are constant.

For each $x \neq 0$ the quantity $T_b(x) + U_b(x)$ is the total mechanical energy of the system right after a jump. The quantity $T_f(x)$ is the total mechanical energy of the system after a maximal[2] flow, that is, right before a jump. The difference between these two energies corresponds to the dissipation during flows.

The reset of θ injects energy into the system in the form of potential energy. This fact and the central symmetry of the phase portrait (namely, if ϕ is a solution to (4.2), $-\phi$ is a solution as well) imply that a hybrid periodic orbit corresponds to the set of points satisfying the energy balance

$$T_b(x) + U_b(x) = T_f(x) + \frac{1}{2}k\hat{\theta}^2, \tag{4.6}$$

---

1 A nontrivial hybrid periodic orbit comprises more than one point.
2 In the same sense of *maximal* solutions as in Definition 2.4, namely that it can not be extended further.
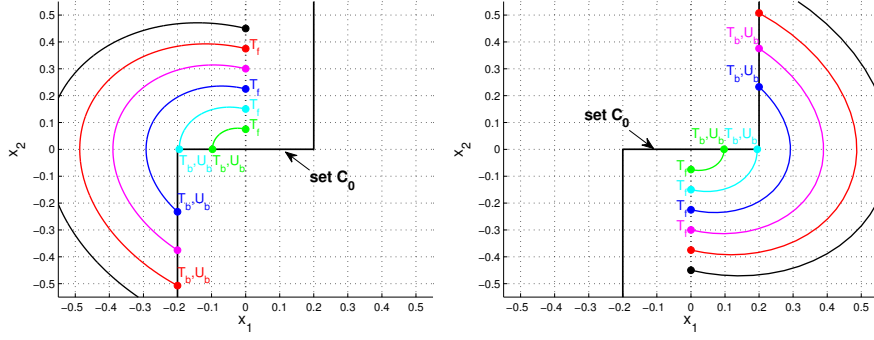
Figure 4.3: Set $\mathcal{C}_0$. Flowing solutions. The curves from $\mathcal{C}_0$ to $\mathcal{D}$ are level sets of T_b, U_b and T_f.

where the last term represents precisely the potential energy injected by a reset. Given the mentioned central symmetry, $x \neq 0$ belongs to a hybrid *periodic* orbit only if $U_b(x) = \frac{1}{2}k\hat{\theta}^2$, so that (4.6) is equivalent to

$$T_b(x) = T_f(x). \tag{4.7}$$

Indeed, suppose that there exist x on the hybrid periodic orbit with $U_b(x) < \frac{1}{2}k\hat{\theta}^2$. Then, for the periodicity of the hybrid orbit, it must be possible to jump to $\mathcal{C}_0 \cap \{x \colon |x_1| < \hat{\theta}\}$. But this is not admitted by the jump map in (4.2c), so it must be $U_b(x) = \frac{1}{2}k\hat{\theta}^2$.

The energy dissipated by solutions starting on $\mathcal{C}_0$ is derived in the next Lemma, proven in Section 4.7.1.
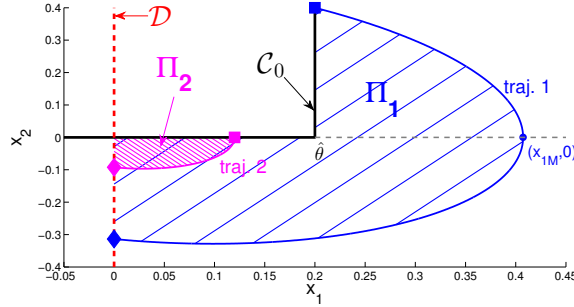
Figure 4.4: The hatched area is proportional to the energy dissipated by damping.

LEMMA 4.1 *Consider any solution x to (4.2) flowing from $\mathcal{C}_0 \setminus \{0\}$ at ordinary time t_1 to $\mathcal{D}$ at ordinary time $t_2 \geqslant t_1$ and define the total mechanical energy at x as*

$$E(x) := \frac{1}{2}mx_2^2 + \frac{1}{2}kx_1^2.$$

The dissipated energy between t_1 and t_2 is $E(x(t_1)) - E(x(t_2))$ and equal to $c\Pi$, where Π is the (unsigned) area within the curves given by the image of the solution, the set $\mathcal{C}_0$ and the set $\mathcal{D}$ (hatched area in Figure 4.4).

As flowing solutions cannot intersect, it is clear from Figure 4.4 that for $x = (x_1, x_2) \in \mathcal{C}_0$ the area $\Pi(x)$ is a strictly increasing function of $|x|$, and so is the dissipation. Its monotonicity with respect to initial conditions on $\mathcal{C}_0$ implies that there is only one initial condition on $\mathcal{C}_0$ for which (4.6) holds, that is, there exists a unique hybrid periodic orbit. We have then the following Theorem.

THEOREM 4.1 *Under Assumption 4.1, there exists a unique nontrivial hybrid periodic orbit for the hybrid system (4.2). $T_b(x) = T_f(x)$ at each point x of the hybrid periodic orbit.*

REMARK 4.2 *Because of the monotonicity property we have established, the role of parameter* $\hat{\theta}$ *can be further commented on. Since $\frac{1}{2}k\hat{\theta}^2$ corresponds to the potential energy introduced at switches, larger $\hat{\theta}$'s result in larger periodic orbits. This is evident when comparing Figures 4.2 and 4.6, corresponding to values of $\hat{\theta}$ equal to respectively 0.2 m and 0.3 m.* ⌐

4.4   GLOBAL ASYMPTOTIC STABILITY OF THE HYBRID PERIODIC ORBIT

The stability of the nontrivial hybrid periodic orbit is a set stability problem. Consider the attractor given by

$$\mathcal{A} := \{x \in \mathcal{C}: T_b(x) = T_f(x), x \neq 0\}. \tag{4.8}$$

Energy considerations similar to those in the previous section readily show that $\mathcal{A}$ is compact and forward invariant (see the proof of Lemma 4.2). The images of all nontrivial hybrid periodic solutions of (4.2) coincide with $\mathcal{A}$. Attractivity and stability of the periodic motion follow from the next theorem.

THEOREM 4.2 *Under Assumption 4.1, the set $\mathcal{A}$ in (4.8) is an asymptotically stable attractor for the hybrid system (4.2) with basin of attraction $\mathcal{B}_{\mathcal{A}} = \mathbb{R}^2 \setminus \{0\}$.*

The origin $x = 0$ is not in $\mathcal{B}_{\mathcal{A}}$ because it is a weak equilibrium: solutions to (4.2) starting from the origin can flow forever staying at the origin; they may jump to $-\hat{\theta}$ or $\hat{\theta}$ and then converge to the hybrid periodic orbit or they may flow in the origin for a while and then jump to $-\hat{\theta}$ or $\hat{\theta}$. Moreover, all x's not belonging to $\mathcal{C} \cup \mathcal{D}$ are in the basin of attraction as noted after Definition 2.11.

We remark that the stability of the set $\mathcal{A}$ does *not* require an explicit characterization of the hybrid periodic orbit. We only need to ensure the feasibility of the balance in (4.6) (or, equivalently, (4.7)). Therefore, by Theorems 4.1 and 4.2, the reset feedback law induces a hybrid periodic solution for every parameter selection that satisfies Assumption 4.1.
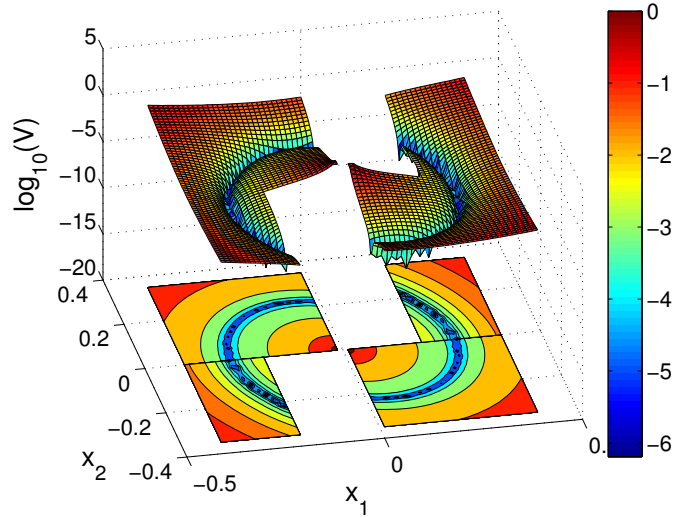
Figure 4.5: The Lyapunov function V in logarithmic scale.

The proof of Theorem 4.2 is based on a Lyapunov argument. Using the definitions in (4.5), consider the Lyapunov function candidate for $\mathcal{A}$ given by

$$V(x) := \frac{(U_b(x) + T_b(x) - T_f(x) - \frac{1}{2}k\hat{\theta}^2)^2}{U_b(x)}. \tag{4.9}$$

The shape and the level sets of V are illustrated in Figure 4.5. Note that the Lyapunov function V blows up as x approaches 0 (the boundary of $\mathcal{B}_{\mathcal{A}}$) and as x grows unbounded, as shown in Figure 4.5 for the same parameter selection of Figure 4.2.

The next lemma is a key step towards proving Theorem 4.2, and is proven in Section 4.7.2.

LEMMA 4.2 *Under Assumption 4.1, the set $\mathcal{A}$ in (4.8) is nonempty and compact and the Lyapunov function V in (4.9)*

(i) is positive definite with respect to $\mathcal{A}$ on $\mathcal{B}_{\mathcal{A}} \cap (\mathcal{C} \cup \mathcal{D})$, namely

$$
\begin{aligned}
V(x) &= 0 \quad \text{if } x \in \mathcal{A} \\
V(x) &> 0 \quad \text{if } x \in \mathcal{B}_{\mathcal{A}} \cap (\mathcal{C} \cup \mathcal{D}) \backslash \mathcal{A} \\
&\lim_{\substack{|x| \to 0^+ \\ |x| \to +\infty}} V(x) = +\infty
\end{aligned}
\tag{4.10a}
$$

(ii) is constant in the flow direction[3]

$$
\langle \nabla V(x), f(x) \rangle = 0, \quad \forall x \in \mathcal{C}
\tag{4.10b}
$$

(iii) provides strict decrease across jumps[4]

$$
V(G(x)) - V(x) < 0, \quad \forall x \in \mathcal{B}_{\mathcal{A}} \cap \mathcal{D} \backslash \mathcal{A}.
\tag{4.10c}
$$

REMARK 4.3 *Item (i) of Lemma 4.2 implies that for any indicator function ω of $\mathcal{A}$ on $\mathcal{B}_{\mathcal{A}}$ (see Definition 2.15) there exists class $\mathcal{K}_\infty$ functions $\underline{\alpha}$ and $\overline{\alpha}$ such that*

$$
\underline{\alpha}(\omega(x)) \leqslant V(x) \leqslant \overline{\alpha}(\omega(x)).
\tag{4.11}
$$

This is just a local version of Lemma 2.1. Moreover, from the global version of Fact 2.6 we obtain that the asymptotic stability property established in Theorem 4.2 is robust on $\mathcal{B}_{\mathcal{A}}$. ⌟

To obtain Theorem 4.2, we need to combine the properties of V in Lemma 4.2 with the next Lemma, which is proven in Section 4.7.3.

LEMMA 4.3 *Solutions to (4.2) enjoy a semiglobal persistent jumping property (enunciated within Fact 2.15 and in Remark 2.1).*

Based on Lemma 4.2, the proof of Theorem 4.2 is a mere application of Lyapunov results described in Section 2.5. In particular, Lemma 4.2 establishes that function V in (4.9) is a weak Lyapunov function for the compact attractor $\mathcal{A}$, in the sense of Equations (2.42) in Fact 2.15. Indeed, the fact that $\mathcal{A}$ is compact is sufficient to obtain that (4.10a) implies (4.11) for any indicator function ω and suitable class $\mathcal{K}_\infty$ functions $\underline{\alpha}$, $\overline{\alpha}$. Moreover, (4.10b) coincides with (2.42b) and (4.10c) coincides with (2.42c) because $\mathcal{A}$ is compact. As a consequence, we may apply a local generalization of Fact 2.15 and Remark 2.1, as already illustrated in Application 2.4, because of the semiglobal persistent jumping established in Lemma 4.3.

4.5 SIMULATION RESULTS

We simulate the hybrid system (4.2) with the same parameters adopted in Figure 4.2, corresponding to $m = 1$ kg, $c = 0.3$ Ns/m, $k = 1$ N/m (eigenvalues $s_{1,2} = -0.15 \pm i0.9887$, consistent with Assumption 4.1). Instead of $\hat{\theta} = 0.2$ m we enforce a reset to the larger value $\hat{\theta} = 0.3$. Compared to Figure 4.2, the hybrid periodic orbit becomes larger as shown in the upper part of Figure 4.6. The bottom part of Figure 4.6 shows the values of the Lyapunov function and of the states (x_1, x_2) as functions of the ordinary time.

---

3 We do not give a formal proof of smoothness of V in our derivation, therefore it would be more appropriate to use the directional derivative of V in (4.10b). We use here the gradient notation to keep the discussion simple.

4 Note that $\overline{\mathrm{sgn}}(x_2)$ is single-valued for all $x \in \mathcal{D} \cap \mathcal{B}_{\mathcal{A}} = \{x \in \mathbb{R}^2 : x_1 = 0, x_2 \neq 0\}$ because it is set-valued only at $x_2 = 0$.
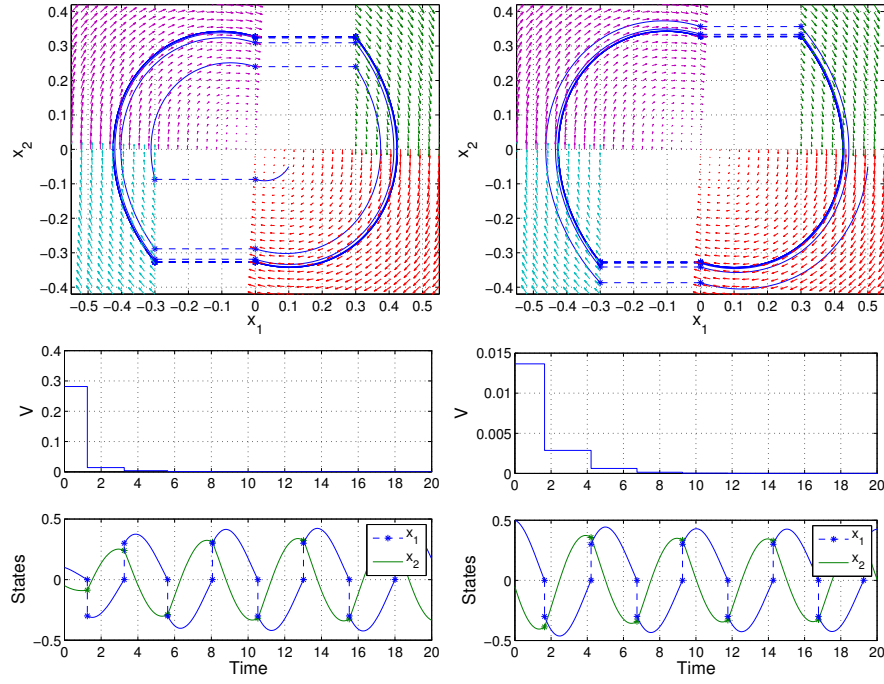
Figure 4.6: Upper part: phase plot of the solutions. Bottom part: Lyapunov function and hybrid solutions projected on ordinary time for the two initial conditions. Left: initial condition $(0.1, -0.05)$. Right: initial condition $(0.5, -0.05)$.

4.6   CONCLUSIONS AND FUTURE RESEARCH

Following [62], different hybrid periodic orbits can be generated by exploiting different reset laws. Within the hybrid characterization (4.2), one of the switching laws proposed in [62] is captured by the alternative flow and jump sets $\mathcal{C}_{\text{alt}}$ and $\mathcal{D}_{\text{alt}}$ given in Figure 4.7a: $\hat{\theta} \geqslant 2\epsilon_{\phi}$ and $\epsilon_{\phi} > 0$ is a new control parameter, whose role is commented in Remark 4.4. We have then the hybrid system

$$\dot{x} = f(x), \quad x \in \mathcal{C}_{\text{alt}}$$

$$x^+ = G_{\text{alt}}(x) := \begin{bmatrix} x_1 + \hat{\theta}\, \text{sign}(x_2) \\ x_2 \end{bmatrix}, \quad x \in \mathcal{D}_{\text{alt}}. \tag{4.12}$$

With the parameter values of Section 4.5, the simulation of a number of solutions is reported in Figure 4.7b. The approach and results in Sections 4.3 and 4.4 can be extended to capture the stability properties of this new hybrid system, to show the existence of a globally asymptotically stable hybrid periodic orbit. Figure 4.7 shows the potentiality of the hybrid characterization in (4.2) in the sense that a number of reset feedback laws can be modeled by variations on the definitions of the flow and jump sets and of the jump map (see [62]). The monotonicity of the dissipated energy is crucial for the uniqueness of the attractor. Within the family of reset feedback guaranteeing existence and uniqueness of an asymptotically stable hybrid periodic orbit, the system in Chapter 5 is a relevant instance.

REMARK 4.4 *By a suitable change of coordinates, (4.12) can be transformed into (5.8), so that the relationships hold:*

$$-\bar{y} + \bar{u} = \epsilon_{\phi} \tag{4.13a}$$

$$\bar{y} + \bar{u} = -\epsilon_{\phi} + \hat{\theta}, \tag{4.13b}$$

where $\bar{y}$ and $\bar{u}$ are quantities defined in (5.6) in Chapter 5. In Section 5.3, we discuss design guidelines to achieve a desired frequency and amplitude for the oscillations of (5.8), or

(a) Flow and jump sets.   (b) solutions.

Figure 4.7: $\epsilon_\phi = 0.2$ and $\hat{\theta} = 0.6$.

equivalently (4.12), *through the control parameters $\bar{y}$ and $\bar{u}$. Because of the linear transformation in* (4.13), *ϵ_ϕ and $\hat{\theta}$ can be equivalently used to the same end. We refer the reader to Section 5.3 for a more clear discussion on the effect of the two parameters.* ⌙

It is natural to consider mechanical systems with elastic potentials typical of nonlinear springs, so that (4.2a) would read $\dot{x}_2 = -\frac{c}{m}x_2 - \frac{1}{m}\frac{\partial U}{\partial x_1}$ where the potential U is any positive definite function. A necessary condition for the existence of an attractor with basin $\mathbb{R}^2\backslash\{0\}$ is the strict monotonicity of the elastic potential, namely the positivity of the function $x_1 \mapsto x_1\frac{\partial U(x_1)}{\partial x_1}$. In fact, the lack of strict monotonicity may lead to the coexistence of several attractors. The minimal requirement for the existence of globally attractive hybrid periodic orbits is that the linearization of the flow dynamics at the origin has complex conjugate eigenvalues, which is a straightforward generalization of Assumption 4.1. Otherwise, solutions that are sufficiently close to the origin would flow towards it remaining in the second/fourth quadrant, without triggering any reset. Tight sufficient conditions for the existence of a global attractor for general elastic potentials are addressed in Chapter 5.

Finally, the generality of a Lyapunov approach for stability analysis calls for extensions of the method to more general mechanical systems. One further step is the analysis of n-dimensional linear mechanical systems perturbed by resets. We also recall that the model in (4.2), albeit an abstraction, stems from the robotics context. Further analysis in Chapter 5 will investigate the potential of a similar model for robotic applications, in particular the one of legged locomotion.

4.7 TECHNICAL PROOFS

4.7.1 *Proof of Lemma 4.1*

The work performed by the nonconservative viscous force $F_d = cx_2$ in moving the point mass from a position 1 to a position 2 causes a change $E_2 - E_1$ in the total mechanical energy [84, Page 9]. With the aid of Figure 4.4, let us exemplify it on solutions like "traj. 1" and denote x_{1M} the value at which a solution crosses the line $x_2 = 0$, so that *on the solution* x_2 can be expressed as function of x_1 for each half-plane $x_2 > 0$, $x_2 < 0$. Then, by splitting the integral relative to the work in two pieces, we get $E(x(t_2)) - E(x(t_1)) = \int_{\hat{\theta}}^{x_{1M}} -(cx_2)dx_1 + \int_{x_{1M}}^{0} -(cx_2)dx_1 = -c\Pi < 0$.

4.7.2   *Proof of Lemma 4.2*

The proof of this fact relies on Lemma 4.1. From (4.9),

$$V(x) = \frac{\left(\overbrace{U_b(x) + T_b(x)}^{E_b(x)} - \overbrace{T_f(x)}^{E_f(x)} - \overbrace{\frac{1}{2}k\hat{\theta}^2}^{=:\hat{U}} \right)^2}{U_b(x)} = \frac{(c\Pi(x) - \hat{U})^2}{U_b(x)}, \qquad (4.14)$$

where E_b and E_f are the total energies of the system right after and right before a jump, respectively; $\hat{U}$ is the potential energy at $\left[\begin{smallmatrix} \hat{\theta} \\ 0 \end{smallmatrix} \right] \in \mathcal{C}_0$; $\Pi(x)$ is the (positive) area spanned by the solution passing through x during a flow from $\mathcal{C}_0$ (where E_b is evaluated) to $\mathcal{D}$ (where E_f is evaluated); and $c > 0$ is the damping coefficient in (4.1). Figure 4.4 provides two examples for $\Pi(x)$.

We are now ready to prove Lemma 4.2. First notice that, due to the uniqueness of flowing solutions, the function $x \mapsto \Pi(x)$ is necessarily strictly increasing as x moves farther from the origin (or any compact set). Denote by $c\Pi_0 := c\Pi\left(\left[\begin{smallmatrix} \hat{\theta} \\ 0 \end{smallmatrix} \right] \right)$ the dissipated energy when starting from the corner of set $\mathcal{C}_0$ in (4.4). Moreover, denote by $c\Pi^\star := \frac{1}{2}k\hat{\theta}^2 = \hat{U}$ the dissipated energy associated to the hybrid periodic orbit. Note that $\Pi^\star > \Pi_0$ necessarily, because $c\Pi_0$ cannot be larger than the total energy $\hat{U} = c\Pi^\star$ at the beginning of the corresponding solution starting from the corner of $\mathcal{C}_0$. Then,

$$\mathcal{A} = \{x \in \mathcal{C} : \Pi(x) = \Pi^\star, \ x \neq 0\}, \qquad (4.15)$$

which proves that it is non-empty and compact. We prove now the three items of the Lemma.

Item (i). Since $V(x)$ in (4.14) is non-negative and zero if and only if $\Pi(x) = \Pi^\star$, from expression (4.15) we obtain $V(x) = 0$ if and only if $x \in \mathcal{A}$ and positive otherwise. Moreover, as x approaches zero, we have that $U_b(x)$ tends to zero, which implies $V(x) \to \infty$. Since $U_b(x) \leqslant \hat{U}$ for all x due to the structure of $\mathcal{C}_0$, $\lim_{|x| \to \infty} \Pi(x) = +\infty$ implies $\lim_{|x| \to \infty} V(x) = +\infty$.

Item (ii). This item follows straightforwardly from the fact that by construction $V(x)$ remains constant during flow.

Item (iii). First of all notice that $x = \left[\begin{smallmatrix} x_1 \\ x_2 \end{smallmatrix} \right] \in \mathcal{D}$ implies $x_1 = 0$ and that $G(x) = \left[\begin{smallmatrix} \hat{\theta}\mathrm{sign}(x_2) \\ x_2 \end{smallmatrix} \right]$ for all $x \in \mathcal{D} \cap \mathcal{B}_{\mathcal{A}}$. We split the proof in three cases. We only consider jumps from points in the negative part of $\mathcal{D}$ (namely $x_2 < 0$) because of the central symmetry of the phase portrait. We also use the simplified notation Π^+ to denote $\Pi(x^+)$. Similar simplifications will be used for other quantities.
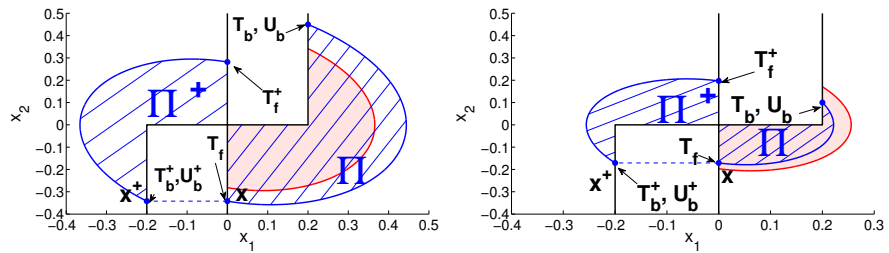
Figure 4.8: Left: $\Pi > \Pi^\star > \Pi_0$. Right: $\Pi^\star > \Pi > \Pi_0$. Pink areas are Π^+ mirrored about the origin.

Case 1: $\Pi > \Pi^\star > \Pi_0$. First of all, by uniqueness of solutions $\Pi^+ > \Pi^\star$, otherwise the flow would intersect the hybrid periodic orbit. Consider the left part of Figure 4.8 and note that $\Pi > \Pi^\star$ implies $\Pi^+ < \Pi$. Indeed, exploiting $U_b^+ = U_b = \hat{U} = c\Pi^\star$ and $T_b + U_b = T_f + c\Pi$ and $T_f^+ = T_f$, we get $T_b = T_f + c\Pi - c\Pi^\star > T_f = T_b^+$. $\Pi > \Pi^+$ follows by monotonicity. Finally, the result is proven from

$$0 = c\Pi^\star - \hat{U} < c\Pi^+ - \hat{U} < c\Pi - \hat{U}.$$

Case 2: $\Pi^\star > \Pi > \Pi_0$. First of all, $\Pi^+ < \Pi^\star$ again from uniqueness of solutions. Consider the right-part of Figure 4.8 and note that $\Pi_0 < \Pi < \Pi^\star$ implies $\Pi^+ > \Pi$. In fact, following the argument of Case 1, we have that $U_b^+ = U_b = \hat{U} = c\Pi^\star$ and $T_b + U_b = T_f + c\Pi$ and $T_b^+ = T_f$ thus $T_b = T_f + c\Pi - c\Pi^\star < T_f = T_b^+$. The result is proven from

$$0 = c\Pi^\star - \hat{U} > c\Pi^+ - \hat{U} > c\Pi - \hat{U}.$$
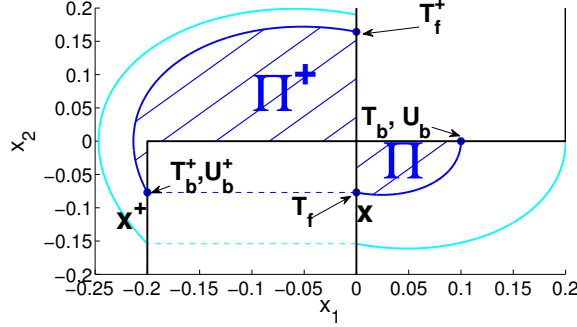
Figure 4.9: Case 3: $0 < \Pi < \Pi_0$.

Case 3: $0 < \Pi < \Pi_0$. Consider Figure 4.9. In this case we have $U_b < \hat{U}$ because U_b is evaluated on the horizontal part of $\mathcal{C}_0$. Then

$$
\begin{aligned}
V^+ - V &= \frac{(c\Pi^+ - \hat{U})^2}{\hat{U}} - \frac{(c\Pi - \hat{U})^2}{U_b} \\
&< \frac{(c\Pi^+ - \hat{U})^2}{\hat{U}} - \frac{(c\Pi - \hat{U})^2}{\hat{U}}.
\end{aligned}
$$

Now, observe that $c\Pi^+ < \hat{U} = c\Pi^\star$ because otherwise the forward solution from x^+ would intersect the flowing portion of the hybrid periodic orbit (thus contradicting uniqueness). Then, using $\hat{U} > 0$, we get $V^+ - V < 0$ from

$$(c\Pi^+ - \hat{U})^2 - (c\Pi - \hat{U})^2 = c\underbrace{(\Pi^+ - \Pi)}_{>0}(\underbrace{c\Pi^+ - \hat{U}}_{<0} + \underbrace{c\Pi - \hat{U}}_{<0}) < 0,$$

where we used *(i)* $\Pi^+ > \Pi$ from Π^+ being evaluated from the vertical part of $\mathcal{C}_0$ and *(ii)* $c\Pi < \hat{U}$ from $c\Pi < U_b$.

4.7.3 *Proof of Lemma 4.3*

This property is verified combining semiglobal practical persistent jumping defined within Fact 2.15 and in Remark 2.1, and in principle it involves the set $\mathfrak{S}_\Delta := ((\mathcal{A} + \Delta\mathbb{B})\backslash\mathcal{A}) \cap \mathcal{B}_\mathcal{A}$ for each $\Delta > 0$ (the intersection with the basin of attraction is introduced to have a local version of semiglobal persistent jumping). However, for a simpler verification of the property, we can always find Δ' generating the set $\mathfrak{S}'_\Delta := \Delta'\mathbb{B} \cap \mathcal{B}_\mathcal{A}$ such that $\mathfrak{S}'_\Delta \supset \mathfrak{S}_\Delta$ and then the solutions corresponding to the restrictions $\mathcal{C} \cap \mathfrak{S}'_\Delta$, $\mathcal{D} \cap \mathfrak{S}'_\Delta$ from (2.41) are a subset of the solutions corresponding to the restrictions $\mathcal{C} \cap \mathfrak{S}_\Delta$, $\mathcal{D} \cap \mathfrak{S}_\Delta$. Then we set out to verify the semiglobal persistent jumping property on solutions corresponding to the restriction with $\mathfrak{S}'_\Delta$.

For solutions that are not complete, a large enough $N \geqslant 0$ can always be found to satisfy (2.43).

On the other hand, for each $\Delta' > 0$ and complete solutions, there exists a maximum time τ_{RD} between each pair of consecutive jumps in the domain of the solutions[5] to the restricted hybrid system, and τ_{RD} is strictly less than the length of the first flow interval of a solution to the nonrestricted hybrid system starting from

---

5 That is, a uniform reverse dwell time.
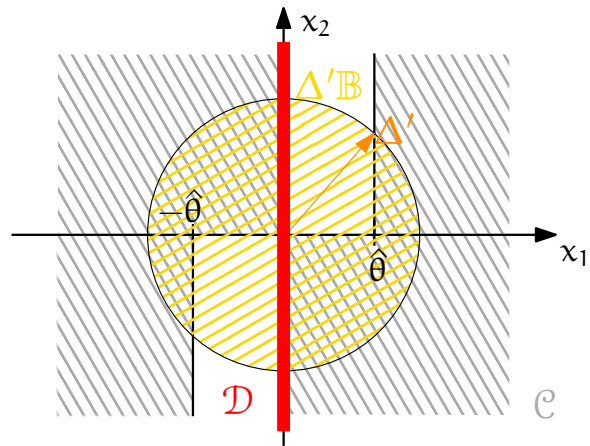
Figure 4.10: Flow set $\mathcal{C}$ and jump set $\mathcal{D}$ and $\Delta'\mathbb{B}$.

$x(0,0) = \begin{bmatrix} \hat{\theta} \\ \Delta' \end{bmatrix}$. This upper bound of τ_{RD} holds because the flow map is given by the linear system in (2.3a), for which solutions starting on the same ray take the same time to reach the ray $\{x \colon x_1 = 0, x_2 \leqslant 0\}$ (where they jump), and a ray passing through $\begin{bmatrix} \hat{\theta} \\ \Delta' \end{bmatrix}$ bounds from above the one taking the largest time. An illustration is provided in Figure 4.10. Moreover, complete solutions cannot jump twice at the same ordinary time but there is always a flow portion between any two consecutive jumps. Therefore, for each Δ' and complete solutions, (2.43) is satisfied with $j \geqslant t/\tau_{RD}$.

5

RESET CONTROL OF MINIMAL-ORDER MECHANICAL
SYSTEMS

In this Chapter we present for the same second order nonlinear mechanical system two reset control strategies allowing to either sustain or damp oscillations. These two behaviors are seen here as complementary aspects, in the sense that a suitable mirroring of the jump map associated to the reset strategy suffices to go from one behaviour to the other. We first present our results building on classical tools from reset control (relay feedback) applied to nonlinear mechanical systems. Then we take some first steps toward turning our stability results into a design procedure for the case of sustaining oscillations. We show the applicability of the two reset control strategies to the case of a hopping mass and an automotive suspension. The final section contains the proofs of the results, where some powerful facts from the hybrid system framework can be exploited after we provide a hybrid system formulation of the closed-loop system. The arguments of the proofs also draw many conclusions from the physically intuitive notions of energy for the considered mechanical system.

The content of this chapter is based on [17].

5.1 INTRODUCTION: LITERATURE CONNECTIONS AND APPLICABILITY OF THE FRAMEWORK

This chapter focuses on nonlinear mechanical systems and two fundamental behaviors that can be induced by reset control, namely, sustain or damp oscillations. Both behaviors can be obtained through suitable reset strategies on the same reference mechanical system, which is a second order system with nonlinear potential gradient modulated by the control input, and a damping coefficient that can depend on both position and velocity, as long as the damping increases with the absolute value of the velocity.

In the same spirit of [45] (or [55] for a broader approach encompassing neurobiology and biomechanics) and the templates mentioned in [43], we claim the use of *minimal order* mechanical systems in this chapter because they *can* provide the fundamental explanation to the phenomena of reset-sustained and reset-damped oscillations, as we show for the applications in Section 5.4. At the same time, considering minimal order systems allows us to come up with design procedures like in Section 5.3. (As future work, we intend to show that the properties of these phenomena are preserved also when we consider more complex models under suitable timescale separations.)

We decide to present our results in the settled framework of reset control, in Sections 5.2.1 for sustaining oscillations and in Section 5.2.2 for damping them. The promising features of reset control for generating limit cycles have been extensively studied for a linear system with a relay feedback interconnection (see, e.g., [70, §18.1.8] and references therein). Indeed, in the case of sustained oscillations with linear potential gradient, our results boil down to the classical work in [7] (see also Remark 5.1). The reset framework is intended to make the results more accessible because their scope is at an intersecting point among different technical fields (control theory, robotics and automotive, as we will discuss later). At the same time, the system described here can be presented through the state-dependent switching [72, §1.1.1]. At any rate, the reset framework (as well as the switching framework, see [47, §1.4]) can be included in the larger class of hybrid dynamical systems in Chapter 2, upon whose formalism a more rigorous description and the proofs of the results rely heavily. Therefore, a hybrid system formulation is provided in the exposition before the proofs in Sections 5.5.1 and 5.5.2, respectively parallel to Sections 5.2.1 and 5.2.2. Our analysis also draws arguments from the classical tools of Poincaré section and map [54].

Strictly connected to the minimal order of the model, our reset control laws have the virtue of simplicity, both in terms of the sensing and the actuation required. Indeed, we need one sensor to detect when the position reaches a certain threshold and our actuation is limited to a discrete number of values for the input u (two). In this sense, our results can be viewed as an instance of quantized control, although the focus of this chapter is different from the typical objectives in such a scientific area, which are to guarantee stabilizability of an equilibrium in a semiglobal practical sense and at the same time to provide upper bounds on the rate of transitions in the control action [32, 44]. On the other hand, our objective for reset-sustained oscillations is the global asymptotic stability of the periodic orbit, and for reset-damped oscillations it is to preserve the global asymptotic stability of the natural equilibrium of the unactuated solution while draining more energy with respect to that unactuated solution (thereby accelerating the convergence to the natural equilibrium). The two behaviours of reset-sustained and reset-dampened oscillations are unified in the sense that they arise for the same underlying mechanical system and a simple mirroring of the jump set can produce one behaviour or the other.

We discuss now the relationship with Chapter 4, which constitutes preliminary work for the results in this chapter. We address here a fairly more general mechanical system in view of the allowed nonlinearities that we have just discussed. Additionally, for this same system we also use a reset approach to favour the reduction of mechanical vibrations. Finally, in Section 5.4 we present two relevant engineering applications of the proposed framework, namely a hopping mass from robotics and a (semi-active) suspension from automotive. On the other hand, Chapter 4 has its own interest because because of the Lyapunov construction associated to the periodic orbit, which is not pursued here.

The framework in this chapter is motivated by some newly devised actuators, such as the variable impedence actuators in [121] and [68] for legged locomotion, whose very fast action resembles the introduction of a kick of energy to the mechanical system and can be modelled by a controller reset (an alternative approach close to the nature of this work would be [106]).

We show the applicability of the proposed framework to two relevant engineering applications: a hopping mass from robotics illustrates the main result of Section 5.2.1 (sustain oscillations), and a (semi-active) suspension from automotive the one of Section 5.2.2 (damp oscillations). The hopping mass is the first milestone in legged locomotion for robots, as witnessed by the impact of the seminal work [100]. [68, 101, 126] testify to the applicability of the present reset approach to legged locomotion. A similar approach can be found also in [66]. Moreover, the potentiality of applying hybrid system techniques in the context of legged locomotion is pointed out in [50], and addressed in technical terms in [119] using the same hybrid system formalism as here (or in [107], for the close setting of juggling systems). In locomotion, the presence of unilateral constraints due to contact forces leads naturally also to the hybrid systems formalism of complementarity systems in [111]. For the suspension, the proposed reset actuation makes it fall into the category of semi-active suspensions, for which we refer the reader to the survey [96] (or [110] and references therein).

The chapter is organized as follows. Section 5.2 introduces the second order mechanical system and the common ingredients in the reset control law. Section 5.2.1 addresses how to sustain oscillations in this mechanical system through reset control by presenting the overall closed-loop system and the asymptotic stability result. Section 5.2.2 addresses how to damp oscillation in the same mechanical system through a suitably modified reset strategy. Section 5.3 presents a design procedure in a simple linear setting, and discusses its applicability to weakly nonlinear oscillators. Section 5.4 describes two significant applications of the proposed framework, namely a hopping mass in Section 5.4.1 and an automotive suspension in Section 5.4.2. Finally, a formulation according to the hybrid systems formalism, the proofs and the more technical analysis of the various sections are collected in Section 5.5.

Notation. $\mathbb{Z}_{\geqslant 0}$ denotes the nonnegative integers. For a solution $t \mapsto \psi$, domψ denotes its domain; for a hybrid solution $(t, j) \mapsto \phi$, domϕ denotes its hybrid time

Figure 5.1: Curve $s \mapsto \gamma(s)$ and related sets C_i and D_i.

domain (see Definition 2.2). For any set S, $\overline{S}$ denotes its closure. $\mathbb{B}$ denotes the closed unit ball.

5.2 TWO BEHAVIOURS FOR ONE MECHANICAL SYSTEM THROUGH RESET CONTROL

We present in this section how to sustain or damp oscillations in the same mechanical system. For convenience of presentation, the system is recalled within each of the following subsections 5.2.1 and 5.2.2, and the different reset laws are described therein. However, we show here the unifying features of the two approaches.

We start from the same nonlinear planar mechanical system

$$m\ddot{y} + c(y, \dot{y})\dot{y} + \frac{\partial U}{\partial y}(y, u) = 0, \tag{5.1}$$

where y is the position, $\dot{y}$ is the velocity, $\ddot{y}$ is the acceleration, m is the mass, $c(y, \dot{y})$ is the nonlinear damping coefficient, and $U(y, u)$ is the nonlinear potential whose dependence on the position y is modulated by u, that we use as a control input to the system. The underlying properties that we require of (5.1) are essentially contained in Assumption 5.1 (with minor additions for the damping case in Assumption 5.2).

Oscillations in (5.1) are sustained or damped by simple, piecewise constant, reset laws for the input u. Indeed, we partition the state space $(y, \dot{y})$ in two regions through a curve γ or γ' as in the Figures 5.1 and 5.3. These partitions are C_i, $i = 1, 2$, where $u = u_i$ is applied. Resets occur when the curve γ or γ' are crossed at positions y_i, $i = 1, 2$. In this way, both minimal actuation (a limited number of u_i) and minimal sensing (detection of a limited number of thresholds y_i) are achieved.

5.2.1 Reset-sustained oscillation

We show now that

$$m\ddot{y} + c(y, \dot{y})\dot{y} + \frac{\partial U}{\partial y}(y, u) = 0, \tag{5.2a}$$

whose quantities were defined after (5.1), can be controlled into steady state oscillations by simple, piecewise constant, reset laws for the input u with the approach we outlined above at the beginning of Section 5.2.

Based on Figure 5.1, consider the curve

$$\gamma(s) := \begin{cases} (y_2, s - y_2) & s \leqslant y_2 \\ (s, 0) & y_2 \leqslant s \leqslant y_1 \\ (y_1, s - y_1) & s \geqslant y_1, \end{cases} \tag{5.2b}$$

where y_1 and y_2 are two *constant* values. γ divides the plane $(y, \dot{y})$ into the two regions

$$C_1 := \{(y, \dot{y}) : (\dot{y} < 0, y_2 < y \leqslant y_1) \text{ or } y > y_1\} \tag{5.2c}$$

$$C_2 := \{(y, \dot{y}) : (\dot{y} > 0, y_2 \leqslant y < y_2) \text{ or } y < y_2\}. \tag{5.2d}$$

We pursue minimal actuation complexity, so we resort to a binary control action u depending on the state $(y, \dot{y})$ as

$$u = \begin{cases} u_1 & \text{if } (y, \dot{y}) \in C_1 \\ u_2 & \text{if } (y, \dot{y}) \in C_2, \end{cases} \tag{5.2e}$$

where u_1 and u_2 are two *constant* values. At the same time, we also keep a minimal sensing complexity because the resets are triggered when the state $(y, \dot{y})$ is detected to cross the branches

$$\{\gamma(s) \colon s \geqslant y_1\} =: D_1 \tag{5.2f}$$
$$\{\gamma(s) \colon s \leqslant y_2\} =: D_2. \tag{5.2g}$$

Solutions are well defined in view of their hybrid definition that we postpone to Section 5.5.1. We define then the following standard concepts.

DEFINITION 5.1 *Orbit denotes the image of a solution to* (5.2). *A periodic solution is a solution* ψ *defined for all nonnegative times for which there exists* $T > 0$ *such that* $t \in \mathrm{dom}(\psi)$ *implies* $t + T \in \mathrm{dom}(\psi)$ *and, moreover,*

$$\psi(t) = \psi(t + T).$$

A periodic orbit is the image of a periodic solution, and is nontrivial *if it comprises more than one point.*

Based on this definition, we can characterize the asymptotic stability for system (5.2) according to the classical notions for nonlinear systems. The resets act as a "kick" of energy for the system, with oscillations arising from the balance between the energy introduced by the resets and the energy dissipated during the flow. The uniqueness of a globally asymptotically stable steady-state oscillation is guaranteed under mild conditions on the reset law and on the system nonlinearities.

ASSUMPTION 5.1 *The functions* $(y, \dot{y}) \mapsto c(y, \dot{y})\dot{y}$ *is Lipschitz in each of the domains* $\overline{C}_1$ *and* $\overline{C}_2$, *and the functions* $y \mapsto \frac{\partial U}{\partial y}(y, u_1)$ *and* $y \mapsto \frac{\partial U}{\partial y}(y, u_2)$ *are Lipschitz in* $\overline{C}_1$ *and* $\overline{C}_2$, *respectively. Moreover,*

$$c(y, \dot{y}) \geqslant c_\epsilon > 0 \quad \text{for all } (y, \dot{y}) \tag{5.3a}$$

$$\left.\begin{aligned} \frac{\partial c}{\partial \dot{y}}(y, \dot{y}) \geqslant 0 \quad \text{for all } \dot{y} > 0 \text{ and all } y \\ \frac{\partial c}{\partial \dot{y}}(y, \dot{y}) \leqslant 0 \quad \text{for all } \dot{y} < 0 \text{ and all } y \end{aligned}\right\} \tag{5.3b}$$

$$\left.\begin{aligned} \frac{\partial U}{\partial y}(y, u_1) > 0 \quad \text{for all } y \text{ such that } (y, \dot{y}) \in \overline{C}_1 \\ \frac{\partial U}{\partial y}(y, u_2) < 0 \quad \text{for all } y \text{ such that } (y, \dot{y}) \in \overline{C}_2. \end{aligned}\right\} \tag{5.3c}$$

Condition (5.3a) is trivially satisfied by any (nonideal) mechanical system. Conditions (5.3b) and (5.3c) restrict the nonlinearity of the damping coefficient and the potential to monotone functions in regions defined by the sign of $\dot{y}$ and in the regions $\overline{C}_i$, respectively. We have the following general result.

THEOREM 5.1 *For the mechanical system* (5.2) *satisfying Assumption 5.1, there exists a unique nontrivial periodic orbit that is globally asymptotically stable.*

A hybrid system formulation of (5.2) and the proofs of the presented results are postponed to Section 5.5.1.

REMARK 5.1 *The result in Theorem 5.1 is connected to the classical contribution [7], where the input to a linear time invariant single-input-single-output system is obtained through*
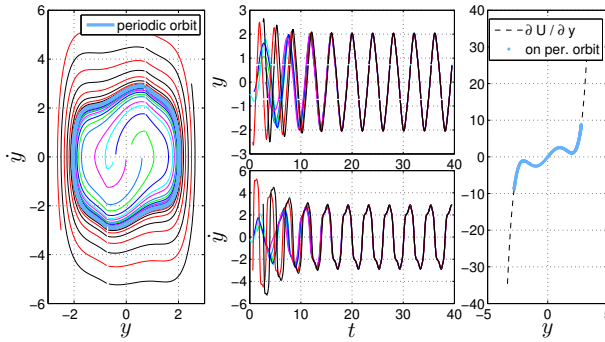
Figure 5.2: Example 5.1 for a nonlinear potential gradient. Left: periodic orbit. Center, top: position y. Center, bottom: velocity $\dot{y}$. Right: potential gradient curve (black), and portion explored when y is on the periodic orbit (light blue).

a feedback relay and necessary conditions are provided for the local stability of the resulting periodic solution, possibly in the presence of time delays on the input. System (5.8) in Section 5.3 can be recast using a formulation with a relay. However, in this chapter we provide sufficient conditions for global asymptotic stability of a fully nonlinear mechanical system in the previous theorem (directly for asymmetric oscillations, that is, $|u_1| \neq |u_2|$ and $|y_1| \neq |y_2|$).

EXAMPLE 5.1 *We illustrate Theorem 5.1 on a simple mass-spring-damper whose nonlinear stiffness is modulated by the input u. We choose the parameters $m = 1$ kg, $c = 0.3$ Ns/m, $\frac{\partial U}{\partial y}(y, u) = 4(y - u) - \frac{5}{3}(y - u)^3 + \frac{1}{5}(y - u)^5$. The potential gradient $\frac{\partial U}{\partial y}(y, 0)$ is the black curve in the right part of Figure 5.2, which we design to have a local minimum that could represent the drop in the stress curve after a yield point for ductile materials. As for the reset law, fix $u_2 = -u_1 = 0.75$ m and $y_1 = -y_2 = 0.75$ m, in a symmetric fashion. u acts trivially as a horizontal translation in $\frac{\partial U}{\partial y}(y, u)$, so that (5.3c) is easily satisfied. The results are shown in Figure 5.2. In the left part, orbits for different initial conditions are depicted together with the periodic orbit they converge to. In the the center part we plot the corresponding solutions y and $\dot{y}$ for the same initial conditions. In the right part we add to the curve $\frac{\partial U}{\partial y}(y, 0)$ (shown in black) the pairs $\left(y, \frac{\partial U}{\partial y}(y, 0)\right)$ (shown in light blue) such that y lies on the periodic orbit depicted with the same color in the left part of the figure.*

5.2.2 *Reset-damped oscillations*

For the nonlinear mechanical system in (5.1)

$$m\ddot{y} + c(y, \dot{y})\dot{y} + \frac{\partial U}{\partial y}(y, u) = 0 \tag{5.4a}$$

simple reset laws can also be used to damp oscillations, by increasing the natural dissipation of the system, as we discussed above at the beginning of Section 5.2. In particular, we assume that (5.4a) has a globally asymptotically stable equilibrium point $(y_0, 0)$ when the input is at rest ($u = u_0$), so that a faster damping of the oscillations through resets accelerates the convergence to this attractor.

The damping of the oscillations is obtained by a reset law parallel to the one adopted in Section 5.2.1. Based on Figure 5.3, a suitable mirroring γ' of the reset

Figure 5.3: Reset law in (5.4): relevant quantities and sets.

curve γ in (5.2b) induces earlier reset instants, with the goal of extracting energy from the system. Then, u is determined according to

$$u = \begin{cases} u_1 & \text{if } (y, \dot{y}) \in C_1 \\ u_2 & \text{if } (y, \dot{y}) \in C_2 \end{cases} \tag{5.4b}$$

$$C_1 := \{(y, \dot{y}) \colon (\dot{y} > 0, y_1 < y \leqslant y_2) \text{ or } y > y_2\} \tag{5.4c}$$

$$C_2 := \{(y, \dot{y}) \colon (\dot{y} < 0, y_1 \leqslant y < y_2) \text{ or } y < y_1\}. \tag{5.4d}$$

Resets are triggered when the state $(y, \dot{y})$ crosses the branches

$$D_1 := \{(y, \dot{y}) \colon y = y_1, \dot{y} \geqslant 0\} \tag{5.4e}$$

$$D_2 := \{(y, \dot{y}) \colon y = y_2, \dot{y} \leqslant 0\} \tag{5.4f}$$

$$D_0 := \{(y, \dot{y}) \colon y_1 \leqslant y \leqslant y_2, \dot{y} = 0\}. \tag{5.4g}$$

When D_1 or D_2 are crossed, the control u toggles between u_1 and u_2, like in Section 5.2.1. On the other hand, when the branch D_0 is crossed, the system resets its actuation u to the rest value u_0, which globally stabilizes the equilibrium $(y_0, 0)$, with $y_1 < y_0 < y_2$, from any point of $C_0 := \mathbb{R}^2$. To ensure global asymptotic stability of $(y_0, 0)$ when $u = u_0$ is applied, we need the following sector assumption (5.5a) on the potential. Moreover, (5.5b)-(5.5c) guarantee a decrease in the potential energy when crossing the branch D_0, that is, resetting from u_1 to u_0 or from u_2 to u_0.

ASSUMPTION 5.2 *Given $y_1 < y_0 < y_2$,*

$$(y - y_0) \frac{\partial U}{\partial y}(y, u_0) > 0 \quad \text{for } y \neq y_0 \tag{5.5a}$$

$$\begin{rcases} U(y, u_0) - U(y, u_1) < 0 \\ U(y, u_0) - U(y, u_2) < 0 \end{rcases} \quad \text{for all } y \in [y_1, y_2]. \tag{5.5b} \tag{5.5c}$$

Proposition 5.1 establishes that each reset sequence causes a nonzero decrease of the total energy of the system, as compared to the case with no actuation ($u = u_0$). Draining energy from the system helps achieving faster damping of oscillations.

PROPOSITION 5.1 *Each solution to (5.4) undergoes a finite number of jumps that induce a nonzero decrease of the total energy defined in (5.27). In particular, for each $\bar{e} > 0$, there exists $N(\bar{e})$ such that all solutions with initial total energy smaller than $\bar{e}$ perform at most $N(\bar{e})$ jumps.*

REMARK 5.2 *Assumptions (5.5b)-(5.5c) are required to guarantee a nonzero decrease for each reset sequence (in particular for the tail of the sequence). Higher energy levels $\bar{e}$ induce more jumps $N(\bar{e})$. An upper bound on $N(\bar{e})$ is explicitly derived at the end of the proof of Proposition 5.1 on page 84, as a function of the bound δ on the dissipated energy at jumps in (5.44).*

Figure 5.4: Reset-controlled linear oscillator. (The quantity v will be defined and used in Section 5.5.3.)

Proposition 5.1 clarifies the desirable features of the proposed law, but also constitutes a key ingredient for proving Theorem 5.2, which establishes that the introduction of the resets preserves asymptotic stability.

THEOREM 5.2 *For the mechanical system* (5.4) *satisfying Assumptions 5.1 and 5.2,* $(y_0, 0)$ *is a globally asymptotically stable equilibrium point.*

A hybrid system formulation of (5.4) and the proofs of the presented results are postponed to Section 5.5.2.

5.3 DESIGN PROCEDURES

Section 5.2.1 showed that simple reset laws are an effective way to induce oscillations on a nonlinear mechanical system. In this section we discuss design guidelines on the reset law to achieve a desired frequency and amplitude for the closed-loop steady-state oscillations associated to the periodic orbit of Theorem 5.1, in the simple case of linear dynamics and symmetric curves and symmetric actuation for the reset law. We also discuss the applicability of these guidelines to a weakly nonlinear setting.

We set then

$$c(y, \dot{y}) = c > 0 \tag{5.6a}$$

$$\frac{\partial U}{\partial y}(y, u) = k(y - u) \tag{5.6b}$$

$$u_2 = -u_1 = \bar{u} > 0 \tag{5.6c}$$

$$y_1 = -y_2 = \bar{y} > 0, \tag{5.6d}$$

as represented in Figure 5.4. In Assumption 5.1, (5.3a)-(5.3b) are satisfied by selection (5.6a) and, given selections (5.6b)-(5.6d), (5.3c) becomes

$$1 < \frac{\bar{u}}{\bar{y}} =: \lambda. \tag{5.7}$$

The ratio λ is a relevant parameter for a coincise characterization of the closed-loop steady-state oscillations, as it will become evident in the following.

We rewrite conveniently system (5.2) under the simplifications in (5.6) as:

$$\ddot{y} + 2\xi\omega_n\dot{y} + \omega_n^2 y = \omega_n^2(-\bar{u}), \qquad (y, \dot{y}) \in C_1 \tag{5.8a}$$

$$\ddot{y} + 2\xi\omega_n\dot{y} + \omega_n^2 y = \omega_n^2\bar{u}, \qquad (y, \dot{y}) \in C_2, \tag{5.8b}$$

with natural frequency and damping ratio given by

$$\omega_n = \sqrt{\frac{k}{m}} \quad \text{and} \quad \xi = \frac{c}{2m\omega_n}. \tag{5.9}$$

The main result of this section shows that the frequency of the closed-loop steady-state oscillations is proportional to the natural frequency of the system, whereas

their amplitude is proportional to the magnitude of the reset parameter $\bar{y}$ shaping the switching curve γ.

THEOREM 5.3 *For all $\xi > 0$, the frequency ω_{reset} and the amplitude $y_{\max}$ of the closed-loop steady-state oscillations are given by*

$$\omega_{\text{reset}} = \omega_n \, \kappa(\xi, \lambda) \tag{5.10a}$$

$$y_{\max} = \bar{y} \, \psi(\xi, \lambda), \tag{5.10b}$$

for some suitable functions κ, ψ.
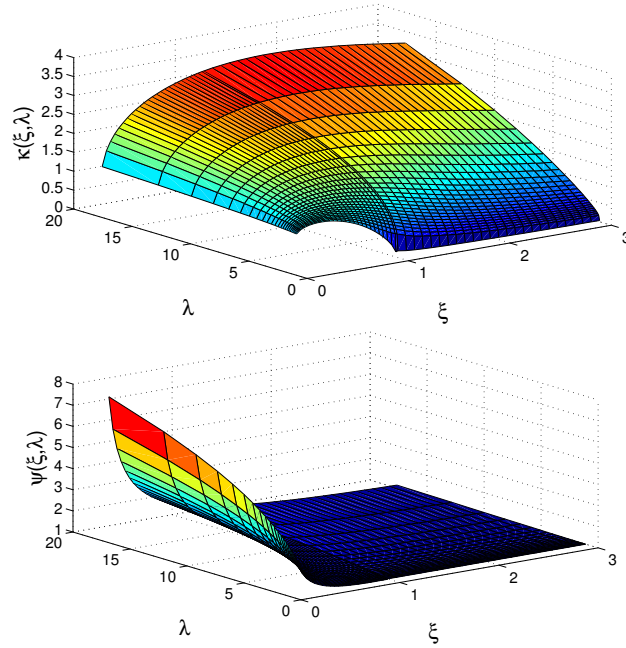
Figure 5.5: Top: $\omega_{\text{reset}} = \omega_n \kappa(\xi, \lambda)$ in (5.10a). Bottom: $y_{\max} = \bar{y}\psi(\xi, \lambda)$ in (5.10b).

An explicit expression for κ and ψ cannot be derived, but their shape in the parameter space (ξ, λ) is as shown in Figure 5.5 and is obtained through the solution of a numerical problem, which we detail in Section 5.5.3 together with the rest of the proof of Theorem 5.3.
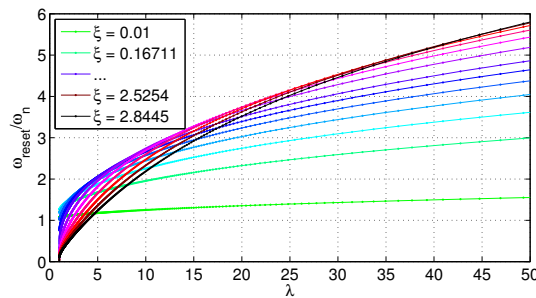
Figure 5.6: ω_{reset} as a function of λ for some (fixed) values of ξ.

Equations (5.10) and Figure 5.5 provide design guidelines to achieve a desired oscillation frequency ω_{reset} and amplitude $y_{\max}$ in closed loop. Suppose that the mechanical system is given, that is, ω_n and ξ have a predefined specific value.

1. Based on the desired value of ω_{reset}, we choose the corresponding value of λ according to the curve κ in (5.10a). In particular, in this phase we regard ξ as fixed, so that it is helpful to depict in Figure 5.6 the shape of ω_{reset} as a function of λ, for some fixed values of ξ. For fixed ξ, such curves are monotone with respect to λ. As it is evident also in Figure 5.5, only if $\xi > 1$ the image of κ can extend from 0 to $+\infty$.

2. Based on the desired value of y_{max}, we choose the corresponding value of $\bar{y}$ according to (5.10b) now that $\psi(\xi, \lambda)$ is fixed. Together with the value of λ in previous point, this determines $\bar{u} = \lambda\bar{y}$ from (5.7).

Adaptation laws can be implemented on top of the proposed guidelines to guarantee robustness with respect to parameter uncertainties.
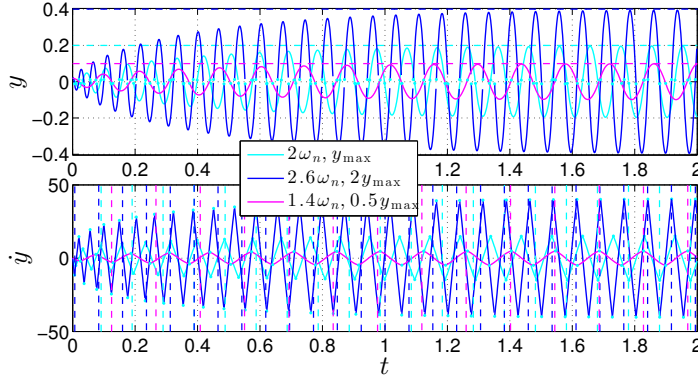
Figure 5.7: Solutions for different desired ω_{reset} and y_{max}.

EXAMPLE 5.2 *We illustrate the previous design criterion in Figure 5.7. The (open loop) parameters of (5.8) are $\omega_n = 2\pi 5.03$ rad/s and $\xi = 0.0316$, and we want to achieve through reset three different pairs $(\omega_{reset}, y_{max})$, that is, $(2\omega_n, 0.2)$, $(2.6\omega_n, 0.4)$ and $(1.4\omega_n, 0.1)$. The design criterion above returns the following pairs $(\lambda, \bar{y})$: $(55.51, 0.0087)$, $(157.13, 0.0119)$ and $(8.21, 0.0094)$. The solutions corresponding to each case (turquoise, blue and magenta, respectively) are shown in Figure 5.7. The fact that the desired frequency and height $(\omega_{reset}, y_{max})$ are achieved asymptotically is shown by the vertical and horizontal dashed lines. The horizontal lines in the upper part show the desired height y_{max} for each case. The vertical lines in the lower part mark the desired period $2\pi/\omega_{reset}$ (starting from the last reset) for each case. It is evident that after a transient the solutions converge to the desired height, and synchronize with the desired period of oscillation, which is different from their natural frequency.*

REMARK 5.3 *The design guidelines derived from Theorem 5.3 extend to weakly nonlinear mechanical systems (5.2a) with symmetric reset laws. If the nonlinear periodic behaviour can be approximated by a linear one with fitted parameters c_L and k_L, a simple input-to-state stability (ISS, [59, §4.9]) argument bounds the error between the unique (by Theorem 5.1) periodic solutions to the linear approximation and to the nonlinear system. This argument shows then that the frequency and amplitude of the closed-loop steady-state oscillations predicted in (5.10) are essentially preserved in the nonlinear setting.*

In particular, consider approximating the nonlinear dynamics in (5.2a) coupled with a symmetric reset law (characterized by $\bar{u}$ and $\bar{y}$) with the linear fitting considered in this section:

$$m\ddot{z} + c_L\dot{z} + k_L(z - u) = 0, \tag{5.11}$$
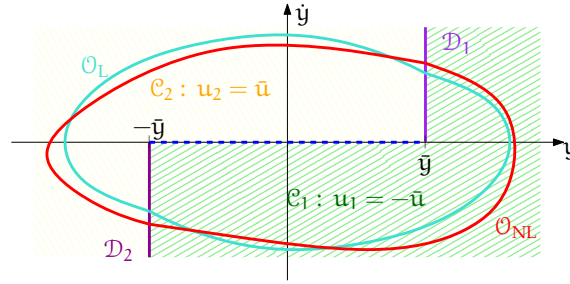
Figure 5.8: Fitting the parameters k_L and c_L of the linear oscillator unique periodic orbit $\mathcal{O}_L$ such that $\delta^\star$ is small, given the nonlinear oscillator unique periodic orbit $\mathcal{O}_{NL}$.

and write the error dynamics $e := z - y$

$$m\ddot{e} + c_L\dot{e} + k_L e = \delta(y, \dot{y}) :=$$
$$\left(c(y, \dot{y}) - c_L\right)\dot{y} + \frac{\partial U}{\partial y}(y, u(y, \dot{y})) - k_L(y - u(y, \dot{y})). \quad (5.12)$$

Consider Figure 5.8 where we depict the unique periodic orbits $\mathcal{O}_L$ for the flow in (5.11) and $\mathcal{O}_{NL}$ for the flow in (5.2a). On the compact region $\mathcal{O}_{NL}$, k_L and c_L are selected to obtain

$$\delta^\star := \min_{k_L, c_L > 0} \max_{y, \dot{y} \in \mathcal{O}_{NL}} |\delta(y, \dot{y})|. \quad (5.13)$$

For positive k_L and c_L, the error dynamics is ISS relative to the input δ in (5.12) because of [59, Lemma 4.6], so there exist a class $\mathcal{KL}$ function β_{ISS} and a class $\mathcal{K}$ function[1] γ_{ISS} such that

$$|e(t)| \leqslant \beta_{ISS}(|(e(0), \dot{e}(0))|, t) + \gamma_{ISS}(\sup_t |\delta(y, \dot{y})|).$$

As noted in [59, p. 175], e will be ultimately bounded by $\gamma_{ISS}(\sup_t |\delta(y, \dot{y})|)$: we are actually interested in this ultimate bound by γ_{ISS} because our objective is to bound the error when approximating (5.2a) with (5.11) and using then (approximately) the relations (5.10) for the asymptotic nonlinear periodic orbit. Moreover, by construction (5.13),

$$\gamma_{ISS}(\sup_t |\delta(y, \dot{y})|) \leqslant \gamma_{ISS}(\delta^\star). \quad (5.14)$$

The linear steady-state behavior is a good predictor of the nonlinear steady-state behavior when the gain γ_{ISS} is small and when the bound on the nonlinearity $\delta^\star$ is small. ⌐

5.4   APPLICATIVE EXAMPLES

We show in this section that the main previous results (Theorem 5.1 in Section 5.2.1 and Theorem 5.2 in Section 5.2.2) can already be applied fruitfully to two relevant engineering applications.

5.4.1   *Hopping robot*

Consider the hopping robot [100] in Figure 5.9, described by position y_h and velocity $\dot{y}_h$ and acted upon by the piecewise constant input u. The standard hopping behavior of the robot is defined by two main phases. During the *stance* phase the robot is attached to the ground and follows the dynamics of an oscillator. During the *flight* phase the robot is no longer attached to the ground and follows a ballistic

---

1 For a state space realization matrices (A, B) of the linear system (5.12) we have $\gamma_{ISS}(r) = \frac{2\lambda_{MAX}(P)^2 |B|}{\lambda_{min}(P)} r$ where P is the solution to the Lyapunov equation $PA + A^\top P = -I$.
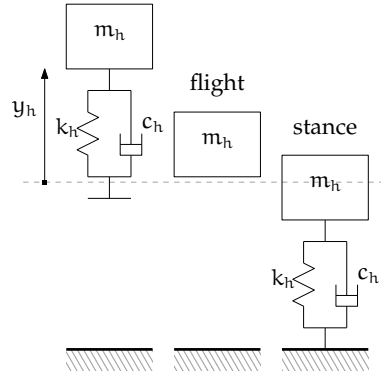
Figure 5.9: Hopping robot on a fixed spot.

motion. The transitions from stance to flight and from flight to stance correspond approximately to the spring being undeformed after having been loaded during the stance, and to the bottom end of the spring touching the ground after the flight, respectively. As in [68], the hopper is equipped with a motor that preloads the spring during the flight phase by a length θ (we assume that the spring can be shortened and preloaded fast enough during a flight phase). This storage of energy is then released via a clutch mechanism at the contact with the ground.

The preceding physical description motivates us to use the formulation in Section 5.2.1 and write a simplified model of the hopper. We specialize the reset curve γ in (5.2b) by setting $y_1 = \theta - \epsilon$ and $y_2 = 0$. The curve divides the space $(y_h, \dot{y}_h)$ into the regions

$$C_1 := \{(y_h, \dot{y}_h) \colon y_h > \theta - \epsilon \text{ or } (\dot{y}_h < 0, 0 < y_h \leqslant \theta - \epsilon)\} \tag{5.15a}$$

$$C_2 := \{(y_h, \dot{y}_h) \colon y_h < 0 \text{ or } (\dot{y}_h > 0, 0 \leqslant y_h < \theta - \epsilon)\} \tag{5.15b}$$

where C_1 correspond to the flight, and C_2 to the stance. The (small) parameter $\epsilon > 0$ is introduced to take into account uncertainties in the transition between stance and flight phases. $\epsilon = 0$ corresponds to the transition from stance to flight occuring *exactly* when the spring is undeformed after being loaded during stance. In practice the system enters into ballistic motion even if the spring is not fully extended yet. Our model does not capture this level of detail but the parameter $\epsilon > 0$ is used to model the anticipation of the transition from stance to flight.

In the flow regions the input takes the values

$$u = \begin{cases} 0 & \text{if } (y_h, \dot{y}_h) \in C_1 \\ \theta & \text{if } (y_h, \dot{y}_h) \in C_2 \,. \end{cases} \tag{5.15c}$$

Resets are triggered when crossing the curve

$$D_1 := \{(y_h, \dot{y}_h) \colon y_h = \theta - \epsilon, \dot{y}_h \geqslant 0\} \tag{5.15d}$$

$$D_2 := \{(y_h, \dot{y}_h) \colon y_h = 0 \; \dot{y}_h \leqslant 0\} \,. \tag{5.15e}$$

Finally, the continuous evolution in (5.2a) during flight ($u = u_1 = 0$ and potential $y_h \mapsto U(y_h, u_1) = mgy_h$) becomes

$$m\ddot{y}_h + c_1\dot{y}_h + mg = 0, \tag{5.15f}$$

where m is the mass, g is the gravity, and c_1 is the (small) air friction. During stance ($u = u_2 = \theta$ and potential $y_h \mapsto U(y_h, u_2) = \frac{1}{2}k(y_h - \theta)^2 + mgy_h$) (5.2a) becomes

$$m\ddot{y}_h + c_2\dot{y}_h + k(y_h - \theta) + mg = 0, \tag{5.15g}$$

where k is the stiffness, and c_2 combines possibly an actual mechanical damper, the structural damping and the dissipation occuring at the impact, so that typically

$c_2 \gg c_1$. Note that (5.15f) and (5.15g) can be merged into the single equation corresponding to (5.2a)

$$m\ddot{y}_h + c(y_h, \dot{y}_h)\dot{y}_h + \frac{\partial U}{\partial y_h}(y_h, u) = 0 \qquad (5.16)$$

where the damping c can be defined from c_1 and c_2, and $\frac{\partial U}{\partial y_h}$ from the two above potentials $y_h \mapsto U(y_h, u_1)$ and $y_h \mapsto U(y_h, u_2)$. The control u is determined by (5.15c).

For $\epsilon > 0$, consider a spring stiffness k such that

$$k\epsilon > mg.$$

Then, Assumption 5.1 is satisfied since $\frac{\partial U}{\partial y_h}(y_h, u_2) = k(y_h - \theta) + mg < 0$ in $\overline{C}_2$, therefore Theorem 5.1 guarantees that the hopper has a unique nontrivial periodic orbit which is asymptotically stable. We illustrate this result in the following example.
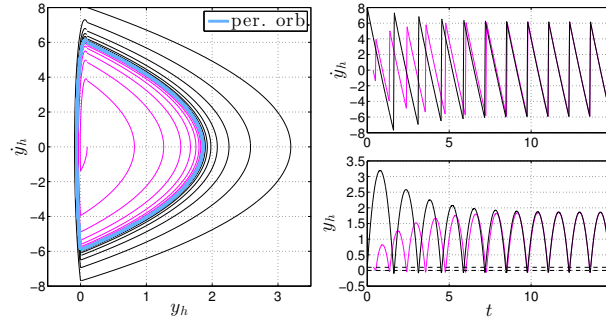
Figure 5.10: Hopping robot. Left: phase portrait with the periodic solution (light blue) and two other solutions (magenta, black) starting inside and outside the periodic orbit. Right, bottom: time evolution of y_h (magenta, black) with the position thresholds 0 and $\theta - \epsilon$ (dashed) determining the transitions between flight and stance. Right, top: time evolution of $\dot{y}_h$ (magenta, black).

EXAMPLE 5.3 *Consider for (5.15) the parameters* $m = 50$ *kg*, $c_1 = 5$ *Ns/m*, $c_2 = 400$ *Ns/m*, $k = 100$ *kN/m*, $g = 9.81$ *m/s^2*, $\theta = 0.1$ *m. The stance phase begins when the solution crosses the lower dashed threshold at 0 downwards, and ends when it crosses the upper dashed threshold at $\theta - \epsilon$ upwards. The periodic orbit (in light blue) arises when the energy injected by the spring preload (and released through a clutch mechanism when touching ground as in [68]) balances the energy dissipated along the orbit.*

5.4.2 *Automotive suspension*

Consider the simplified planar model of an automotive suspension represented on the left of Figure 5.11 with sprung mass m_s, where y_s is the displacement of the sprung mass from its equilibrium position, $\dot{y}_s$ is the corresponding velocity, y_r is the displacement of the road and the parameters k_s and c_s are the stiffness and damping relative to the suspension. The corresponding model is

$$m_s\ddot{y}_s + c_s(\dot{y}_s - \dot{y}_r) + k_s(y_s - y_r - u) = 0, \qquad (5.17a)$$

where in the following we consider $y_r(t) = 0$ for all positive times t, leaving to future work the validation of the proposed control law in the presence of road excitation. u denotes the reset action in terms of spring preload that is chosen according to Section 5.2.2, with the symmetric selections

$$u_2 = -u_1 = \bar{u} > 0 \qquad (5.17b)$$

$$y_2 = -y_1 = \bar{y} > 0. \qquad (5.17c)$$
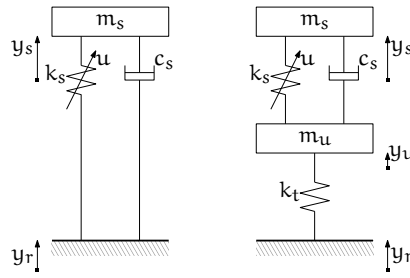
Figure 5.11: Simplified and full quarter car model.
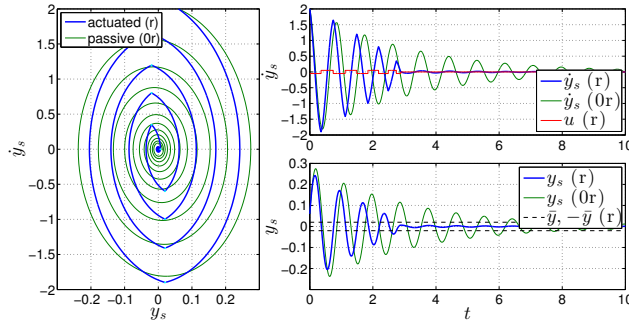
Figure 5.12: Left: phase portrait for actuated suspension and passive suspension $(u(t) = 0$ for all t). Right, bottom: time evolution of y_s. Right, top: time evolution of $\dot{y}_s$ and u for the actuated suspension.

The rest value of u is $u_0 = 0$, which is applied after crossing the set $D_0 = \{(y_s, \dot{y}_s): -\bar{y} \leqslant y_s \leqslant \bar{y}, \dot{y}_s = 0\}$ and is associated to the equilibrium $y_0 = 0$ of the free dynamics.

Under the condition

$$\bar{y} < \frac{\bar{u}}{2}, \tag{5.18}$$

Assumptions 5.1 and 5.2 are satisfied, and Theorem 5.2 establishes that the equilibrium $(0, 0)$ of the reset suspension is globally asymptotically stable.

The simple reset actuation guarantees that energy is drained from the system at each reset, as per Proposition 5.1: note that $\bar{u} > 0$, $\bar{y} > 0$ suffice to drain energy when resetting from D_1 to D_2, or vice versa, since in both these resets the drained energy is $-\frac{1}{2}k(2\bar{u})(2\bar{y})$. This improves the suspension performance compared to the case when no actuation is present ($u(t) = 0$ for all positive times t), as we illustrate in the following example.

EXAMPLE 5.4 *Fix the parameters* $m_s = 400$ *kg*, $c_s = 260$ *Ns/m*, $k_s = 20 \cdot 10^3$ *N/m*, $\bar{u} = 0.05$ *m*, $\bar{y} = 0.02$ *m in* (5.17). *Figure* 5.12 *shows the improvement of the reset suspension (blue) with respect to the unactuated one (green). Note that for the actuated suspension the segment* D_0 *is intersected at about 2.9 s and afterwards the mechanical system evolves according to its free dynamics.*

We also show that the proposed reset law can be generalized to the complete quarter car model [110, Chapter 3.1] on the right of Figure 5.11, *where* y_u *is the displacement of the unsprung mass from its equilibrium position,* $\dot{y}_u$ *is the corresponding velocity and* k_t *is the stiffness relative to the tire. For this model we have:*

$$m_s \ddot{y}_s + c_s(\dot{y}_s - \dot{y}_u) + k_s(y_s - y_u - u) = 0 \tag{5.19a}$$

$$m_u \ddot{y}_u - c_s(\dot{y}_s - \dot{y}_u) - k_s(y_s - y_u - u) + k_t(y_u - y_r) = 0, \tag{5.19b}$$

where u *is reset based only on the position* y_s, *as in* (5.17) *with only* one *degree of freedom. With the additional parameters* $m_u = 50$ *kg and* $k_t = 250 \cdot 10^3$ *N/m, we show at the top of*
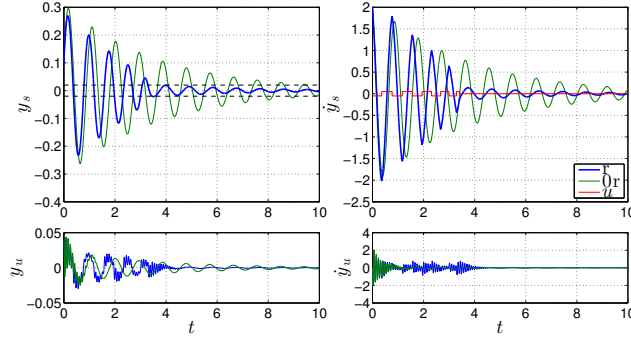
Figure 5.13: Time evolutions of the state variables for the actuated (blue) and passive (green) suspension. Top, left: chassis dispacement y_s. Top, right: chassis velocity $\dot{y}_s$. Bottom, left: tire displacement y_u. Bottom, right: tire velocity $\dot{y}_u$.

Figure 5.13 the improvement of the reset law in damping oscillations and achieving a faster convergence of the chassis coordinate y_s to its equilibrium (we report also the unsprung-mass coordinate y_u for completeness at the bottom). The generalizability of the reset law from one to two degrees of freedom rests essentially upon a timescale separation between the natural frequency of the tire $\sqrt{\frac{k_t}{m_u}} = 70.7$ rad/s and the natural frequency of the chassis $\sqrt{\frac{k_s}{m_s}} = 7.07$ rad/s as in [59, Example 11.4].

5.5 HYBRID FORMULATION, TECHNICAL ANALYSIS AND PROOFS

This final section is devoted to collecting the proofs of our results in Sections 5.2.1, 5.2.2 and 5.3.

5.5.1 *Hybrid formulation and proof of Theorem 5.1*

In Section 5.2.1, solutions were parametrized only by the ordinary time t as $\psi \colon \mathbb{R}_{\geqslant 0} \to \mathbb{R}^2$, and the results involved the classical notions of asymptotic stability of compact sets (the unique periodic orbit in Theorem 5.1) for nonlinear continuous-time systems. Assume now that we track the number of resets j undergone by the solutions, and that we make this additional parametrization explicit in a solution $\psi \colon \mathbb{R}_{\geqslant 0} \times \mathbb{Z}_{\geqslant 0} \to \mathbb{R}^2$. Consider also the control action u as a *state*, which is constant whenever $(y, \dot{y})$ belongs to C_1 or C_2 and is updated at a reset.

These points lead seamlessly to a formulation according to the hybrid dynamical systems formalism in Section 2.1. Using the pictorial representation in Figure 5.14, we write then (5.2) as

$$
\left.
\begin{aligned}
m\ddot{y} + c(y, \dot{y})\dot{y} + \frac{\partial U}{\partial y}(y, u) &= 0 \\
\dot{u} &= 0
\end{aligned}
\right\} \quad (y, \dot{y}, u) \in \mathcal{C} \tag{5.20a}
$$

$$
\left.
\begin{aligned}
y^+ &= y \\
\dot{y}^+ &= \dot{y} \\
u^+ &= u_i
\end{aligned}
\right\} \quad (y, \dot{y}, u) \in D_i \times \{u_{3-i}\}, i \in \{1, 2\} \tag{5.20b}
$$

$$
\mathcal{C} := \mathcal{C}_1 \cup \mathcal{C}_2 := (\overline{C}_1 \times \{u_1\}) \cup (\overline{C}_2 \times \{u_2\}) \tag{5.20c}
$$

$$
\mathcal{D} := \mathcal{D}_1 \cup \mathcal{D}_2 := (D_1 \times \{u_2\}) \cup (D_2 \times \{u_1\}) \tag{5.20d}
$$

where $\overline{C}_1$ and $\overline{C}_2$ denote the closure of C_1 and C_2 in (5.2c)-(5.2d). Thanks to the shift to a hybrid system formulation in (5.20) from (5.2) and its regularity in terms
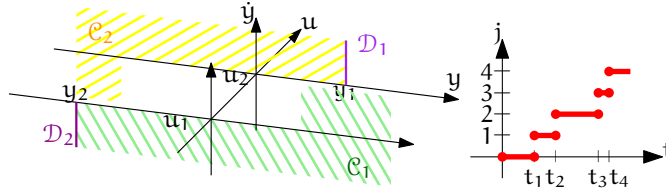
Figure 5.14: Left: hybrid system formulation (5.20) of system (5.2). Right: a typical hybrid time domain for (5.20) (see (5.23) for the definition of $t_1, \ldots, t_4$).

of the hybrid basic conditions of Section 2.2, we establish for instance in the proof of Proposition 5.2 that the periodic orbit is globally asymptotically stable by just characterizing the behaviour of solutions through a Poincaré map, as is done in Lemma 5.2 below.

The concept of solution for a hybrid dynamical system like (5.20) was discussed in Definition 2.4, and the typical (cf. Lemma 5.1) appearance of hybrid time domains (see Definition 2.2) for (5.20) is in Figure 5.14, with the two time directions t and j. Then, given a hybrid solution ϕ with hybrid time domain $\text{dom}\phi$, define the function that associates to each time t the least index j such that $(t, j) \in \text{dom}\phi$ as

$$\underline{j}(t) := \min_{(t,j) \in \text{dom}\phi} j. \tag{5.21}$$

Using (5.21), we can project a hybrid solution

$$(t, j) \mapsto \phi(t, j) = \big(y(t, j), \dot{y}(t, j), u(t, j)\big)$$

onto the ordinary time direction as

$$t \mapsto \phi(t, \underline{j}(t)) = \bar{\phi}(t) = \big(\bar{y}(t), \bar{\dot{y}}(t), \bar{u}(t)\big).$$

$\bar{\phi}$ satisfy by construction (5.2e) and, given the signal $t \mapsto \bar{u}(t)$, $(\bar{y}, \bar{\dot{y}})$ is a solution to the following reformulation of (5.2a)

$$m\ddot{y} + c(y, \dot{y})\dot{y} + \frac{\partial U}{\partial y}(y, \bar{u}(t)) = 0$$

in the sense of Carathéodory as in [37, Page 3]. Then, solutions to (5.20) are also solutions to (5.2), and since the former are well-defined we could define in Section 5.2.1 the concepts in Definition 5.1, and characterize the stability properties in Theorem 5.1. Repeating Definition 4.1 in Chapter 4 for convenience, we can then parallel Definition 5.1 in the following Definition 5.2. The notions of solution and complete solution can be found in Definitions 2.4 and 2.5, respectively.

DEFINITION 5.2 *Orbit denotes the image of a hybrid solution to* (5.20). *A hybrid periodic solution is a complete solution ϕ for which there exists a pair of nonnegative scalars (T, J) with $T + J > 0$, such that $(t, j) \in \text{dom}\phi$ implies $(t + T, j + J) \in \text{dom}\phi$ and, moreover,*

$$\phi(t, j) = \phi(t + T, j + J), \quad \forall (t, j) \in \text{dom}\phi.$$

A hybrid periodic orbit is the image of a hybrid periodic solution, and is nontrivial *if it comprises more than one point.*

First we establish in Lemma 5.1 the solution properties that are needed for Lemma 5.2, among which uniqueness and completeness.

LEMMA 5.1 *For each initial condition, solutions to* (5.20) *are unique, each flow interval of their hybrid time domain is bounded, they jump from $\mathcal{D}_1$ infinitely many times and they are complete.*

Proof of Lemma 5.1. We divide the proof in three steps each proving a part of our statement, and we always refer to Figure 5.14.

(a) For each initial condition, solutions to (5.20) are unique.
The flow and jump maps in (5.20a)-(5.20b) are Lipschitz single-valued functions by Assumption 5.1, and no flow is possible from the jump set because in $\mathcal{C} \cap \mathcal{D}_1$ ($\mathcal{C} \cap \mathcal{D}_2$) the velocity $\dot{y}$ is positive (negative, respectively).

(b) For each initial condition, each flow interval of the hybrid time domain of the solutions to (5.20) is bounded.
Take any initial condition in $\mathcal{C}_1$. The solution is bound to leave in finite time the set $\mathcal{C}_1 \cap \{(y, \dot{y}, u) \colon \dot{y} \geqslant 0\}$ because

$$x \in \mathcal{C}_1 \cap \{(y, \dot{y}, u) \colon \dot{y} \geqslant 0\} \Rightarrow \ddot{y} < 0 \tag{5.22}$$

since $m\ddot{y} = -c(y, \dot{y})\dot{y} - \frac{\partial u}{\partial y}(y, u_1) < 0$ thanks to (5.3a) and (5.3c). Moreover, after crossing $\dot{y} = 0$, $\dot{y}$ remains negative and bounded away from zero, so that $\mathcal{D}_2$ is reached in finite time. A parallel reasoning holds for any initial condition in $\mathcal{C}_2$. Then each flow interval is bounded.

(c) For each initial condition, solutions to (5.20) jump from $\mathcal{D}_1$ infinitely many times and they are complete.
By the argument in the previous step *(b)*, a solution in $\mathcal{C}_1$ necessarily reaches $\mathcal{D}_2$ in finite time and the jump map in (5.20b) guarantees that a solution in $\mathcal{D}_2$ necessarily reaches $\mathcal{C}_2$. The same argument guarantees then that a solution in $\mathcal{C}_2$ necessarily reaches $\mathcal{D}_1$ in finite time and the jump map guarantees that a solution in $\mathcal{D}_1$ reaches $\mathcal{C}_1$. We can then conclude that solutions jump infinitely many times from $\mathcal{D}_1$, which implies completeness (see Definition 2.5). $\qquad\square$

Thanks to Lemma 5.1, we can parametrize solutions by their initial condition $x_0 = (y^0, \dot{y}^0, u^0)$ as

$$(t, j) \mapsto \phi^{x_0}(t, j) = (\phi_y^{x_0}(t, j), \phi_{\dot{y}}^{x_0}(t, j), \phi_u^{x_0}(t, j)).$$

In the following we consider extensively solutions with x_0 in $\mathcal{D}_1$. Moreover, given a hybrid solution ϕ^x with hybrid time domain $\mathrm{dom}\phi^x$, define the function that associates to each jump index j the least time t such that $(t, j) \in \mathrm{dom}\phi^x$ as

$$t_j := \min_{(t,j) \in \mathrm{dom}\phi^x} t, \tag{5.23}$$

corresponding then to the time when the jump index increases from $j - 1$ to j. Based on the parametrization by the initial condition and on (5.23), we define for each $x \in \mathcal{D}_1$ the function $P \colon \mathcal{D}_1 \to \mathcal{D}_1$ as

$$P(x) := \phi^x(t_3, 2), \tag{5.24}$$

which is well defined because of Lemma 5.1 and plays the role of a Poincaré map for the equation

$$x^+ = P(x), \quad x \in \mathcal{D}_1. \tag{5.25}$$

The existence of a hybrid periodic orbit follows from the properties of P that are presented in the next Lemma.

LEMMA 5.2 $P \colon \mathcal{D}_1 \to \mathcal{D}_1$ *is continuous. There exists a unique equilibrium*

$$x^\star = P(x^\star), \tag{5.26}$$

which is globally asymptotically stable for (5.25).

Proof of Lemma 5.2. We divide the proof in steps.
$P \colon \mathcal{D}_1 \to \mathcal{D}_1$ *is continuous.*
Lemma 5.1 guarantees that for each initial condition (then also for an initial condition in $\mathcal{D}_1$), solutions reach $\mathcal{D}_1$ in finite time. In particular, any solution reaches
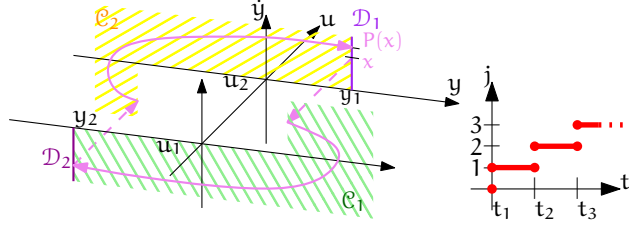
Figure 5.15: Left: the orbit of ϕ^x (violet). Right: its hybrid time domain.

$\mathcal{D}_1$ after a first jump occurring at $t_1 = t_0 = 0$, a flowing interval $[t_1, t_2]$, a second jump at t_2, and a second flowing interval $[t_2, t_3]$. Therefore, according to (5.24), the range of P is indeed $\mathcal{D}_1$. Since the sets $\mathcal{C}$ and $\mathcal{D}$ in (5.20c)-(5.20d) are closed and the flow and jump maps in (5.20a)-(5.20b) are continuous functions by Assumption 5.1, hybrid system (5.20) satisfies the hybrid basic conditions of Section 2.2, which imply nominal well-posedness [47, Theorem 6.8] in the sense of [47, Definition 6.2]. Then, [47, Proposition 6.14] concludes that for every $\epsilon > 0$ and $\tau \geqslant 0$, solutions ϕ^{x_0} and ϕ^x (with $x_0 \in \mathcal{D}_1$, $x \in \mathcal{D}_1$ and $|x - x_0| \leqslant \delta$) are such that ϕ^{x_0} and ϕ^x are (τ, ϵ)-close [47, Definition 5.23]. From (τ, ϵ)-closeness, *uniqueness* and completeness of ϕ^{x_0} and ϕ^x, we can deduce $|P(x) - P(x_0)| \leqslant \epsilon$ for a sufficiently small δ.

Energy injected at jumps and dissipated along flow.
For any point $x = (y, \dot{y}, u) \in \mathcal{C} \cup \mathcal{D}$, define its total energy as the sum of kinetic and potential energy, that is,

$$e(x) := \frac{1}{2} m\dot{y}^2 + U(y, u), \tag{5.27}$$

which can be specialized for a point $x \in \mathcal{D}_1$ (that is, $x = (y_1, \dot{y}, u_2)$ for some $\dot{y} \geqslant 0$) as

$$E(x) := \frac{1}{2} m\dot{y}^2 + U(y_1, u_2). \tag{5.28}$$

In the sequel, for the convenience of the reader, we will use $e(x)$ for a generic $x \in \mathcal{C} \cup \mathcal{D}$ and $E(x) = e(x)$ whenever addressing points $x \in \mathcal{D}_1$. For each $x \in \mathcal{D}_1$, consider the solution ϕ^x. Because of Lemma 5.1, ϕ^x is bound to jump from $\mathcal{D}_1$, flow for a finite time in $\mathcal{C}_1$, jump from $\mathcal{D}_2$ and flow for a finite time in $\mathcal{C}_2$ before reaching again $\mathcal{D}_1$. Such a solution and the jump times t_1, t_2, t_3 (defined in (5.23)), corresponding to the previous transitions, are depicted in Figure 5.15, to which the reader is referred for the rest of the proof. For such a portion of the solution up to $(t_3, 2)$, we want to characterize as a function of $x \in \mathcal{D}_1$ the injected energy I and the dissipated energy D.

Using the total energy definition in (5.27), the energy injected at the two jumps is for $x \in \mathcal{D}_1$

$$\begin{aligned} I &:= \left[e(\phi^x(t_1, 1)) - e(\phi^x(t_1, 0)) \right] + \left[e(\phi^x(t_2, 2)) - e(\phi^x(t_2, 1)) \right] \\ &= \left[U(y_1, u_1) - U(y_1, u_2) \right] + \left[U(y_2, u_2) - U(y_2, u_1) \right] \\ &= \text{constant} > 0 \end{aligned} \tag{5.29}$$

in accordance with the jump map (5.20b). I is a positive constant because $U(y_1, u_1) - U(y_2, u_1) > 0$ and $U(y_2, u_2) - U(y_1, u_2) > 0$ due to (5.3c).

As for the dissipated energy D, the derivative along solutions of the total energy e in (5.27) is from (5.20a):

$$\dot{e} = -c(y, \dot{y})\dot{y}^2. \tag{5.30}$$

Then, for each $x \in \mathcal{D}_1$ and the solution ϕ^x, the dissipated energy $D: \mathcal{D}_1 \to \mathbb{R}_{\geqslant 0}$ is

$$
\begin{aligned}
D(x) &:= -\int_{t_1}^{t_2} \dot{e}\big(\phi^x(t,1)\big)\,dt - \int_{t_2}^{t_3} \dot{e}\big(\phi^x(t,2)\big)\,dt \\
&= \int_{t_1}^{t_2} c\big(\phi_y^x(t,1), \phi_{\dot{y}}^x(t,1)\big)\phi_{\dot{y}}^x(t,1)^2\,dt \\
&\quad + \int_{t_2}^{t_3} c\big(\phi_y^x(t,2), \phi_{\dot{y}}^x(t,2)\big)\phi_{\dot{y}}^x(t,2)^2\,dt,
\end{aligned}
\tag{5.31}
$$

where the integrals are restricted to the flow intervals.

Monotonicity of the dissipated energy.

We can show that D is strictly increasing with respect to the velocity of points in $\mathcal{D}_1$, that is,

$$
\left.\begin{aligned}
x_a &= (y_1, \dot{y}_a, u_2) \in \mathcal{D}_1 \\
x_b &= (y_1, \dot{y}_b, u_2) \in \mathcal{D}_1 \\
0 &\leqslant \dot{y}_a < \dot{y}_b
\end{aligned}\right\} \Rightarrow D(x_a) < D(x_b),
\tag{5.32}
$$

which we prove in two steps.

First, restate the integrals in (5.31) in terms of orbits. In each of the two integrals in (5.31), the time direction j is fixed to $\bar{j} \in \{1, 2\}$. For the fixed $\bar{j}$, we further split the computation of the corresponding integral in subintervals where $\phi_{\dot{y}}^x > 0$ or $\phi_{\dot{y}}^x < 0$ ($\phi_{\dot{y}}^x(\cdot, \bar{j})$ can be zero only on a set of zero measure because of (5.22)), on each of which $\phi_{\dot{y}}^x$ is an increasing or decreasing function of t, respectively, because $\dot{y} = \frac{dy}{dt}$. Then, in each one of such subintervals, $t \mapsto \phi_{\dot{y}}^x(t, \bar{j})$ is invertible with inverse $y \mapsto t(y)$, and

$$
\frac{dt(y)}{dy} = \frac{1}{\frac{d\phi_y^x(t,\bar{j})}{dt}\Big|_{t(y)}} = \frac{1}{\phi_{\dot{y}}^x(t,\bar{j})|_{t(y)}}
$$

(note that $\phi_y^x(\cdot, \bar{j})$ is absolutely continuous so that $\phi_y^x(\cdot, \bar{j})$ is continuously differentiable). We can then change the integration variable from time t to position y. For instance, for one such subinterval $[\tau_a, \tau_b]$ where either $\phi_{\dot{y}}^x \geqslant 0$ or $\phi_{\dot{y}}^x \leqslant 0$, the dissipated energy (taken positive as in (5.31)) is

$$
\begin{aligned}
&e\big(\phi^x(\tau_a, \bar{j})\big) - e\big(\phi^x(\tau_b, \bar{j})\big) \\
&= \int_{\tau_a}^{\tau_b} c\big(\phi_y^x(t,\bar{j}), \phi_{\dot{y}}^x(t,\bar{j})\big)\phi_{\dot{y}}^x(t,\bar{j})^2\,dt \\
&= \int_{\phi_y^x(\tau_a,\bar{j})}^{\phi_y^x(\tau_b,\bar{j})} c\big(y, \phi_{\dot{y}}^x(t(y),\bar{j})\big)\phi_{\dot{y}}^x(t(y),\bar{j})^2 \frac{dt(y)}{dy}\,dy \\
&= \int_{\phi_y^x(\tau_a,\bar{j})}^{\phi_y^x(\tau_b,\bar{j})} c\big(y, \phi_{\dot{y}}^x(t(y),\bar{j})\big)\phi_{\dot{y}}^x(t(y),\bar{j})\,dy \\
&= \int_{\phi_y^x(\tau_b,\bar{j})}^{\phi_y^x(\tau_a,\bar{j})} c\big(y, \phi_{\dot{y}}^x(t(y),\bar{j})\big)\big(-\phi_{\dot{y}}^x(t(y),\bar{j})\big)\,dy
\end{aligned}
$$

(5.33a)

(5.33b)

so that this integral is always positive regardless of the sign of $\phi_{\dot{y}}^x$ over $[\tau_a, \tau_b]$ ($\phi_{\dot{y}}^x$ negative implies $\phi_y^x(\tau_b, \bar{j}) < \phi_y^x(\tau_a, \bar{j})$). Consider also Lemma 4.1 for a physical interpretation in terms of work when $c(y, \dot{y})$ is constant.

Second, consider $D(x_a)$ and $D(x_b)$ for $\dot{y}_a < \dot{y}_b$ as in (5.32). Take the two solution ϕ^{x_a} and ϕ^{x_b} with $\dot{y}_b > \dot{y}_a$ and split the integrals expressing the respective dissipated energies according to the integration principle just described. Up to reaching $\mathcal{D}_1$, the orbit of ϕ^{x_a} is in the interior of the area spanned by the orbit of ϕ^{x_b} (see Figure 5.16) because two orbits can *not* intersect during flow (if they did, uniqueness of solutions in Lemma 5.1 would be violated), and y and $\dot{y}$ do not change across jumps. Due to this fact and Assumption (5.3b), when $\phi_{\dot{y}}$ is positive (cf. Figure 5.16 in $\mathcal{C}_2$ and Equation (5.33a)) the integrand $c\big(y, \phi_{\dot{y}}(t(y),\bar{j})\big)\phi_{\dot{y}}(t(y),\bar{j})$ relative to ϕ^{x_a} is strictly smaller than that of ϕ^{x_b}. The same holds for $\phi_{\dot{y}}$ negative (cf. Figure 5.16
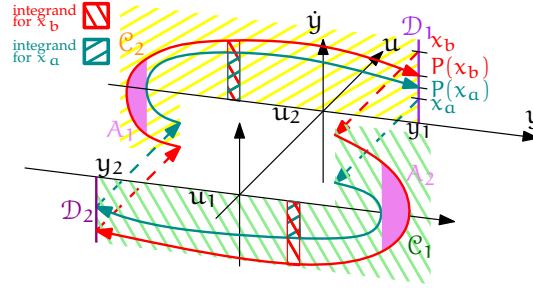
Figure 5.16: Integrand relative to the dissipated energy by damping for two orbits.

in $\mathcal{C}_1$ and Equation (5.33b)), beside the fact that the dissipated energy along ϕ^{x_b} has additional (positive) contributions (denoted by A_1 and A_2 in Figure 5.16). We conclude that the dissipated energy relative to ϕ^{x_a} is strictly less than that of ϕ^{x_b}.

Balance and uniqueness of equilibrium $P(x^\star) = x^\star$.

Property (5.32) implies that there exist a unique value of $x \in \mathcal{D}_1$, that we call $x^\star$, satisfying

$$D(x^\star) = I. \tag{5.34}$$

We show now that $P(x^\star) = x^\star$, so that (5.26) is proven. Suppose by contradiction that $P(x^\star) \neq x^\star$, hence $E(x^\star) \neq E(P(x^\star))$. Then, by the energy balance

$$E(x^\star) + I - D(x^\star) = E(P(x^\star)) \tag{5.35}$$

we can deduce $D(x^\star) \neq I$, which is a contradiction.

Asymptotic stability.

For the global asymptotic stability of the unique equilibrium $x^\star$ of (5.25), consider the Lyapunov function $V \colon \mathcal{D}_1 \to \mathbb{R}_{\geqslant 0}$ defined for $x = (y_1, \dot{y}, u_2)$ and $x^\star = (y_1, \dot{y}^\star, u_2)$ as

$$V(x) := |x - x^\star|^2 = (\dot{y} - \dot{y}^\star)^2. \tag{5.36}$$

Because in (5.25) P is continuous and $\mathcal{D}_1$ is closed (so it satisfies the hybrid basic conditions relative to the discrete part only) and the attractor is the point $x^\star$, we need to prove (as from Fact 2.10):

$$V(P(x)) - V(x) < 0 \quad \forall x \in \mathcal{D}_1, \, x \neq x^\star,$$

or, equivalently,

$$\left(\dot{y}^+ - \dot{y}\right)\left(\dot{y}^+ - \dot{y}^\star + \dot{y} - \dot{y}^\star\right) < 0 \quad \forall \dot{y} \geqslant 0, \dot{y} \neq \dot{y}^\star \tag{5.37}$$

once we substitute (5.36) and we use $(y_1, \dot{y}^+, u_2) = P(x)$ from (5.25). Property (5.37) is true if the following implications hold

$$\dot{y}^+ > \dot{y} \Rightarrow \dot{y} < \dot{y}^+ < \dot{y}^\star \tag{5.38a}$$
$$\dot{y}^+ < \dot{y} \Rightarrow \dot{y} > \dot{y}^+ > \dot{y}^\star. \tag{5.38b}$$

Indeed, since $\dot{y}^+ = \dot{y}$ holds true only for $\dot{y} = \dot{y}^\star$ due to (5.26), either (5.38a) or (5.38b) holds, under either of which (5.37) is true. To conclude the proof, we then show the validity of (5.38). To prove (5.38a), we just need to prove $\dot{y}^+ > \dot{y} \Rightarrow \dot{y}^+ < \dot{y}^\star$. $\dot{y}^+ > \dot{y}$ implies $E(P(x)) > E(x)$ by (5.28). From an energy balance

$$E(P(x)) - E(x) = I - D(x),$$

so $I - D(x) > 0$. By (5.32) and (5.34), $I - D(x) > 0$ implies $\dot{y}^\star > \dot{y}$. Consider the two solutions $\phi^{x^\star}$ and ϕ^x. Due to (5.20b), the velocity remains the same across jumps, so

$$\dot{y}^\star = \phi_{\dot{y}}^{x^\star}(0, 1) > \phi_{\dot{y}}^{x}(0, 1) = \dot{y}.$$
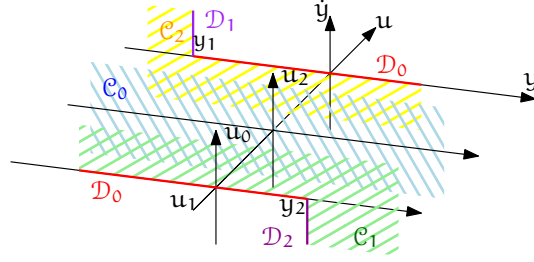
Figure 5.17: Hybrid formulation of system (5.4).

While flowing in $\mathcal{C}_1$, uniqueness of solutions from Lemma 5.1 holds, meaning that the orbits of the two solutions cannot intersect. So, after the flow in $\mathcal{C}_1$, $\phi_{\dot{y}}^{x^\star}(t_2^{x^\star}, 1) < \phi_{\dot{y}}^{x}(t_2^{x}, 1)$. Repeating the reasoning for $\mathcal{D}_2$ and $\mathcal{C}_2$, we obtain finally that

$$\dot{y}^\star = \phi_{\dot{y}}^{x^\star}(t_3, 2) > \phi_{\dot{y}}^{x}(t_3, 2) = \dot{y}^+.$$

(5.38b) is proven with parallel considerations to those for (5.38a).   □

We proved in Lemma 5.1 that all solutions jump from $\mathcal{D}_1$ after a finite time and we proved in Lemma 5.2 that there exists a unique $x^\star \in \mathcal{D}_1$ such that $P(x^\star) = x^\star$. The unique periodic orbit starting from $x^\star := (y_1, \dot{y}^\star, u_2)$ has a finite continuous period $T > 0$ and a discrete period $J = 2$, as from Definition 5.2, and defines the attractor $\mathcal{A}$ as

$$\mathcal{A} := \{x \colon x = \phi^{x^\star}(t, j) \text{ for some } (t, j)\}. \tag{5.39}$$

Therefore the existence of a unique nontrivial periodic orbit that is globally asymptotically stable (Theorem 5.1) is an immediate consequence of the following proposition.

PROPOSITION 5.2   *$\mathcal{A}$ in (5.39) is globally asymptotically stable.*

Proof of Proposition 5.2. Stability follows from Lemma 5.2 (stability of $x^\star$) and continuity of solutions on compact time intervals, as established in [47, Proposition 6.14]. Global attractivity follows from Lemma 5.2 (attractivity of $x^\star$), persistent jumping in Lemma 5.1 and again continuity of solutions on compact time intervals. These properties are also uniform because the hybrid basic conditions are satisfied, as established in Fact 2.4.   □

5.5.2   *Hybrid formulation and proofs of Proposition 5.1 and Theorem 5.2*

As we did in Section 5.5.1 for system (5.2), let us reformulate system (5.4) as a hybrid dynamical system:

$$\left.\begin{array}{l} m\ddot{y} + c(y, \dot{y})\dot{y} + \dfrac{\partial U}{\partial y}(y, u) = 0 \\[2mm] \dot{u} = 0 \end{array}\right\} \quad (y, \dot{y}, u) \in \mathcal{C} \tag{5.40a}$$

$$\left.\begin{array}{l} y^+ = y \\ \dot{y}^+ = \dot{y} \\ u^+ = u_i \end{array}\right\} \quad (y, \dot{y}, u) \in \mathcal{D}_i, i \in \{0, 1, 2\} \tag{5.40b}$$

$$\begin{aligned} \mathcal{C} &:= (\overline{C}_1 \times \{u_1\}) \cup (\overline{C}_2 \times \{u_2\}) \cup (\overline{C}_0 \times \{u_0\}) \\ &=: \mathcal{C}_1 \cup \mathcal{C}_2 \cup \mathcal{C}_0 \end{aligned} \tag{5.40c}$$

$$\mathcal{D} := \bigcup_{i \in \{1,2,3\}} \mathcal{D}_i \quad \text{with} \quad \begin{cases} \mathcal{D}_1 := D_1 \times \{u_2\} \\ \mathcal{D}_2 := D_2 \times \{u_1\} \\ \mathcal{D}_0 := D_0 \times \{u_1, u_2\}. \end{cases} \tag{5.40d}$$

We first prove Proposition 5.1.

Proof of Proposition 5.1. We divide the proof in steps.

Variation of total energy across jumps.

Using the definition of total energy in (5.27), we define its variations across jumps for all $y \in [y_1, y_2]$

$$\Delta_{1 \to 2} := e\big((y_2, \dot{y}, u_2)\big) - e\big((y_1, \dot{y}, u_1)\big) = U(y_2, u_2) - U(y_2, u_1) \tag{5.41a}$$

$$\Delta_{2 \to 1} := e\big((y_2, \dot{y}, u_1)\big) - e\big((y_2, \dot{y}, u_2)\big) = U(y_1, u_1) - U(y_1, u_2) \tag{5.41b}$$

$$\Delta_{1 \to 0}(y) := e\big((y, 0, u_0)\big) - e\big((y, 0, u_1)\big) = U(y, u_0) - U(y, u_1) \tag{5.41c}$$

$$\Delta_{2 \to 0}(y) := e\big((y, 0, u_0)\big) - e\big((y, 0, u_2)\big) = U(y, u_0) - U(y, u_2), \tag{5.41d}$$

where each of these $\Delta_{i \to j}$ is the variation due to a jump that resets the control from u_i to u_j.

$$U(y_1, u_1) < U(y, u_1) < U(y_2, u_1) \tag{5.42a}$$

$$U(y_2, u_2) < U(y, u_2) < U(y_1, u_2). \tag{5.42b}$$

Using the relations in (5.41), we can obtain that for all $y \in [y_1, y_2]$ (the equation number over the inequality sign justifies the corresponding bound)

$$\Delta_{1 \to 2} + \Delta_{2 \to 1} \overset{(5.42a),(5.42b)}{<} 0 \tag{5.43a}$$

$$\Delta_{1 \to 2} + \Delta_{2 \to 0}(y) \overset{(5.42b)}{\leqslant} U(y, u_0) - U(y_2, u_1)$$

$$\overset{(5.42a)}{\leqslant} U(y, u_0) - U(y, u_1) = \Delta_{1 \to 0}(y) \overset{(5.5b)}{<} 0 \tag{5.43b}$$

$$\Delta_{2 \to 1} + \Delta_{1 \to 0}(y) \overset{(5.42a)}{\leqslant} U(y, u_0) - U(y_1, u_2)$$

$$\overset{(5.42b)}{\leqslant} U(y, u_0) - U(y, u_2) = \Delta_{2 \to 0}(y) \overset{(5.5c)}{<} 0 \tag{5.43c}$$

In light of (5.43), a scalar $\delta > 0$ can then be found such that for all $y \in [y_1, y_2]$

$$\Delta_{1 \to 2} + \Delta_{2 \to 1} < -\delta \tag{5.44a}$$

$$\Delta_{1 \to 2} + \Delta_{2 \to 0}(y) \leqslant \Delta_{1 \to 0}(y) < -\delta \tag{5.44b}$$

$$\Delta_{2 \to 1} + \Delta_{1 \to 0}(y) \leqslant \Delta_{2 \to 0}(y) < -\delta. \tag{5.44c}$$

Finite number of jumps $N(\bar{e})$ and nonzero decrease of total energy.

If solutions to (5.40) start in $\mathcal{C}_0$, no jumps are allowed because of (5.40d) and $u = u_0$. Therefore, the jumps are clearly finite.

Solutions in $\mathcal{D} \cap \mathcal{C}$ can only jump because any flowing solution along the vector field (5.40a) would flow outside $\mathcal{C}$. Indeed,

- $\dot{y} < 0$ in $\mathcal{D}_2 \cap \mathcal{C}_1 \backslash \{(y_2, 0, u_1)\}$, and then solutions would flow to the forbidden set $y < y_2$;

- $\ddot{y} = -\frac{1}{m} \frac{\partial U}{\partial y}(y, u_1) < 0$ in $\mathcal{D}_0 \cap \mathcal{C}_1$ due to (5.22) and then forbidden flow to $\dot{y} < 0$, $y < y_2$ would occur.

Analogous reasonings hold in $\mathcal{D} \cap \mathcal{C}_2$.

Consider now a solution starting in $\mathcal{C}_1$ (a parallel reasoning holds when starting in $\mathcal{C}_2$). The solution is bound to reach (and jump from) either $\mathcal{D}_0$ or $\mathcal{D}_2$ *after a finite time* because *(i)* $\ddot{y} < 0$ in $\mathcal{C}_1 \cap \{(y, \dot{y}, u_1) : \dot{y} \geqslant 0\}$ due to (5.22) and *(ii)* $\dot{y} < 0$ elsewhere in $\mathcal{C}_1$ (see also step *(b)* in the proof of Lemma 5.1). Given this fact, assume by contradiction that the number of jumps is not finite. This is only possible if there

exists a complete solution ϕ_c that keeps jumping from $\mathcal{D}_1$ and $\mathcal{D}_2$, but never from $\mathcal{D}_0$ because from $\mathcal{D}_0$ solutions can only jump to $\mathcal{C}_0$. Take any jump time t_j as defined in (5.23) such that $\phi_c(t_j, j-1) \in \mathcal{D}_1$. Then we have $\phi_c(t_j, j) \in \mathcal{C}_1$, $\phi_c(t_{j+1}, j) \in \mathcal{D}_2$, $\phi_c(t_{j+1}, j+1) \in \mathcal{C}_2$ and $\phi_c(t_{j+2}, j+1) \in \mathcal{D}_1$ (refer also to Figure 5.17), and the following holds:

$$
\begin{aligned}
e\big(\phi_c(t_{j+2}, j+1)\big) &- e\big(\phi_c(t_j, j-1)\big) \\
&= e(\phi_c(t_j, j)) - e(\phi_c(t_j, j-1)) + \int_{t_j}^{t_{j+1}} \frac{d}{dt} e(\phi_c(t, j)) dt \\
&\quad + e(\phi_c(t_{j+1}, j+1)) - e(\phi_c(t_{j+1}, j)) + \int_{t_{j+1}}^{t_{j+2}} \frac{d}{dt} e(\phi_c(t, j+1)) dt \\
&\leqslant \Delta_{1\to 2} + \Delta_{2\to 1} < -\delta,
\end{aligned}
\tag{5.45}
$$

where we used (5.30) and (5.3a) for bounding the integrals, and then (5.44a). Equation (5.45) shows that such a "bad" solution ϕ_c cannot exist because the total energy e when crossing $\mathcal{D}_1$ would decrease arbitrarily due to persistent jumping from $\mathcal{D}_1$, and this contradicts

$$
e(x) = \tfrac{1}{2} m \dot{y}^2 + U(y_1, u_2) \geqslant U(y_1, u_2)
$$

which recurrently holds in $\mathcal{D}_1$.

Equation (5.45) also holds for a solution jumping a finite number of times from $\mathcal{D}_1$ and the same number of times from $\mathcal{D}_2$. After that, solutions can jump a next to last time from $\mathcal{D}_1$ or from $\mathcal{D}_2$, and then jump from $\mathcal{D}_0$. Note that the energy also decreases by at least $-\delta$ in these tail jumps as established by (5.44b) and (5.44c). This implies that for each $\bar{e}$, all solutions with initial total energy smaller than $\bar{e}$ perform at most $N(\bar{e}) \leqslant 2\frac{\bar{e}}{\delta} + 3$ jumps.   □

To prove Theorem 5.2, we use the following fact, which is a consequence of [48, Theorem 31], when all jumps are treated as events:

FACT 5.1 ([48, Theorem 31]) *Suppose that the hybrid system $\mathcal{H} = (\mathcal{C}, F, \mathcal{D}, G)$ with state $x \in \mathbb{R}^n$ satisfies the hybrid basic conditions. Let the compact set $\mathcal{A} \subset \mathbb{R}^n$ satisfy $G(\mathcal{D} \cap \mathcal{A}) \subset \mathcal{A}$, and assume that $\mathcal{A}$ is globally asymptotically stable for the hybrid system with no jumps $\mathcal{H}^0 = (\mathcal{C}, F, \emptyset, \emptyset)$. Also suppose that, for the hybrid system $\mathcal{H}$ and each compact set $\mathcal{K} \subset \mathbb{R}^n$, there exists $N > 0$ such that each solution starting in $\mathcal{K}$ experiences no more than N jumps. Then the set $\mathcal{A}$ is globally asymptotically stable for the system $\mathcal{H}$.*

Proof. To prove the fact, we simply need that $\mathcal{D}^0$ and G^0 in [48, Theorem 31] are both the empty set for a suitable outer semicontinuous event indicator $\mathcal{E}$ (an event is a pair $(g, x) \in \mathbb{R}^n \times \mathbb{R}^n$ such that $\mathcal{E}(g, x) = \emptyset$). By identifying jumps with events ($\mathcal{E}(g, x) := \emptyset$ for all $x \in \mathcal{D}$, $g \in G(x)$), we get precisely $G^0 = \emptyset$, and $\mathcal{D}^0 = \emptyset$.   □

Proof of Theorem 5.2. The proof of this theorem is a concatenation of Fact 5.1 applied to (5.40) with Proposition 5.1, after noting that in each compact set $\mathcal{K}$ there is a maximum value $\bar{e}$ of the total energy.   □

5.5.3   *Technical analysis and proof of Theorem 5.3*

In this Section we prove the proportionality for $\omega_{\text{reset}}/\omega_n$ and $y_{\max}/\bar{y}$, and we set up the nonlinear algebraic equations of the numerical problem through which κ and ψ in Theorem 5.3 are obtained. Because of the symmetry induced by (5.6) in (5.8), the solutions enjoy central symmetry (if ψ is a solution of (5.8), then $-\psi$ is a solution). Moreover, a solution starting at $t = 0$ from D_1, flowing in C_1 and reaching D_2 at $t = t_1$, must satisfy $\dot{y}(0) = -\dot{y}(t_1)$ to be periodic. Therefore, we can consider just one of the symmetric portions of the unique periodic solution guaranteed by

Theorem 5.1, for instance the one in C_1 where (5.8a) holds. Based on Figure 5.4, this portion satisfies then the boundary conditions:

$$y(0) = \bar{y}, \quad \dot{y}(0) = \bar{v}, \quad y(t_1) = -\bar{y}, \quad \dot{y}(t_1) = -\bar{v} \tag{5.46}$$

for some velocity $\bar{v} > 0$ and time $t_1 > 0$. To obtain the unique solution to (5.46), we impose also that t_1 be the *least* positive time[2] satisfying (5.46). Problem (5.46) sets a system of four equations in the four unknowns $\bar{v}$, t_1 and the two parameters relative to initial conditions in the solution to (5.8a). Once the system is solved, ω_{reset} follows from

$$\omega_{reset} = \frac{\pi}{t_1},$$

and y_{max} is obtained from the time when the periodic solution has zero velocity. In Theorem 5.3 we only assumed $\xi > 0$: to express in (5.46) the solution y, $\dot{y}$ of (5.8a), we split the analysis in the two[3] cases $0 < \xi < 1$ (underdamped) and $\xi > 1$ (overdamped).

Underdamped system ($0 < \xi < 1$). The solution to the linear dynamics (5.8a) has the form parametrized by the unknowns Y, φ

$$y(t) = Y e^{-\xi \omega_n t} \cos(\omega_n \sqrt{1-\xi^2} t + \varphi) - \bar{u} \tag{5.47a}$$

$$\dot{y}(t) = -\xi \omega_n Y e^{-\xi \omega_n t} \cos(\omega_n \sqrt{1-\xi^2} t + \varphi) \tag{5.47b}$$
$$- Y \omega_n \sqrt{1-\xi^2} e^{-\xi \omega_n t} \sin(\omega_n \sqrt{1-\xi^2} t + \varphi).$$

This expression, used in (5.46), yields

$$\bar{y} = Y \cos(\varphi) - \bar{u} \tag{5.48a}$$

$$\bar{v} = -\xi \omega_n Y \cos(\varphi) - Y \omega_n \sqrt{1-\xi^2} \sin(\varphi) \tag{5.48b}$$

$$-\bar{y} = Y e^{-\xi \omega_n t_1} \cos(\omega_n \sqrt{1-\xi^2} t_1 + \varphi) - \bar{u} \tag{5.48c}$$

$$-\bar{v} = -\xi \omega_n Y e^{-\xi \omega_n t_1} \cos(\omega_n \sqrt{1-\xi^2} t_1 + \varphi) \tag{5.48d}$$
$$- Y \omega_n \sqrt{1-\xi^2} e^{-\xi \omega_n t_1} \sin(\omega_n \sqrt{1-\xi^2} t_1 + \varphi).$$

Substitute $Y = \frac{\bar{u}+\bar{y}}{\cos(\varphi)}$ from (5.48a) and $\bar{v}$ from (5.48b) into (5.48c)-(5.48d), use the definition of λ in (5.7) and set $\tau_1 := \omega_n t_1$:

$$(\lambda-1)/(\lambda+1) = e^{-\xi \tau_1} \cos(\sqrt{1-\xi^2} \tau_1 + \varphi)/\cos(\varphi)$$

$$\xi \cos(\varphi) + \sqrt{1-\xi^2} \sin(\varphi) = \tag{5.49}$$
$$- \xi e^{-\xi \tau_1} \cos(\sqrt{1-\xi^2} \tau_1 + \varphi) - \sqrt{1-\xi^2} e^{-\xi \tau_1} \sin(\sqrt{1-\xi^2} \tau_1 + \varphi).$$

Note again that t_1, and so τ_1, is the least positive time satisfying (5.46). It is apparent that in (5.49) τ_1 and φ depend *only* on ξ and λ, so

$$\omega_{reset} = \omega_n \frac{\pi}{\tau_1} =: \omega_n \kappa, \tag{5.50}$$

where for simplicity we drop the dependence of κ on ξ and λ.

Find now y_{max}. Substitute back τ_1 and φ to obtain Y in (5.47), and consider the time $t^\star$ such that $\dot{y}(t^\star) = 0$, $t^\star \in [0, t_1]$ with $\dot{y}$ in (5.47b). Then $y_{max} = y(t^\star)$. Set $\tau^\star := \omega_n t^\star$ to obtain

$$\frac{-\xi}{\sqrt{1-\xi^2}} = \tan(\sqrt{1-\xi^2} \tau^\star + \varphi).$$

---

2 We use here for simplicity only the ordinary times since the analysis involves a single flow interval of the periodic orbit. However, t_1 corresponds indeed to the time defined in (5.23) using hybrid time domains.

3 We refrain from considering also the case $\xi = 1$ (real and coincident roots) as it can be seen as the limit of the above cases for $\xi \to 1^+$ and $\xi \to 1^-$.

Solve for $\tau^\star$ that again depends only on ξ and λ. With $\tau^\star$, (5.47a), (5.7), obtain ψ (dropping the dependence on ξ and λ) as:

$$y_{\max} = \bar{y}\left(\frac{\lambda+1}{\cos\varphi}e^{-\xi\tau^\star}\cos(\sqrt{1-\xi^2}\tau^\star+\varphi)-\lambda\right) =: \bar{y}\psi.$$

Overdamped system ($\xi > 1$). The solution to (5.8a) has the form parametrized by the unknowns Y_1, Y_2

$$\begin{aligned}
y &= Y_1 e^{-\omega_n l_1(\xi)t} + Y_2 e^{-\omega_n l_2(\xi)t} - \bar{u} \\
\dot{y} &= -\omega_n l_1(\xi)Y_1 e^{-\omega_n l_1(\xi)t} - \omega_n l_2(\xi)Y_2 e^{-\omega_n l_2(\xi)t},
\end{aligned} \tag{5.51}$$

where

$$l_1(\xi) := \xi + \sqrt{\xi^2-1} > l_2(\xi) := \xi - \sqrt{\xi^2-1} > 0.$$

For simplicity drop the dependence of l_1 and l_2 on ξ. Set

$$r := \frac{\lambda-1}{\lambda+1} \quad \text{and} \quad \tau_1 := \omega_n t_1,$$

solve (5.46) obtaining intermediately

$$Y_1 = \bar{u} + \bar{y} - Y_2 \quad \text{and} \quad \frac{Y_2}{\bar{u}+\bar{y}} = \frac{r - e^{-l_1\tau_1}}{e^{-l_2\tau_1} - e^{-l_1\tau_1}},$$

and finally:

$$\frac{(1+e^{l_2\tau_1})(-1+e^{l_1\tau_1}r)}{(1+e^{l_1\tau_1})(-1+e^{l_2\tau_1}r)} = \frac{l_1}{l_2}. \tag{5.52}$$

Solve for τ_1 (again depending only on ξ through l_1, l_2 and on λ) and get κ as in (5.50). With the same reasoning as in $0 < \xi < 1$, find $\tau^\star$ and then ψ:

$$\begin{aligned}
y_{\max} = \bar{y}\Bigg(&(\lambda+1)\frac{(r-e^{-\tau_1 l_2})e^{-l_1\tau^\star}}{e^{-\tau_1 l_1}-e^{-\tau_1 l_2}} \\
&- (\lambda+1)\frac{(r-e^{-\tau_1 l_1})e^{-l_2\tau^\star}}{e^{-\tau_1 l_1}-e^{-\tau_1 l_2}} - \lambda\Bigg) := \bar{y}\psi. \tag{5.53}
\end{aligned}$$

GLOBAL ASYMPTOTIC STABILITY OF A PID CONTROL SYSTEM WITH COULOMB FRICTION

In this Chapter we characterize the properties of a differential inclusion model of the feedback interconnection of a sliding mass with a proportional-integral-derivative (PID) controller under Coulomb friction. We prove global asymptotic stability of the largest set of closed-loop equilibria using a discontinuous Lyapunov-like function, and a weak version of the LaSalle's invariance principle. Simulations are also provided to illustrate our statements. Due to the regularity of the differential inclusion model, global asymptotic stability is intrinsically robust. Additionally, taking as input the size of the inflation of a perturbed model, the dynamics is input-to-state (ISS) stable, and this perturbation includes the well-known Stribeck effect. Future work will address further the case of static friction force larger than the Coulomb one and will propose for that setting compensation schemes.

The content of this Chapter is entirely based on [16].

6.1 INTRODUCTION: LITERATURE REVIEW

Classical results on friction in mechanical systems acknowledge that, for a moving mass, the friction force is proportional to the normal force through a kinetic coefficient (Coulomb friction) and presents possibly a term proportional to the velocity (viscous friction), whereas at rest the friction force is bounded by the product of the normal force and a static coefficient, generally greater than the kinetic coefficient.

Within the control community, the interest in the dynamical properties of friction had its peak in the 1990's, and the control engineering reasons for this interest are lucidly argued in [90, §1]. These dynamical properties have been studied along a modeling direction in the Dahl model [31], the LuGre model [8, 24], the models by Bliman and Sorine [21] and the Leuven model [117] (the characteristics of these models are also collectively outlined in [36]). When a mass moves with steady velocity and the corresponding friction force is measured, there is a small interval of velocities near zero where the friction force decreases before increasing again due to viscous friction and this behaviour is given the name of *Stribeck effect*. Other typical experimental friction phenomena are presliding/sliding and rate independence, for which the reader is referred to [90, §2.1-2.3]. In [21], considering friction as depending only on the path, allows using the theory of hysteresis operators [60, 122] and the LuGre model itself proved to be amenable to theoretical analysis, as [11] presents necessary and sufficient conditions for the passivity of its underlying operator from velocity to friction force.

In this chapter, we propose to characterize Coulomb friction in terms of differential inclusions [9], and we apply this characterization to the case of a point mass under such a friction force and actuated by a proportional-integral-derivative (PID) controller. This problem is a classical one in the friction literature (together with the point mass on a moving belt) and we will be able to prove the global asymptotic stability of the attractor having zero velocity, zero position and a bounded integral error. The use of a set-valued map for the friction force is quite natural in mechanics (see, e.g., [46, §10] and the references in [69, §1.5]) and is taken into consideration in [1, 21, 98, 125]: in [1] it is applied to a second-order uncontrolled mechanical system, in [125] to uncontrolled multi-degree-of-freedom mechanical systems, in [98] to a PD controlled 1 degree-of-freedom system. The combination of set-valued friction laws and Lyapunov tools is also the subject of [69, Chap. 5-6]. Other controlling strategies such as impulsive control are explored in [120]. The mathematical challenges associated with Coulomb friction are also illustrated in [116] and references therein.

To the best of the author's knowledge, global asymptotic stability has not been proved so far. In particular, it was proved (see [6, Thm. 1] and the related works
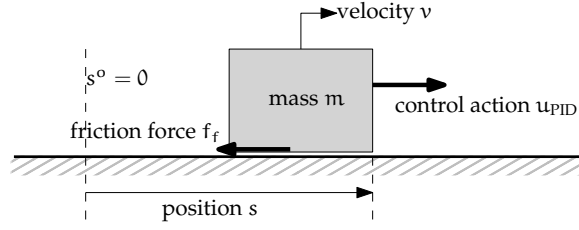
Figure 6.1: Mass under the action of friction and controlled by a PID controller.

[4, 5]) that in our same setting there exists no stick-slip limit cycle (the so-called hunting phenomenon, see [6, p. 679] and [24, §V-A.]; see [6] and Remark 6.3 for the definitions of stick and slip), which is the detrimental signature of a stiction greater than the Coulomb friction. As an overall achievement, Lyapunov tools applied to a differential-inclusion model enable proving global asymptotic stability of the largest set of equilibria. Additionally, the established properties and the regularity of our model imply robustness of asymptotic stability. This, in turn, allows us to prove an input-to-state stability (ISS) property for the perturbed dynamics, establishing that more general friction phenomena (including the Stribeck effect) cause a gradual deterioration of the response, in an ISS sense. This chapter can be regarded as a stepping stone to stiction larger than Coulomb where nontrivial jump set and maps can be identified (see [8, p. 106]), and to proposing compensation schemes using hybrid friction laws.

The chapter is structured as follows. We present the proposed model and the main results in Section 6.2. Then Section 6.3 contains an illustration by simulation of the established properties. The end of the paper contains the Lyapunov-based proof, separated into the proof of global attractivity (Section 6.4) and of stability (Section 6.5).

Notation. The sign function is defined as: $\text{sign}(x) := 1$ if $x > 0$, $\text{sign}(0) := 0$, $\text{sign}(x) := -1$ if $x < 0$. The saturation function is defined as: $\text{sat}(x) := \text{sign}(x)$ if $|x| > 1$, $\text{sat}(x) := x$ if $|x| \leqslant 1$. For $c \neq 0$, the function $x \mapsto \text{dz}_c(x)$ is defined as $\text{dz}_c(x) := x - c\,\text{sat}\left(\frac{x}{c}\right)$. $|x|$ denotes the Euclidean norm of vector x. $\langle \cdot, \cdot \rangle$ defines the inner product between its two vector arguments. The distance of a vector $x \in \mathbb{R}^n$ to a closed set $\mathcal{A} \subset \mathbb{R}^n$ is defined by $|x|_{\mathcal{A}} := \inf_{y \in \mathcal{A}} |x - y|$. A function $f: \mathbb{R}^n \to \mathbb{R}$ is lower semicontinuous if it satisfies $\liminf_{x \to x_0} f(x) \geqslant f(x_0)$ for each point x_0 of its domain.

6.2 PROPOSED MODEL AND MAIN RESULT

In Section 6.2.1 we derive the model we are using for the PID control system with Coulomb friction from a standard description of the friction force; we also prove that solutions to this model are unique, therefore coinciding with the ones of the standard description. Next, we present our main result in terms of global attractivity and stability in Section 6.2.2 together with some generalizations.

6.2.1 *Derivation of the model*

Consider a point mass m described by position s and velocity v, as in Figure 6.1. The overall friction force f_f acting on the mass comprises both Coulomb and viscous friction. Its classical description (see [4, Eq. (3)], or similarly [90, Eq. (5)]) is parametrized by a Coulomb friction constant $\bar{f}_c > 0$ and by the viscous friction constant $\alpha_v > 0$. The expression of f_f reads

$$f_f(f_r, v) := \begin{cases} \bar{f}_c \, \text{sign}(v) + \alpha_v v, & \text{if } v \neq 0 \\ f_r, & \text{if } v = 0, \ |f_r| < \bar{f}_c \\ \bar{f}_c \, \text{sign}(f_r), & \text{if } v = 0, \ |f_r| \geqslant \bar{f}_c \end{cases} \tag{6.1}$$

where f_r is the resultant tangential force. The mass is actuated by the PID control u_{PID}

$$u_{PID}(t) := -\bar{k}_p s(t) - \bar{k}_i \int_0^t s(\tau)d\tau - \bar{k}_d \frac{ds(t)}{dt}$$
$$= -\bar{k}_p s(t) - \bar{k}_i e_i(t) - \bar{k}_d v(t),$$

(6.2)

where e_i is defined to be the integral of the position error and is the state of the controller, satisfying $\dot{e}_i = s$ and $e_i(0) = 0$.

Using Newton's law, we write the mechanical dynamics $\dot{s} = v$ and $m\dot{v} = u_{PID} - f_f(u_{PID}, v)$. The convenient definitions $u := \frac{u_{PID} - \alpha_v v}{m}$, $(k_p, k_v, k_i) := (\frac{\bar{k}_p}{m}, \frac{\bar{k}_d + \alpha_v}{m}, \frac{\bar{k}_i}{m})$ and $f_c := \frac{\bar{f}_c}{m}$ yield then

$$\dot{e}_i = s \tag{6.3a}$$
$$\dot{s} = v \tag{6.3b}$$

$$\dot{v} = \begin{cases} u - f_c & \text{if } v > 0 \text{ or } (v = 0, u \geqslant f_c) \\ 0 & \text{if } (v = 0, |u| < f_c) \\ u + f_c & \text{if } v < 0 \text{ or } (v = 0, u \leqslant -f_c) \end{cases} \tag{6.3c}$$

$$u = -k_p s - k_v v - k_i e_i, \tag{6.3d}$$

where we used that $u_{PID} = m\,u$ for $v = 0$.

Model (6.3) arises from a relatively intuitive description of the mechanical principles behind the model of Figure 6.1. Its discontinuous right hand side makes it hard to prove existence of solutions for any initial conditions, even though such a property can be shown to hold on a case-by-case basis. Moreover, it seems to be hard to use dynamics (6.3) for establishing some stability properties and certifying that the position s converges to zero.

In this chapter we use the monotone set-valued friction law [69, Eq. 5.36] for which existence of solutions is structurally guaranteed. By defining the overall state $z := (e_i, s, v)$, this is equivalent to applying the Filippov [37] or Krasovskii regularization to the discontinuous dynamics (6.3) and obtaining

$$\dot{z} \in \begin{bmatrix} s \\ v \\ -k_i e_i - k_p s - k_v v \end{bmatrix} - f_c \begin{bmatrix} 0 \\ 0 \\ 1 \end{bmatrix} \text{SGN}(v) =: \tilde{F}(z) \tag{6.4a}$$

where the function SGN is a set-valued map defined as

$$\text{SGN}(v) := \begin{cases} \text{sign}(v), & \text{if } v \neq 0 \\ [-1, 1], & \text{if } v = 0. \end{cases} \tag{6.4b}$$

REMARK 6.1 *Although this model (and the equivalent one (6.16), after a change of coordinate) does not present a jump map and set, it is still useful to see it in terms of a purely continuous hybrid dynamical system $\mathcal{H} = (\tilde{F}, \mathbb{R}^3, \emptyset, \emptyset)$ consistently with Section 2.1 because the properties proven for the hybrid setting of Chapter 2 are carried over for this purely continuous system. Theorem 6.1, Corollary 6.1, the proof in Section 6.4.2 are examples of the usefulness of such a hybrid interpretation of model (6.4).* ⌟

Note that model (6.4) recognizes that the Coulomb friction can be selected as any force in the set $[-\bar{f}_c, \bar{f}_c]$ when v is zero and has magnitude $\bar{f}_c$ and direction opposite to v whenever $v \neq 0$. One may wonder whether any artificial solution[1] is introduced

---

1 We consider a solution to (6.3) or (6.4) a function that satisfies the sole continuous part of Definition 2.4 (or (2.8), since we will see that the hybrid basic conditions are satisfied), that is, any locally absolutely continuous function ψ satisfying respectively $\dot{\psi}(t) = \tilde{f}(\psi(t))$ or $\dot{\psi}(t) \in \tilde{F}(\psi(t))$ for almost all t in its domain.

by such an enriched description of the dynamics. The following result establishes uniqueness of the solutions to (6.4), which implies that the unique solution to (6.4) must necessarily be the unique solution to (6.3). Indeed, dynamics (6.3) allows for only some selections of $\dot{v}$ compared to those allowed by (6.4), so that any solution to (6.3) is also a solution to (6.4).

LEMMA 6.1 *For any initial condition $z(0) \in \mathbb{R}^3$, system (6.4) has a unique solution defined for all $t \geqslant 0$.*

Proof. Existence of solutions follows from [37, §7, Thm. 1] because the mapping in (6.4) is outer semicontinuous and locally bounded with nonempty compact convex values (see also [47, Prop. 6.10]). Completeness of maximal solutions follows from local existence and no finite escape times, as (6.4) can be regarded as a linear system forced by a bounded input. To prove uniqueness, consider two solutions $z_1 = (z_{1,e_i}, z_{1,s}, z_{1,v})$, z_2 both starting at z_0 and define $\delta(t) = (\delta_{e_i}(t), \delta_s(t), \delta_v(t)) := z_1(t) - z_2(t)$, for all $t \geqslant 0$. Then, $\delta(0) = 0$ and, for almost all $t \geqslant 0$,

$$\dot{\delta}(t) \in A_\delta \delta(t) - f_c \begin{bmatrix} 0 \\ 0 \\ 1 \end{bmatrix} \big(\mathrm{SGN}(z_{1,v}(t)) - \mathrm{SGN}(z_{1,v}(t) - \delta_v(t)) \big),$$

with

$$A_\delta := \begin{bmatrix} 0 & 1 & 0 \\ 0 & 0 & 1 \\ -k_i & -k_p & -k_v \end{bmatrix}, \tag{6.5}$$

whose maximum singular value is λ_δ. Therefore we can write for almost all nonnegative t

$$\frac{\mathrm{d}}{\mathrm{d}t} \frac{|\delta(t)|^2}{2} = \delta(t)^\top \dot{\delta}(t) \leqslant \lambda_\delta |\delta(t)|^2 + M(t)$$

$$M(t) := \max_{\substack{f_1 \in f_c \, \mathrm{SGN}(z_{1,v}(t)) \\ f_2 \in f_c \, \mathrm{SGN}(z_{1,v}(t) - \delta_v(t))}} \delta_v(t)(f_2 - f_1).$$

Whether $z_{1,v}(t)$ and $z_{1,v}(t) - \delta_v(t)$ are positive, zero or negative, by trivial inspection of all the cases it can be shown that $M(t) \leqslant 0$ for all $t \geqslant 0$. Therefore,

$$\frac{\mathrm{d}}{\mathrm{d}t} \frac{|\delta(t)|^2}{2} \leqslant \lambda_\delta |\delta(t)|^2 \text{ for almost all } t \geqslant 0,$$

and from standard comparison theorems $\delta(0) = 0$ implies $\delta(t) = 0$ for all $t \geqslant 0$, that is, $z_1(t) = z_2(t)$ for all $t \geqslant 0$. □

6.2.2 *Main result*

The advantage in the use of the compact dynamics (6.4) is that we may adopt Lyapunov tools to study the asymptotic stability properties of the rest position under the following standard assumption (see, for example, [6]).

ASSUMPTION 6.1 *The parameters in (6.3d) are such that*

$$k_i > 0, \quad k_p > 0, \quad k_v k_p > k_i.$$

According to the Routh stability test, Assumption 6.1 holds if and only if the origin of the dynamics in (6.4) with $f_c = 0$ is globally exponentially stable.

Under Assumption 6.1, one readily sees that all possible equilibria of dynamics (6.4) correspond to $(e_i, s, v) = (\bar{e}_i, 0, 0)$ with $|\bar{e}_i| \leqslant \frac{f_c}{k_i}$, that is, whenever the mass is at rest at zero position and the size of the integral error e_i is bounded by the specific threshold $\frac{f_c}{k_i}$. Any of these points is an equilibrium for (6.4) because in (6.4) a value can be selected from $f_c \, \mathrm{SGN}(0)$ such that the (unique) solution maintains $\dot{z}$ identically zero. Note that here we consider the problem of tracking a position setpoint $s^o = 0$, but the result can be generalized to piecewise constant setpoints s^o, thanks to a shift in the position coordinate to $s - s^o$ and the global nature of our results. Denote then the set of these equilibria as

$$\mathcal{A} := \left\{ (e_i, s, v) : \, s = 0, \, v = 0, \, e_i \in \left[-\frac{f_c}{k_i}, \frac{f_c}{k_i} \right] \right\}. \tag{6.6}$$

PROPOSITION 6.1 *Under Assumption 6.1, the attractor $\mathcal{A}$ in (6.6) is 1) globally attractive and 2) Lyapunov stable for dynamics (6.4).*

The global attractivity of $\mathcal{A}$ is proven in Section 6.4 and its stability in Section 6.5. For attractivity, we use a suitable discontinuous Lyapunov-like function and a non-smooth version of LaSalle's invariance principle: these tools are applicable to our scenario because of the desirable structural properties of the regularization in (6.4). Note that no smaller set could be proven to be globally attractive because $\mathcal{A}$ is a union of equilibria.

REMARK 6.2 *For our results in Proposition 6.1 and Theorem 6.1 to hold, we just need the PID-related parameters k_i, k_p and k_v to guarantee asymptotic stability when no friction is present, as in Assumption 6.1. However, it requires a nontrivial analysis to determine their influence in term of convergence rate of the state when friction is present. In particular, since our analysis is based on a Lyapunov-like function, it is a nontrivial extension to use these Lyapunov tools to determine the convergence rate of the solutions, based on suitable properties of the Lyapunov function.* ⌐

For $\mathbb{B}$ denoting the closed unit ball, $\overline{\mathrm{co}}$ the closed convex hull of a set, and $\rho : \mathbb{R}^3 \to \mathbb{R}_{\geqslant 0}$ a suitable continuous perturbation function satisfying $z \notin \mathcal{A} \Rightarrow \rho(z) > 0$ and vanishing in $\mathcal{A}$, we have the following perturbation of dynamics (6.4):

$$\dot{z} \in \overline{\mathrm{co}}\tilde{F}(z + \rho(z)\mathbb{B}) + \rho(z)\mathbb{B}. \tag{6.7}$$

Note that (6.7) represents precisely the ρ-perturbation of $\mathcal{H} = (\tilde{F}, \mathbb{R}^3, \emptyset, \emptyset)$ in Definition 2.17 (see also Remark 6.1).

The main result in Theorem 6.1 establishes the following two relevant robust stability properties of $\mathcal{A}$ involving the solutions to the perturbed dynamics (6.7). By specializing Definitions 2.18 and 2.19 in the purely continuous setting and for $\mathcal{U} = \mathbb{R}^3$ (since the present results are global), *robust uniform global asymptotic stability of $\mathcal{A}$* corresponds to the property that $\mathcal{A}$ is uniformly globally asymptotically stable for (6.7) (see Definition 2.14), and *robust global $\mathcal{KL}$ asymptotic stability of $\mathcal{A}$* to the existence of $\beta_0 \in \mathcal{KL}$ such that all solutions to (6.7) satisfy $|z(t)|_{\mathcal{A}} \leqslant \beta_0(|z(0)|_{\mathcal{A}}, t)$ for all $t \geqslant 0$. Note that robust uniform global asymptotic stability is equivalent to robust global $\mathcal{KL}$ asymptotic stability due to [47, Thm. 3.40].

THEOREM 6.1 *Under Assumption 6.1, the attractor $\mathcal{A}$ in (6.6) is robustly uniformly globally asymptotically stable and robustly globally $\mathcal{KL}$ asymptotically stable.*

The hybrid basic conditions are satisfied by $\tilde{F}$ and $\mathcal{A}$ is compact: from Fact 2.6, Proposition 6.1 implies robust global $\mathcal{KL}$ asymptotic stability of $\mathcal{A}$, and thus Theorem 6.1, as already noted in Example 2.8.

A specific perturbation of interest arises when selecting a constant scalar $\rho_v \in \mathbb{R}$ and perturbing the friction effect as follows:

$$\dot{z} \in \begin{bmatrix} s \\ v \\ -k_i e_i - k_p s - k_v v \end{bmatrix} - f_c \begin{bmatrix} 0 \\ 0 \\ 1 \end{bmatrix} \mathrm{SGN}_{\rho_v}(v) \tag{6.8a}$$

$$\mathrm{SGN}_{\rho_v}(v) := \begin{cases} [\mathrm{sign}(v) - |\rho_v|, \mathrm{sign}(v) + |\rho_v|], & \text{if } |v| > |\rho_v| \\ [-1 - |\rho_v|, 1 + |\rho_v|], & \text{if } |v| \leqslant |\rho_v|. \end{cases} \tag{6.8b}$$

Note that (6.8b) coincides with the inflation of a set-valued mapping defined for the flow map in Definition 2.17, as we saw in Example 2.7. In the special case $\rho_v = 0$, SGN_0 clearly coincides with SGN. This perturbation is of interest because it comprises the Stribeck effect, as shown after the proof of Corollary 6.1. Its proof exploits an interesting consequence of the robustness result established in Theorem 6.1, namely the semiglobal practical robust asymptotic stability of attractor $\mathcal{A}$ that was presented in Definition 2.20. This consequence follows from Facts 2.4 and 2.7.

COROLLARY 6.1 *Under Assumption 6.1, the attractor $\mathcal{A}$ in (6.6) is globally input-to-state stable for dynamics (6.8a) from input ρ_v.*

Proof. The solutions to (6.8a) are a subset of the solutions to $\dot{z} = A_\delta z - f_c \begin{bmatrix} 0 \\ 0 \\ 1 \end{bmatrix} \mathfrak{m}$, where: A_δ in (6.5) is Hurwitz from Assumption 6.1, and $\mathfrak{m}$ is a locally integrable signal satisfying $\mathfrak{m}(t) \leqslant 1 + |\rho_v|$ for all t because, for the constant scalar ρ_v, $\mathrm{SGN}_{\rho_v}(v(t)) \leqslant 1 + |\rho_v|$ for all t. From BIBO stability of exponentially stable linear systems, there exist positive c and λ such that all solutions satisfy

$$|z(t)| \leqslant ce^{-\lambda t}|z(0)| + c(1 + |\rho_v|). \tag{6.9}$$

From the two distances

$$|z|_{\mathcal{A}}^2 := s^2 + v^2 + \left(dz_{f_c/k_i}(e_i)\right)^2$$
$$|z|^2 := s^2 + v^2 + e_i^2,$$

we have $|z|_{\mathcal{A}} \leqslant |z|$ and $|z|^2 \leqslant 2|z|_{\mathcal{A}}^2 + 2\left(\frac{f_c}{k_i}\right)^2$ (by splitting into the cases $|e_i| \geqslant \frac{f_c}{k_i}$ and $|e_i| < \frac{f_c}{k_i}$), which implies $|z| \leqslant \sqrt{2}\left(|z|_{\mathcal{A}} + \frac{f_c}{k_i}\right)$. These relationships between the two distances and (6.9) imply that there exist positive constants κ_1, κ_2, κ_3 such that all solutions satisfy

$$|z(t)|_{\mathcal{A}} \leqslant |z(t)| \leqslant ce^{-\lambda t}|z(0)| + c(1 + |\rho_v|)$$
$$\leqslant \kappa_1 e^{-\lambda t}|z(0)|_{\mathcal{A}} + \kappa_2 + \kappa_3|\rho_v|, \ \forall t \geqslant 0. \tag{6.10}$$

By Theorem 6.1 and the semiglobal practical robustness of $\mathcal{KL}$ asymptotic stability following from Facts 2.4 and 2.7, one can transform the semiglobal practical δ-ϵ argument into a class $\mathcal{K}$ function γ_ℓ by following similar steps to [59, Lemma 4.5], as we did in Application 2.1. Moreover, using a similar approach to [114, Thm. 2] relating the size of the initial condition and of the input, we obtain the following:

$$|z(0)|_{\mathcal{A}} \leqslant \frac{1}{\delta_\ell}, |\rho_v| \leqslant \delta_\ell \Rightarrow |z(t)|_{\mathcal{A}} \leqslant \beta_\ell(|z(0)|_{\mathcal{A}}, t) + \gamma_\ell(|\rho_v|), \ \forall t \geqslant 0, \tag{6.11}$$

for some suitable class $\mathcal{KL}$ and class $\mathcal{K}$ functions β_ℓ and γ_ℓ, and for a small enough scalar $\delta_\ell > 0$. Without loss of generality, consider now using in (6.11) a small enough δ_ℓ such that $(2\delta_\ell)^{-1} \geqslant \kappa_2 + \kappa_3\delta_\ell$. Introduce the function $T^\star \colon \mathbb{R}_{\geqslant 0} \to \mathbb{R}_{\geqslant 0}$ with $T^\star(s) := \max\{0, \lambda^{-1}\log(2\delta_\ell\kappa_1 s)\}$, which satisfies:

$$\kappa_1 e^{-\lambda T^\star(s)} s + \kappa_2 + \kappa_3\delta_\ell \leqslant \delta_\ell^{-1}, \quad \forall s \geqslant 0. \tag{6.12}$$

Finally, we conclude the proof by establishing the following (global) ISS bound from ρ_v:

$$|z(t)|_{\mathcal{A}} \leqslant \beta(|z(0)|_{\mathcal{A}}, t) + \gamma(|\rho_v|), \ \forall z(0), \ \forall \rho_v, \ \forall t \geqslant 0, \tag{6.13}$$

where functions β and γ of class $\mathcal{KL}$ and class $\mathcal{K}$, respectively, are built starting from the following inequalities:

$$\beta(s, t) \geqslant \begin{cases} \kappa_1 e^{-\lambda t}s + \kappa_2 + \kappa_3\delta_\ell, & \text{if } s \geqslant \frac{1}{\delta_\ell}, t \leqslant T^\star(s) \tag{6.14a} \\ \mathfrak{b}(s, t), & \text{otherwise} \tag{6.14b} \end{cases}$$

$$\mathfrak{b}(s, t) := \max\left\{\beta_\ell(s, \max\{0, t - T^\star(s)\}), \kappa_1 e^{-\lambda t}s\right\} \tag{6.14c}$$

$$\gamma(s) \geqslant \begin{cases} \kappa_2 + \kappa_3 s, & \text{if } s \geqslant \delta_\ell \tag{6.14d} \\ \gamma_\ell(s), & \text{if } s \leqslant \delta_\ell. \tag{6.14e} \end{cases}$$

The effectiveness of selections (6.14) for establishing the ISS bound (6.13) can be verified case by case.

CASE 1 ($|\rho_v| \geqslant \delta_\ell$): use (6.10), (6.14d), and bound $\kappa_1 e^{-\lambda t}s$ in (6.14c)-(6.14b).

CASE 2 ($|\rho_v| \leqslant \delta_\ell$ and $|z(0)|_{\mathcal{A}} \leqslant \delta_\ell^{-1}$): use (6.11), (6.14e), and the bound in (6.14c)-(6.14b) for $\beta_\ell(s, \max\{0, t - T^\star(s)\})$.

CASE 3 ($|\rho_v| \leqslant \delta_\ell$ and $|z(0)|_{\mathcal{A}} \geqslant \delta_\ell^{-1}$): for $t \leqslant T^\star(|z(0)|_{\mathcal{A}})$ use (6.14a) and nonnegativity of γ, whereas for $t \geqslant T^\star(|z(0)|_{\mathcal{A}})$ use $|z(T^\star(|z(0)|_{\mathcal{A}}))|_{\mathcal{A}} \leqslant \delta_\ell^{-1}$ (from (6.10) and (6.12)) and the semigroup property of solutions to fall again into case 2 above. $\square$

A consequence of Corollary 6.1 is that the Stribeck effect, which is known to lead to persistent oscillations (the so-called *hunting* phenomenon), produces solutions that are graceful degradations in the ISS sense of the asymptotically stable solutions to the unperturbed dynamics because small Stribeck deformations lead to graphs included in the graph of $f_c \, \mathrm{SGN}_{\rho_v}(v)$, as shown in Figure 6.2.
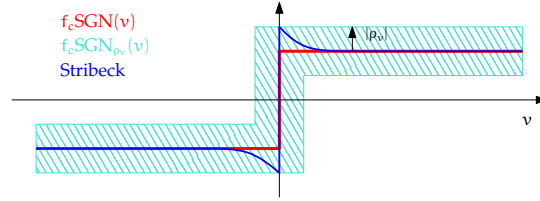
Figure 6.2: Stribeck effect is included in the perturbation (6.8a).

6.3 ILLUSTRATION BY SIMULATION

Before we prove our main result in Sections 6.4-6.5, in this section we illustrate by simulation the typical behaviour of solutions to (6.4) and their convergence to the attractor. Simulations capture, for each initial condition, the unique solution to (6.4) because of Lemma 6.1. When $f_c = 0$, (6.4) reduces to a linear system with characteristic polynomial $s^3 + k_v s^2 + k_p s + k_i = 0$, whose roots have negative real part from Assumption 6.1. Although our subsequent proof does not differentiate anyhow among the possible locations of these roots in the complex plane, we present our simulations for two representative cases, complex conjugate and three distinct real roots. Specifically, roots $\{-6.01, -0.19 \pm i0.79\}$ and $\{-0.8, -0.5, -0.2\}$ are obtained for parameters $(k_v, k_p, k_i) = (6.4, 3, 4)$ and $(k_v, k_p, k_i) = (1.5, 0.66, 0.08)$, respectively. $f_c = 1 \text{ m/s}^2$ is common to all simulations.

First, we present the solutions to (6.4) for different sets of initial conditions for the complex conjugate and real root cases, respectively in the left and right top plots of Figure 6.3. In the solution represented by a heavier dark violet line, two different phases are visible: the mass is in motion (called *slip phase* in the friction literature), or the mass is at rest (called *stick phase*) and the velocity is zero on a nonzero time interval. Whenever the mass is in a slip phase, the PID control acts in the direction of getting the mass closer to the position setpoint at zero. During a stick phase starting at t_i, only the error integral builds up linearly in time as $e_i(t) = e_i(t_i) + s(t_i)(t - t_i)$ until the control action u overcomes the Coulomb friction, that is, $|u| = |-k_i e_i - k_p s| = f_c$. So, the closer the mass is to the zero position (smaller $s(t_i)$), the longer it takes the error to build up and exit a stick phase. As a consequence, solutions converge asymptotically to the attractor, but not exponentially. Moreover, position and velocity converge to zero, but the error integral does not in general: it continues to oscillate and enters asymptotically the set $\left[-\frac{f_c}{k_i}, \frac{f_c}{k_i}\right]$ as the position approaches zero for complex conjugate roots (top, left); it approaches the equilibria $\frac{f_c}{k_i}$ or $-\frac{f_c}{k_i}$ for distinct real roots (top, right) because after a stick phase the position and the velocity converge to zero exponentially, so that v remains always nonzero.

Second, we present in the left and right center plots of Figure 6.3 a phase portrait for the same solutions in the top plots. In these figures it is evident that solutions converge to the attractor in (6.6), with the two different behaviors described above. In the left center plot, we can also appreciate the presence of a strip in the plane $v = 0$ expressed by equation $-f_c \leqslant -k_i e_i - k_p s \leqslant f_c$ (as in [99, Page 7]), that is, the region of the state space where stick is bound to occur.

Third, we keep the same initial conditions and parameters and we anticipate the evolution along solutions of the Lyapunov-like function introduced in the next section (see its definition in (6.19)). In particular, this function is nonincreasing along solutions, it can be discontinuous (for example, the left, bottom, dark blue and violet curves close to $t = 0$ s), and remains constant during stick (as pointed out by the same heavier dark violet curves).
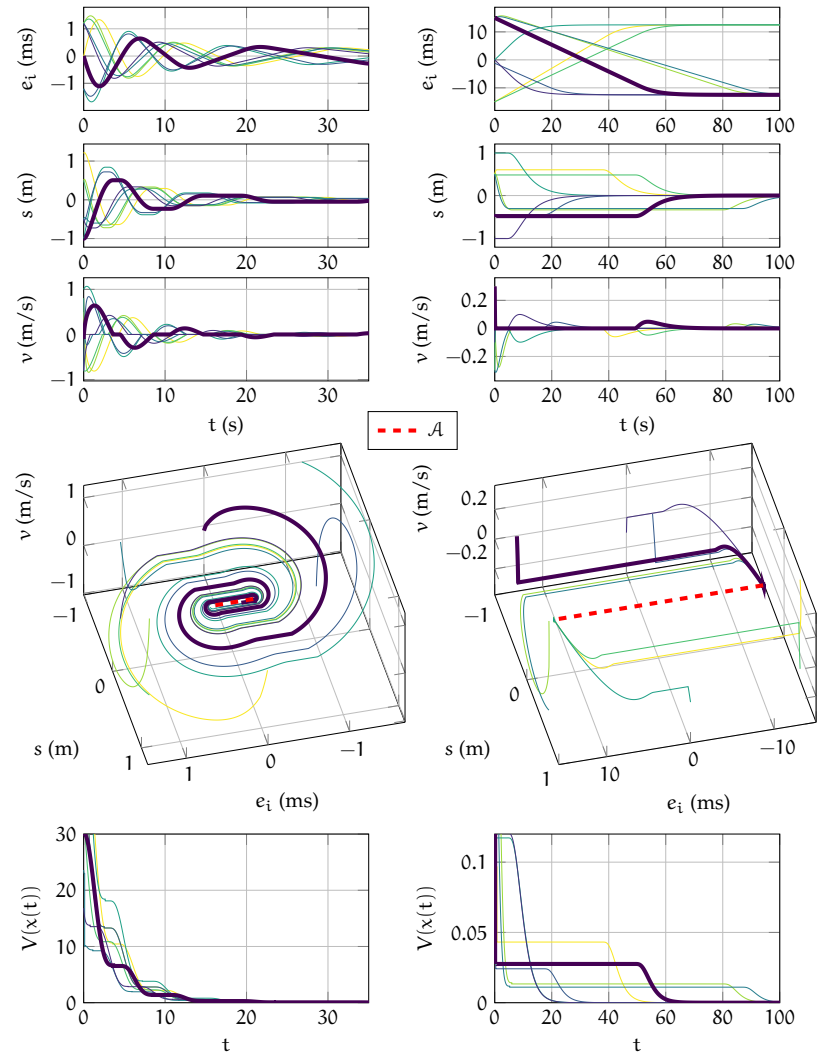
Figure 6.3: Top: solutions to (6.4) for different initial conditions. Center: phase portraits for (6.4) for the same solutions. Bottom: Lyapunov-like function V in (6.19) evaluated along the same solutions. All the figures to the left (resp., right) refer to the PID parameters $(k_v, k_p, k_i) = (6.4, 3, 4)$ (resp., $(1.5, 0.66, 0.08)$).

6.4   PROOF OF PROPOSITION 6.1: GLOBAL ATTRACTIVITY

In Section 6.4.1 we state a change of coordinate for model (6.4) that allows us to define a Lyapunov-like function. Its properties in Lemma 6.2 are the key to establish global attractivity and stability. The proof of the lemma is postponed to Section 6.4.3, whereas global attractivity is proven directly in Section 6.4.2.

6.4.1   *Coordinate change and discontinuous LaSalle function*

For the following analysis we adopt a specific change of coordinates for (6.4), that is,

$$\sigma := -k_i s$$
$$\phi := -k_i e_i - k_p s \qquad\qquad (6.15)$$
$$v := v.$$

The change of coordinates is nonsingular thanks to Assumption 6.1 (k_i, k_p strictly positive) and it rewrites (6.4) as

$$
\dot{x} := \begin{bmatrix} \dot{\sigma} \\ \dot{\phi} \\ \dot{v} \end{bmatrix} \in \begin{bmatrix} -k_i v \\ \sigma - k_p v \\ \phi - k_v v - f_c \, \mathrm{SGN}(v) \end{bmatrix}
$$

$$
= \underbrace{\begin{bmatrix} 0 & 0 & -k_i \\ 1 & 0 & -k_p \\ 0 & 1 & -k_v \end{bmatrix}}_{=:A} \begin{bmatrix} \sigma \\ \phi \\ v \end{bmatrix} - \underbrace{\begin{bmatrix} 0 \\ 0 \\ f_c \end{bmatrix}}_{=:b} \mathrm{SGN}(v) \tag{6.16}
$$

$$
= Ax - b\,\mathrm{SGN}(v) =: F(x).
$$

In the new coordinates x, the attractor $\mathcal{A}$ in (6.6) can be expressed as

$$
\mathcal{A} = \{(\sigma, \phi, v): |\phi| \leqslant f_c, \sigma = 0, v = 0\}. \tag{6.17}
$$

Among other things, the simple expression in (6.17) allows writing explicitly the distance of a point x from $\mathcal{A}$ as

$$
|x|^2_{\mathcal{A}} := \Big(\inf_{y \in \mathcal{A}} |x - y| \Big)^2 = \sigma^2 + v^2 + dz_{f_c}(\phi)^2 \tag{6.18}
$$

where $dz_{f_c}(\phi) := \phi - sat_{f_c}(\phi)$ is the symmetric scalar deadzone function returning zero when $\phi \in [-f_c, f_c]$. Indeed, the rightmost expression in (6.18) follows from separating the cases $\phi < -f_c$, $|\phi| \leqslant f_c$, $\phi > f_c$ and applying Definition 2.7 for the distance to a set. See also Figure 2.8 for the level sets of $|x|^2_{\mathcal{A}}$.

Based on the set-valued model (6.4) for the friction and the form of the attractor in (6.17), it is rather intuitive to introduce the following discontinuous Lyapunov-like function

$$
V(x) := \begin{bmatrix} \sigma \\ v \end{bmatrix}^T \begin{bmatrix} \frac{k_v}{k_i} & -1 \\ -1 & k_p \end{bmatrix} \begin{bmatrix} \sigma \\ v \end{bmatrix} + \min_{f \in f_c \, \mathrm{SGN}(v)} |\phi - f|^2 \tag{6.19a}
$$

$$
= \min_{f \in f_c \, \mathrm{SGN}(v)} \begin{bmatrix} \sigma \\ \phi - f \\ v \end{bmatrix}^T P \begin{bmatrix} \sigma \\ \phi - f \\ v \end{bmatrix}
$$

where the matrix P is given by

$$
P := \begin{bmatrix} \frac{k_v}{k_i} & 0 & -1 \\ 0 & 1 & 0 \\ -1 & 0 & k_p \end{bmatrix}, \tag{6.19b}
$$

and satisfies $PA + A^T P \leqslant 0$ relative to (6.16) with $f_c = 0$. Note that for $v \neq 0$ the minimization in (6.19a) becomes trivial because f can take only the value $f_c \, \mathrm{sign}(v)$. It is emphasized that function V is discontinuous. For example, if we evaluate V along the sequence of points $(\sigma_i, \phi_i, v_i) = (0, 0, \varepsilon_i)$ for $\varepsilon_i \in (0, 1)$ converging to zero, V converges to f_c^2, even though its value at zero is zero. Nevertheless, function V enjoys a number of useful properties established in the next lemma whose proof is given in Section 6.4.3.

LEMMA 6.2 *The Lyapunov-like function in (6.19) is lower semicontinuous and enjoys the following properties:*

1. *$V(x) = 0$ for all $x \in \mathcal{A}$ and there exists $c_1 > 0$ such that $c_1 |x|^2_{\mathcal{A}} \leqslant V(x)$ for all $x \in \mathbb{R}^3$,*

2. *there exists $c > 0$ such that each solution $x = (\sigma, \phi, v)$ to (6.16) satisfies for all $t_2 \geqslant t_1 \geqslant 0$*

$$
V(x(t_2)) - V(x(t_1)) \leqslant -c \int_{t_1}^{t_2} v(t)^2 \, dt. \tag{6.20}
$$

REMARK 6.3 *In [6] it is proven that if a solution is in a* slip phase *in the nonempty time interval* (t_i, t_{i+1}) *(namely, for all* $t \in (t_i, t_{i+1})$, $v(t) \neq 0$*) and the slip phase is preceded and followed by a* stick phase *(namely, there exist* $\delta > 0$ *such that, for all* $t \in [t_i - \delta, t_i] \cup [t_{i+1}, t_{i+1} + \delta]$, $v(t) = 0$ *and* $|\phi(t)| \leqslant f_c$*), then*

$$|\sigma(t_{i+1})| < |\sigma(t_i)|. \tag{6.21}$$

This relation is illustrated in Figure 6.4.
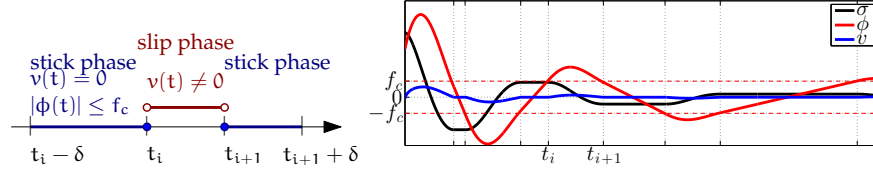
Figure 6.4: Illustration of the slip and stick phases, and of a specific state evolution. The satisfaction of (6.21) from [6] is also visible.

[6, Lemma L2] uses the explicit form of solutions (depending on the nature of the eigenvalues of A) to prove (6.21). Instead, we can conclude easily (6.21) from (6.20) (implying $V(x(t_i)) < V(x(t_{i+1})$ *because during a slip phase the velocity is strictly nonzero), and from the definition (6.19a) and* $|\phi(t_i)| \leqslant f_c$, $|\phi(t_{i+1})| \leqslant f_c$ *(implying* $V(x(t_i)) = \frac{k_v}{k_i} \sigma(t_{i+1})^2$, $V(x(t_{i+1})) = \frac{k_v}{k_i} \sigma(t_i)^2$*).*

⌟

6.4.2 *Proof of item 1) of Proposition 6.1 (global attractivity)*

In this section we prove the first item of Proposition 6.1 (that is, global attractivity): first we rely on results given originally for hybrid dynamical systems and presented in Section 2.5.6, second we present an alternative proof that relies only on results for differential inclusions.

Proof of item 1) of Proposition 6.1 (global attractivity of A). All solutions[2] $x = (\sigma, \phi, v)$ to (6.16) are complete by Lemma 6.1, and the pair $(F, \mathbb{R}^3)$ in (6.16) satisfies the hybrid basic conditions stated in Assumption 2.1. Furthermore, all solutions are bounded because from Lemma 6.2, $V(x(t)) \leqslant V(x(0))$ (item 2) and $c_1 |x(t)|_{\mathcal{A}}^2 \leqslant V(x(t))$ (item 1) imply $|x(t)|_{\mathcal{A}}^2 \leqslant \frac{V(x(0))}{c_1}$ for all $t \geqslant 0$.

There exist a lower semi-continuous $\ell : \mathbb{R}^3 \to [0, \infty]$ defined for $\chi = (\chi_\sigma, \chi_\phi, \chi_v)$ as $\ell(\chi) := \chi_v^2$ such that $t \mapsto \ell(x(t))$ is summable, and then weakly meagre (see the discussion after Definition 2.24). Indeed, apply (6.20) from 0 to t, and obtain $c \int_0^t v(\tau)^2 d\tau \leqslant V(x(0)) - V(x(t)) \leqslant V(x(0))$ because $V(x(t)) \geqslant 0$ from Lemma 6.2, item 1. Then we have $\int_0^t v(\tau)^2 d\tau \leqslant \frac{V(x(0))}{c}$, and if $t \to +\infty$ we get the required summability of $\ell(x(\cdot))$, that is, the boundedness of its integral from 0 to $+\infty$. We can then use Fact 2.19 to conclude that for each solution x

$$\Omega(x) \subset \{\chi = (\chi_\sigma, \chi_\phi, \chi_v) \in \overline{\text{rge}(x)} : \chi_v = 0\}, \tag{6.22}$$

as we anticipated in Application 2.6.

Fact 2.18 establishes two relevant properties of the ω-limit set $\Omega(x)$ of a solution x.

1. $\Omega(x)$ is invariant for each solution x. It is weakly forward and backward invariant because the hybrid basic conditions are satisfied and each x is complete and bounded as noted above. Because of uniqueness of solutions, weak forward invariance is actually strong forward invariance (see Definition 2.26). Because of (6.22), each element χ of $\Omega(x)$ has $\chi_v = 0$ and because of the

---

2 Solutions to (6.16) are the functions $t \mapsto x(t)$, with components $t \mapsto \sigma(t)$, $t \mapsto \phi(t)$, $t \mapsto v(t)$. Points in the Euclidean space $\mathbb{R}^3$ are denoted by χ, with components $\chi_\sigma, \chi_\phi, \chi_v$.

invariance of $\Omega(x)$, each element must have $\chi_\sigma = 0$ and $|\chi_\phi| \leqslant f_c$ in addition to $\chi_\nu = 0$. Indeed, if it were $\chi_\sigma \neq 0$, a solution x starting from such a point χ would present a ramp in the component ϕ that eventually exceeds f_c in absolute value and drives the component ν away from zero, so that $\Omega(x)$, which has $\chi_\nu = 0$ by (6.22), would no longer be invariant. The same reasoning establishes $|\chi_\phi| \leqslant f_c$ in $\Omega(x)$. Therefore, $\Omega(x)$ is contained in $\mathcal{A}$.

2. The second property of Fact 2.18 is: $|x(t)|_{\Omega(x)} \to 0$ as $t \to \infty$, $t \geqslant 0$, which implies $|x(t)|_{\mathcal{A}} \to 0$ by the previous item.

Since the previous conclusions hold for each solution, they prove global attractivity. □

In the remainder of the section, we present an alternative proof of global attractivity that builds only on results given for differential inclusions, in particular on a generalized version of the invariance principle [59, §4.2] for differential inclusions. The following fact comes indeed from specializing such a result in [103, Thm. 2.10] to our case, where the differential inclusion (6.4) has actually unique solutions defined for all nonnegative times (as established in Lemma 6.1). We also select $G = \mathbb{R}^3$, $U = \mathbb{R}^3$ in the original result of [103].

FACT 6.1 [103] *Let $\ell : \mathbb{R}^3 \to \mathbb{R}_{\geqslant 0}$ be lower semicontinuous and such that $\ell(\chi) \geqslant 0$, for all $\chi \in \mathbb{R}^3$. If x is a complete and bounded solution to (6.4) satisfying $\int_0^{+\infty} \ell(x(t))\mathrm{d}t < +\infty$, then x converges to the largest forward invariant subset $\mathcal{M}$ of $\Sigma := \{\chi \in \mathbb{R}^3 : \ell(\chi) = 0\}$.*

Proof of item 1) of Proposition 6.1 (global attractivity of $\mathcal{A}$). The proof exploits Fact 6.1, where we take $\ell(\chi) = \chi_\nu^2$. From Lemma 6.2, $V(x(t)) \leqslant V(x(0))$ (item 2) and $c_1|x(t)|_{\mathcal{A}}^2 \leqslant V(x(t))$ (item 1) for any nonnegative t, so that $c_1|x(t)|_{\mathcal{A}}^2 \leqslant V(x(0))$ and then all solutions to (6.16) are bounded (their completeness is established in Lemma 6.1). Apply (6.20) from 0 to t, and obtain $c\int_0^t \nu^2(\tau)\mathrm{d}\tau \leqslant V(x(0)) - V(x(t)) \leqslant V(x(0))$ because $V(x(t)) \geqslant 0$ from Lemma 6.2, item 1. Then we have $\int_0^t \nu^2(\tau)\mathrm{d}\tau \leqslant \frac{V(x(0))}{c}$, and if $t \to +\infty$ we get the required boundedness of the integral of $\ell(x(\cdot))$. Then Fact 6.1 guarantees that the solution x converges to the largest forward invariant subset $\mathcal{M}$ of $\Sigma = \{\chi = (\chi_\sigma, \chi_\phi, \chi_\nu) : \chi_\nu = 0\}$. We claim that such a subset is $\mathcal{A}$. Indeed, $\mathcal{M} \subset \Sigma$ implies $\chi_\nu = 0$ in $\mathcal{M}$. Moreover, $\chi_\sigma = 0$ in $\mathcal{M}$ because each solution x starting from $\chi_\nu = 0$ and $\chi_\sigma \neq 0$ causes a ramp of the ϕ component of x that eventually exceeds f_c and drives the ν component away from zero (therefore out of Σ). Finally, in $\mathcal{M}$ we must have $|\chi_\phi| \leqslant f_c$ otherwise the ν component would become nonzero again. Therefore the largest forward invariant set $\mathcal{M}$ in Σ is the attractor $\mathcal{A}$. □

6.4.3 *Proof of Lemma 6.2*

To the end of proving Lemma 6.2, we note that model (6.16) and function (6.19) suggest that there are three relevant affine systems and smooth functions associated to the three cases in (6.3c) that are worth considering (and will be used in our proofs). They correspond to

$$\dot{\xi} = f_1(\xi) := A\xi - b, \qquad\qquad \xi(0) = \xi_1, \qquad\qquad (6.23\text{a})$$

$$\dot{\xi} = f_0(\xi) := \begin{bmatrix} 0 & 0 & 0 \\ 1 & 0 & 0 \\ 0 & 0 & 0 \end{bmatrix} \xi, \qquad\qquad \xi(0) = \xi_0, \qquad\qquad (6.23\text{b})$$

$$\dot{\xi} = f_{-1}(\xi) := A\xi + b, \qquad\qquad \xi(0) = \xi_{-1}, \qquad\qquad (6.23\text{c})$$

and, with the definition $|\xi|_P^2 := \xi^\mathsf{T} P \xi$,

$$V_1(\xi) := \left\| \begin{bmatrix} \sigma \\ \phi - f_c \\ \nu \end{bmatrix} \right\|_P^2, \; V_0(\xi) := \left\| \begin{bmatrix} \sigma \\ 0 \\ 0 \end{bmatrix} \right\|_P^2, \; V_{-1}(\xi) := \left\| \begin{bmatrix} \sigma \\ \phi + f_c \\ \nu \end{bmatrix} \right\|_P^2. \qquad (6.23\text{d})$$

Based on the description above, we can state the following claim relating (6.23) to solutions of (6.16) and to V in (6.19). Its proof mostly relies on straightforward inspection of the various cases and is given at the end of the present section.

CLAIM 6.1 *There exists* $c > 0$ *such that, for each initial condition* $(\bar{\sigma}, \bar{\phi}, \bar{v})$, *one can select* $k \in \{-1, 0, 1\}$ *and* $T > 0$ *satisfying the following:*

1. *the unique solution* $\xi = (\xi_\sigma, \xi_\phi, \xi_v)$ *to the* k-*th initial value problem among* (6.23a)-(6.23c) *with initial condition* $\xi_k = (\bar{\sigma}, \bar{\phi}, \bar{v})$ *coincides in* $[0, T]$ *with the unique solution to* (6.16);

2. *the solution* ξ, *mentioned above satisfies for all* $t \in [0, T]$

$$V(\xi(t)) = V_k(\xi(t)), \tag{6.24a}$$

$$\frac{d}{dt} V_k(\xi(t)) \leqslant -c|\xi_v(t)|^2. \tag{6.24b}$$

Additionally, we restate a fact from [52] that is beneficial to proving Lemma 6.2. Specifically, we use [52, Theorem 9] together with the variant in [52, Section 5 (point a.)]. We also specialize the statement, using the fact that when the function g is integrable, the standard integral can replace the upper integral (as noted after [52, Definition 8]). The lower right Dini derivative D_+h of h is defined as $D_+h(t) := \liminf_{\epsilon \to 0^+} \frac{h(t+\epsilon)-h(t)}{\epsilon}$.

FACT 6.2 *[52] Given* $t_2 > t_1 \geqslant 0$, *suppose that* h *is lower semicontinuous and that* l *is locally integrable in* $[t_1, t_2]$. *If* $D_+h(\tau) \leqslant l(\tau)$ *for all* $\tau \in [t_1, t_2]$, *then*

$$h(t_2) - h(t_1) \leqslant \int_{t_1}^{t_2} l(\tau)d\tau.$$

Building on Claim 6.1 and Fact 6.2 we can prove Lemma 6.2.

Proof of Lemma 6.2. We show first that V is lower semicontinuous. Define the set-valued mapping

$$G(x) := \bigcup_{f \in SGN(v)} g(\sigma, \phi, v, f), \quad g(\sigma, \phi, v, f) := \begin{bmatrix} \sigma \\ \phi - f \\ v \end{bmatrix}^T P \begin{bmatrix} \sigma \\ \phi - f \\ v \end{bmatrix},$$

and consider the additional set-valued mapping

$$(\sigma, \phi, v) \rightrightarrows H(\sigma, \phi, v) := (\sigma, \phi, v, f_c SGN(v)).$$

By the very definition of set-valued mapping, we can write $G = g \circ H$ (the composition of g and H), that is,

$$(\sigma, \phi, v) \rightrightarrows g(\sigma, \phi, v, f_c SGN(v)) = G(x).$$

Then, G is outer semicontinuous by [102, Proposition 5.52, item (b)] because both g and H are outer semicontinuous and H is locally bounded. Finally, by the definition of distance $d(u, S)$ between a point u and a closed set S, we can write $V(x) = d(0, G(x))$. Then, V is lower semicontinuous by [102, Proposition 5.11, item (a)] because G was proven to be outer semicontinuous.

We prove now the properties of V item by item.

Item 1). There exists $\mathfrak{g} > 0$ such that

$$\begin{bmatrix} \sigma \\ v \end{bmatrix}^T \begin{bmatrix} \frac{k_v}{k_i} & -1 \\ -1 & k_p \end{bmatrix} \begin{bmatrix} \sigma \\ v \end{bmatrix} \geqslant \mathfrak{g}(\sigma^2 + v^2)$$

because the inner matrix is positive definite by Assumption 6.1. Moreover, we have from (6.19a) that

$$\min_{f \in f_c SGN(v)} (\phi - f)^2 \geqslant \min_{f \in [-f_c, f_c]} (\phi - f)^2 = dz_{f_c}(\phi)^2.$$

Therefore, (6.18) yields $V(x) \geqslant c_1|x|_{\mathcal{A}}^2$ with $c_1 := \min\{\mathfrak{g}, 1\}$.

Item 2). Equation (6.20) is a mere application of Fact 6.2 for $h(\cdot) = V(x(\cdot))$ and $\ell(\cdot) = -c(v(\cdot))^2$ where $x = (\sigma, \phi, v)$ is a solution to (6.16) and c is from Claim 6.1. So, we need to check that the assumptions of Fact 6.2 are verified.

We already established above that V is lower semicontinuous. Solutions x to (6.16) are absolutely continuous functions by definition. Then, because the composition of a lower semicontinuous and a continuous function is lower semicontinuous (see [102, Exercise 1.40]), the Lyapunov-like function (6.19a) evaluated along the solutions of (6.16) is lower semicontinuous in t. Since solutions are absolutely continuous, $-cv^2$ is locally integrable.

Finally, it was proven in Claim 6.1, item 1 that for each initial condition, the unique solution to (6.16) coincides with the solution to one of the three affine systems in (6.23) (numbered k) on a finite time interval T. Moreover, from Claim 6.1, item 2 V coincides in $[0, T]$ with the function V_k in (6.24), which is differentiable, then $t \mapsto V(x(t))$ at $t = 0$ is at least differentiable from the right and the lower right Dini derivative coincides with the right derivative. In particular, we established in (6.24) that this right derivative is upper bounded by $-cv^2$. □

6.4.3.1 *Proof of Claim 6.1*

Proof of Claim 6.1. For each possible initial condition $(\bar{\sigma}, \bar{\phi}, \bar{v})$, items 1) and 2) are satisfied by choosing the suitable k as in the table below ($\vee, \wedge$ are respectively the logical OR, AND).

Initial condition	k
$(\bar{v} > 0) \vee (\bar{v} = 0 \wedge \bar{\phi} > f_c) \vee (\bar{v} = 0 \wedge \bar{\phi} = f_c \wedge \bar{\sigma} > 0)$	1
$(\bar{v} = 0 \wedge \bar{\phi} = f_c \wedge \bar{\sigma} = 0) \vee (\bar{v} = 0 \wedge \bar{\phi} = f_c \wedge \bar{\sigma} < 0)$ $\vee (\bar{v} = 0 \wedge \|\bar{\phi}\| < f_c) \vee (\bar{v} = 0 \wedge \bar{\phi} = -f_c \wedge \bar{\sigma} > 0)$ $\vee (\bar{v} = 0 \wedge \bar{\phi} = -f_c \wedge \bar{\sigma} = 0)$	0
$(\bar{v} = 0 \wedge \bar{\phi} = -f_c \wedge \bar{\sigma} < 0) \vee (\bar{v} = 0 \wedge \bar{\phi} < -f_c) \vee (\bar{v} < 0)$	-1

Table 1: How to choose k in Claim 6.1 depending on the initial condition.

The proof of item 1) consists in showing that for each possible initial condition, the k in the table is such that the solution $\xi := (\xi_\sigma, \xi_\phi, \xi_v)$ to the affine system $\dot{\xi} = f_k(\xi)$ among (6.23a)-(6.23c) is also solution to (6.16) on the interval $[0, T]$. To verify (6.24a), we evaluate V and V_k along ξ.

We address only the case $\bar{v} = 0 \wedge \bar{\phi} > f_c$ because all other cases rely on similar reasonings. The third state equation of (6.23) reads $\dot{\xi}_v = \xi_\phi - k_v \xi_v - f_c$ with $\xi_v(0) = 0$, $\xi_\phi(0) > f_c$, so that $\dot{\xi}_v(0) > 0$. Then there exists $T > 0$ such that $\xi_v(t) > 0$ for all $t \in (0, T]$. Substitute the solution ξ to (6.23a) into (6.16). Because $-f_c \, \mathrm{SGN}(\xi_v(t)) = \{-f_c\}$ for all $t \in (0, T]$, (6.16) becomes $\dot{\xi}(t) = A\xi(t) - b$, and this holds true for all $t \in (0, T]$ precisely because ξ arises from (6.23a) ($k = 1$). Then the solution ξ is also a solution to (6.16) for $t \in [0, T]$ because they have the same initial conditions and $\dot{\xi}(t) \in F(\xi(t))$. For the same case, we prove $V(\xi(t)) = V_1(\xi(t))$ for all $t \in [0, T]$: at $t = 0$, $\xi_\phi(0) > f_c$ and the minimizer in (6.19a) is $f = f_c$; for $t \in (0, T]$, $\xi_v(t) > 0$ and $f = f_c$ is the only possible selection in (6.19a).

For each initial condition and the corresponding k, $c = 2(k_v k_p - k_i) > 0$ (by Assumption 6.1) verifies (6.24b). For $k = 1$,

$$\frac{d}{dt} V_1(\xi(t)) = \frac{d}{dt} \left(\begin{bmatrix} \xi_\sigma \\ \xi_\phi - f_c \\ \xi_v \end{bmatrix}^T P \begin{bmatrix} \xi_\sigma \\ \xi_\phi - f_c \\ \xi_v \end{bmatrix} \right)$$

$$= (A\xi - b)^T P \begin{bmatrix} \xi_\sigma \\ \xi_\phi - f_c \\ \xi_v \end{bmatrix} + \begin{bmatrix} \xi_\sigma \\ \xi_\phi - f_c \\ \xi_v \end{bmatrix}^T P(A\xi - b)$$

$$= -c\xi_v^2,$$

which satisfies (6.24b) in $[0, T]$. Parallel computations hold for $k = -1$. For $k = 0$, $V_0(\xi(t)) = \frac{k_v}{k_i} \xi_v(t)^2$ so that $\frac{d}{dt} V_0(\xi(t)) = 2\frac{k_v}{k_i} \xi_\sigma \dot{\xi}_\sigma = 0 \leqslant 0 = -c\xi_v(t)^2$. □
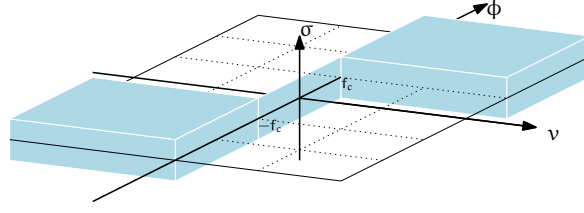
Figure 6.5: R is the (closed) blue region in Lemma 6.3, $\hat{R}$ is its complement.

6.5 PROOF OF PROPOSITION 6.1: STABILITY

This section is devoted to proving stability of the attractor.

The Lyapunov-like function introduced in (6.19) of the previous section is unfortunately not enough to prove stability. Indeed, its discontinuity on the attractor $\mathcal{A}$ prevents us from obtaining a uniform continuous upper bound depending on the distance from $\mathcal{A}$. However, a stability bound can be constructed through an auxiliary function defined as

$$\hat{V}(x) := \tfrac{1}{2}k_1\sigma^2 + \tfrac{1}{2}k_2\big(dz_{f_c}(\phi)\big)^2 + k_3|\sigma||v| + \tfrac{1}{2}k_4v^2. \tag{6.25}$$

Function $\hat{V}$ allows establishing bounds in the directions of discontinuity of V. In particular, we define the two subsets

$$R := \{x \colon v(\phi - \mathrm{sign}(v)f_c) \geqslant 0\}$$
$$\hat{R} := \mathbb{R}^3 \setminus R$$

represented in Figure 6.5. The following Lemma 6.3 holds. Based on the setting of its proof (and Case (i) of the proof of item 2) of Proposition 6.1 on page 101), Fact 2.17 in Chapter 2 aimed at generalizing the idea behind it, and in Application 2.5 we also provided some more details about the computation of the (Clarke) generalized gradient $\partial\hat{V}(x)$ appearing in (6.26c).

LEMMA 6.3 *For suitable positive scalars* $k_1, \ldots, k_4$ *in* (6.25), *there exist positive scalars* c_1, c_2, $\hat{c}_1$, $\hat{c}_2$ *such that*

$$c_1|x|^2_{\mathcal{A}} \leqslant V(x) \leqslant c_2|x|^2_{\mathcal{A}}, \qquad\qquad \forall x \in R, \tag{6.26a}$$

$$\hat{c}_1|x|^2_{\mathcal{A}} \leqslant \hat{V}(x) \leqslant \hat{c}_2|x|^2_{\mathcal{A}}, \qquad\qquad \forall x \in \hat{R}, \tag{6.26b}$$

$$\hat{V}^\circ(x) := \max_{\mathfrak{v}\in\partial\hat{V}(x),\mathfrak{f}\in F(x)} \langle\mathfrak{v},\mathfrak{f}\rangle \leqslant 0, \qquad\qquad \forall x \in \hat{R}, \tag{6.26c}$$

where $\partial\hat{V}(x)$ *denotes the generalized gradient of* $\hat{V}$ *at* x *(see the definition in* (2.53) *and [27, §1.2]) and* F *is the set-valued map in* (6.16).

Proof. Note that

$$\min_{f \in f_c\,\mathrm{SGN}(v)} \big(\phi - f\big)^2 = dz_{f_c}(\phi)^2$$

whenever $x \in R$. Since P in (6.19b) is positive definite and

$$V(x) = \left[\begin{smallmatrix} \sigma \\ dz_{f_c}(\phi) \\ v \end{smallmatrix}\right]^{\mathrm{T}} P \left[\begin{smallmatrix} \sigma \\ dz_{f_c}(\phi) \\ v \end{smallmatrix}\right] \quad \forall x \in R,$$

positive c_1 and c_2 can be chosen to satisfy (6.26a), using the definition (6.18). (The lower bound in (6.26a) was already established for all $x \in \mathbb{R}^3$ in Lemma 6.2, item 1.) For positive $k_1, \ldots, k_4$ and $k_1k_4 > k_3^2$, the inner matrix in

$$\hat{V}(x) = \frac{1}{2}\left[\begin{smallmatrix} |\sigma| \\ |dz_{f_c}(\phi)| \\ |v| \end{smallmatrix}\right]^{\mathrm{T}} \begin{bmatrix} k_1 & 0 & k_3 \\ 0 & k_2 & 0 \\ k_3 & 0 & k_4 \end{bmatrix} \left[\begin{smallmatrix} |\sigma| \\ |dz_{f_c}(\phi)| \\ |v| \end{smallmatrix}\right]$$

is positive definite and (6.26b) can be satisfied for the same reason.

To prove (6.26c), we consider only the set $\hat{R}_> := \hat{R} \cap \{x \colon \nu > 0\}$ because a parallel reasoning can be followed in $\hat{R} \cap \{x \colon \nu < 0\}$. For $x \in \hat{R}_>$, we have $\nu > 0$, $\phi < f_c$ and (6.16) reduces to the differential equation

$$\dot{\sigma} = -k_i \nu =: \mathfrak{f}_\sigma(x)$$
$$\dot{\phi} = \sigma - k_p \nu =: \mathfrak{f}_\phi(x) \tag{6.27a}$$
$$\dot{\nu} = -k_\nu \nu + \phi - f_c =: \mathfrak{f}_\nu(x) \leqslant -k_\nu |\nu| - |dz_{f_c}(\phi)|.$$

Consistently, we check the max in (6.26c) only for the singleton $\mathfrak{f} = (\mathfrak{f}_\sigma(x), \mathfrak{f}_\phi(x), \mathfrak{f}_\nu(x))$ to which $F(x)$ reduces for all $x \in \hat{R}_>$. Moreover,

$$\frac{d}{d\phi}\left(\tfrac{1}{2}\left(dz_{f_c}(\phi)\right)^2\right) = dz_{f_c}(\phi), \ \partial\left(|\sigma|\right) = \mathrm{SGN}(\sigma), \tag{6.27b}$$

where $\partial\left(|\sigma|\right)$ denotes the generalized gradient of $\sigma \mapsto |\sigma|$ according to the definition in (2.53). We need then to find suitable positive constants $k_1, \dots, k_4$ satisfying $k_1 k_4 > k_3^2$ and such that $\hat{V}^\circ(x)$ is negative semidefinite in $\hat{R}_>$. Since in $\hat{R}_>$ we have $\nu = |\nu|$ and $dz_{f_c}(\phi) = -|dz_{f_c}(\phi)|$, then we get

$$\max_{\zeta \in \partial |\sigma|}\left(-k_i k_3 |\nu|^2 \zeta\right) = k_i k_3 |\nu|^2$$

for all $x \in \hat{R}_>$, which gives in turn:

$$\hat{V}^\circ(x) \leqslant [k_i k_3 |\nu|^2 - k_4 k_\nu |\nu|^2] + [k_2 \sigma dz_{f_c}(\phi) - k_3 |\sigma| |dz_{f_c}(\phi)|]$$
$$+ [-k_1 k_i \sigma \nu - k_3 k_\nu |\nu| |\sigma|] + [k_2 k_p |\nu| |dz_{f_c}(\phi)| - k_4 |\nu| |dz_{f_c}(\phi)|].$$

Since $k_1, \dots, k_4$ are positive by assumption, in each pair in brackets the second term is negative semidefinite and dominates the first (sign-indefinite or nonnegative) term if $k_3 > \max\left\{\frac{k_i}{k_\nu} k_1, k_2\right\}$ and $k_4 > \max\left\{\frac{k_i}{k_\nu} k_3, k_p k_2, \frac{k_3^2}{k_1}\right\}$. With this selection, (6.26b) and (6.26c) are simultaneously satisfied. $\square$

With Lemma 6.3 we can finally prove the stability of the attractor.

Proof of item 2) of Proposition 6.1 (stability of $\mathcal{A}$). Based on the constants c_1, c_2, $\hat{c}_1$, $\hat{c}_2$ introduced in Lemma 6.3, the following stability bound for each solution x to (6.16)

$$|x(t)|_{\mathcal{A}} \leqslant \sqrt{\frac{c_2 \hat{c}_2}{c_1 \hat{c}_1}} |x(0)|_{\mathcal{A}}, \quad \forall t \geqslant 0 \tag{6.28a}$$

is proven by splitting the analysis in two cases.

Case (i): $x(t) \notin R$, $\forall t \geqslant 0$.

Since $R \cup \hat{R} = \mathbb{R}^3$, $x(t) \in \hat{R}$ for all $t \geqslant 0$. $\hat{V}^\circ(x(t)) \leqslant 0$ for all $t \geqslant 0$ from (6.26c) implies $\hat{V}(x(t)) \leqslant \hat{V}(x(0))$ for all $t \geqslant 0$, as it was shown in the proof of Fact 2.17 before Equation (2.66). Using bound (6.26b) we obtain

$$\hat{c}_1 |x(t)|_{\mathcal{A}}^2 \leqslant \hat{V}(x(t)) \leqslant \hat{V}(x(0)) \leqslant \hat{c}_2 |x(0)|_{\mathcal{A}}^2, \quad \forall t \geqslant 0,$$

which implies (6.28a) because $1 \leqslant \sqrt{c_2/c_1}$ from (6.26a).

Case (ii): $\exists t_1 \geqslant 0$ such that $x(t_1) \in R$.

Consider the smallest $t_1 \geqslant 0$ such that $x(t_1) \in R$ (the existence of such a *smallest* time follows from R being closed). Then, following the analysis of Case (i) for the (possibly empty) time interval $[0, t_1)$ and using continuity of solutions, we obtain

$$\hat{c}_1 |x(t)|_{\mathcal{A}}^2 \leqslant \hat{c}_2 |x(0)|_{\mathcal{A}}^2, \quad \forall t \in [0, t_1]. \tag{6.28b}$$

At t_1 we apply (6.26a) (because $x(t_1) \in R$) and (6.28b) to get $V(x(t_1)) \leqslant c_2 \left(\frac{\hat{c}_2}{\hat{c}_1} |x(0)|_{\mathcal{A}}^2\right)$. Finally, by the bounds in items 1 and 2 of Lemma 6.2,

$$c_1 |x(t)|_{\mathcal{A}}^2 \leqslant V(x(t)) \leqslant V(x(t_1)) \leqslant c_2 \frac{\hat{c}_2}{\hat{c}_1} |x(0)|_{\mathcal{A}}^2, \quad \forall t \geqslant t_1. \tag{6.28c}$$

Since $\sqrt{\frac{c_2}{c_1}} \geqslant 1$, (6.28b) implies

$$c_1 |x(t)|_{\mathcal{A}}^2 \leqslant c_2 \frac{\hat{c}_2}{\hat{c}_1} |x(0)|_{\mathcal{A}}^2, \quad \forall t \in [0, t_1],$$

which proves (6.28a) when combined with (6.28c). $\square$

7

CONCLUSIONS AND FUTURE PERSPECTIVES

In this work we proposed to model a number of electrical and mechanical systems according to the hybrid systems formalism in [47, 48]. We characterized then their properties according to the notions of stability and attractivity, suitably extended for the hybrid setting. To this end, we exploited Lyapunov functions that were weak, either because their derivatives and increments along solutions did not show a strict decrease, or because of their lack of differentiablity, or because they satisfied only generalized invariance principle conditions.

On a general level, then, one main contribution of this work was to show on a set of relevant applications the modeling capabilities of the chosen hybrid system formalism, whose power also resides in the possibility of tweaking Lyapunov tools and using weak Lyapunov functions to certify asymptotic stability.

On a detailed level, the problem of each chapter presented its own conclusions and future perspectives.

RIPPLE We already noted in Chapter 3 that the presented scheme (without the knowledge of the switching instants) was conceived directly for on-line usage. The application to which we linked this observer scheme was the ripple disturbance in the feedback signal of the JET tokamak. Because of the delicacy of this application, a further necessary theoretical step would be to enhance the presented scheme and ensure global (or semiglobal practical) asymptotic stability. On the other hand, AC/DC converters are an off-the-shelf component in high power electronics, which would allow for a ready experimental on-line validation of the proposed scheme. Apart from the enhancement we have just suggested, the scheme appears quite mature with respect to the problem we wanted to solve. In a broader sense, further research could concentrate on applying hybrid dynamical systems techniques to high power electronics, whose components induce quite naturally discontinuities due to the switchings, or to brushless DC motors, which suffer from a similar ripple disturbance in the torque [67, 112].

RESET Since Chapter 5 already constitutes an extension of Chapter 4, we discuss here conclusions and future developments mainly relative to Chapter 5. The framework in Chapter 5 characterized successfully the two controlled systems of a hopping mass and an automotive suspension. The analysis and the proofs are carried out for a second order nonlinear mechanical system. One interesting direction of future work is to extend the framework to mechanical systems with more degrees of freedom, exploiting timescale separation arguments (see [123] for singularly perturbed hybrid dynamical systems, [106] relative to fast actuation, and also more generally [34]). Hybrid dynamical systems seem particularly relevant to the case of legged locomotion, not only in terms of reset laws, but also because they can account for the unilateral constraints of the stance phase. This would also suggest a connection to the works concerning hybrid systems and impacts. The concrete applicability of such a framework in the robotics context is testified by the works cited in the chapters, and the full development of variable impedance actuators might spur the applicability also to the automotive context. Although the perspective of quantized control is different (see the discussion in Section 5.1), the type of actuation we considered suggests interesting connections with that scientific area.

FRICTION Chapter 6 has the largest potential in terms of future research. As for now, its main contribution is the proof of global asymptotic stability for the considered system. This result could be turned from an analysis problem into a design problem by inserting suitable compensation schemes for the friction. In the same context then, a compensator could achieve exponential instead

of just asymptotic stability. However, a more realistic physical scenario is the presence of a static force whose magnitude f_s is greater than the magnitude f_c of the Coulomb force. In this case, the insertion of a friction compensator is all the more needed because the use of a PID controller leads to undesired persistent oscillations (the so-called hunting phenomenon). Since this system evolves discrete-wise by toggling between the two logical states of stick and slip without Zeno phenomena, such an automaton representation may help in the design of the compensator. A further fact to consider is that the parameters f_c and f_s are typically known with large uncertainty because they depend on many exogenous factors (like wear, lubrication, temperature...). Compensation schemes must necessarily face this limitation, and present then a high degree of robustness.

BIBLIOGRAPHY

[1] S. Adly. "Attractivity theory for second order non-smooth dynamical systems with application to dry friction." In: *Journal of mathematical analysis and applications* 322.2 (2006), pp. 1055–1070.

[2] P. J. Antsaklis. "A brief introduction to the theory and applications of hybrid systems." In: *Proceedings IEEE, Special Issue on Hybrid Systems: Theory and Applications*. 2000.

[3] P. J. Antsaklis and A. Nerode. "Hybrid control systems: An introductory discussion to the special issue." In: *IEEE Transactions on Automatic Control* 43.4 (1998), pp. 457–460.

[4] B. Armstrong-Hélouvry and B. Amin. *PID control in the presence of static friction*. Tech. rep. EE-93–2. Dept. of Electrical Engineering and Computer Science, University of Wisconsin – Milwaukee, 1993.

[5] B. Armstrong-Hélouvry and B. Amin. "PID control in the presence of static friction: exact and describing function analysis." In: *American Control Conference*. Vol. 1. 1994, pp. 597–601.

[6] B. Armstrong and B. Amin. "PID control in the presence of static friction: A comparison of algebraic and describing function analysis." In: *Automatica* 32.5 (1996), pp. 679–692.

[7] K. J. Åström. "Oscillations in systems with relay feedback." In: *Adaptive Control, Filtering, and Signal Processing*. Springer, 1995, pp. 1–25.

[8] K. J. Åström and C. Canudas-de-Wit. "Revisiting the LuGre friction model." In: *IEEE Control Systems* 28.6 (2008), pp. 101–114.

[9] J. P. Aubin and A. Cellina. *Differential Inclusions. Set-valued Maps and Viability Theory*. Springer-Verlag, 1984.

[10] A. A. Ball and H. K. Khalil. "High-gain observers in the presence of measurement noise: A nonlinear gain approach." In: *47th IEEE Conference on Decision and Control*. 2008, pp. 2288–2293.

[11] N. Barahanov and R. Ortega. "Necessary and sufficient conditions for passivity of the LuGre friction model." In: *IEEE Transactions on Automatic Control* 45.4 (2000), pp. 830–832.

[12] J.P. Barbot, H. Saadaoui, M. Djemai, and N. Manamanni. "Nonlinear observer for autonomous switching systems with jumps." In: *Nonlinear Analysis: Hybrid Systems* 1.4 (2007), pp. 537–547.

[13] A. Bisoffi, F. Biral, M. Da Lio, and L. Zaccarian. "Longitudinal jerk estimation of driving intentions for intelligent vehicle applications." Under review in the IEEE/ASME Transactions on Mechatronics.

[14] A. Bisoffi, F. Biral, M. Da Lio, and L. Zaccarian. "Longitudinal Jerk Estimation for Identification of Driver Intention." In: *IEEE 18th International Conference on Intelligent Transportation Systems*. 2015, pp. 1855–1861.

[15] A. Bisoffi, M. Corno, C. Ongini, and S. M. Savaresi. "Sistema di segnalazione per ottimizzare i consumi di un veicolo nella percorrenza di strade semaforizzate." Italian Patent MI 2014A001024. Applicant: Politecnico di Milano. 2014.

[16]   A. Bisoffi, M. Da Lio, A. R. Teel, and L. Zaccarian. "Global asymptotic stability of a PID control system with Coulomb friction." In: *arXiv* (2016). Available at https://arxiv.org/abs/1609.09103. Under review in the IEEE Transactions on Automatic Control.

[17]   A. Bisoffi, F. Forni, M. Da Lio, and L. Zaccarian. "Reset control of minimal-order mechanical systems with applications." In preparation.

[18]   A. Bisoffi, F. Forni, M. Da Lio, and L. Zaccarian. "Global results on reset-induced periodic trajectories of planar systems." In: *European Control Conference*. 2016, pp. 2644–2649.

[19]   A. Bisoffi, M. Da Lio, and L. Zaccarian. "A hybrid ripple model and two hybrid observers for its estimation." In: *IEEE 53rd Conference on Decision and Control*. Los Angeles (CA), USA, 2014.

[20]   A. Bisoffi, L. Zaccarian, M. Da Lio, and D. Carnevale. "Hybrid cancellation of ripple disturbances arising in AC/DC converters." In: *Automatica* 77 (2017), pp. 344–352.

[21]   P.-A. Bliman and M. Sorine. "Easy-to-use realistic dry friction models for automatic control." In: *European Control Conference*. Vol. 113. 1995, pp. 267–272. URL: https://who.rocq.inria.fr/Pierre-Alexandre.Bliman/publis.htm.

[22]   C. I. Byrnes and C. F. Martin. "An integral-invariance principle for nonlinear systems." In: *IEEE Transactions on Automatic Control* 40.6 (1995), pp. 983–994.

[23]   C. Cai, R. Goebel, and A. R. Teel. "Smooth Lyapunov functions for hybrid systems part II: (pre) asymptotically stable compact sets." In: *IEEE Transactions on Automatic Control* 53.3 (2008), pp. 734–748.

[24]   C. Canudas-de-Wit, H. Olsson, K. J. Åström, and P. Lischinsky. "A new model for control of systems with friction." In: *IEEE Transactions on Automatic Control* 40.3 (1995), pp. 419–425.

[25]   D. Carnevale, S. Galeani, and L. Menini. "Output regulation for a class of linear hybrid systems. Parts 1 & 2." In: *IEEE 51st Conference on Decision and Control*. 2012.

[26]   D. Carnevale, S. Galeani, and M. Sassano. "Necessary and sufficient conditions for output regulation in a class of hybrid linear systems." In: *IEEE 52nd Conference on Decision and Control*. 2013, pp. 2659–2664.

[27]   F. H. Clarke. *Optimization and nonsmooth analysis*. Vol. 5. SIAM, 1990.

[28]   F. Clarke. "Lyapunov functions and discontinuous stabilizing feedback." In: *Annual reviews in control* 35.1 (2011), pp. 13–33.

[29]   M. Corno, A. Bisoffi, C. Ongini, and S. M. Savaresi. "An energy-driven road-to-driver assistance system for intersections." In: *European Control Conference*. 2015, pp. 3035–3040.

[30]   N. Cox, L. Marconi, and A. R. Teel. "High-gain observers and linear output regulation for hybrid exosystems." In: *International Journal of Robust and Nonlinear Control* (2013).

[31]   P. R. Dahl. *A solid friction model*. Tech. rep. The Aerospace Corporation El Segundo CA, 1968.

[32]   C. De Persis. "Robust stabilization of nonlinear systems by quantized and ternary control." In: *Systems & Control Letters* 58.8 (2009), pp. 602–608.

[33] W. Desch, H. Logemann, E. P. Ryan, and E. D. Sontag. "Meagre functions and asymptotic behaviour of dynamical systems." In: *Nonlinear Analysis: Theory, Methods & Applications* 44.8 (2001), pp. 1087–1109.

[34] F. El Hachemi, M. Sigalotti, and J. Daafouz. "Stability analysis of singularly perturbed switched linear systems." In: *IEEE Transactions on Automatic Control* 57.8 (2012), pp. 2116–2121.

[35] R. J Evans and A. V. Savkin. "Guest Editorial: Hybrid control systems." In: *Systems & Control Letters* 38 (1999), p. 139.

[36] G. Ferretti, G. Magnani, and P. Rocco. "Single and multistate integral friction models." In: *IEEE Transactions on Automatic Control* 49.12 (2004), pp. 2292–2297.

[37] A. F. Filippov. *Differential equations with discontinuous righthand sides: control systems*. Kluwer Academic Publishers, 1988.

[38] S. Formentin, A. Bisoffi, and T. Oomen. "Asymptotically exact direct data-driven multivariable controller tuning." In: *IFAC-PapersOnLine* 48.28 (2015), pp. 1349–1354.

[39] F. Forni, A. R. Teel, and L. Zaccarian. "Follow the bouncing ball: global results on tracking and state estimation with impacts." In: *IEEE Transactions on Automatic Control* 58.6 (2013), pp. 1470–1485.

[40] F. Forni, A. R. Teel, and L. Zaccarian. "Reference Mirroring for Control with Impacts." In: *Hybrid Systems with Constraints*. Ed. by J. Daafouz, S. Tarbouriech, and M. Sigalotti. Wiley, 2013, pp. 211–249.

[41] F. Forni, A. Teel, and L. Zaccarian. "Reference mirroring for control with impacts." In: *Hybrid Systems with Constraints* (2013), pp. 211–246.

[42] B. A. Francis and W. M. Wonham. "The internal model principle of control theory." In: *Automatica* 12.5 (1976), pp. 457–465.

[43] R. J. Full and D. E. Koditschek. "Templates and anchors: neuromechanical hypotheses of legged locomotion on land." In: *Journal of Experimental Biology* 202.23 (1999), pp. 3325–3332.

[44] A. Garulli, A. Giannitrapani, and M. Leomanni. "Minimum switching control for systems of coupled double integrators." In: *Automatica* 60 (2015), pp. 115–121.

[45] R. M. Ghigliazza, R. Altendorfer, P. Holmes, and D. Koditschek. "A simply stabilized running model." In: *SIAM review* 47.3 (2005), pp. 519–549.

[46] C. Glocker. *Set-valued force laws: dynamics of non-smooth systems*. Vol. 1. Springer Science & Business Media, 2013.

[47] R. Goebel, R. G. Sanfelice, and A. R. Teel. *Hybrid Dynamical Systems: modeling, stability, and robustness*. Princeton University Press, 2012.

[48] R. Goebel, R. Sanfelice, and A. R. Teel. "Hybrid dynamical systems." In: *IEEE Control Systems* 29.2 (2009), pp. 28–93.

[49] J. Grasman. *Asymptotic methods for relaxation oscillations and applications*. 1st ed. Applied Mathematical Sciences. Springer, 1987.

[50] J. W. Grizzle, C. Chevallereau, R. W. Sinnet, and A. D. Ames. "Models, feedback control, and open problems of 3D bipedal robotic walking." In: *Automatica* 50.8 (2014), pp. 1955–1988.

[51] F. Gunther and F. Iida. "Preloaded hopping with linear multi-modal actuation." In: *IEEE/RSJ International Conference on Intelligent Robots and Systems*. 2013, pp. 5847–5852.

[52] J. W. Hagood and B. S. Thomson. "Recovering a function from a Dini derivative." In: *The American Mathematical Monthly* 113.1 (2006), pp. 34–46.

[53] W. Hahn. *Stability of motion*. Translated by Arne P. Baartz. Springer-Verlag, 1967.

[54] M. W. Hirsch and S. Smale. *Differential Equations, Dynamical Systems, and Linear Algebra (Pure and Applied Mathematics, Vol. 60)*. Academic Press, 1974.

[55] P. Holmes, R. J. Full, D. Koditschek, and J. Guckenheimer. "The dynamics of legged locomotion: Models, analyses, and challenges." In: *SIAM Review* 48.2 (2006), pp. 207–304.

[56] A. Isidori. *Nonlinear Control Systems*. 3rd. Springer, 1995.

[57] C. M. Kellett. "A compendium of comparison function results." In: *Mathematics of Control, Signals, and Systems* 26.3 (2014), pp. 339–374.

[58] C. M. Kellett and A. R. Teel. "Discrete-time asymptotic controllability implies smooth control-Lyapunov function." In: *Systems & Control Letters* 52.5 (2004), pp. 349–359.

[59] H. K. Khalil. *Nonlinear Systems*. 3rd. Prentice Hall, 2002.

[60] M. A. Krasnosel'skii and A. V. Pokrovskii. *Systems with hysteresis*. Springer-Verlag, 1989.

[61] J. Kurzweil. "On the inversion of Lyapunov's second theorem on stability of motion." In: *American Mathematical Society Translations, Series 2.24* (1956), pp. 19–77.

[62] D. Lakatos and A. Albu-Schäffer. "Switching based limit cycle control for compliantly actuated second-order systems." In: *Proceedings of the 19th IFAC World Congress*. 2014, pp. 6392–6399.

[63] D. Lakatos, G. Garofalo, A. Dietrich, and A. Albu-Schäffer. "Jumping control for compliantly actuated multilegged robots." In: *IEEE International Conference on Robotics and Automation*. 2014, pp. 4562–4568.

[64] D. Lakatos, G. Garofalo, F. Petit, C. Ott, and A. Albu-Schäffer. "Modal limit cycle control for variable stiffness actuated robots." In: *IEEE International Conference on Robotics and Automation*. 2013, pp. 4934–4941.

[65] D. Lakatos, F. Petit, and A. Albu-Schäffer. "Nonlinear oscillations for cyclic movements in variable impedance actuated robotic arms." In: *IEEE International Conference on Robotics and Automation*. 2013, pp. 508–515.

[66] D. Lakatos, D. Seidel, W. Friedl, and A. Albu-Schäffer. "Targeted jumping of compliantly actuated hoppers based on discrete planning and switching control." In: *IEEE/RSJ International Conference on Intelligent Robots and Systems*. 2015, pp. 5802–5808.

[67] H. Le-Huy, R. Perret, and R. Feuillet. "Minimization of torque ripple in brushless dc motor drives." In: *IEEE Transactions on Industry Applications* 4 (1986), pp. 748–755.

[68] D. Leach, F. Gunther, N. Maheshwari, and F. Iida. "Linear multimodal actuation through discrete coupling." In: *IEEE/ASME Transactions on Mechatronics* 19.3 (2014), pp. 827–839.

[69] R. I. Leine and N. van de Wouw. *Stability and convergence of mechanical systems with unilateral constraints*. Vol. 36. Springer Science & Business Media, 2007.

[70] W. S. Levine. *The Control Systems Handbook: Control System Advanced Methods*. CRC press, 2010.

[71] Y. Li and R. G. Sanfelice. "A finite-time convergent observer with robustness to piecewise-constant measurement noise." In: *Automatica* 57 (2015), pp. 222–230.

[72] D. Liberzon. *Switching in systems and control*. Springer Science & Business Media, 2012.

[73] H. Lin and P. J. Antsaklis. "Hybrid Dynamical Systems: An Introduction to Control and Verification." In: *Foundations and Trends® in Systems and Control* 1.1 (2014), pp. 1–172.

[74] H. Logemann and E. P. Ryan. "Asymptotic behaviour of nonlinear systems." In: *American Mathematical Monthly* (2004), pp. 864–889.

[75] A. M. Lyapunov. "The general problem of the stability of motion." In: *International Journal of Control* 55.3 (1992). translated from Russian into French by E. Davaux, translated from French into English by A. T. Fuller, pp. 531–534.

[76] J. Lygeros. "Lecture notes on hybrid systems." In: *Notes for an ENSI-ETA workshop*. 2004.

[77] M. Malisoff and F. Mazenc. *Constructions of strict Lyapunov functions*. Springer Science & Business Media, 2009.

[78] L. Marconi and L. Praly. "Uniform practical nonlinear output regulation." In: *IEEE Transactions on Automatic Control* 53.5 (2008), pp. 1184–1202.

[79] L. Marconi and A. R. Teel. "A note about hybrid linear regulation." In: *IEEE 49th Conference on Decision and Control*. 2010, pp. 1540–1545.

[80] L. Marconi and A. R. Teel. "Internal model principle for linear systems with periodic state jumps." In: *IEEE Transactions on Automatic Control* 58.11 (2013), pp. 2788–2802.

[81] C. G. Mayhew, R. G. Sanfelice, and A. R. Teel. "Quaternion-based hybrid control for robust global attitude tracking." In: *IEEE Transactions on Automatic Control* 56.11 (2011), pp. 2555–2566.

[82] F. Mazenc and D. Nešić. "Lyapunov functions for time varying systems satisfying generalized conditions of Matrosov theorem." In: *44th IEEE Conference on Decision and Control and European Control Conference*. 2005, pp. 5432–5437.

[83] R. I. McLachlan, G. R. W. Quispel, and N. Robidoux. "Unified approach to Hamiltonian systems, Poisson systems, gradient systems, and systems with Lyapunov functions or first integrals." In: *Physical Review Letters* 81.12 (1998), p. 2399.

[84] L. Meirovitch. *Fundamentals of Vibrations*. McGraw-Hill Companies, 2000.

[85] P. E. Moraal and J. W. Grizzle. "Observer design for nonlinear systems with discrete-time measurements." In: *IEEE Transactions on Automatic Control* 40.3 (1995), pp. 395–404.

[86] A. S. Morse. "Supervisory control." In: *Adaptive Control, Filtering, and Signal Processing*. Springer, 1995, pp. 241–270.

[87] A. S. Morse, C. C. Pantelides, S. Sastry, J. M. Schumacher, et al. "Introduction to the special issue on hybrid systems." In: *Automatica* 35.3 (1999), pp. 347–348.

[88] A. Neto, G. De Tommasi, R. Albanese, G. Ambrosino, M. Ariola, G. Artaserse, A. J. N. Batista, B. Carvalho, F. Crisanti, H. Fernandes, et al. "Exploitation of modularity in the JET tokamak vertical stabilization system." In: *Control Engineering Practice* 20.9 (2012), pp. 846–856.

[89] M. Ó Searcóid. *Metric spaces*. Springer Science & Business Media, 2006.

[90] H. Olsson, K. J. Åström, C. Canudas-de-Wit, M. Gäfvert, and P. Lischinsky. "Friction models and friction compensation." In: *European Journal of Control* 4.3 (1998), pp. 176–195.

[91] F. M. Pait and A. S. Morse. "A cyclic switching strategy for parameter-adaptive control." In: *IEEE Transactions on Automatic Control* 39.6 (1994), pp. 1172–1183.

[92] S. Petterson. "Switched state jump observers for switched systems." In: *Proceedings of the 16th IFAC World Congress*. 2005.

[93] S. Pettersson. "Observer design for switched systems using multiple quadratic Lyapunov functions." In: *Proceedings of the 2005 IEEE International Symposium on Intelligent Control, Mediterrean Conference on Control and Automation*. 2005, pp. 262–267.

[94] S. Pettersson. "Designing switched observers for switched systems using multiple Lyapunov functions and dwell-time switching." In: *2nd IFAC Conference on Analysis and Design of Hybrid Systems*. Vol. 2. 2006, pp. 18–23.

[95] A. Pironti and M. Walker. "Fusion, tokamaks, and plasma control: an introduction and tutorial." In: *IEEE Control Systems* 25.5 (2005), pp. 30–43.

[96] C. Poussot-Vassal, C. Spelta, O. Sename, S. M. Savaresi, and L. Dugard. "Survey and performance evaluation on some automotive semi-active suspension control methods: A comparative study on a single-corner model." In: *Annual Reviews in Control* 36.1 (2012), pp. 148–160.

[97] C. Prieur, A. R. Teel, and L. Zaccarian. "Relaxed persistent flow/jump conditions for uniform global asymptotic stability." In: *IEEE Transactions on Automatic Control* 59.10 (2014), pp. 2766–2771.

[98] D. Putra, H. Nijmeijer, and N. van de Wouw. "Analysis of under-compensation and overcompensation of friction in 1 DOF mechanical systems." In: *Automatica* 43.8 (2007), pp. 1387–1394.

[99] C. J. Radcliffe and S. C. Southward. "A property of stick-slip friction models which promotes limit cycle generation." In: *American Control Conference*. 1990, pp. 1198–1205.

[100] M. H. Raibert. *Legged robots that balance*. MIT press, 1986.

[101] M. Reis and F. Iida. "An energy-efficient hopping robot based on free vibration of a curved beam." In: *IEEE/ASME Transactions on Mechatronics* 19.1 (2014), pp. 300–311.

[102] R. T. Rockafellar and R. J.-B. Wets. *Variational analysis*. Vol. 317. Springer Science & Business Media, 2009.

[103] E. P. Ryan. "An integral invariance principle for differential inclusions with applications in adaptive control." In: *SIAM Journal on Control and Optimization* 36.3 (1998), pp. 960–980.

[104]   C. O. Saglam, A. R. Teel, and K. Byl. "Lyapunov-based versus Poincaré Map Analysis of the Rimless Wheel." In: *IEEE 53rd Conference on Decision and Control*. 2014, pp. 1514–1520.

[105]   R. G. Sanfelice, R. Goebel, and A. R. Teel. "Invariance principles for hybrid systems with connections to detectability and asymptotic stability." In: *IEEE Transactions on Automatic Control* 52.12 (2007), pp. 2282–2297.

[106]   R. G. Sanfelice and A. R. Teel. "On singular perturbations due to fast actuators in hybrid control systems." In: *Automatica* 47.4 (2011), pp. 692–701.

[107]   R. G. Sanfelice, A. R. Teel, and R. Sepulchre. "A hybrid systems approach to trajectory tracking control for juggling systems." In: *46th IEEE Conference on Decision and Control*. 2007, pp. 5282–5287.

[108]   M. Sassano, D. Carnevale, and A. Astolfi. "Extremum seeking-like observer for nonlinear systems." In: *IFAC Proceedings Volumes* 44.1 (2011). 18th IFAC World Congress, pp. 1849 –1854.

[109]   M. Sassano and L. Zaccarian. "Hierarchical stability of nonlinear hybrid systems." In: *arXiv* (2016). Available at https://arxiv.org/abs/1601.01271.

[110]   S. M. Savaresi, C. Poussot-Vassal, C. Spelta, O. Sename, and L. Dugard. *Semi-active suspension control design for vehicles*. Elsevier, 2010.

[111]   A. J. van der Schaft and J. M. Schumacher. "Complementarity modeling of hybrid systems." In: *IEEE Transactions on Automatic Control* 43.4 (1998), pp. 483–490.

[112]   J.-H. Song and I. Choy. "Commutation torque ripple reduction in brushless DC motor drives using a single DC current sensor." In: *IEEE Transactions on Power Electronics* 19.2 (2004), pp. 312–319.

[113]   E. D. Sontag. "Smooth stabilization implies coprime factorization." In: *IEEE Transactions on Automatic Control* 34.4 (1989), pp. 435–443.

[114]   E. D. Sontag. "Further facts about input to state stabilization." In: *IEEE Transactions on Automatic Control* 35.4 (1990), pp. 473 –476.

[115]   E. D. Sontag and H. J. Sussmann. "Further comments on the stabilizability of the angular velocity of a rigid body." In: *Systems & Control Letters* 12.3 (1989), pp. 213–217.

[116]   D. E. Stewart. "Rigid-body dynamics with friction and impact." In: *SIAM Review* 42.1 (2000), pp. 3–39.

[117]   J. Swevers, F. Al-Bender, C. G. Ganseman, and T. Projogo. "An integrated friction model structure with improved presliding behavior for accurate friction compensation." In: *IEEE Transactions on Automatic Control* 45.4 (2000), pp. 675–686.

[118]   A. R. Teel, F. Forni, and L. Zaccarian. "Lyapunov-based sufficient conditions for exponential stability in hybrid systems." In: *IEEE Transactions on Automatic Control* 58.6 (2013), pp. 1591–1596.

[119]   A. R. Teel, R. Goebel, B. Morris, A. D. Ames, and J. W. Grizzle. "A stabilization result with application to bipedal locomotion." In: *IEEE 52nd Conference on Decision and Control*. 2013, pp. 2030–2035.

[120]   N Van De Wouw and RI Leine. "Robust impulsive control of motion systems with uncertain friction." In: *International Journal of Robust and Nonlinear Control* 22.4 (2012), pp. 369–397.

[121] B. Vanderborght, A. Albu-Schäffer, A. Bicchi, E. Burdet, D. G. Cald-
       well, R. Carloni, M. Catalano, O. Eiberger, W. Friedl, G. Ganesh, et
       al. "Variable impedance actuators: A review." In: *Robotics and Au-
       tonomous Systems* 61.12 (2013), pp. 1601–1614.

[122] A. Visintin. *Differential models of hysteresis*. Vol. 111. Springer-Verlag,
       1994.

[123] W. Wang, A. R. Teel, and D. Nešić. "Analysis for a class of singularly
       perturbed hybrid systems via averaging." In: *Automatica* 48.6 (2012),
       pp. 1057–1068.

[124] E.R. Westervelt, J.W. Grizzle, C. Chevallereau, J.H. Choi, and B. Mor-
       ris. *Feedback control of dynamic bipedal robot locomotion*. Control and
       automation. Boca Raton: CRC Press, 2007.

[125] N. van de Wouw and R. I. Leine. "Attractivity of equilibrium sets of
       systems with dry friction." In: *Nonlinear Dynamics* 35.1 (2004), pp. 19–
       39.

[126] X. Yu and F. Iida. "Minimalistic models of an energy-efficient vertical-
       hopping robot." In: *IEEE Transactions on Industrial Electronics* 61.2
       (2014), pp. 1053–1062.